UNCLASSIFIED

63-2-4

1

QUARTERLY PROGRESS REPORT

No. 68

752 500

JANUARY 15, 1963

752 500

MASSACHUSETTS INSTITUTE OF TECHNOLOGY
RESEARCH LABORATORY OF ELECTRONICS
CAMBRIDGE, MASSACHUSETTS

$17.50

The Research Laboratory of Electronics is an interdepartmental laboratory in which faculty members and graduate students from numerous academic departments conduct research.

The research reported in this document was made possible in part by support extended the Massachusetts Institute of Technology, Research Laboratory of Electronics, jointly by the U.S. Army, the U.S. Navy (Office of Naval Research), and the U.S. Air Force (Office of Scientific Research), under Contract DA36-039-sc-78108, Department of the Army Task 3-99-25-001-08; and in part by Contract DA-SIG-36-039-61-G14.

Partial support for work in Plasma Dynamics is provided by the U.S. Atomic Energy Commission under Contract AT(30-1)-1842; the National Science Foundation (Grant G-24073); the U.S. Air Force (Electronic Systems Division) under Contract AF 19(604)-5992; and the U.S. Air Force (Aeronautical Systems Division) under Contract AF 33(616)-7624.

Partial support for work in Communication Sciences is provided by the National Science Foundation (Grant G-16526) and the National Institutes of Health (Grant MH-04737-02).

Additional support of specific projects is acknowledged in footnotes to the appropriate sections.

MASSACHUSETTS INSTITUTE OF TECHNOLOGY

RESEARCH LABORATORY OF ELECTRONICS

QUARTERLY PROGRESS REPORT No. 68

January 15, 1963

Submitted by: H. J. Zimmermann
G. G. Harvey
W. B. Davenport, Jr.

TABLE OF CONTENTS

CONTENTS

CONTENTS

CONTENTS

PERSONNEL

Administration

Professor H. J. Zimmermann, Director
Professor G. G. Harvey, Associate Director
Professor W. B. Davenport, Jr., Associate Director
Mr. R. A. Sayers, Personnel and Business Manager

Advisory Committee

Dean G. S. Brown (Ex officio)
Professor W. W. Buechner
Professor W. B. Davenport, Jr.
Professor P. Elias
Professor G. G. Harvey
Professor A. G. Hill
Professor I. W. Sizer
Professor H. J. Zimmermann (Chairman)

Faculty

Allis, W. P. (Absent)
Arden, D. N. (Absent)
Barrett, A. H.
Bekefi, G.
Bers, A.
Billman, K. W.
Bitter, F.
Bose, A. G.
Brazier, Mary A. B. (Visiting)
Brown, S. C.
Carabateas, E. N.
Chomsky, A. N.
Chorover, S. L.
Chu, L. J.
Cochran, J. F.
Davenport, W. B., Jr.
Dennis, J. B.
Dupree, T. H.
Eden, M.
Edgerton, H. E.
Elias, P.
Fano, R. M.
Freedman, S. I.
Gallager, R. G.
Garland, C. W.
Getty, W. D.
Goldstein, M. H., Jr.
Graham, J. W.
Green, D. M.
Guillemin, E. A.
Gyftopoulos, E. P.
Halle, M.
Hammes, G. G.
Harvey, G. G.
Hatsopoulos, G. N. (Absent)
Haus, H. A.
Heinz, J. M.
Heiser, W. H.
Hennie, F. C., III
Hill, A. G.
Hoffman, M. A.
Hofstetter, E. M.
Huffman, D. A.
Ingard, K. U.
Jackson, W. D.
Jacobs, I. M.
Jakobson, R.
Javan, A.
Kerrebrock, J. L.
King, J. G.
Kinsey, J. L.
Klima, E. S.
Kyhl, R. L.
Lee, Y. W.
Lettvin, J. Y.
Lidsky, L. M.
Manders, A. M.
Mason, S. J.
Maxwell, E. (Visiting)
Meissner, H. P.
Melcher, J. R.
Melzack, R.
Minsky, M. L.
More, T., Jr.
Nottingham, W. B.
Oates, G. C.
Peake, W. T.
Penfield, P. L., Jr.
Penhune, J. P.
Perry, C.
Putnam, H.
Rafuse, R. P.
Reiffen, B. (Visiting)
Reynolds, J. M.
Rose, D. J.
Rosenblith, W. A.
Sakrison, D. J.
Schetzen, M.
Schreiber, W. F.
Schwab, W. C.
Searle, C. L.
Shannon, C. E.
Shapiro, A. H.
Siebert, W. McC.
Smith, J. L., Jr.
Smullin, L. D.
Stevens, K. N. (Absent)
Stickney, R. E.
Stockham, T. G., Jr.
Strandberg, M. W. P.
Swets, J. A. (Absent)
Teager, H. M.
Teuber, H. L.
Thornton, R. D.
Tisza, L. (Absent)
Townes, C. H.
Troxel, D. E.
Van Trees, H. L., Jr.
Wall, P. D.
Warren, B. E.
Waugh, J. S.
Whitehouse, D. R.
Whitney, W. M.
Woodson, H. H.
Wozencraft, J. M.
Young, L. R.
Zacharias, J. R.
Zadeh, L. A. (Visiting)
Zimmermann, H. J.

PERSONNEL

Instructors

Alter, R.
Bohacek, P. K.
Bruce, J. D.
Cooper, R. S.
Crystal, T. H. (Absent)
Cummings, J. R.
Dean, L. W., III
East, D. A.
Hall, J. L., II
Kellner, W. G.
Kennedy, R. S.
Kincaid, T. G.
Kliman, G. B.
Koskinen, M. F.
Krishnayya, J. G.
Liu, C. L.
MacDonald, J. S.
Oppenheim, A. V.
Parente, R. B.
Perlmutter, D. M.
Pierson, E. S.
Schneider, A. J.
Shavit, A.
Widnall, W. S.

Lecturers

Pitts, W. H.
Rines, R. H.
Stroke, G. W.
Stroke, H. H.

Research Associates

Barlow, J. S.
Bradley, L. C., III
Burke, J. J., Jr.
Cavaggioni, A.
Cerrillo, M. V.
Dupress, J.
Fiocco, G.
Gerstein, G. L.
Gesteland, R. C.
Hermann, H. T.
House, A. S.
Kilmer, W. L.
Matthews, G. H.
Stark, L.
Thompson, E.
Yngve, V. H.

Staff Members

Arndt, R. W.
Badessa, R. S.
Bates, V. J.
Bosche, Carol M.
Brown, R. M.
Campbell, Elizabeth J.
Chang, Yi
Charney, Elinor K.
Clark, W. A., Jr. (Lincoln Laboratory)
Clayton, R. J.
Congleton, Ann
Crist, A. H.
Darlington, J. L.
Duffy, D. F.
Edwards, D. J.
Farley, B. G. (Lincoln Laboratory)
Ferretti, E. F.
Fields, H.
Garber, M.
Giberman, E.
Hewitt, J. H.
Howland, B. (Lincoln Laboratory)
Ingersoll, J. G.
Ingraham, E. C.
Jaseja, T. S.
Kannel, Muriel
Katz, J. J.
Kerllenevich, N.
Keyes, R. V., Jr.
Kiang, N. Y-S.
Kuiper, J. W.
Kusse, B. R.
Lindsley, V. Susan
Majumdar, S. K.
McCarthy, J. J.
McCulloch, W. S.
Molnar, Donna A.
Mulligan, W. J.
O'Brien, F. J.
Pennell, Martha M.
Percival, W. K.
Pitts, W. H.
Postal, P. M.
Rao, B. D. N.
Reid, M. H.
Rosebury, F.
Ryan, L. W.
Saltalamacchia, A. J.
Sandel, T. T. (Lincoln Laboratory)
Satterthwait, A. C.
Sayers, R. A.
Shiffman, C. A.
Smith, P. L.
Stroke, H. H.
Stucki, M. J.
Svihula, G. F.
Szoke, A.
Thomas, Helen L.
Vidale, Eda B.
Viertel, J. J.
Whitney, R. E.
Willis, P. A.
Wilson, G. L.
Yaqub, M.

PERSONNEL

Visitors

Baker, F. H. (Postdoctoral Fellow of the National Institutes of Health)
Gross, C. (Postdoctoral Fellow of the National Institutes of Health)
Hall, R. D. (Postdoctoral Fellow of the National Institute of Mental Health)
Imai, N.
Isami, Y. (Fulbright Research Scholar in Linguistics)
Keyser, S. J.

Kornacker, K. (Postdoctoral Fellow of the National Institutes of Health)
Menyuk, Paula (Postdoctoral Fellow of the National Institutes of Health)
Molnar, C. E.
Onesto, N. M. (R.L.E. Postdoctoral Fellow)
Parks, J. H.
Rojas, J. A. (Postdoctoral Fellow of the National Institutes of Health)

Schiller, P. H. (Postdoctoral Fellow of the National Institutes of Health)
Siatkowski, Z.
Toschi, R. (Fulbright Research Scholar)
Troelstra, A. (NATO Science Fellow)
Walker, D. E.
Walter, W. T.
Wojnar, A. (R.L.E. Postdoctoral Fellow)
Wu, K. (R.L.E. Postdoctoral Fellow)
Yasui, S.

Graduate Students

Adcock, T. G.
Addison, R. C., Jr. (Raytheon Fellow)
Aldrich, J. A. (RCA Fellow)
Algazi, V. R.
Allen, R. J.
Alvarez de Toledo, F.
Anderson, A. T., III
Anderson, T. M. (USN Fellow)
Andrews, J. M., Jr.
Andrews, M. L.
Arbib, M. A.
Arnstein, D. S.
Arunasalam, V.
Austin, M. E. (National Science Foundation Fellow)
Axelrod, F. S.
Bartsch, R. R.
Bauer, R. F.
Berlekamp, E. R.
Bever, T. G.
Blackford, B. L.
Blinn, J. C., III
Blum, M.
Bobrow, D. G.
Bolen, N. E.
Bosco, J. A.
Brabson, B. B. (National Science Foundation Fellow)
Brassert, W. L.

Brendel, P. J. (National Science Foundation Fellow)
Briggs, R. J. (RCA Fellow)
Brown, J. E.
Buntschuh, C. D.
Burgiel, J. C.
Burns, S. K. (Teaching Assistant)
Bush, A. M.
Cahlander, D. A.
Capranica, R. R. (Communications Development Training Program Fellow of Bell Telephone Laboratories, Inc.)
Chamberlain, S. G.
Chandra, A. N.
Cheadle, G.
Chiao, R. Y.
Clarke, J. F.
Clemens, J. K.
Coccoli, J. D.
Cogdell, J. R.
Coggins, J. L.
Cornew, R. W.
Crowley, J. M. (U.S. AEC Fellow)
Cunningham, J. E.
Davis, J. A. (National Science Foundation Fellow)

Dethlefsen, R.
Diamond, B. L.
Domen, J. K.
Donadieu, L. J.
Drouet, M. G. A.
Dym, H.
Ebert, P. M. (National Science Foundation Fellow)
Ellis, J. R., Jr.
Falconer, D. D. (Whitney Fellow)
Fohl, T.
Forney, G. D., Jr.
Fraim, F. W., IV
Gann, A. G. (Raytheon Fellow)
Garmire, Elsa M.
Garosi, G. A.
Gerstmann, J. (National Science Foundation Fellow)
Ghosh, S. K.
Glenn, W. H., Jr. (Hughes Aircraft Fellow)
Golub, R. (I.T.T. Fellow)
Gothard N.
Gray, C. E. (Teaching Assistant)
Gray, P. R. (Teaching Assistant)
Grayzel, A. I.

Graduate Students (continued)

Greenspan, R. L.
Gronemann, U. F.
Guttrich, G. L.
Hall, Barbara C.
(National Science Foundation Fellow)
Halverson, W. D.
Hambrecht, F. T.
Hart, T. P.
Hartenbaum, B. A.
Haruta, K.
Hegblom, E. R.
Henke, W. L.
(National Science Foundation Fellow)
Heywood, J. B.
Holsinger, J.
Hooper, E. B., Jr.
Houk, J. C., Jr.
(IBM Fellow)
Hsieh, H. Y.
Huang, T. S.
(Teaching Assistant)
Huibonhoa, R.
(Teaching Assistant)
Impink, A. J., Jr.
Ingraham, J. C.
(National Science Foundation Fellow)
Ivie, E. L.
Jameson, P. W.
(Schlumberger Fellow)
Johnston, W. D., Jr.
Jones, J. S.
Kamen, E. L.
Karvellas, P. H.
Katona, P. G.
Kellen, P. F.
Kelly, W. F.
(Sperry-Rand Corporation Fellow)
Ketterer, F. D.
Kiparsky, R. P. V.
Kniazzeh, A. G. F.
Kocher, D. G.
Kramer, A. J.
(Teaching Assistant)
Kronquist, R. L.
Kukolich, S. G.
Kuroda, S. Y.
(Whitney Fellow)
Langendoen, D. T.
Lastovka, J. B.
Lerman, S. H.
Levine, J. D.
Levine, R. C.
(Teaching Assistant)
Levison, W. H.
Lewis, A. T.
Liégeois, F. A.
Lightner, T. M.
Little, R. G.
Llewellyn-Jones, D. T.
Lontai, L. N.
Lowry, E. S.
Luce, D. A.
Luckham, D. C.
Luther, A. H.
Lutz, M. A.
Macomber, J. D.
Mandics, P. A.
Mark, R. G.
Masek, T. D.
Mayo, J. W.
McCawley, J. D.
(Teaching Assistant)
McMorris, J. A., II
Mendell, L.
Mendelson, J.
Mermelstein, P.
Minoo, H.
Morse, D. L.
Mussi, R. N. F.
Navas, F.
Nelson, D. E.
(Teaching Assistant)
Nolan, J. J., Jr.
Nowak, R. T.
Oder, R. R.
Olsen, J. H.
Omura, J. K.
(National Science Foundation Fellow)
Paul, A. P.
Pauwels, H.
Petrie, L. M., Jr.
(Teaching Assistant)
Pfaff, D. W.
Pfeiffer, R. R.
Phipps, C. R., Jr.
Pilla, M. A.
(Teaching Assistant)
Prabhu, V. K.
Praddaude, H. C.
Pruslin, D. H.
Qualls, C. B.
Rahmani, Mahin
Redi, O.
Rizzo, J.
Roberts, L. G.
Rogoff, G. L.
Rook, C. W., Jr.
Rosenbaum, P. S.
Rosenshein, J. S.
Rowe, A. W.
Rummler, W. D.
Sandberg, A. A.
Savage, J. E.
Schlossberg, H.
Schuler, C. J., Jr.
Serafim, P. E.
Shane, J. R.
(Kennicot-Copper Fellow)
Shimony, U.
Simon, R. W.
Simpson, J. I.
Sklar, J. R.
Smith, R. S.
Smith, W. W.
Smythe, D. L., Jr.
(Teaching Assistant)
Snodderly, D. M., Jr.
Sobel, I.
Sohn, S. J.
(Teaching Assistant)
Spangler, P. S.
Staelin, D. H.
Stanton, S. F. (Hughes Aircraft Fellow)
Steele, D. W.
(Sloan Fellow)
Steelman, J. E.
(Teaching Assistant)
Steinbrecher, D. H.
Stiglitz, I. G.
Strong, W. J.
Sutherland, W. R.
(National Science Foundation Fellow)
Taub, A. (National Institutes of Health Fellow)
Tepley, N.
Theodoridis, G.
Thiele, A. A.
Thomae, I. H.
(National Science Foundation Fellow)
Thomas, L. C.
Thompson, W. B.
Thornburg, C. O., Jr.
Tobey, M. C., Jr.
(Teaching Assistant)
Tomlinson, W. J., III

Graduate Students (continued)

Tretiak, O. J.
(R.L.E. Fellow)
Tse, F. Y-F.
Tulenko, J. S.
(U.S. AEC Fellow)
Vanderweil, R. G.
Van Horn, E. C., Jr.
Wade, C. G.
Wagner, C. E.
(Teaching Assistant)
Waletzko, J. A.
Wang, G. Y-C.
Ward, R. L.
(IBM Fellow)
Wasserman, G. S.
Weinreb, S.
Weiss, T. F.
Welch, J. R.
(Teaching Assistant)
Wemple, S. H.
Whitman, E. C.
Wiederhold, M. L.
Wilde, D. U.
(Teaching Assistant)
Wilde, G. R.
Wilensky, S.
Williamson, R. C.
Willke, H. L., Jr.
Wilson, W. J.
(Teaching Assistant)
Witting, H. L.
(U.S. AEC Fellow)
Witting, J. M.
(I.T.T. Fellow)
Witzke, K. G.
Wolf, R. P.
Woo, J. C.
Wright, B. L.
Yudkin, H. L.
Zeiger, H. P.
Zuber, B. L.
Zuckerman, B. M.
Zwicky, A. M., Jr.
(National Defense Education Act Fellow)

Undergraduates

Addis, J. L.
Aponick, A. A.
Bayles, R. U.
Brincko, A. J.
Butterfield, B. O.
Byers, F. H.
Carson, J. F.
Deininger, C. C.
Diephuis, R. J.
Ecklein, D.
Gadzuk, J. W.
Grabowski, R. E.
Hamlin, R. M., Jr.
Harlem, G. S.
Hartman, P. W.
Hirschfeld, R. A.
Hutson, R. L.
Johnson, I. S. C.
Koons, H. C.
Libman, S. M.
Lindes, P.
McDowell, G. Q.
Mann, C. A., Jr.
Marchese, P. S., Jr.
Murray, J. R.
Nelson, G. P.
Ng, L. C.
Norris, R. B., Jr.
Parchesky, J.
Perrolle, P. M.
Peterson, B. A.
Piner, S. D.
Rome, J. A.
Schindall, J. E.
Siemens, P. J.
Smith, D. F.
Speer, E. R., Jr.
Stark, M. F.
Ter-Minassian, V.
Turnbull, R. J.
Wan, A. C. M.
Wolf, W. J., Jr.
Wolfberg, M.
Yap, B. K.
Yansen, D. E.

Senior Thesis Students

Baecker, R. M.
Baugh, W. H., III
Bender, M. H.
Books, G. E.
Chu, Y. H.
Cohn, T. E.
Dralle, A. V.
Ellms, S. R.
Emelianoff, M. D.
Emerson, S. T.
Evans, S. A.
Fevrier, A.
Fiory, A. T.
Flicker, J. K.
Hadden, W. J., Jr.
Hassan, A. R.
Hegyi, D. J.
Jansen, R. H.
Jordan, H. D.
Joseph, D. K.
Kinzer, T. J., III
Kosdon, F. J.
Kotler, S. J.
Landowne, D.
Langbein, D.
Lennon, W. J.
Lynch, J. T.
McClees, H. C., Jr.
MacDonald, J. F. P.
Manheimer, W. M.
Marble, C. W.
Meyer, J. S.
Miller, S. W.
Milner, P.
Mudama, E. L.
Okereke, S. A.
Pearlman, M. R.
Porter, R. P.
Reznek, S. R.
Sarraquigne, M. R.
Schlessinger, L.
Solin, S. A.
Spira, P. M.
Stavn, M. J.
Stokowski, S. R.

PERSONNEL

Senior Thesis Students (continued)

Tomes, C. F.
Valby, L. R.
Wachtel, J. M.
Wawzonek, J. J.
Weintraub, A. C.
Wende, C. D.
Winsor, N. K.
Zilles, S. N.

Assistants and Technicians

Aquinde, P.
Arnold, Jane B.
Atlas, H.
Babcock, E. B.
Barrett, J. W.
Barrows, F. W.
Beaton, Catherine M.
Bella, C. J.
Berg, A. E.
Butler, R. E., Jr.
Carbone, Marie L.
Chance, Eleanor K.
Connolly, J. T.
Cook, J. F.
Coyle, J. E.
Cranmer, R. E.
Crist, F. X.
Donahue, P. D.
Engler, R. R.
Fitzgerald, E. W., Jr.
French, Marjorie A.
Gay, H. D.
Grande, Esther D.
Greenwood, E. L.
Gregor, C. A.
Hallett, J. G.
Karas, P.
Kelly, M. A.
Kierstead, J. D.
Leonard, E. T.
Major, Diane
McKenzie, J. A.
McLean, J. J.
Mitchell, W. S., Jr.
Molin, A. H.
Neal, R. W.
Nolund, J. F.
North, D. K.
Overslvizen, T.
Papa, D. C.
Peck, J. S.
Porcaro, R. J.
Pyle, Cynthia M.
Samson, P. R.
Schwabe, W. J.
Sears, A. R.
Smith, Gabriella W.
Solomon, R. W.
Sprague, L. E.
Stroud, Marion B.
Thompson, D. S.
Tortolano, A. J.
Weiss, Aurice V.
Yaffee, M. A.
Yee, F. Q.

Document Room

Hewitt, J. H.
Hurvitz, Rose S.
Laurendeau, Carole A.

Drafting Room

Navedonsky, C. P., Foreman
Donahue, J. B.
Elliot, Claire L.
Porter, Jean M.
Rollins, I. E.

Machine Shop

Keefe, J. B., Foreman
Barnet, F. J.
Bletzer, P. W.
Brennan, J.
Bunick, F. J.
Cabral, M., Jr.
Carter, C. E.
Daniels, W. M.
Gibbons, W. D.
Liljeholm, F. H.
Marshall, J. J.
Muse, W. J.
Reimann, W.
Ryan, J. F.
Sanromá, J. B.
Shmid, E.
Smart, D. A.
Tucker, C. L.

Secretaries

Amidon, Willa T.
Barron, Gladys G.
Bertozzi, Norma

PERSONNEL

Secretaries (continued)

Blais, Gisele G.
Boyajian, Judith A.
Brown, Eileen A.
Brunetto, Deborah A.
Canniff, Kathleen A.
Carbone, Angelina
Cavanaugh, Mary C.
Chapman, Carol A.
Cormier, Bertha
Crimmings, Anne F.
Daly, Marguerite A.
Dordoni, Joan M.
Epstein, Elinor F.
Galbraith, Joan B.
Gazan, Margaret M.

Geller, Elaine J.
Gordon, Linda S.
Greulach, Vicki E.
Hall, Nancy K.
Hall, Sandra T.
Healy, Sylvia K.
Johnson, Barbara A.
Johnson Judith N.
Kaloyanides, Venetia
Keim, Norma R.
Lannoy, Doris E.
Lepore, Elaine C.
Litchman, Sandra H.
Loeb, Charlotte G.
McEntee, Doris C.

Morneault, Beverly A.
Morneault, Diane M.
Omansky, Betsey G.
Petone, Rosina C.
Pettee, Lorraine M.
Rose, Martha G.
Scalleri, Mary B.
Scanlon, Dorothea C.
Scherr, Marsha H.
Smith, Clare F.
Solomon, Cynthia
Staffiere, Rose Carol
Thomson, Susan M.
Toebes, Rita K.
Vesey, Patricia A.

Technical Typists

Barnes, R. A.
Fleming, Patricia L.

Katan, Ann
Levin, L.
Levine, R. I.

Lombard, Mary C.
Rabkin, W. I.

Stock Rooms

Doiron, E. J., Foreman
Audette, A. G.
Haggerty, R. H.

Joyce, T. F.
Lucas, W. G.
McDermott, J. F.
Masszi, L. N.

Riley, J. F.
Sharib, G.
Sincuk, J., Jr.

Technicians' Shop

Lorden, G. J., Foreman
Calileo, D. W.

DiPietro, P. J.
Fownes, Marilyn R.
Howell, W. B.

Lander, H. J.
MacDonald, K. B.

Tube Laboratory

Staff

Rosebury, F.
Ryan, L. W.

Glass Blowers

DiGiacomo, R. M.
Doucette, W. F.

Technicians

Aucella, Alice A.
Griffin, J. L.
Leach, G. H., Jr.
MacDonald, A. A.

PUBLICATIONS AND REPORTS

MEETING PAPERS PRESENTED

Annual General Meeting, Australian Mathematical Society, Sydney, N.S.W., Australia
August 17, 1962

M. A. Arbib, Monogenic Normal Systems Are Universal

International Symposium on Information Theory, Free University of Brussels, Belgium
September 2-7, 1962

G. L. Gerstein, Mathematical Models for the All-or-None Activity of Some Neurons

M. C. Goodall, Cognition as Two-Way Communication

D. A. Huffman, The Generation of Impulse-Equivalent Pulse Trains

Fourth International Congress on Microwave Tubes, The Hague
September 3-7, 1962

A. Bers, Waves on Electron Beams of High Charge Density

H. A. Haus, Quantum Noise in Linear Amplifiers

ACM 1962 National Conference, Syracuse, New York
September 4-7, 1962

V. H. Yngve, Toward Better Programming Languages (invited)

Symposium on Magnetoplasmadynamic Electrical Power Generation, King's College, University of Durham, Newcastle-on-Tyne, England
September 6-8, 1962

W. D. Jackson and E. S. Pierson, Operating Characteristics of the MHD Induction Generator

American Chemical Society One Hundred Forty-second National Meeting, Atlantic City, New Jersey
September 9-14, 1962

G. G. Hammes and P. Fasella, A Kinetic Study of Glutamic-Aspartic Transaminase

G. G. Hammes and J. L. Steinfeld, Relaxation Spectra of Metal Complexes in Aqueous Solution

International Congress of Surgeons, New York
September 10, 1962

N. Y-S. Kiang, Electrical Responses from the Auditory Nerve Recorded by Means of Gross and Microelectrodes (invited)

MEETING PAPERS PRESENTED (continued)

XXII International Congress of Physiological Sciences, Leiden, The Netherlands

September 10-17, 1962

L. Stark, A Servoanalytic Concept of the Rigidity of Parkinson Syndrome

VIIIth International Conference on Low Temperature Physics, Queen Mary College, University of London, London, England

September 16-22, 1962

M. S. Dresselhaus, D. H. Douglass, Jr., and R. L. Kyhl, Measurement of the Magnetic Field Dependence of the Surface Impedance of Superconducting Tin at X-band

High-Power Microwave Tube Symposium, U. S. Army Signal Research and Development Laboratory, Fort Monmouth, New Jersey

September 25, 1962

L. B. Anderson and A. Bers, A Broadband Megawatt Hollow-Beam Multicavity Klystron

AIEE Fall General Meeting, Chicago, Illinois

October 7-12, 1962

W. D. Jackson, Liquid Metal Faraday-type MHD Generators

National Electronics Conference, Chicago, Illinois

October 10, 1962

I. M. Jacobs, Method and Merit of Binary Coding for Analog Channels (invited)

Fifteenth Gaseous Electronics Conference, Boulder, Colorado

October 10-12, 1962

J. F. Waymouth, The Influence of Ion Temperature on Langmuir Probe Characteristics

Otolaryngology Research Seminar, Massachusetts Eye and Ear Infirmary, Boston, Massachusetts

October 11, 1962

J. S. Barlow, Some Studies on Eye Movements in Relation to Vestibular Mechanisms in Man (invited)

Fortieth Annual Meeting of the New England Section of the American Society for Engineering Education, Dartmouth College, Hanover, New Hampshire

October 13, 1962

M. H. Goldstein, Jr., Chairman and Discussant of the Engineering Life Sciences Session on "The Biomedical Engineer – Does He and Should He Exist?" (invited)

MEETING PAPERS PRESENTED (continued)

AIEE Professional Group on Engineering, Writing, and Speech Meeting, Massachusetts Institute of Technology, Cambridge, Massachusetts

October 24, 1962

V. H. Yngve, Computer Programs for Translation (invited)

Symposium on Pyridoxal Catalysis, Rome, Italy

October 25-31, 1962

G. G. Hammes and P. Fasella, The Mechanism of Enzymatic Transamination

Linguistic Colloquium, Ohio State University, Columbus, Ohio

October 26, 1962

E. S. Klima, Problems in Grammatical Analysis (invited)

Seminar, Computation Laboratory, Princeton University, Princeton, New Jersey

October 29, 1962

M. Eden, Production and Recognition of Handwriting (invited)

Fifteenth Annual Conference on Engineering in Biology and Medicine, Chicago, Illinois

November 5-7, 1962

J. S. Barlow, Analysis of Control of Eye Movements in Man by Means of Autocorrelation and Crosscorrelation (invited)

J. C. Houk, Jr. and L. Stark, An Engineering Model of Motor Coordination in Man (invited)

L. R. Young and L. Stark, Discontinuous Biological Control – The Eye Movement System (invited)

Sixteenth Annual Northeast Electronics Research and Engineering Meeting, Boston, Massachusetts

November 5-7, 1962

J. B. Dennis, Time-Shared Operation of a Small Computer

G. Fiocco, Some Applications of Optical Radar to Astronomy and Geophysics

H. A. Haus and J. A. Mullen, Photon Noise

L. D. Smullin, Strong Beam-Plasma Interactions

Sixty-fourth Meeting, Acoustical Society of America, Seattle, Washington

November 7-10, 1962

D. M. Green, Masking with Two Sinusoids

U. Ingard, Sound Radiation from Perforated and Other Pervious Vibrating Surfaces

MEETING PAPERS PRESENTED (continued)

Lecture, University of Minnesota Medical School, Minneapolis, Minnesota
November 8, 1962

J. S. Barlow, Models of Circadian Rhythms (invited)

Lecture, Cambridge State School and Hospital, Cambridge, Minnesota
November 9, 1962

J. S. Barlow, Studies on Periodic Phenomena in the EEG (invited)

Seminar, Department of Biophysics, Johns Hopkins University Medical School, Baltimore, Maryland
November 12, 1962

N. Y-S. Kiang, Analysis of Responses in Single Auditory Nerve Fibers (invited)

American Rocket Society Meeting, Los Angeles, California
November 13, 1962

L. Stark and L. R. Young, Defining the Human Equation (invited)

First Congress on the Information System Sciences, Hot Springs, Virginia
November 19-21, 1962

R. M. Fano, A Heuristic Discussion of Probabilistic Decoding (invited)

L. Stark, M. Okajima, and G. H. Whipple, Computer Pattern Recognition Techniques; Electro-Cardiographic Diagnosis (invited)

American Physical Society Meeting, Cleveland, Ohio
November 23-24, 1962

T. S. Jaseja, A. Javan, J. Murray, and C. H. Townes, Stability and Resettability of He-Ne Masers

Long Island Chapter IRE Professional Group on Microwave Theory and Techniques Meeting, Long Island City, New York
November 27, 1962

P. Penfield, Jr., Some of the Less Exotic Varactor Applications

Seminar on Theoretical Biology, University of Maryland, College Park, Maryland
November 28, 1962

M. Eden, Generative Models of Biology (invited)

MEETING PAPERS PRESENTED (continued)

Fourth Annual Meeting, Division of Plasma Physics, American Physical Society, Atlantic City, New Jersey

November 28 - December 1, 1962

S. C. Brown, Far Infrared Studies of High-Density Plasmas (invited)

T. H. Dupree, Kinetic Theory of Plasma and Electromagnetic Field

G. Fiocco and E. Thompson, Thomson Scattering of Optical Radiation from an Electron Beam

W. D. Getty, B. Hartenbaum, H. Y. Hsieh, and L. D. Smullin, The Beam-Plasma Discharge

W. G. Homeyer, A. J. Impink, Jr., D. J. Rose, and I. Kaplan, Thermal and Material Problems in a Controlled Fusion Blanket

W. G. Homeyer, I. Kaplan, and D. J. Rose, Tritium Regeneration in a Controlled Fusion Blanket

L. M. Lidsky and D. J. Rose, The Interaction of a Directed Plasma with a Magnetic Mirror

S. D. Rothleder and D. J. Rose, Diffusion of a Finite Cylindrical Plasma in a Magnetic Field

Applied Science and Computation Center Colloquium, Tufts University, Medford, Massachusetts

November 29, 1962

V. H. Yngve, Language Translation by Machine (invited)

JOURNAL ARTICLES ACCEPTED FOR PUBLICATION

(Reprints, if available, may be obtained from the Document Room, 26-327, Research Laboratory of Electronics, Massachusetts Institute of Technology, Cambridge 39, Massachusetts.)

W. P. Allis and S. J. Buchsbaum, Coupling between Electromagnetic and Electron Waves in a Plasma (Nuclear Fusion)

M. Clark, Jr., D. Luce, R. Abrahms, H. Schlossburg, and J. Rome, Results of Preliminary Experiments on the Aural Significance of Segments of Tones of Orchestral Instruments and of Choral Tones (Audio Engr.)

H. Fields, G. Bekefi, and S. C. Brown, Microwave Emission from Non-Maxwellian Plasmas (Phys. Rev.)

O. Fujimura, Analysis of Nasal Consonants (J. Acoust. Soc. Am.)

J. V. Gaven, J. S. Waugh, and W. H. Stockmayer, Self-diffusion and Impurity-Controlled Proton Relaxation in Liquid Methane (J. Chem. Phys.)

G. L. Gerstein, Review of "Electroencephaloscopy" by M. N. Livanov and V. M. Anan (EEG Clin. Neurophysiol.)

F. T. Hambrecht, P. D. Donahue, and R. Melzack, A Multiple-Channel EEG Telemetering System (EEG Clin. Neurophysiol.)

JOURNAL ARTICLES ACCEPTED FOR PUBLICATION (continued)

G. G. Hammes and P. Fasella, A Kinetic Study of Glutamic-Aspartic Transaminase (J. Am. Chem. Soc.)

G. G. Hammes and J. L. Steinfeld, Relaxation Spectra of Some Ni(II) and Co(II) Complexes (J. Am. Chem. Soc.)

U. Ingard and D. S. Wiley, Instabilities of a Liquid Conductor (Phys. Fluids)

T. Ogawa, A Circularly Polarized Maser Oscillator (J. Appl. Phys.)

P. Penfield, Jr., The Minimum Noise of Varactor Amplifiers (Trans. IRE, PGMIL)

H. C. Praddaude, A Perturbation Solution of the Equation of Motion for the Density Matrix (Ann. Phys.)

L. Stark, Biological Rhythms, Noise, and Asymmetry in the Pupil-Retinal Control System (Ann. New York Acad. Sci.)

L. Stark, Environmental Clamping of Biological Systems: Pupil Servomechanisms (J. Opt. Soc. Am.)

L. Stark and H. T. Hermann, Prerequisite for a Photoreceptor Structure in the Crayfish Tail Ganglion (Anat. Record)

L. Stark and H. T. Hermann, Single-Unit Responses in a Primitive Photoreceptor Organ (J. Neurophysiol.)

L. Stark, H. T. Hermann, and P. A. Willis, Instrumentation for Processing Neural Signals (EEG Clin. Neurophysiol.)

L. Stark, M. Okajima, and G. H. Whipple, Computer Pattern Recognition Techniques: Electrocardiographic Diagnosis (Communs. Assoc. Computing Machinery)

L. Stark, R. Payne, and Y. Okabe, On-line Digital Computer for Measurement of a Neurological Control System (Communs. Assoc. Computing Machinery)

L. Stark, L. R. Young, and G. Vossius, Predictive Control of Eye-Tracking Movements (Trans. IRE, PGHFE)

G. W. Stroke and H. H. Stroke, Tandem Use of Gratings and Echelles to Increase Resolution, Luminosity, and Compactness of Spectrometers and Spectrographs (J. Opt. Soc. Am.)

LETTERS TO THE EDITOR ACCEPTED FOR PUBLICATION

P. Penfield, Jr., The Prime-Number Paradox in Multiplier Chains (Proc. IRE)

TECHNICAL REPORTS PUBLISHED

(These and previously published technical reports, if available, may be obtained from the Document Room, 26-327, Research Laboratory of Electronics, Massachusetts Institute of Technology, Cambridge 39, Massachusetts.)

399 Jacob Ziv, Coding and Decoding for Time-Discrete Amplitude-Continuous Memoryless Channels

TECHNICAL REPORTS PUBLISHED (continued)

400 Göran Einarsson, A Communication Analysis of High-Frequency Ionospheric Scattering

402 David Ellis Baldwin, The Effect of Close Collisions on the Two-Body Distribution Function in a Plasma

406 John F. Waymouth, Perturbation of a Plasma by a Probe

407 Ward D. Getty, Investigation of Electron-Beam Interaction with a Beam-Generated Plasma

SPECIAL PUBLICATIONS

G. Bekefi, Emission of Microwaves from Plasmas (Proc. Third Symposium on the Engineering Aspects of Magnetohydrodynamics, Gordon and Breach, Inc., Science Publishers, New York)

F. Bitter, Flows in a Steady Plasma (Lecture to be published by Cornell University Press)

N. Chomsky and M. P. Schützenberger, Algebraic Theory of Context-free Languages (Studies in Logic, North-Holland Publishing Company, Amsterdam, The Netherlands)

J. B. Dennis, Computer Control of an Analog Vocal Tract (Proc. Speech Communication Seminar, Stockholm, Sweden, 30 August - 1 September 1962)

R. C. Gesteland, Odor Specificities of the Frog's Olfactory Receptors (Proc. First International Symposium on Olfaction and Taste, Stockholm, Sweden, September 2-5, 1962)

J. M. Heinz, An Analysis of Speech Spectra in Terms of a Model of Articulation (Proc. Fourth International Congress on Acoustics, Copenhagen, 21-28 August 1962)

A. S. House, A. P. Paul, K. N. Stevens, and Jane B. Arnold, Acoustical Description of Syllabic Nuclei: Data Derived by Automatic Analysis Procedures (Proc. Fourth International Congress on Acoustics, Copenhagen, 21-28 August 1962)

A. S. House and K. N. Stevens, Acoustical Description of Syllabic Nuclei: An Interpretation in Terms of a Dynamic Model of Articulation (Proc. Fourth International Congress on Acoustics, Copenhagen, 21-28 August 1962)

S. Inomata, Program for Active Segmentation and Reduction of Phonetic Parameters (Proc. Fourth International Congress on Acoustics, Copenhagen, 21-28 August 1962)

W. S. McCulloch, The Colloquy of Living Things (Bio-Telemetry, edited by L. E. Slater, The Foundation for Instrumentation Education and Research, Inc., New York)

W. B. Nottingham, The Energy Distribution for Electrons in a Thermionic Diode Plasma Cannot Be Truly Maxwellian

Ionization of Cesium at Surfaces

(Advanced Energy Conversion, Pergamon Press, Oxford, 1962)

V. H. Yngve, Toward Better Programming Languages (Digest of Technical Papers, ACM 1962 National Conference, Syracuse, New York, September 4-7, 1962)

Introduction

This report, the sixty-eighth in a series of quarterly progress reports issued by the Research Laboratory of Electronics, contains a review of the research activities of the Laboratory for the three-month period ending November 30, 1962. Since this is a preliminary report, no results should be considered final.

Following our custom of the past several years, in this issue of January 15, 1963 we preface the report of each research group with a statement of the objectives of the group. These summaries of our aims are presented in an effort to give perspective to the detailed reports of this and ensuing quarters.

RADIO PHYSICS

I. PHYSICAL ELECTRONICS

Prof. W. B. Nottingham
B. L. Blackford
J. L. Coggins
L. E. Sprague

RESEARCH OBJECTIVES

1. Theory of Energy Conversion Electronics

The effectiveness of energy conversion by means of thermionic emission from an emitter depends upon the existence of a suitable difference in work-function between the emitter and the collector. Many aspects of the physics of electronics are involved in this application and need to be examined in considerable detail, with theory compared with experiment. Thermionic converters are, at present, very difficult to make. The application of thermionic-emission theory, gas-discharge theory, and space-charge theory all contribute to a better understanding of the phenomena found in practical converters. It is, therefore, one of our objectives to organize these various branches of physics and relate them to experimental work that is generally carried on in laboratories.

2. Work-Function Determination by the Electron Energy Distribution Method

The maintenance of the collector work-function at a low and controllable value is of prime importance in the design and operation of an efficient thermionic converter. It is not enough to say that the collector work-function should be the absolute minimum attainable because, for particular surface conditions, this minimum might occur only at a relatively high temperature that, in turn, would indicate an excessive thermionic emission from the collector. It is important, therefore, to devise a scheme for determining the collector work-function for selected surfaces, especially single-crystal surfaces, in the presence of cesium.

The experimental method that is being used here involves the production of electron emission from a ribbon filament source. Parallel to this source there will be three conducting surfaces with a single small circular opening in each one, so lined up that electrons collimated by means of a magnetic field will be able to pass through all three of these apertures. This collimated beam of electrons will then impinge on the collector, which is similar in construction to the emitter. The part of the surface that receives the beam will be a single crystal with a selected crystallographic orientation. In order to determine the work-function of the collector by this means, it is necessary to study the current-voltage characteristic in the retarding range to determine the characteristic temperature that describes the electron-energy distribution. This temperature must be the same as that of the emitter for the experiment to be correctly interpreted. If this test proves satisfactory, the work-function of the collector can be determined directly from the knowledge of the current density and the applied voltage. In order to make this study in the temperature range for which an appreciable electron emission from the collector can take place, the center diaphragm of the three can be modulated by the application of a square-wave, cutoff potential, and a sharply tuned amplifier can detect the modulated current in the presence of a considerable background of direct current.

3. Adsorption Properties of Single Crystals of Tungsten before and after Carburization

Experiments with clean tungsten crystals show that different crystallographic orientations adsorb cesium with specific characteristics. Generally speaking, the (110) direction and the (112) direction hold cesium best. This is indicated by the fact that at a given cesium pressure these originally high work-function surfaces become the lowest of all. Experience in the field of thermionic emission from thoriated tungsten has led to the commercialized technique of carburizing the surface layer. After carburization, this layer holds thorium better than it did before. The purpose of this experiment is to find out whether or not surface treatment of tungsten can create a situation in which cesium will hold on to give a suitably low work-function at a very high temperature and not also require an excessive arrival rate of cesium.

Selected tungsten wire can be polished and processed in such a manner as to make long single crystals grow in the wire. These single crystals exhibit all of the available crystal directions that combine as (11x), with x taking on values from zero to infinity. The electron emission is seen on a concentric fluorescent screen. After the crystal is grown and its orientation determined, it can be carburized. Cesium is then admitted and the emission pattern reinvestigated to see to what extent the carburization has influenced the adsorption properties of the single crystal.

4. Cesium Ionization on a Thoriated Filament

Surface ionization of cesium depends on the effective work-function of the surface and its temperature. The total number of ions produced depends also on the arrival rate of cesium. Under most conditions, the work-function itself depends on the cesium arrival rate and temperature and, therefore, it is very difficult to evaluate the influence of the work-function itself. A thoriated tungsten filament can be controlled to have an effective work-function between ~ 3 electron volts and ~ 4.5 electron volts. After having brought about the activation, its temperature can be raised sufficiently high so that practically no cesium atoms stick to the surface if the cesium pressure is not too high, and also no additional thorium activation takes place. It is the purpose of this experiment to try to evaluate qualitatively at least, and quantitatively if possible, the direct influence of the surface work-function on the cesium ion production rate.

5. McLeod Gauge Evaluation

Vacuum technology depends on there being some good standard of pressure measurement as a means of calibration for measuring devices that depend on other phenomena and, in particular, depend on the ionization that takes place in an ion gauge. There has been reason to believe that the McLeod gauge, which depends on the application of Boyle's law, does not always yield results as unambiguous as desired. An experiment is under way to test two McLeod gauges, one against the other, when both are constructed as nearly alike as possible. This comparison will be made with a static system, in contrast to a later comparison that will be made with gas flowing through apertures. The scheme involves the control of gas flow from a high-pressure region to a medium-pressure region and, finally, to a very low-pressure region. One McLeod gauge can be calibrated against another in terms of the areas of the apertures that connect these regions. It is the objective of this research to try to evaluate the influence of capillarity and other disturbances that may make the McLeod gauge inaccurate in unexpected ways.

W. B. Nottingham

A. TEMPERATURE DEPENDENCE OF ELECTRICAL LEAKAGE CAUSED BY CESIUM ON GLASS

Experiments concerned with the measurement of small currents (electron emission, ion emission, and so forth) in the presence of cesium vapor are often harassed by electrical leakage caused by cesium atoms which adsorb on the glass walls and presses of the tube. The adverse effects of this leakage are commonly reduced by raising the glass temperature and by the use of "guard rings." The experiments reported here relate specifically to the quantitative investigation of the effect of glass wall temperature and cesium bath temperature on the leakage resistance.

1. Experimental Arrangement

The experimental tube is sketched in Fig. I-1. Potentials of 0-45 volts are applied across the two electrodes and the corresponding currents measured with a sensitive dc electrometer. The entire tube is contained in a shielded temperature-regulated oven.

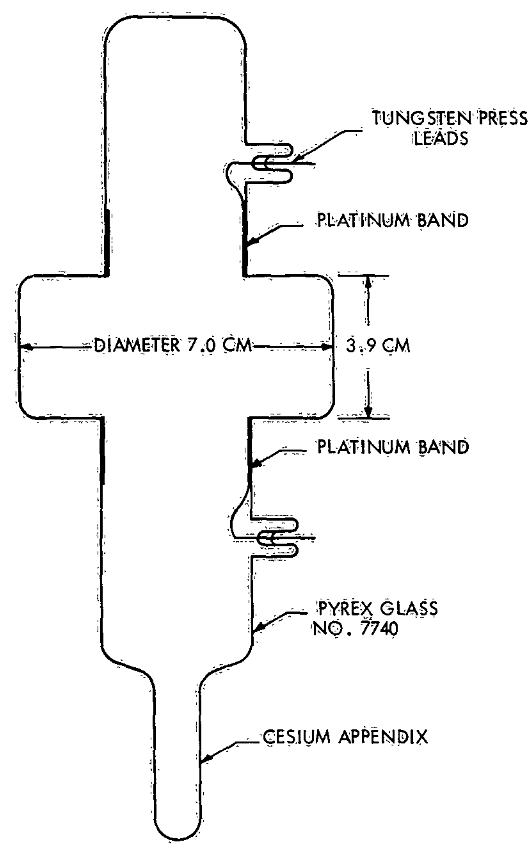

Fig. I-1. Experimental tube.

The cesium appendix is immersed in a water bath whose temperature is regulated independently of the oven. The enlarged section of the tube is equipped with a heating tape powered by direct current to avoid pickup in the electrometer circuitry.

The oven temperature is always maintained higher than that of the cesium bath so that the pressure in the tube is controlled by the bath temperature.

2. Experimental Results

The leakage values are characterized by a quantity ρ_s which denotes the resistance of a square of the cesium covered glass surface. The resistance R of a rectangular shaped surface is given by

$$R = \frac{\rho_s \ell}{d}, \tag{1}$$

where ℓ is the length parallel to the current, and d the length in the perpendicular direction.

Figure I-2 shows ρ_s as a function of the glass temperature T_G at two different values of cesium bath temperature T_{Cs}. It is seen that ρ_s has an exponential dependence on $1/T_G$ for T_G less than 100°C, and that the constant in the exponential is nearly independent of T_{Cs} in the measured temperature range. The decrease of ρ_s at the higher

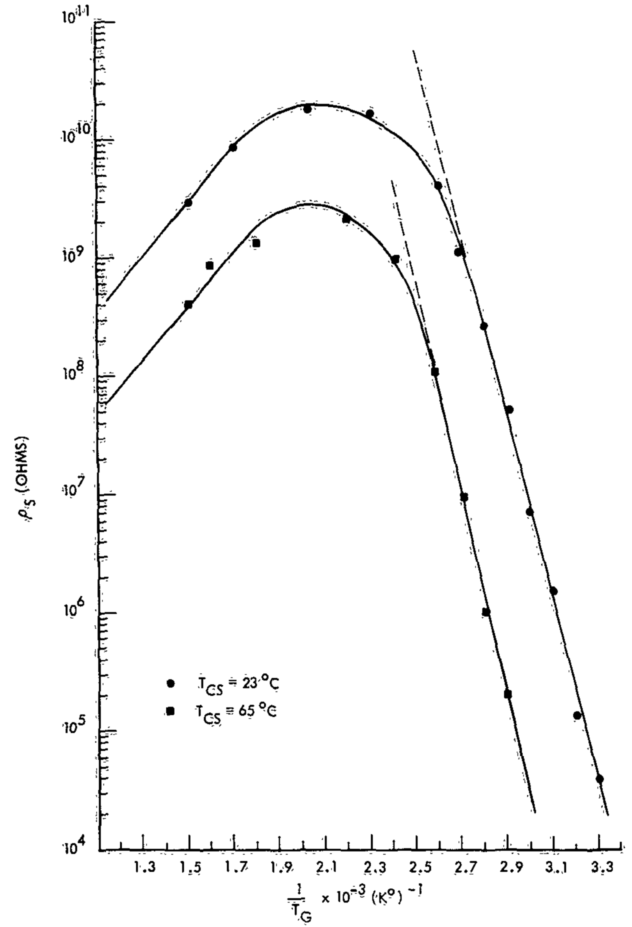

Fig. I-2. Resistance of a square as a function of glass temperature at two values of cesium bath temperature. T_G varies from 30°C to 400°C.

temperatures is caused by leakage through the glass itself rather than across the surface. This statement was verified by measurements made on the bare glass before cesium was admitted into the tube. At the lowest value of T_G and T_{Cs} a waiting period of several hours is required for the leakage current to increase to equilibrium when the glass is free of cesium initially. The fact that both curves do not approach the same value at high temperatures is assumed to be due to a permanent reaction that occurs between the glass and cesium during high-temperature operation. Evidence for this assumption is obtained from an earlier curve taken at $T_{Cs} = 23°C$. It had a maximum value of ρ_s approximately three times greater than the curve for $T_{Cs} = 23°C$ in Fig. I-2. This earlier curve is not reported here because it represents nonequilibrium data at the low values of T_G. The data at $T_{Cs} = 65°C$ were taken after those at $T_{Cs} = 23°C$.

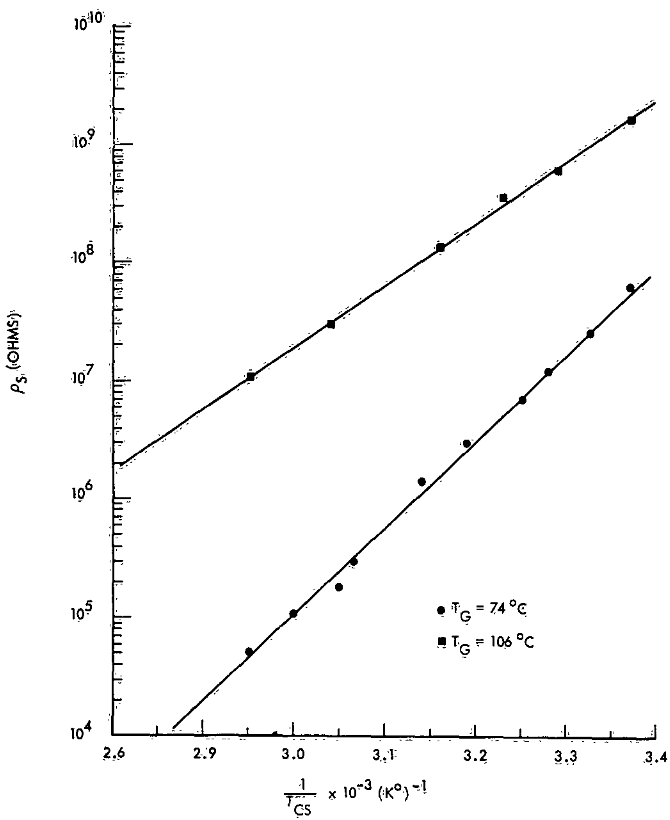

Fig. I-3. Resistance of a square as a function of cesium bath temperature at two values of glass temperature. T_{Cs} varies from 20°C to 65°C.

Figure I-3 shows ρ_s as a function of T_{Cs} at two different values of T_G. Here again

ρ_s depends exponentially on $1/T_{Cs}$ but the slope has a noticeable dependence on T_G. At $T_G = 74°C$, ρ_s is approximately proportional to the square of the cesium vapor pressure; this indicates that ρ_s is strongly dependent on atom arrival rate.

Regarding the amount of cesium present on the glass surface at given values of T_G and T_{Cs}, a simple interpretation of the data gives evidence that the coverage is somewhat less than a monolayer in the temperature ranges of Fig. I-3.

Photocurrents were observed when the tube was subjected to external light. With ordinary room light they are of such magnitude as to mask the leakage current at $T_{Cs} = 23°C$ and T_G above ~ 100°C. This made it necessary to take the data with the tube shielded from all light. Several simple experiments gave evidence that these photocurrents are produced by photoemission of electrons from the cesium-covered glass, particularly in the regions near the electrodes.

3. Summary

The significant results of this report can be conveniently summarized as follows. (a) Useful data relating electrical leakage across cesium-covered glass surfaces to glass temperature and cesium-bath temperature have been obtained for a limited range of temperature. (b) Photocurrents capable of masking leakage currents over a large temperature range were observed.

Further work with ceramic surfaces used is planned. This will allow data to be obtained over a larger temperature range.

B. L. Blackford

II. SOFT X-RAY SPECTROSCOPY

Prof. G. G. Harvey F. H. Byers S. R. Reznek
Prof. K. W. Billman J. B. Lastovka N. K. Winsor

RESEARCH OBJECTIVES

The soft x-ray spectroscopy program has as its objective the experimental study of the structure of the conduction band of electrons in a series of metals, particularly the alkalis, alkaline earths, and some of the transition metals. The filled portion of such a band can be studied by observing the emission spectrum produced by transitions from this band to the nearest available sharp levels below this band. In most metals this corresponds to an energy in the range 15-250 ev (wavelength in the range 50-900 A), so that techniques of extreme ultraviolet vacuum spectroscopy need be applied. The energy widths of these bands usually lie in the range 2-10 ev.

In order to avoid the serious contamination of the metal that is being investigated, which arises in a conventional system, an ultrahigh vacuum (5×10^{-10} Torr) spectrometer has been constructed. Another feature of the device is the elimination of a grating as a dispersion element. This is accomplished through the use of a neutral atomic beam from which photoelectrons are ejected upon soft x-ray bombardment. The photoelectron energies are then analyzed with a low-energy electron spectrometer. This instrument is still under development.

Another objective of the group is to investigate metals in view of recent theoretical advances in the "many-body formulation" of solids. The experimental consequences of this theory should be evident in the volumetric photoelectric effect, in soft x-ray emission and absorption spectra, and in reflection and transmission experiments in this wavelength range.

An experiment performed recently on the volumetric photoelectric effect in nickel was nicely interpreted in view of the plasma oscillations in a metal, which are predicted by this many-body theory. A current effort is to observe plasma radiation from a thin film in which the valence electrons are undergoing collective oscillations. Further experiments along these lines are contemplated. A modification of existing apparatus is being made to allow ultrahigh vacuum conditions to prevail so that data obtained can be interpreted as being due to the metal specimen, rather than to contamination which so often obscures the results in the soft x-ray wavelength region.

G. G. Harvey, K. W. Billman

III. X-RAY DIFFRACTION STUDIES

Prof. B. E. Warren
K. Haruta

RESEARCH OBJECTIVES

We are working on the application of x-ray diffraction methods to the study of problems of interest in solid state physics. Applications of current interest are:

1. The determination of interatomic force constants and frequency distributions in simple structures from a measurement of the temperature diffuse scattering of x-rays.

2. Measurement of long-range and short-range order parameters in binary alloys that show order-disorder changes.

3. Studies of the imperfections that characterize the structures of real materials; in particular, the nature of cold work in a deformed metal. Changes in integrated intensities, peak broadening, and peak shifts are used to measure domain sizes, strains, and faulting. Present emphasis is on the use of ordered alloys such as Cu_3Au in which there are both fundamental and superstructure reflections. The superstructure reflections are much more sensitive to cold work, and give considerably more information than the x-ray reflections from an element.

B. E. Warren

IV. PHYSICAL CHEMISTRY

Prof. C. W. Garland
J. S. Jones

RESEARCH OBJECTIVES

There is a variety of problems in the physics and chemistry of solids in which phonons (lattice vibrations) play an important role. The theory of lattice dynamics can be used to calculate dispersion curves, the vibrational frequency spectrum, and the bulk thermodynamic properties of a crystalline material if appropriate interatomic force constants are known. The adiabatic elastic constants of a single crystal can be measured with high precision by ultrasonic pulse techniques. Such constants provide direct information about the dispersion curves and frequency spectrum at low frequencies, and thus determine the low-temperature thermal properties. They also provide a way of testing or evaluating the force constant parameters in various force models of a solid.

Considerable emphasis has been given to studies of highly anisotropic solids, such as cadmium and zinc, which have nonideal hexagonal close-packed structures. In these cases, data at liquid-helium temperatures determine the harmonic contribution, while the temperature variation is related to anharmonic effects. Recently, attention has been focussed on the elastic properties of crystals near lambda-point transitions. There are "anomalous" changes in the elastic constants of a solid such as NH_4Cl near the critical temperature for an order-disorder transition. The various independent elastic constants of a single crystal behave quite differently in the vicinity of a lambda point, and such differences are related to the detailed structural changes that occur and the nature of the interatomic forces involved.

C. W. Garland

V. BIOPHYSICAL CHEMISTRY*

Prof. G. G. Hammes
Dr. J. J. Burke

RESEARCH OBJECTIVES

In recent years, considerable effort has been expended in the elucidation of biochemical mechanisms by utilizing physical chemical techniques. This project, while we are still making use of general physical chemical techniques, is primarily concerned with kinetic studies of chemical reactions of biochemical interest. Techniques have recently been developed which permit the study of chemical reactions with half times as short as 5×10^{-10} sec.[1] The advantage of being able to carry out kinetic studies over an extended time range is that the entire course of a chemical reaction can be observed. Since reaction intermediates are directly detected, detailed chemical mechanisms can be obtained.

In order to better understand complex biological reactions, the behavior of some simpler model systems is being investigated. This work includes studies of the interactions of metal ions with amino acids, peptides, and polymers in an effort to try and understand the role of metal ions in enzyme catalysis.[2] Also, since macromolecules are of extreme importance in biological systems, chemical processes involving simple polymers, polypeptides, proteins, and polynucleotides are being examined, particularly with regard to possible fast conformational changes.

In addition to model systems, several enzymatic systems are being studied. Fast reaction techniques have already yielded a detailed mechanism for one enzyme system[3] and results for other systems will be available soon. Also, the catalytic role of the macromolecule is being explored.

By coupling kinetic studies with known information about molecular structures, it ultimately should be possible to understand enzymatic mechanisms on a molecular basis.

G. G. Hammes

References

1. G. G. Hammes, Quarterly Progress Report No. 65, Research Laboratory of Electronics, M.I.T., April 15, 1962, p. 5.

2. G. G. Hammes and J. I. Steinfeld, Relaxation spectra of some Ni(II) and Co(II) complexes, J. Am. Chem. Soc. (in press).

3. G. G. Hammes and P. Fasella, A kinetic study of glutamic-aspartic transaminase, J. Am. Chem. Soc. (in press).

*This project is supported in part by the National Institutes of Health (Grant RG-7803).

VI. MICROWAVE SPECTROSCOPY*

Prof. M. W. P. Strandberg
Prof. R. L. Kyhl
J. M. Andrews, Jr.
J. C. Burgiel
Y. H. Chu
D. W. Covington
R. Huibonhoa
J. G. Ingersoll
P. F. Kellen
J. D. Kierstead
S. H. Lerman
J. W. Mayo
Mahin Rahmani
W. J. Schwabe
J. R. Shane
N. Tepley
C. F. Tomes
S. H. Wemple

RESEARCH OBJECTIVES

During the past year, electron paramagnetic resonance studies in solids have concentrated on the interaction processes within the spin system and between the spins and the lattice. A detailed analysis of the line-broadening mechanism and line shape in ruby has been completed and gives a very satisfactory interpretation of experimentally observed line shapes. Spin-lattice relaxation studies have continued; apparatus for generation of coherent microwave phonons has been constructed and is now operating in an understandable fashion. Electron paramagnetic resonance (EPR) techniques were used as a sensitive detection mechanism for recombination studies in gases. An application of a detailed understanding of the physics of electron paramagnetism to microwave maser technology was successfully concluded with the operation of a broadband cavity maser at X-band.

In a different direction, a series of studies of superconductivity in thin films was carried out and the microwave measurement techniques developed for EPR were applied to the measurement of microwave surface impedance of superconductors.

The direction that our work will be taking in the future will include not only further EPR studies but, to an increasing degree, studies on metals and superconductors. The work now in progress on spin-lattice relaxation should confirm our basic understanding of this process and demonstrate the way to obtain meaningful connection between theory and experiment. Our maser work and other recent studies indicate lack of understanding of basic cross-relaxation behavior in dilute paramagnetic systems. We hope to resolve some of these difficulties to allow use of this tool to obtain further physical information.

A major effort will be concentrated on the coherent phonon work, which will be extended for the study of metals and semiconductors because it is such a useful source of information, especially for the metallic state. There is no doubt that information that is useful for understanding the physics of metals is obtainable with electromagnetic radiation in other spectral regions from the soft x-ray region (on which research has been carried out by another group at the Research Laboratory of Electronics; see Section II), through the optical region, to the microwave region. We are now carrying out preliminary experiments on metal plasmas in the optical region using a laser source; this we hope will encourage further effort. The microwave surface impedance studies using our high speed plotter have shown that very useful information is available from surface impedance studies, and we hope to extend this work with improved apparatus and the use of the facilities of the National Magnet Laboratory, especially for the study of the effect of magnetic fields on the surface impedance – monotonic, resonant or oscillatory – of ordinary metals. These studies will require strong support on the theoretical side both in our group and from other groups at M. I. T. and elsewhere. This means that this program is large not only in effort, but also in time scale.

M. W. P. Strandberg, R. L. Kyhl

*This work was supported in part by the U. S. Army Signal Corps under Contract DA36-039-sc-87376; and in part by Purchase Order DDL B-00368 with Lincoln Laboratory, a center for research operated by Massachusetts Institute of Technology with the joint support of the U. S. Army, Navy, and Air Force under Air Force Contract AF19(604)-7400.

VI A. OPTICAL AND INFRARED MASERS

Prof. C. H. Townes
Prof. A. Javan
R. C. Addison, Jr.
R. Y. Chiao
Elsa M. Garmire
T. S. Jaseja
J. H. Parks
M. R. Pearlman
H. Schlossberg
S. R. Stokowski
A. Szoke

RESEARCH OBJECTIVES

This research program on optical and infrared masers is a broad and continuing investigation of the more fundamental aspects of masers and their utilization for physical experiments. The immediate objectives can be described as continuation and completion of a number of experiments launched last year on the applications of masers to spectroscopy and to precision measurements of physical quantities. These include a precise determination of an upper limit to the "ether drift," a modern form of the Michelson and Morley experiment. The spectrum of an optical maser oscillator will be studied further, as will standards of length. For the latter purpose, several new approaches in which an atomic beam is used for the active optical medium will be pursued. We plan to emphasize the generation of a monochromatic source of light in the far infrared, using maser and parametric techniques. The application of such a source of light to far infrared spectroscopy, and of infrared masers to spectroscopic studies, will also be investigated.

C. H. Townes, A. Javan

VII. NUCLEAR MAGNETIC RESONANCE AND HYPERFINE STRUCTURE

Prof. F. Bitter	E. R. Hegblom	H. C. Praddaude
Prof. J. S. Waugh	D. J. Hegyi	O. Redi
Dr. L. C. Bradley III	F. A. Liégeois	C. J. Schuler, Jr.
Dr. H. H. Stroke	R. G. Little	R. W. Simon
Dr. J. F. Waymouth	J. D. Macomber	W. W. Smith
J. C. Chapman	F. Mannis	M. J. Stavn
T. Fohl	P. G. Mennitt	W. J. Tomlinson III
W. D. Halverson	S. R. Miller	W. T. Walter

RESEARCH OBJECTIVES

There are four main objectives in the work of this group: first, the investigation of molecular and solid-state problems by nuclear magnetic-resonance techniques; second, the investigation of the structure of atomic nuclei, particularly of radioactive nuclei, by nuclear magnetic-resonance techniques and by the investigation of atomic hyperfine-structure and isotope shift; third, the development of atomic resonance techniques for the study of resonance radiation; and fourth, the study of the earth's magnetosphere.

1. Nuclear Magnetic Resonance

Our molecular studies by means of nuclear resonance continue to emphasize: (a) the nature of phase transitions, particularly those involving order-disorder phenomena, in solids; (b) intermolecular forces, including their reflection in the transport properties of fluids; and (c) determination of the structures of simple molecules.

J. S. Waugh

2. Hyperfine Structure

Optical pumping and nuclear resonance have been used successfully to achieve new results. The results of our isotope-shift experiments have clarified the causes of the "odd-even staggering" effect observed in atomic spectra of heavy elements. These results show that further systematic study of both isotope and nuclear isomer shifts should provide valuable information on nuclear interactions; in particular, on the polarization of nuclei by nucleons. The theoretical study of the "hyperfine-structure anomaly" and the formalism that we have developed has been used to test explicit assignments of nuclear wave functions. Atomic-beam absorption techniques are being developed and used for precise spectroscopic measurements, as well as for detailed studies of spectral-line profiles. Hyperfine-structure "level crossing" and double-resonance experiments have been carried out with both stable and radioactive atoms. Further work with both types of experiments is expected to yield data on atomic collisions and radiation coherence. An experiment has been performed to test possible parity nonconservation in molecular interactions. This work is being extended to other transitions, and to refining the upper limit on the mixing coefficient of a parity nonconserving state.

L. C. Bradley III, H. H. Stroke, F. Bitter

3. Atomic Resonance Spectroscopy

The detailed analysis of light is becoming increasingly important in such varied fields as atomic and nuclear physics, communication, and astrophysics. In addition to results achieved by spectroscopic instruments that measure wavelengths, the use of magnetically tunable atomic oscillators for measuring frequency distributions offers great promise. In particular, the use of atomic beams in uniform variable magnetic fields promises to become a useful tool for studies of the shape of resonance lines transmitted through radiating and absorbing media.

Also, atoms may be considered as oscillators in which radiofrequencies and optical frequencies are coupled whenever the simultaneous absorption of two such different frequencies involves a common level. Subtle line-narrowing effects resulting from the imprisonment of optical resonance radiation have been detected by using double-resonance techniques. Experimental investigations to determine the relative importance, on the one hand, of interatomic coupling caused by the radiation field, and on the other hand, of the degree of coherence of the light in an absorbing cell should prove to be of value in various investigations.

Work in both of these areas was started some time ago in connection with hyperfine-structure investigations and will now be continued for its own sake.

H. H. Stroke, L. C. Bradley III, F. Bitter

4. The Earth's Magnetosphere

Data obtained from satellites and space probes on the nature of the interplanetary medium are reviving interest in laboratory experiments related to the conditions found in space. We propose to set up models of the earth and its surrounding magnetic field, and to study, first of all, the diffusion of electrons and properties of trapped charges in the surrounding Van Allen belts. The basic condition to be satisfied is that the ratio of the electron cyclotron radius "a",

$$a = \frac{mv}{eB} = \frac{1}{B}\sqrt{\frac{2mV}{e}},$$

have the same ratio to, or should at least be adequately smaller than, the radius of the solid model. If R is the radius of the model, and r the radial distance from the center of the model to any point in space, we have, if the average intensity of magnetization of the spherical dipole is I, the surrounding field in the equatorial plane given by

$$B = \frac{\mu_o}{4\pi}\,\frac{I\left(\frac{4}{3}\pi R^3\right)}{r^3};$$

and therefore the required ratio a/R is

$$\frac{a}{R} = 8\,\frac{\sqrt{V}}{IR}\left(\frac{r}{R}\right)^3.$$

For the earth, we have a magnetic moment 8.2×10^{22} amp-meter^2, $R = 6.4\times10^6$ meters, and an average intensity of magnetization $I = 76$ amp/meter. For the outer edge of the Van Allen belt near the surface of the magnetosphere,

$$\left(\frac{r}{R}\right) = 10$$

$V = 5\times10^4$ electron volts;

and consequently

$$\frac{a}{R} = 8\,\frac{0.71\times10^2}{4.9\times10^8}\times10^3 = 1.2\times10^{-3}.$$

Two spherical dipoles have been designed by Bruce Montgomery of the National Magnet Laboratory. The first is a superconducting coil with an iron core having a magnetic moment 820 amp-m^2 and a diameter of 2". The second is a water-cooled solenoid with an iron core having a magnetic moment 14,000 amp-m^2 and a diameter of 7", requiring 500 kw for its operation. The values of a/R for these dipoles at points distant 10 R from their centers is $3\text{-}4 \times 10^{-2}\sqrt{V}$. These would seem to be adequate models for a convenient range of electron energies. The field of these dipoles at a distance 10 R, or 10" and 35", respectively, would be 20-50 gauss. It would be quite feasible to immerse them in very large coils that produce fields of this order of magnitude to simulate the interplanetary field bounding that of the earth, if it should become desirable for other lines of investigation.

A further requirement of such a model would be that the pressure be made low enough so that electronic mean-free paths would be at least of the order of meters. This indicates operation at pressures below 1 micron, or with an atom density below 10^{13} per cubic centimeter. Insofar as pumping or the production of localized discharges to generate ions and electrons are concerned, this offers no difficulty.

The minimum electron densities required for convenient observations by means of Langmuir probes are of the order of 10^9 per cubic centimeter. This is in a range that would appear to be of interest and practically achievable, at least locally in a large tank. The electronics of the problem is perhaps its most critical aspect. Other approaches for work at very low densities would seem to be desirable.

This program marks the evolution of work on mercury-rare gas discharges, which has been going on for the past two years. The theory of Langmuir-probe measurements in a magnetic field has been developed by J. F. Waymouth.[1] Observations have been made by T. Fohl on the diffusion and thermal conductivity of electrons in a large spherical container with a localized discharge at the center. Magnets for the study of cylindrical plasmas in cusped or uniform longitudinal fields, and in quadrupole or uniform transverse fields are available. It is hoped that these investigations will lead to actual magnetosphere model experiments in the course of the coming year.

F. Bitter, H. H. Stroke

References

1. J. F. Waymouth, Perturbation of a Plasma by a Probe, Technical Report 406, Research Laboratory of Electronics, M.I.T., December 26, 1962.

A. HYPERFINE STRUCTURE AND ISOTOPE SHIFTS IN NEUTRON-DEFICIENT MERCURY ISOTOPES

Production techniques are now under study for the purposes of obtaining Hg^{193} and Hg^{193*} free of Hg^{195} and Hg^{195*} to permit a verification of the preliminary assignment, $I(Hg^{193*}) = 13/2$ and $\mu(Hg^{193*}) \approx \mu(Hg^{195*})$, and to obtain the Hg^{193} spectrum.[1] These results refer solely to the 2537 Å resonance line.

The spectrum of Hg^{194} has been observed over a period of almost one year, in the hope that by comparing its intensity with that of stable Hg^{196}, which was produced simultaneously in the bombardment, we may be able to determine its halflife. At present we are investigating the influence of self-absorption and cleanup on such a determination.

We have also obtained a corrected value for the Hg^{194}-Hg^{196} isotope shift in the 2537 Å line $(0.280 \pm 0.015)\ cm^{-1}$. The result is that $\gamma(195)$ and $\gamma(195^*)$ are even more nearly equal to unity.[2]

W. J. Tomlinson III, H. H. Stroke

References

1. W. J. Tomlinson III and H. H. Stroke, Hyperfine structure and isotope shifts in Hg^{195}, Hg^{195*}, Hg^{194}, and Hg^{193*}, Quarterly Progress Report No. 66, Research Laboratory of Electronics, M.I.T., July 15, 1962, pp. 18-19.

2. W. J. Tomlinson III and H. H. Stroke, Phys. Rev. Letters 8, 436 (1962).

VIII. MICROWAVE ELECTRONICS*

Prof. L. D. Smullin
Prof. H. A. Haus
Prof. A. Bers
R. J. Briggs
P. A. Mandics
A. P. Porter
A. J. Schneider
R. S. Smith

RESEARCH OBJECTIVES

Our group is concerned with theoretical and experimental studies of high-perveance electron beams suitable for interaction with microwave fields.

Experiments on the interaction of a high-density hollow electron beam with fields of klystron-type cavities have been carried out in our laboratory (several reports on this work have appeared in the Quarterly Progress Report). These experiments are being continued and correlated with the theory of gap interaction in such beams. The theory of wave propagation and excitation of electron-beam waveguides is also continuing.

L. D. Smullin, H. A. Haus, A. Bers

*This work is supported in part by Purchase Order DDL B-00368 with Lincoln Laboratory, a center for research operated by Massachusetts Institute of Technology with the joint support of the U.S. Army, Navy, and Air Force under Air Force Contract AF19(604)-7400.

IX. MOLECULAR BEAMS

Prof. J. R. Zacharias
Prof. J. G. King
Prof. C. L. Searle
Dr. G. W. Stroke
R. S. Badessa
V. J. Bates
B. Brabson
R. Golub
G. L. Guttrick
W. D. Johnston, Jr.
S. G. Kukolich
F. J. O'Brien
C. O. Thornburg, Jr.

RESEARCH OBJECTIVES

Three kinds of research are pursued in the molecular beams group:

1. High-precision studies of atomic and molecular radiofrequency spectra, an example being the study of the rotational spectrum of HF.

2. The development and intercomparison of atomic frequency standards. The CS electric resonance studies and the ammonia molecule decelerator are examples. Work is also being done to determine the system properties of a cesium beam tube, and to develop complementary electronics to realize its latent frequency stability. These new clocks and others of different types will be intercompared by using the M. I. T. computer facilities in order to check for possible variations in rate with epoch.

3. Experiments that apply parts of these techniques to interesting problems in any area of physics, as in the following list:

(a) The measurement of the velocity of light in terms of atomic standards,

(b) the search for a charge carried by molecules,

(c) an experiment on an aspect of continuous creation.

These problems are well advanced. In an earlier phase are the following experiments:

(d) the velocity distribution of He atoms from liquid He,

(e) experiments with slow electrons (10^{-6} ev).

J. R. Zacharias, J. G. King, C. L. Searle

A. STARK EFFECT AND HYPERFINE STRUCTURE OF HYDROGEN FLUORIDE

The nuclear hyperfine-structure constants and the electric dipole moment of hydrogen fluoride, H^1F^{19}, in the ground vibration and first excited rotation state have been measured in a molecular beam electric resonance experiment. The hfs constants are

$$c_F = 307.6 \pm 1.5 \text{ kc}$$

$$c_P = -70.6 \pm 1.3 \text{ kc}$$

$$\frac{2}{5}\,\frac{g_P g_F \mu^2_{nm}}{h\langle r^3\rangle} = 57.6 \pm .44 \text{ kc}.$$

The apparatus was calibrated by observing Stark transitions in the ground vibration and first excited rotation state of carbonyl sulfide, $O^{16}C^{12}S^{32}$, and the results were:

$$\frac{\mu_{HF}}{\mu_{OCS}} = 2.554 \pm .0037 \text{ or } \mu_{HF} = 1.8195 \pm .0026 \text{ debye}$$

by using $\mu_{OCS} = 0.7124 \pm .0002$ debye.

An absolute measurement of the OCS electric dipole moment gave

$$\mu_{OCS} = 0.7120 \pm .003 \text{ debye.}$$

A digitally computed solution of the Stark effect with magnetic hyperfine structure was necessary to interpret the data. The theory and experiment are in good agreement over the range of electric field strengths used in the experiment.

The hfs constants are in excellent agreement with the averaged absolute values of these constants as measured in a molecular beam magnetic resonance experiment.[1] The agreement has significance because of discrepancies between the results of the two resonance methods, for some other molecules, in previous experiments.

R. Weiss

References

1. M. R. Baker, M. Nelson, J. A. Leavitt, and N. F. Ramsey, Phys. Rev. 121, 807(1961).

B. CS MASER

The rotational transition ($J = 1 \rightarrow 0$) of CS should provide a more precise molecular frequency standard than other molecular resonances currently used. This transition occurs near 50 kmc.

The principal advantage of using CS, rather than NH_3 or others, is that C^{12} and S^{32} both have zero nuclear moments so there is no spin-spin or spin-rotational interaction.

The permanent dipole moment of CS is rather large (2 debye), so small rf fields are necessary to cause transitions, and small static fields are needed to deflect the beam. The physical construction of the proposed maser would be similar to the original "maser"[2] except that a two-pole deflecting field (state selector) and a two-cavity rf system[3] will be used.

The average lifetime is approximately 30 minutes in an enclosed vessel at room temperature,[4] so the CS must be produced as it is used. Sufficient quantities of CS for a molecular-beam experiment have been produced in our laboratory by dissociation of CS_2 in electrical discharge, and on a hot tungsten wire (2000°C). The resulting vapor is passed through a trap at -100°C, and thus the CS_2 is removed, leaving CS.

S. G. Kukolich

References

1. K. Shimoda, J. Phys. Soc. Japan 12, 1006 (1957).

2. J. P. Gordon, H. J. Zeiger, and C. H. Townes, Phys. Rev. 95, 282 (1954).

3. S. G. Kukolich, Measurements of the 1-1 Inversion Frequency of NH_3 and Experiments with a Two-Cavity Maser, S. B. Thesis, Department of Physics, M.I.T., May 19, 1962.

4. R. C. Mockler and G. R. Bird, Phys. Rev. 98, 1837 (1955).

C. AMMONIA DECELERATION EXPERIMENT

One method of increasing the interaction time of free molecular systems and electromagnetic fields would be to deal with molecules of slow velocity. A linear decelerator designed to provide slow molecules with an intensity that is increased over that predicted by the Boltzmann distribution has been described by Zacharias and King.[1]

The trajectories of ammonia molecules in that device have now been analyzed. We have concluded that the focusing of the last stage was too strong. It is estimated that the transmission of the first 24 stages is greater than $\sim (1/25)$, while the transmission of the last stage is $\sim 10^{-3}$. These estimates make no allowance for possible misalignment of the plates.

Plates with zero focusing have been designed, and the dynamic characteristics of an array of 15 such stages have been studied by using a computer. The duty cycle and bunching characteristics of these stages are not as satisfactory as the parallel plates, but the over-all transmission of the two systems is comparable.

Work is being done, at present, along three lines:

(a) An attempt to improve the characteristics of the nonfocusing plates by considering voltage waveforms other than square waves applied to the plates;

(b) Experiment with a hybrid system consisting of 24 parallel-plate stages and a nonfocusing last stage; and

(c) Consideration of an experiment to demonstrate the principle of deceleration in a limited number (2 or 3) of stages.

R. Golub, B. Brabson

References

1. J. R. Zacharias and J. G. King, Linear decelerator for molecules, Quarterly Progress Report, Research Laboratory of Electronics, M. I. T., January 15, 1958, pp. 56-57.

D. He_3 AND He_4 BEAMS

Initial study has been undertaken on the feasibility of producing and detecting beams of atoms evaporated from the surface of liquid He_3 and He_4 at low temperatures. It is proposed that an "Omegatron" type of radiofrequency mass spectometer[1] be employed as a detector, and such a device has been assembled and operated during the past quarter. A usable sensitivity of ~ 1 ma of ion current per mm Hg for He_4 has been obtained, at a background pressure of 10^{-7} mm Hg in an oil diffusion-pumped system. It is anticipated that this sensitivity is sufficient to permit analysis of beam velocity spectra, and it is hoped that information regarding phenomena in liquid He_3 and He_4 may be gained thereby.

W. D. Johnston, Jr.

References

1. Cf. D. Alpert and R. S. Buritz, J. Appl. Phys. 25, 202 (1954).

E. MEASUREMENT OF THE VEOLCITY OF LIGHT

During the past quarter, all functions of the velocity of light apparatus, electrical, optical, mechanical, for the first time operated simultaneously. The schematic diagram of the apparatus is shown in Fig. IX-1. The figure emphasizes the electronics system

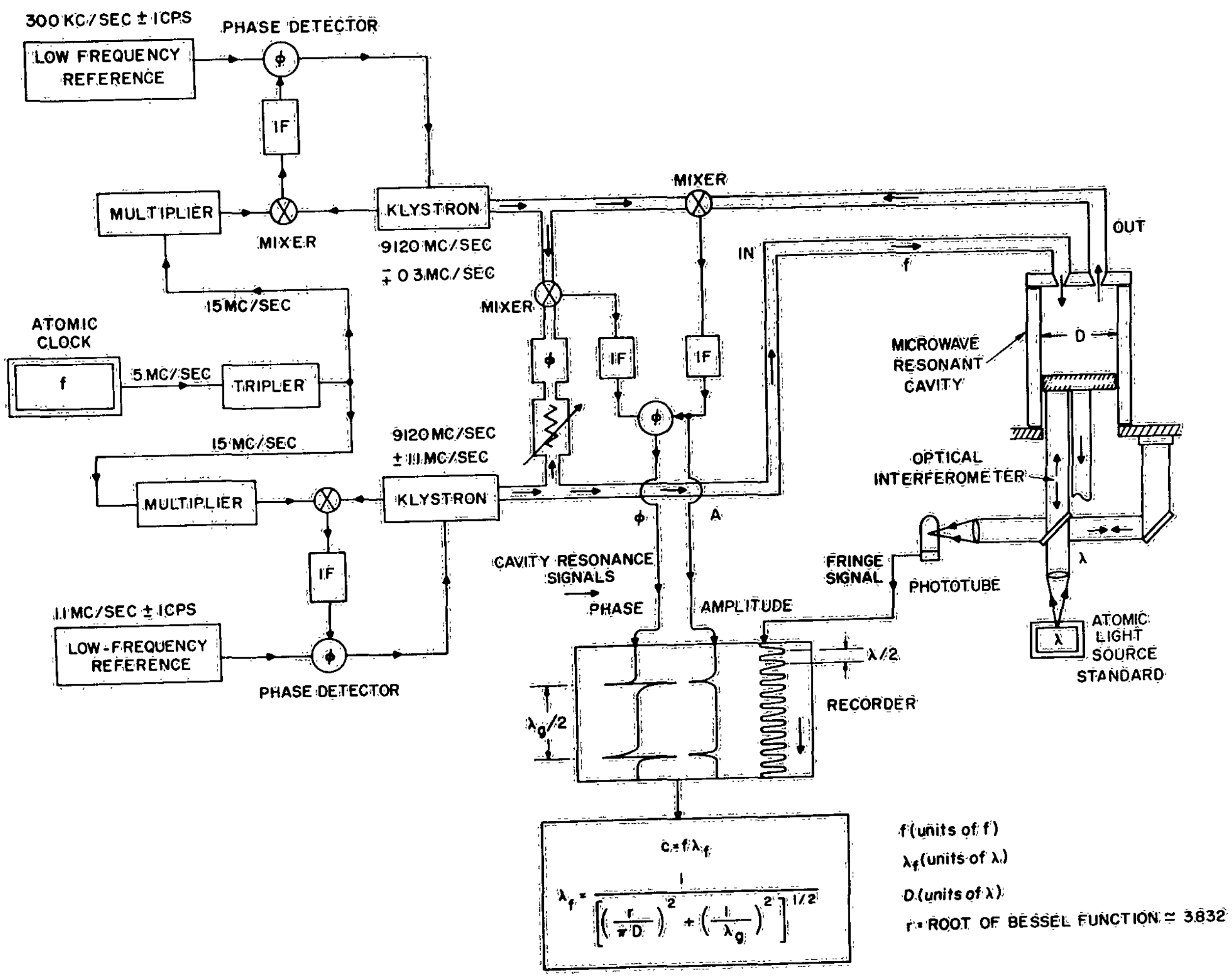

Fig. IX-1. Schematic diagram of velocity-of-light measurement method. The basic equation for the experiment is $c = f\lambda_f$, where λ_f is obtained by measurement of the guide wavelength λ_g in terms of optical interference fringes. Diameter D measurements can be eliminated by measurement of guide wavelengths at two frequences f, both determined with reference to the atomic clock.

because we have already given detailed description of the optical system and the hydraulic drive in previous reports. The system measures the relative phase of the cavity in order to achieve as precise a measurement of λ_g as possible. The signals derived from the microwave and optical systems will be recorded on an FM tape recorder to facilitate data reduction.

We have previously reported that the cylindrical quartz cavity has been optically polished so that its diameter has a precision $\frac{\delta D}{D}$ of approximately $\pm 3 \times 10^{-6}$. Now, from the basic equation

$$\lambda_f = \frac{1}{\left[\left(\frac{r}{\pi D}\right)^2 + \left(\frac{1}{\lambda_g}\right)^2\right]^{1/2}}, \tag{1}$$

which relates the free-space wavelength λ_f to the guide wavelength λ_g, and from the equation

$$c = f\lambda_f, \tag{2}$$

we find that, for the cavity diameter, $D = 161.1$ mm, and the guide wavelength, $\lambda_g \approx 33.88$ mm, used, we have

$$\frac{\partial c}{c} = \left(1 - \frac{6.5}{10^2}\right)\frac{\partial \lambda_g}{\lambda_g} \tag{3}$$

and

$$\frac{\partial c}{c} = \frac{1}{16}\frac{\partial D}{D}, \tag{4}$$

and therefore

$$\frac{\Delta c}{\Delta \lambda_g} \approx 2.25 \frac{\text{km/sec}}{\text{fringe}} \tag{5}$$

and

$$\frac{\Delta c}{\Delta D} \approx \frac{3.2 \text{ km/sec}}{10^2 \text{ fringes}}. \tag{6}$$

In other words, if no diameter corrections at all are made, then the apparatus should yield the value of C within a few parts in 10^7, provided that λg can be measured to within a few parts in 10^7 or approximately 1/100 fringe.

G. W. Stroke, M. A. Yaffee, C. L. Searle,
V. J. Bates, A. T. Funkhouser

X. RADIO ASTRONOMY*

Prof. A. H. Barrett
Prof. J. W. Graham
Prof. R. P. Rafuse
Dr. G. Fiocco
R. J. Allen
A. T. Anderson III
V. J. Bates
J. C. Blinn III
J. A. Bosco
P. J. Brendel
R. K. Breon
J. R. Cummings
G. A. Garosi
J. W. Kuiper
B. R. Kusse
D. H. Staelin
D. H. Steinbrecher
S. Weinreb
C. D. Wende

RESEARCH OBJECTIVES AND SUMMARY

The research areas of this group may be subdivided as follows:

1. The detection and measurement of the radio radiation from extraterrestrial sources, principally at short centimeter and millimeter wavelengths.

2. The application of microwave radiometric techniques to the study of the physical structure of planetary atmospheres, especially the earth's atmosphere.

3. The use of a laser to probe the earth's atmosphere by means of an optical radar, utilizing back scatter from aerosols and molecules.

4. A study of very wide base-line interferometry for radio astronomical measurements.

This program of research requires the development of new techniques in several areas of radiometry. For example, the study of pressure-broadened molecular resonances such as occur in planetary atmospheres dictates the development of a radiometer operating at millimeter wavelengths and having the capability of providing information about line shapes over a frequency interval of several thousands of megacycles. Another example is a result of the need to perform experiments from high-altitude aircraft, balloon-borne platforms, satellites, and space probes, which imposes stringent requirements on equipment design. For purposes of wide base-line interferometry, methods are to be sought by which phase synchronism of local oscillators may be realized and techniques of signal processing and transmission may be utilized to give accurate reproduction of the interference pattern.

In all areas of endeavor listed here, experimental and/or theoretical research and development is under way. During the past year, work has been concentrated in items (1) and (2); items (3) and (4) have recently been initiated. Theoretical studies of the terrestrial H_2O line at $\lambda = 1.35$ cm, and of the microwave spectrum of Venus have been completed. Radiometers operating at K-band, V-band, and E-band have been designed and partially constructed, and preliminary measurements at K-band have been carried out. A 10-ft precision parabolic antenna has been installed on the roof of the Laboratory and is being fitted with a digital control system to allow accurate pointing in celestial coordinates. This facility will be used for lunar and solar research at millimeter wavelengths.

A. H. Barrett, J. W. Graham

A. K-BAND RADIOMETRY

A microwave radiometer operating at 25.5 kmc (λ=1.25 cm) has been constructed and installed in Lincoln Laboratory's 28-ft precision parabolic antenna. The purpose

*This work is supported in part by the National Aeronautics and Space Administration (Contract NaSr-101, Grant NsG-250-62, Grant NsG-264-62); and in part by the U.S. Navy (Office of Naval Research) under Contract Nonr- 3963(02)-Task 2.

of this experiment is twofold:

(i) to provide operational tests of a complete radiometer before it is incorporated into a multichannel system; and

(ii) to observe Venus during the 1962 inferior conjunction.

The frequency was chosen to be compatible with the present antenna feed horn, and to be as near as possible to one of the frequencies of the radiometers aboard the Mariner R-2 Venus spacecraft. Furthermore, by means of a frequency diplexer, measurements are planned simultaneously at 35 kmc (λ=0.8 mm) with a common antenna feed used. The 35-kmc radiometer has been constructed by Lincoln Laboratory personnel. The K-band ground-based measurements are of value because there are no existing measurements of Venusian radiation at this wavelength.

A block diagram of the radiometer is shown in Fig. X-1. The system is a conventional Dicke superheterodyne radiometer employing noise balancing in the antenna input arm. The ferrite switch operates at 94 cps and the bandwidth of the system is 8 mc, as determined by the 30 mc if amplifier. Preliminary tests of the equipment installed on the antenna give an rms temperature fluctuation of approximately 1.2°K with a 5-second integration time.

A multichannel version of this receiver is being built which will incorporate several channel-dropping filters, similar to the diplexer used for frequency separation in

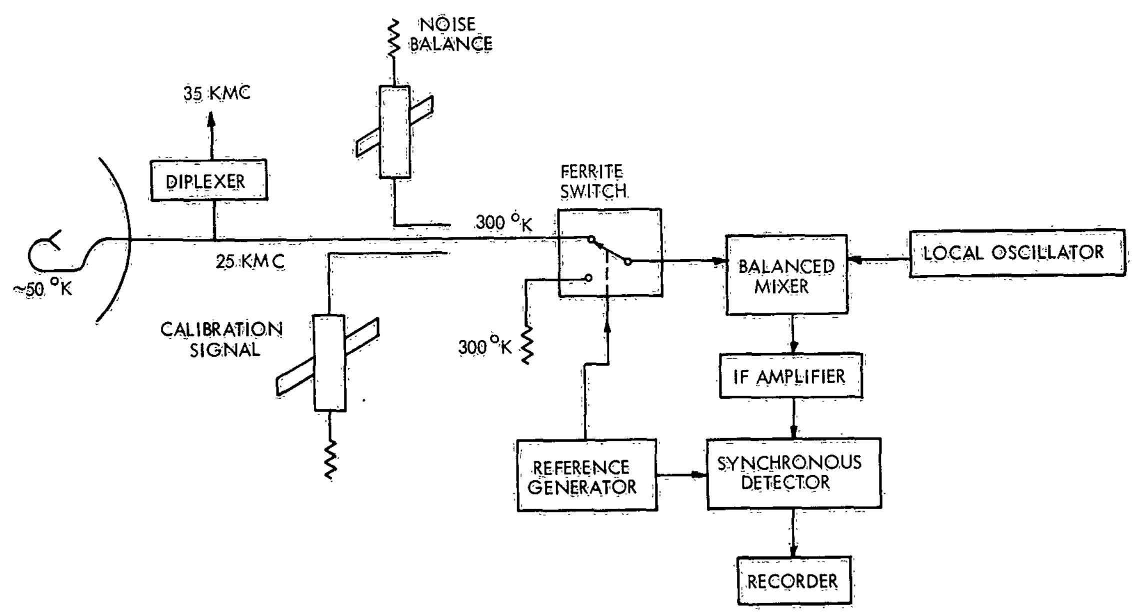

Fig. X-1. K-band radiometer.

Fig. X-1. It is planned to cover the frequency range 18-35 kmc with this arrangement. In addition, a digital synchronous detector for improved long-term stability has been designed and is being tested. The data output will be fed to a tape punch to allow automatic data processing. The completed system will be used for detailed studies of planetary atmospheres.

D. H. Staelin

B. SOLID-STATE LOCAL OSCILLATORS

Two solid-state local oscillators are under development. One will be built to produce 1 mw at 60,152 mc, and the other will produce 2 mw at several frequencies near 22,000 mc (for water-vapor line studies). At present, work is just beginning on the design and synthesis of both chains, and only preliminary design data are available.

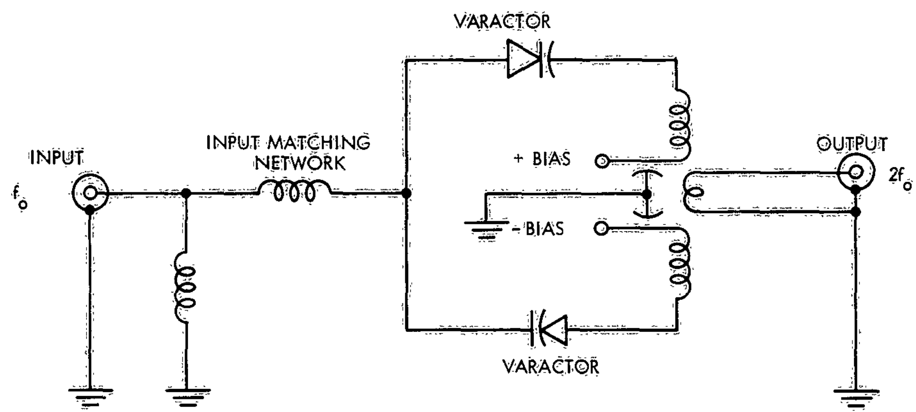

Fig. X-2. Improved doubler circuit.

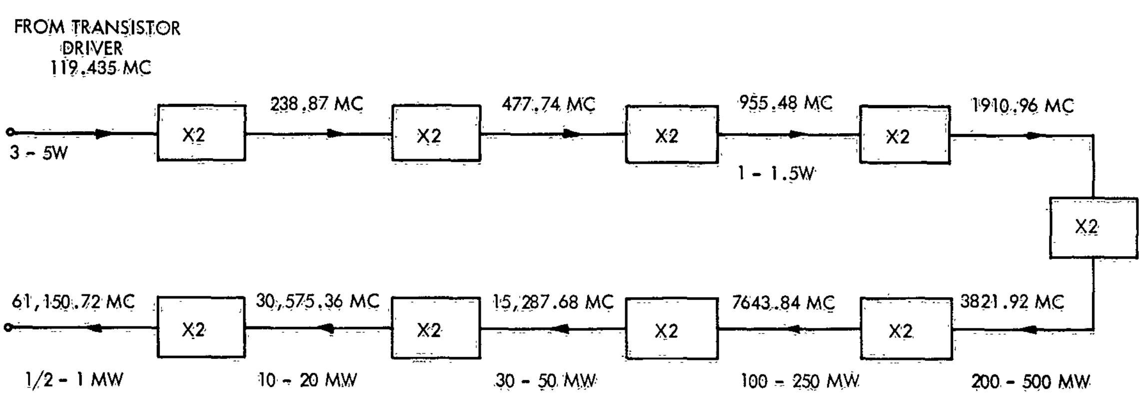

Fig. X-3. 60-Gc chain with expected power levels.

The chain for 60 Gc will be composed of nine doublers starting from 119.435 mc. Designs have been firmed for the first four stages and the last stage. A typical circuit for one of the first four stages is shown in Fig. X-2. This particular circuit is a definite improvement over previous two-diode balanced circuits because it allows the output inductance to be four times larger, and thus facilitates the use of "lumped" circuits at frequencies in excess of 1 Gc. The over-all block diagram is shown in Fig. X-3.

At present, the K-band chain is planned as a string of four doublers to 2200 mc with an output power of 500 mw nominal, followed by a times-ten stage direct to 22 Gc with 2 mw expected output. Considerable attention will have to be paid to spurious signals, and heavy filtering will probably be necessary.

R. P. Rafuse

C. A RELATIONSHIP BETWEEN CURRENT DENSITY $\bar{J}$ AND FAR-ZONE RADIATION FIELDS

An examination of the relation between the source-current distribution and the far-zone electromagnetic field radiated by the current distribution has been made. It has been demonstrated that the curl of the current distribution uniquely determines the far-zone fields. Specifically, it has been shown that $\nabla \times \bar{J}$, where $\bar{J}$ is the current distribution, and the far-zone magnetic field is a three-dimensional, vector, Fourier-transform pair. In the far zone, the magnetic and electric fields uniquely determine one another so that $\nabla \times \bar{J}$ also determines the electric field; in fact, $\nabla \times \nabla \times \bar{J}$ and the far-zone electric field have been shown to be a Fourier-transform pair. The transform variables are position $\bar{p}$ in the radiating current distribution, and direction cosines $\bar{u}$ of the field point measured with respect to a right-hand coordinate system with origin in the radiating body. A proof of the statement that $\nabla \times \bar{J}$ determines the magnetic field follows.

The expression[1] for the magnetic field produced by a current distribution is

$$\bar{H}(\bar{u},\lambda) = \frac{1}{4\pi} \int_V \bar{J} \times (\nabla\phi)\, dv, \tag{1}$$

where

$$\phi = \frac{\exp\left(-j\frac{2\pi r}{\lambda}\right)}{r}.$$

Using the vector identity $\bar{J} \times \nabla\phi = (\nabla \times \bar{J})\phi - \nabla \times (\bar{J}\phi)$, we can rewrite Eq. 1 as

$$\bar{H}(\bar{u},\lambda) = \frac{1}{4\pi} \int_V (\nabla \times \bar{J})\,\phi\, dv - \frac{1}{4\pi} \int_V \nabla \times (\bar{J}\phi)\, dv. \tag{2}$$

The second volume integral can be converted to a surface integral by making use of the known formula

$$\int_V \nabla \times \bar{A}\, dv = \int_S \bar{n} \times \bar{A}\, da,$$

where $\bar{n}$ is the outward directed normal to the surface S bounding the volume V. Equation 2 then becomes

$$\bar{\bar{H}}(\bar{u},\lambda) = \frac{1}{4\pi} \int_V (\nabla \times \bar{J})\, \phi\; dv - \frac{1}{4\pi} \int_S \bar{n} \times (\bar{J}\phi)\; da. \tag{3}$$

If the surface S is taken exterior to the current distribution so that $\bar{J}$ is identically zero on S the surface integral vanishes, and Eq. 3 reduces to

$$\bar{\bar{H}}(\bar{u},\lambda) = \frac{1}{4\pi} \int_V (\nabla \times \bar{J})\, \phi\; dv. \tag{4}$$

Equation 4 is true in all space exterior to the current distribution. We specialize to the far zone and Eq. 4 becomes

$$\bar{\bar{H}}_{FZ}(\bar{u},\lambda) = \frac{\exp\left(-j\frac{2\pi R_1}{\lambda}\right)}{4\pi R_1} \int [\nabla \times \bar{J}(\bar{\bar{\rho}},\lambda)]\, \exp\left(j\frac{2\pi\bar{\bar{\rho}}\cdot\bar{u}}{\lambda}\right) d\bar{\bar{\rho}}, \tag{5}$$

where R_1 is distance to the field point, $\bar{u}$ is a unit vector in the direction of the field point and $d\bar{\bar{\rho}} = dv$; this is clearly a Fourier integral. In the limit $\lambda \to \infty$ the radiation field $\bar{\bar{H}}_{FZ} \to 0$, as it must, since $\int_V \nabla \times \bar{J}\, dv = \int_S \bar{n} \times \bar{J}\, da = 0$ when S is taken exterior to $\bar{J}$.

Equation 5 can be uniquely inverted only if the domain of direction cosines is taken to be infinite. Physically $\bar{u}$ is constrained to the unit sphere, $\|\bar{u}\| = 1$, by the requirement that observation angles be real. It can be shown that inversion of Eq. 5, subject to the unit-sphere constraint yields $\nabla \times \bar{J}$ convolved with the function $(1/\lambda)^3[(\sin 2\pi\|\bar{\rho}\|/\lambda)/(2\pi\|\bar{\rho}\|/\lambda)]$. Hence the physically observable, far-zone magnetic (or electric) field determines a smoothed version of $\nabla \times \bar{J}$.

J. R. Cummings

References

1. J. A. Stratton, Electromagnetic Theory (McGraw-Hill Book Company, Inc., New York, 1941), p. 466.

XI. PHYSICAL ACOUSTICS*

Prof. K. U. Ingard
Dr. L. W. Dean III
A. V. Dralle
S. R. Elms
S. T. Emerson
T. J. Kinzer III
G. C. Maling, Jr.
W. M. Manheimer
H. L. Willke, Jr.
J. M. Witting

RESEARCH OBJECTIVES

In physical acoustics the problems involved concern the emission, propagation, and absorption of sound and vibrations in matter. Specific problems include relaxation phenomena in gases and solids, problems in nonlinear acoustics, and the interaction of sound and turbulence.

In plasma physics our present main interest is in the area of instabilities in plasmas and liquid conductors, and of wave propagation in plasmas.

K. U. Ingard

A. INSTABILITY OF LIQUID CONDUCTORS IN A MAGNETIC FIELD

The study of instability of liquid conductors in a magnetic field has been conducted with an analysis of the experimental results obtained earlier. Some of these results have been mentioned briefly in a previous progress report.[1] The rate of change of the extreme diameter in a pinch instability has been evaluated as a function of the wavelength of the perturbation on the stream for several different values of the current through the stream.

Similarly, the rate of growth of the spiral diameter in an m = 1 type of instability in a longitudinal magnetic field has been determined. This last rate is found empirically to be well described by the expression

$$\beta \approx C\,(IB/\rho d^3)^{1/2}\ \mathrm{sec}^{-1},$$

where I is the current through the stream, B the longitudinal magnetic field, ρ the density, and d the diameter of the liquid conductor. The dimensionless constant C is 4.5. A more detailed account of this investigation will appear in the December issue of The Physics of Fluids.

U. Ingard, D. S. Wiley

References

1. D. S. Wiley and U. Ingard, Bifurcation instability of a liquid conductor in an axial magnetic field, Quarterly Progress Report No. 63, Research Laboratory of Electronics, M.I.T., October 15, 1961, p. 133.

*This work was supported in part by the U.S. Navy (Office of Naval Research) under Contract Nonr-1841(42).

B. SOUND PROPAGATION OVER A PLANE BOUNDARY

The analysis of the influence of turbulence on sound propagated over a plane boundary has been completed. The new analysis of the problem differs from that presented in Quarterly Progress Report No. 55 (pages 141-149) in two respects. First, both amplitude and phase fluctuations have been included in the calculations; and, second, the amplitude and phase fluctuations are assumed to be normally distributed. The experimental results discussed in Quarterly Progress Report No. 66 (pages 69-70) have been

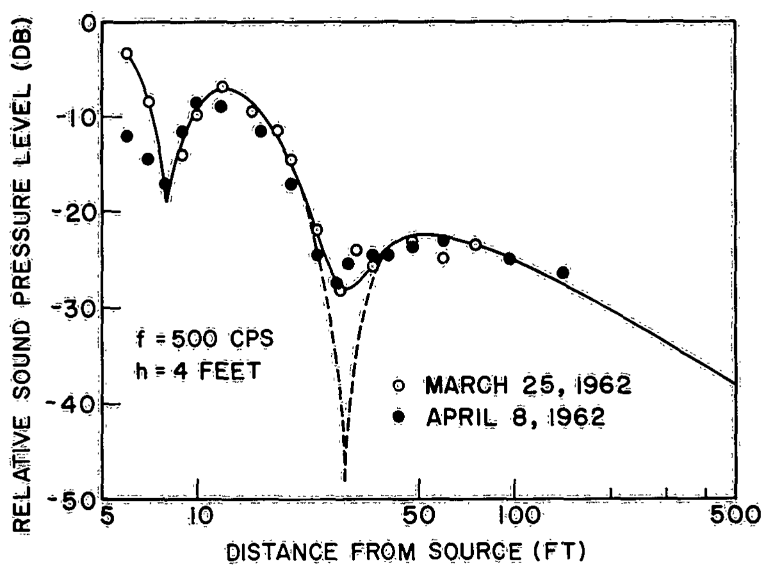

Fig. XI-1. Mean-square sound-pressure level in a turbulent atmosphere over a plane reflecting boundary as a function of distance from the source (frequency, 500 cps). Dashed curve refers to the calculated distribution in a homogeneous atmosphere; solid curve, the calculated distribution for a turbulent atmosphere.

analyzed in detail, and the fractional standard deviation of the mean-square pressure fluctuations (Std. Dev./p^2_{rms}) has been calculated as a function of distance from the source, and compared with the analysis that follows.

If it is assumed that both the amplitude fluctuations (a) and phase fluctuations (δ) are normally distributed, with variance given by

$$\sigma^2 = \langle\delta^2\rangle = \frac{\sqrt{\pi}}{2}\mu_o^2(k_ox)(k_oL)\left(1+\frac{\sqrt{x^2+4h^2}}{x}\right)$$

$$\langle(\ln(1+a))^2\rangle = \frac{\sqrt{\pi}}{2}\mu_o^2(k_ox)(k_oL),$$

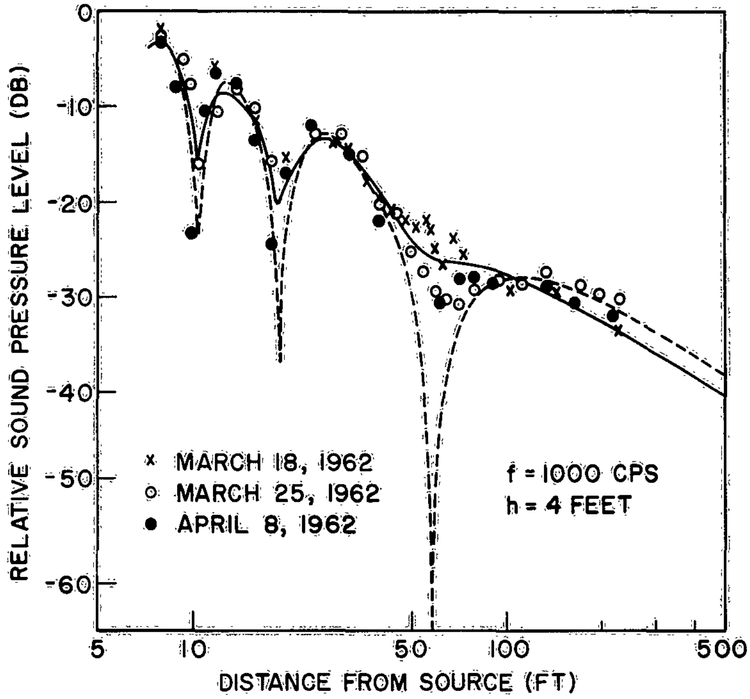

Fig. XI-2. Mean-square sound-pressure level in a turbulent atmosphere over a plane reflecting boundary as a function of distance from the source (frequency, 1000 cps). Dashed curve refers to the calculated distribution in a homogeneous atmosphere; solid curve, the calculated distribution for a turbulent atmosphere.

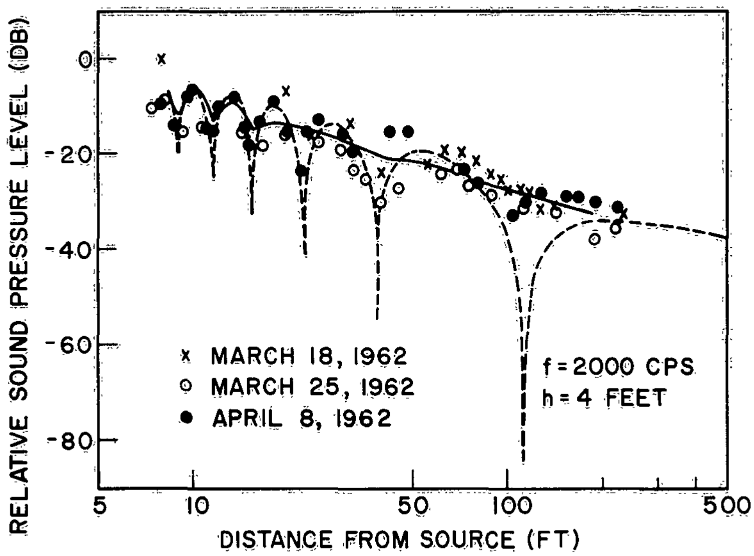

Fig. XI-3. Mean-square sound-pressure level in a turbulent atmosphere over a plane reflecting boundary as a function of distance from the source (frequency, 2000 cps). Dashed curve refers to the calculated distribution in a homogeneous atmosphere; solid curve, the calculated distribution for a turbulent atmosphere.

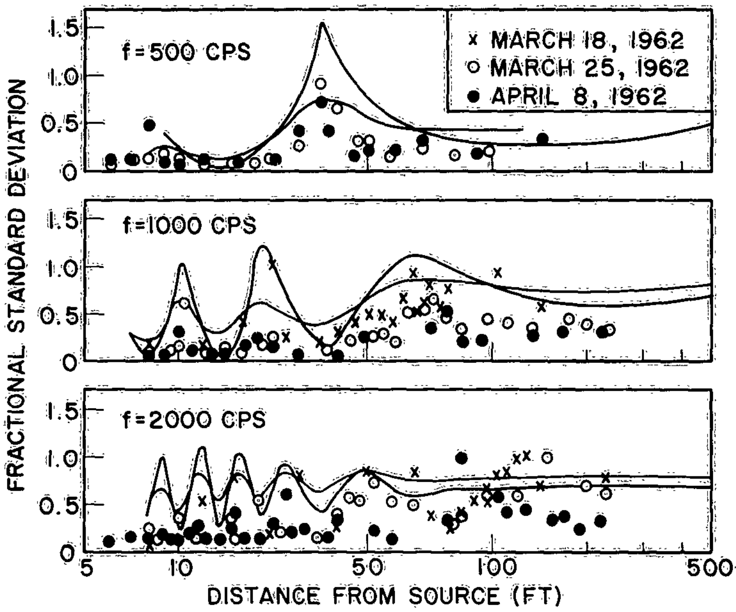

Fig. XI-4. Measured and calculated fluctuations of the sound-pressure amplitude as a function of distance from the source.

then it can be shown that the mean-square sound-pressure level as a function of distance from the source is given approximately by

$$m = \langle \overline{p^2} \rangle \doteq \frac{1}{xr}\left(\langle a^2 \rangle + \frac{r}{2x}\left(1 - \frac{x}{r}\right)^2 + \left(1 + \cos\beta_0 e^{-\sigma^2/2}\right)\right),$$

and the variance of the fluctuations in mean-square pressure, $V = \langle (\overline{p^2})^2 \rangle - \langle (\overline{p^2}) \rangle^2$, may be approximated as

$$V = \frac{1}{2}\left(1 + 2\langle a^2 \rangle\right)\left(1 - e^{-\sigma^2}\right)\left(1 - e^{-\sigma^2} \cos 2\beta_0\right) + 2\langle a^2 \rangle\left(1 + \cos\beta_0 e^{-\sigma^2/2}\right).$$

If the value of the parameter $\mu_0^2 L$ is chosen so that the calculated value of m is in good agreement with experiment at 500 cps, and $x = 28.5$ ft, the correlation at other frequencies and at other distances is as illustrated in Figs. XI-1, XI-2, and XI-3. The dashed curves are the calculated sound pressures for a quiescent atmosphere. Plots of $\sqrt{V/m}$ vs distance are presented in Fig. XI-4. The sharply peaked curves were calculated under the assumption that amplitude fluctuations could be neglected. It is seen that somewhat better agreement with experiment can be obtained if the effect of amplitude fluctuations is included.

U. Ingard, G. C. Maling, Jr.

References

1. L. A. Chernov, Wave Propagation in a Random Medium (McGraw-Hill Book Company, Inc., New York, 1961).

C. STABILITY OF PARALLEL FLOWS

1. Introduction

If $(0, 0, W(x_1))$ is a parallel flow solution for the Navier-Stokes equations and $(u_1(\bar{x}, 0), u_2(\bar{x}, 0), W(x_1) + u_3(\bar{x}, 0))$ represents an infinitesimally disturbed flow condition at $t = 0$, then the disturbed system will evolve according to

$$\frac{\partial u_i}{\partial t} = \nu\nabla^2 u_i - W\frac{\partial u_i}{\partial x_3} - \frac{\partial p}{\partial x_i'} - \delta_{i3}\frac{dW}{dx_1}u_1 \tag{1a}$$

$$\frac{\partial u_i}{\partial x_i} = 0 \tag{1b}$$

with nonlinear terms neglected.

Taking the divergence of (1a), and using (1b), we find that

$$\nabla^2 p = -2\frac{dW}{dx_1}\frac{\partial u_1}{\partial x_3}, \tag{1c}$$

so that, with proper boundary conditions, p can be expressed in terms of the u_i and eliminated from (1a). In fact, taking ∇^2 in the first of Eqs. 1a and substituting $\nabla^2 p$ from (1c), we have

$$\frac{\partial}{\partial t}\nabla^2 u_1 = \nu\nabla^4 u_1 - W\frac{\partial}{\partial x_3}\nabla^2 u_1 + \frac{d^2W}{dx_1^2}\frac{\partial u_1}{\partial x_3}. \tag{2}$$

We have used the fact that W is, at most, quadratic in x_1.

The case $u_i(\bar{x}, t) = e^{\lambda t}u_i(\bar{x})$ has been studied extensively,[1] since for this case the stability analysis reduces to the (difficult) problem of discovering whether (2) has solutions for u_1 with Re $(\lambda) \geq 0$. For many cases of interest, however, there exist no solutions, or only a restricted class of solutions of this simple type, so that the results under such an assumption are not entirely conclusive. We shall discuss a weak instability, not of exponential type, which is common to all inviscid parallel flows.

2. A Weak Instability

The equations of motion (1) and (2) are homogeneous in x_3, so that the u_i will remain independent of x_3 if they are so at $t = 0$. We consider, first, the case $\nu = 0$, for which (1) becomes

$$\frac{\partial u_1}{\partial t} = -\frac{\partial p}{\partial x_1} \tag{3a}$$

$$\frac{\partial u_2}{\partial t} = -\frac{\partial p}{\partial x_2} \tag{3b}$$

$$\frac{\partial u_3}{\partial t} = -\frac{dW(x_1, x_2)}{dx_1} u_1 \quad \frac{dW(x_1, x_2)}{dx_2} u_2 \tag{3c}$$

$$\frac{\partial u_1}{\partial x_1} + \frac{\partial u_2}{\partial x_2} = 0, \tag{3d}$$

in which we now permit W to depend on x_2, as well as on x_1. We suppose that the flow is contained by a boundary $b(x_1, x_2)$, so that the component of u normal to B must vanish along B.

According to (3), $\partial^2 p/\partial x_1^2 + \partial^2 p/\partial x_2^2 = 0$, and the normal derivative of p vanishes at B. The only harmonic function satisfying the boundary conditions (and finite everywhere, if B is not closed) is $p = \text{constant}$. According to (3a) and (3b), then, u_1 and u_2 are time-independent. Equation 3c can be immediately integrated to give

$$u_3(\bar{x}, t) = u_3(\bar{x}, 0) - t\left[\frac{dW}{dx_1} u_1(\bar{x}) + \frac{dW}{dx_2} u_2(\bar{x})\right]. \tag{4}$$

This simple linear analysis thus yields a weak instability, linear in time, which is common to all inhomogeneous inviscid parallel flows. The instability arises from a mixing of parallel streamlines of varied flow strengths by a weak persistent convective motion.

We should expect that in an exact analysis u_3 should grow at first according to (4), and then flatten out or turn back when $u_3 \ll W$ ceases to be valid. We can indeed construct exact solutions of the Navier-Stokes equations which exhibit this behavior. In an exact analysis (4) becomes

$$\left.\begin{aligned} &\frac{\partial u_i}{\partial t} = -u_1 \frac{\partial u_i}{\partial x_1} - u_2 \frac{\partial u_i}{\partial x_2} - \frac{\partial p}{\partial x_1} \\ &u_n\big|_B = 0 \qquad\qquad \frac{\partial u_i}{dx_i} = 0 \end{aligned}\right\} \quad i = 1, 2 \tag{5a}$$

$$\left.\begin{aligned} &\frac{\partial u_3}{\partial t} = -\left[u_1 \frac{\partial}{dx_1} + u_2 \frac{\partial}{\partial x_2} \ u_3\right] \\ &u_3(\vec{x}, t=0) = W(x_1, x_2) \end{aligned}\right\} \tag{5b}$$

Equations 5a are the two-dimensional Navier-Stokes equations, which admit of time-stationary vortical motions $(u_1(\vec{x}), u_2(\vec{x}))$. Equation 5b simply expresses the continuity of $u_3(x_1, x_2)$ in the two-dimensional convective field (u_1, u_2). For small t, u_3 clearly evolves according to (4).

The second case, $\nu \neq 0$, is less transparent, and we consider only plane parallel flow between parallel plates at $x = (\pm\pi)$. Equation 2 in this case reduces to

$$\begin{aligned} &\frac{d}{dt} \nabla^2 u_1 = \nu \nabla^4 u_1 \\ &\frac{du_1}{dx_1}(\pm\pi) = u_1(\pm\pi) = 0. \end{aligned} \tag{6}$$

Equation 6 can also be written

$$\begin{aligned} &\frac{d}{dt} w = \nu \nabla^2 w \\ &w(\pm\pi) = f(\pm\pi) \\ &\frac{dw}{dx}(\pm\pi) = \frac{df}{dx}(\pm\pi), \end{aligned} \tag{7}$$

where $f = f(x_1 x_2 t)$, and $\nabla^2 f = 0$, so that $u_1 = w - f$ clearly satisfies (1). We expand

$u_1 = \int_{-\infty}^{\infty} \int_C \tilde{u}_1\left(x_1, k_2, \lambda^{(o)}\right) \exp(\lambda^{(o)} t) \exp(ik_2 x_2)\, d\lambda^{(o)} dk_2$, etc., so that (2) becomes

$$\begin{aligned} &\lambda^{(o)} \tilde{w} = \nu \left(\frac{d^2}{dx_1^2} - k_2^2\right) \tilde{w} \\ &\frac{d\tilde{w}}{dx}(\pm\pi) = \frac{d\tilde{f}}{dx}(\pm\pi) \\ &\tilde{w}(\pm\pi) = \tilde{f}(\pm\pi). \end{aligned} \tag{8a}$$

Here, $\left(\frac{d^2}{dx_1^2} - k_2^2\right) \tilde{f} = 0$, so that $\tilde{f} = a \cosh k_2 x_1 + b \sinh k_2 x_1$, $k_2 \neq 0$.

With $\lambda = \frac{\lambda^{(o)}}{\nu} + k_2^2$, we have

$$\lambda\tilde{w} = \frac{d^2}{dx_1^2}\tilde{w}. \tag{8b}$$

Note that if $\tilde{w}_\lambda(x)$ is a solution of (8a) for some (λ, a, b), then $\tilde{w}_\lambda(-x)$ will be a solution for $(\lambda, a, -b)$. It follows that the even and odd parts of $\tilde{w}_\lambda$ separately will be solutions for $(\lambda, a, 0)$ and $(\lambda, 0, b)$, respectively. Thus we seek $\tilde{w}^{(e)}$ even, and $\tilde{w}^{(o)}$odd, satisfying

$$\begin{aligned} & w^{(e)}(\pm\pi) = a \cosh k_2\pi \\ & \frac{dw^{(e)}(\pm\pi)}{dx} = \pm k_2 a \sinh k_2\pi \\ & w^{(o)}(\pm\pi) = \pm b \sinh k_2\pi \\ & \frac{dw^{(o)}(\pm\pi)}{dx} = k_2 b \cosh k_2\pi \\ & \lambda w = \frac{d^2}{dx_1^2} w \end{aligned} \tag{9a}$$

or, more concisely,

$$\frac{1}{w^{(e)}}\frac{dw^{(e)}}{dx}(\pm\pi) = \pm k_2 \tanh k_2\pi$$

and (9b)

$$\frac{1}{w^{(o)}}\frac{dw^{(o)}}{dx}(\pm\pi) = \pm k_2 \coth k_2\pi.$$

With the given boundary conditions, we have

$$\begin{aligned} \left(\frac{d^2u}{dx_1^2}, v\right) &= \int_{-\pi}^{\pi} \frac{d^2u}{dx_1^2}\bar{v}\, dx_1 = \frac{du}{dx_1}\bar{v}\Big|_{-\pi}^{\pi} - \int_{-\pi}^{\pi} \frac{du}{dx_1}\frac{d\bar{v}}{dx_1}\, dx_1 \\ &= \frac{du}{dx_1}\bar{v}\Big|_{-\pi}^{\pi} - u\frac{d\bar{v}}{dx_1}\Big|_{-\pi}^{\pi} + \int_{-\pi}^{\pi} u\frac{d^2\bar{v}}{dx_1^2}\, dx_1 \\ &= u\bar{v}\left(\frac{1}{u}\frac{du}{dx_1} - \overline{\frac{1}{v}\frac{dv}{dx_1}}\right)\Big|_{-\pi}^{\pi} + \left(u, \frac{d^2v}{dx_1^2}\right). \end{aligned} \tag{10}$$

The conditions (9b) ensure the vanishing of the iterated term in (10).

The system is thus a regular self-adjoint one, so that the eigenfunctions of (9a) will be complete for the purposes of expansion. Even solutions of (9a) have the form

$$w^{(e)} = A \cosh \sqrt{\lambda}\, x_1$$

for which λ must be chosen so that (11)

$$\frac{1}{w^{(e)}} \frac{dw^{(e)}}{dx}(\pi) = \sqrt{\lambda} \tanh \sqrt{\lambda}\, \pi = k_2 \tanh k_2\pi.$$

The only solution with $\lambda \geq 0$ is $w^{(e)} = A \cosh k_2x_1$, for $\lambda = k_2^2$. In case $\lambda < 0$, we write $\sqrt{\lambda} \tanh \pi\sqrt{\lambda} = -p \tan p\pi = k_2 \tanh k_2\pi$, so that p is real, $(-p^2=\lambda)$. We get eigenvalues p_n with $n - \frac{1}{2} < p_n < n$, $n = 1, 2 \ldots$, so that $\lambda_n = -p_n^2$ and $\lambda_n^{(o)} = -\nu\left(p_n^2+k_2^2\right)$. The only odd solution of (9a) with $\lambda \geq 0$ is $w_o^{(o)} = A \sinh k_2x_1$, for $\lambda = k_2^2$.

For $\lambda < 0$, we set $\lambda = -q^2$ and write

$$w^{(o)} = B \sin qx_1, \tag{12}$$

where

$$\frac{1}{w^{(o)}} \frac{dw^{(o)}}{dx}(\pi) = q \cot q\pi = k_2 \coth k_2\pi,$$

or

$$\tan q\pi = \frac{q}{k_2} \tanh k_2\pi.$$

We get eigenvalues q_n with $n < q_n < n + \frac{1}{2}$, $n = 1, 2 \ldots$, ($q_n = 0$ is spurious). Thus we have solutions

$$\begin{aligned} u_1^{(e)}(x_1k_2p_n) &\propto \frac{\cos p_nx_1}{\cos p_n\pi} - \frac{\cosh k_2x_1}{\cosh k_2\pi} \qquad & \lambda_n^{(o)} &= -\nu\left(p_n^2+k_2^2\right) \\ u_1^{(o)}(x_1k_2q_n) &\propto \frac{\sin q_nx_1}{\sin q_n\pi} - \frac{\sinh k_2x_1}{\sinh k_2\pi} \qquad & \lambda_n^{(o)} &= -\nu\left(q_n^2+k_2^2\right) \end{aligned} \tag{13}$$

Finally, if $u_1(x_1, x_2, 0)$ is any perturbation that is continuous and piecewise smooth in x_1 and x_2, satisfies the boundary conditions on x_1, and $\in L_1(X_2)$, we obtain

$$\begin{aligned} u_1(x_1x_2t) = &\int_{-\infty}^{\infty} \sum_{p_n(k_2)} \exp\left[-\nu\left(p_n^2+k_2^2\right)t\right] u_1^{(e)}(p_n,k_2) \left[\frac{\cos p_nx_1}{\cos p_n\pi} - \frac{\cosh k_2x_1}{\cosh k_2\pi}\right] \cdot \exp(ik_2x_2)\, dk_2 \\ &+ \int_{-\infty}^{\infty} \sum_{q_n(k_2)} \exp\left[-\nu\left(q_n^2+k_2^2\right)t\right] u_1^{(o)}(q_n,k_2) \left[\frac{\sin q_nx_1}{\sin q_2\pi} - \frac{\sinh k_2x_1}{\sinh k_2\pi}\right] \cdot \exp(ik_2x_2)\, dk_2. \end{aligned} \tag{14a}$$

Here,

$$u_1^{(e)}(p_u, k_2) = \frac{1}{2\pi}\int_{-\infty}^{\infty} \exp(-ik_2x_2)\,\frac{\int_{-\pi}^{\pi} u_1(x_1x_2, o)\cos p_nx_1\,dx_1}{\cos p_n\pi\left(\pi + \dfrac{\sin 2p_n\pi}{2p_n}\right)}\,dx_2$$

$$u_1^{(o)}(q_n, k_2) = \frac{1}{2\pi}\int_{-\infty}^{\infty} \exp(-ik_2x_2)\,\frac{\int_{-\pi}^{\pi} u(x_1, x_2, o)\sin q_nx_1\,dx_1}{\sin q_nx_1\left(\pi - \dfrac{\sin 2q_n\pi}{2q_n}\right)}\,dx_2. \tag{14b}$$

This expansion is of a type that is well known from the theory of heat conduction, and is shown to converge uniformly for all x_1 and $t \geq t_o$ $(t_o > 0)$ and thus to satisfy the boundary conditions for all $t > 0$, and to converge to the series expansion for $u_1(x_1, x_2, 0)$ for $t \to 0$. This solution is unique under the given conditions.

If $u_1(x_1, x_2, 0)$ is taken to be periodic in x_2 instead of being $\in L_1(X_2)$, the solution above remains valid if we replace the integrals in (14a) by summations on k_2, and the symbols $\frac{1}{2\pi}\int_{-\infty}^{\infty}$ in (14b) by $\frac{1}{2L}\int_{-L}^{L}$.

To complete the problem, we compute u_3. According to (1a),

$$\frac{\partial u_3}{\partial t} = \nu\nabla^2 u_3 - W'u_1 \qquad u_3\Big|_{x_1=\pm\pi} = 0, \tag{15}$$

where $W' = \frac{dW}{dx_1} = \frac{d}{dx_1}(V_o+V_1x+V_2x^2)$.

Equation 15 is the inhomogeneous heat equation in two dimensions. If u_3 and u_1 are continuous, piecewise smooth and periodic in x_2 of period $2L$, we have the unique uniformly convergent series expansion

$$u_3(x_1, x_2, t) = \sum_{\substack{k_2=\pm\frac{\pi}{L}, \pm\frac{2\pi}{L}\dots \\ n=1,2,\dots}} \exp\left(-\nu\left[k_2^2+\left(n+\tfrac{1}{2}\right)^2\right]t\right)\cos\left(n+\tfrac{1}{2}\right)x_1$$

$$\cdot\left\{f_{k_2n}^e - \int_0^t \exp\left(\nu\left[k_2^2+\left(n+\tfrac{1}{2}\right)^2\right]s\right) g_{k_2n}^e(s)\,ds\right\} e^{ik_2x_2}$$

$$+ \sum_{k_2, n} \exp\left(-\nu[k_2^2+n^2]t\right)\sin nx_1$$

$$\cdot\left\{f^{o}_{k_2n} - \int_0^t \exp\left(\nu\left[k_2^2+n^2\right]s\right) g^{o}_{k_2n}(s)\, ds\right\} e^{ik_2x_2}. \tag{16a}$$

Here,

$$f^{(e)}_{k_2n} = \frac{1}{2\pi L}\int_{-L}^{L}\int_{-\pi}^{\pi} u_3(x_1, x_2, 0)\cos\left(n+\frac{1}{2}\right)x_1\, e^{ik_2x_2}\, dx_1 dx_2$$

$$f^{(o)}_{k_2n} = \frac{1}{2\pi L}\int_{-L}^{L}\int_{-\pi}^{\pi} u_3(x_1, x_2, 0)\sin nx_1\, e^{-ik_2x_2}\, dx_1 dx_2 \tag{16b}$$

and $g_{k_2n}(s)$ corresponds to f_{k_2n} with $W'u_1(x_1, x_2, s)$ replacing $u_3(x_1, x_2, 0)$ in (16b).

There are clearly no true instabilities for $\nu \neq 0$; however, certain of the inhomogeneous terms in (16a) attain large values for finite times before decaying exponentially as $t \to \infty$. Substituting $u_1(x_1, x_2, s)$ from (14a) in (16a), we find terms of the typical magnitude

$$\exp\left(-\nu\left(k_2^2+n^2\right)t\right)\int_0^t \exp\left(\nu\left(n^2-p_n^2\right)s\right) ds\; u_1(p_m, k_2)(c_1V_1+c_2 2V_2)\sin nx_1\, e^{ik_2x_2}, \tag{17}$$

where c_1 and c_2 are constants arising from the integrations in (16a), which are of the order of unity for $m \approx n$, except where they vanish by symmetry. For $n = m$, the argument $\left(n^2-p_n^2\right)$ is always positive, so that

$$\int_0^t \exp\left(\nu\left(n^2-p_m\right)^2\right) ds \geq t.$$

Choosing $n = 1$ and suppressing the spatial dependence in (17), we get the estimate

$$u_3 \approx t\exp\left(-\nu\left(k_2^2+1\right)t\right) Vu_1(0). \tag{18}$$

As $\nu \to 0$, the estimate (18) approaches the form of (4), the solution for $\nu = 0$.

Equation 18 attains a maximum for $t_o = \dfrac{1}{\nu\left(1+k_2^2\right)}$, so that

$$u_{3_{max}} \approx \frac{V}{\nu\left(1+k_2^2\right)} u_1 \approx \frac{R}{\pi^2} u_1(0), \tag{19}$$

showing that after a finite time the initial perturbation in u_1 appears as a term in u_3 and is amplified by a factor of the order of the Reynolds number $R = \frac{\pi^2 V}{\nu}$.

H. L. Willke, Jr.

References

1. C. C. Lin, The Theory of Hydrodynamic Stability (Cambridge University Press, London, 1955).

XII. NOISE IN ELECTRON DEVICES*

Prof. H. A. Haus
Prof. P. L. Penfield, Jr.
Prof. R. P. Rafuse
W. D. Rummler

RESEARCH OBJECTIVES

The research on noise in electron devices has two objectives:

(i) The study of specific devices, such as the parametric amplifier and the maser, to determine the physical sources of noise and the limitations they impose on the noise performance of the amplifier.

The parametric amplifier with coherent input signals at both the signal and idler frequency, and the degenerate parametric amplifier are the impetus for the second objective.

(ii) The determination of a measure of the optimum noise performance of multiterminal linear amplifiers. The optimum noise performance of a linear twoport amplifier is known to be expressible in terms of its minimum noise measure, a quantity that is characteristic of the amplifier. The optimum noise performance of a multiterminal pair amplifier excited by a multiterminal pair source is at present under study for the purpose of devoloping an analogous measure for the optimum noise performance of such an amplifier.

H. A. Haus, P. Penfield, Jr., R. P. Rafuse

A. SOLUTIONS TO THE PROBLEM OF THE OPTIMUM NOISE PERFORMANCE OF MULTITERMINAL AMPLIFIERS

In a previous report[1] we showed that under certain restrictions the stationary values of signal-to-noise ratio which can be obtained for a specified value of exchangeable signal power at a single-output terminal pair by imbedding an n-terminal pair source and an m-terminal pair amplifier in an n + m + 1 terminal pair lossless network are governed by two coupled matrix equations — Eqs. 1 and 2.

$$\overline{E_{na}E_{na}^{\dagger}}x_2 + 2\lambda(Z_a+Z_a^{\dagger})\,x_2 = 0 \tag{1}$$

$$\overline{E_sE_s^{\dagger}}x_1 + \mu\left[\overline{E_nE_n^{\dagger}}+2\lambda(Z+Z^{\dagger})\right]x_1 = 0 \tag{2}$$

By a simpler derivation, it has been established that Eqs. 1 and 2 are valid regardless of the nature of the matrices characterizing the source and amplifier networks; however, for simplicity we shall assume here that $\overline{E_sE_s^{\dagger}}$ is positive definite, $Z + Z^{\dagger}$ is positive definite, and $Z_a + Z_a^{\dagger}$ is indefinite.

Components of the vectors x_1 and x_2 may be interpreted as complex voltage ratios. For instance, with all voltage sources in the source and amplifier short-circuited

*This work was supported in part by Purchase Order DDL B-00368 with Lincoln Laboratory, a center for research operated by Massachusetts Institute of Technology with the joint support of the U. S. Army, Navy, and Air Force under Air Force Contract AF19(604)-7400.

except the source represented by E_{s1}, which is the open-circuit signal voltage at the first terminal pair of the source network, the open-circuit voltage at the output terminal pair is $x_{11}E_{s1}$, where x_{11} is the first component of the vector x_1. Similarly, the components of x_2 relate the open-circuit noise voltage at the output terminal pairs to the open-circuit voltages of the amplifier. Imbedding the source and amplifier networks in a given $n+m+1$ terminal pair lossless network enables us to define a unique pair of vectors x_1 and x_2. The reverse is not true; it can be shown that there are an infinite number of lossless networks corresponding to a particular pair of vectors x_1 and x_2.

For Eq. 1 there are n eigenvalues λ_i and eigenvectors $x_2^{(i)}$. We may express the eigenvalue λ_i in terms of its eigenvectors as

$$\lambda_i = -\frac{x_2^{(i)\dagger}\overline{E_{na}E_{na}^\dagger}x_2^{(i)}}{2x_2^{(i)\dagger}\left(Z_a+Z_a^\dagger\right)x_2^{(i)}}. \tag{3}$$

For convenience later, we shall label the smallest positive eigenvalue as λ_1 and the remaining positive eigenvalues in ascending order, and we shall label the smallest negative eigenvalues λ_m and the remaining negative eigenvalues in descending order.

Equation 2, on the other hand, has n solutions for each of the m eigenvalues λ_i of Eq. 1; this gives us a total of $n \times m$ sets of solutions to Eqs. 1 and 2. Using a double-subscript notation for these eigenvalues and eigenvectors, we may express the eigenvalue μ_{ij} in terms of λ_i and the eigenvector $x_1^{(ij)}$ as

$$\frac{1}{\mu_{ij}} = \frac{x_1^{(ij)\dagger}\overline{E_nE_n^\dagger}x_1^{(ij)} + 2\lambda_i x_1^{(ij)\dagger}(Z+Z^\dagger)\,x_1^{(ij)}}{x_1^{(ij)\dagger}\overline{E_sE_s^\dagger}x_1^{(ij)}}. \tag{4}$$

Here, we number our eigenvalues for a given λ_i by the order of the value of their reciprocals; the minimum value of $1/\mu_i$ (which may be negative) is $1/\mu_{i1}$ and the maximum is $1/\mu_{in}$.

We would now like to relate the quantities of interest, namely the signal-to-noise ratio at the output and the exchangeable signal power at the output, to the eigenvalues derived from Eqs. 1 and 2. For the optimal imbedding network corresponding to a set of values λ_i and μ_{ij} we write the signal-to-noise ratio as

$$\sigma_{ij} = \frac{x_1^{(ij)\dagger}\,\overline{E_sE_s^\dagger}\,x_1^{(ij)}}{x_1^{(ij)\dagger}\overline{E_nE_n^\dagger}x_1^{(ij)} + x_2^{(i)\dagger}\,\overline{E_{na}E_{na}^\dagger}\,x_2^{(i)}}, \tag{5}$$

and the exchangeable signal power as

$$p_{ij} = \frac{x_1^{(ij)\dagger}\, \overline{E_s E_s^\dagger}\, x_1^{(ij)}}{2x_1^{(ij)\dagger}(Z+Z^\dagger)\, x_1^{(ij)} + 2x_2^{(i)\dagger}\left(Z_a + Z_a^\dagger\right) x_2^{(i)}}. \tag{6}$$

We now see why these quantities do not appear directly as eigenvalues. In Eq. 3 we see that λ_i is independent of the magnitude of $x_2^{(i)}$; similarly, μ_{ij} in Eq. 4 is independent of the magnitude of $x_1^{(ij)}$. On the other hand, both of the quantities defined in Eqs. 5 and 6 are dependent on the relative magnitude of $x_2^{(i)}$ and $x_1^{(ij)}$. We can explicitly demonstrate the consequences of this by considering the particular realization of the optimal network that places this fact in evidence.

Consider an imbedding of the m-terminal pair amplifier in an arbitrary m + 1 terminal pair lossless network. We know that we can always pick this network in such a manner that the mean-square voltage and the real part of the impedance at the output terminal pair are $x_2^{(i)'\dagger}\, \overline{E_{na} E_{na}^\dagger}\, x_2^{(i)'}$ and $1/2\, x_2^{(i)'\dagger}\left(Z_a + Z_a^\dagger\right) x_2^{(i)'}$, respectively, where $x_2^{(i)'}$ is a vector that is proportional to $x_2^{(i)}$. Similarly, we can losslessly reduce the source network to a one-terminal pair network with mean-square signal voltage

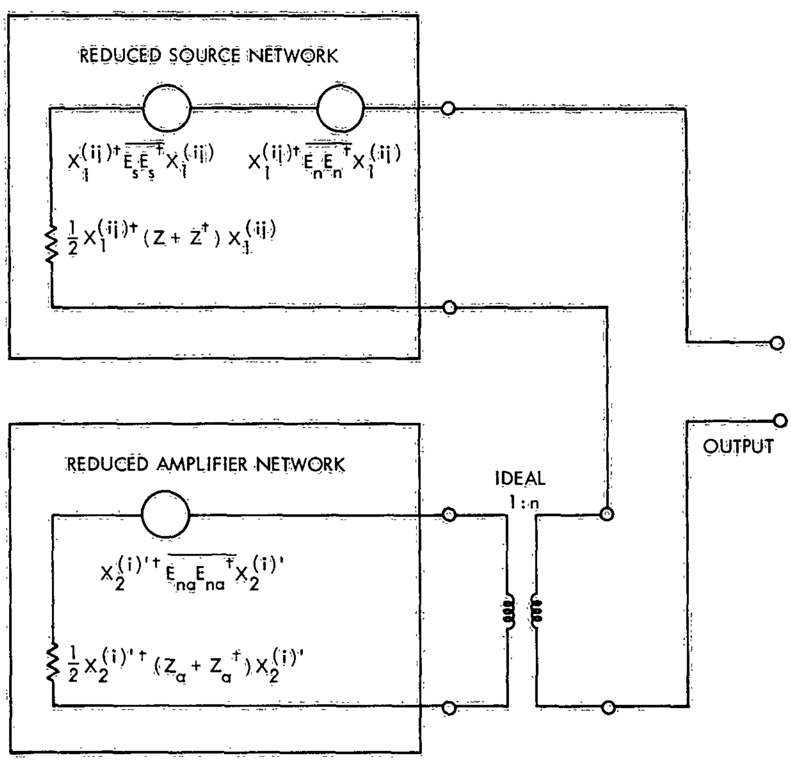

Fig. XII-1. Realization of the optimal network.

$x_1^{(ij)\dagger} \overline{E_s E_s^\dagger} x_1^{(ij)}$, mean-square noise voltage $x_1^{(ij)\dagger} \overline{E_n E_n^\dagger} x_1^{(ij)}$, and impedance $1/2\ x_1^{(ij)\dagger} (Z+Z^\dagger)\ x_1^{(ij)}$. Combining these two reduced networks as shown in Fig. XII-1, we see that the signal-to-noise ratio and the exchangeable signal power at the output are given by Eqs. 5 and 6, respectively, where $x_2^{(i)} = nx_1^{(i)'}$. This network is optimal in the sense of Eqs. 1 and 2 for any value of n. We see that varying the transformer ratio is equivalent to varying the ratio of $\|x_2^{(i)}\|$ to $\|x_1^{(ij)}\|$. Physically, then, when we vary n or $\|x_2^{(i)}\|/\|x_1^{(ij)}\|$, we are changing the amount of our use of the amplifier, since we are changing the exchangeable signal power at the output and, thereby, also changing the signal-to-noise ratio at the output. This interpretation is actually completely general and independent of the particular imbedding network that we are using. However, in general, variation of the ratio of $\|x_2^{(i)}\|$ to $\|x_1^{(ij)}\|$ can correspond to some complex variation of the imbedding network because of the multiple feedback loops that may exist between the source and amplifier networks. Figure XII-1, then, just gives a convenient way of visualizing the effects of varying the ratio of $\|x_2^{(i)}\|$ to $\|x_1^{(ij)}\|$.

We see then that setting the ratio of $\|x_2^{(i)}\|$ to $\|x_1^{(ij)}\|$ equal to zero or, equivalently, setting n=0 is the same as throwing away the amplifier. The values of σ_{ij} and p_{ij} for this limit are just the signal-to-noise ratio and the exchangeable power of the source network alone. We designate these two quantities as

$$\sigma_{ij,s} = \frac{x_1^{(ij)\dagger}\ \overline{E_s E_s^\dagger}\ x_1^{(ij)}}{x_1^{(ij)\dagger}\ \overline{E_n E_n^\dagger}\ x_1^{(ij)}} \tag{7}$$

$$p_{ij,s} = \frac{x_1^{(ij)\dagger}\ \overline{E_s E_s^\dagger}\ x_1^{(ij)}}{2x_1^{(ij)\dagger}\ (Z+Z^\dagger)\ x_1^{(ij)}},$$

respectively.

It follows that for a given pair of eigenvalues λ_i and μ_{ij} we may vary σ_{ij} and p_{ij} by varying the ratio of the magnitudes of the eigenvectors, that is, by varying only the transformer ratio in Fig. XII-1. Such a variation enables us to plot the stationary values of signal-to-noise ratio as a function of the exchangeable signal power at the output corresponding to this particular solution to Eqs. 1 and 2. For this purpose we need the relation

$$1/\sigma_{ij} = 1/\mu_{ij} - \lambda_i/p_{ij}, \tag{9}$$

which may be verified by using Eqs. 3-6. From Eq. 9 we see that it is more convenient to plot characteristic curves of $1/\sigma_{ij}$ as a function of $1/p_{ij}$. In the $1/\sigma_{ij} - 1/p_{ij}$ plane these characteristic curves are straight lines with slopes $-\lambda_i$ and intercepts $1/\mu_{ij}$ with the $1/\sigma_{ij}$ axis. Thus a set of eigenvalues λ_i and μ_{ij} merely determine a characteristic line in the $1/\sigma_{ij} - 1/p_{ij}$ plane; moreover, we see that for the stated problem there are $n \times m$ such lines.

It must be pointed out, however, that only one-half of a characteristic line is realizable. Comparing Eqs. 5 and 7, we see that

$$\frac{1}{\sigma_{ij}} \geq \frac{1}{\sigma_{ij,s}}, \tag{10}$$

and, using Eqs. 4, 7, 8, and 10 in Eq. 9, we find that either

$$\lambda_i > 0 \text{ and } 1/p_{ij} \leq 1/p_{ij,s}$$

$$\text{or} \tag{11}$$

$$\lambda_i < 0 \text{ and } 1/p_{ij} \geq 1/p_{ij,s}.$$

The equality signs in Eqs. 10 and 11 will hold only when $|x_2^{(i)}|/|x_1^{(ij)}|$ is zero, that is, the realizable one-half of the characteristic line ends at the point determined by the source – the point whose coordinates are $1/\sigma_{ij,s}$ and $1/p_{ij,s}$. Hence, in the $1/\sigma_{ij} - 1/p_{ij}$ plane we can realize only the one-half of the characteristic line that is above and to the left of the source point for negative λ_i, and above and to the right of the source point for positive λ_i. We can only achieve a signal-to-noise ratio equal to μ_{ij} at infinite exchangeable signal power if $1/p_{ij} = 0$ satisfies one of the inequalities of Eq. 11.

In displaying the solution to the optimization problem in the $1/\sigma_{ij} - 1/p_{ij}$ plane, we shall show only those solutions for a given λ_i which correspond to $1/\mu_{i1}$, the minimum value of $1/\mu_i$, and $1/\mu_{in}$, the maximum value of $1/\mu_i$. We would like to find where the end points of these characteristic curves lie in the $1/\sigma_{ij} - 1/p_{ij}$ plane. If we consider how these end points change as λ_i changes, we find that they generate a closed curve. This is illustrated in Fig. XII-2, in which several of these characteristic curves are shown as they must appear for positive λ's and minimum $1/\mu_i$. With reference to Fig. XII-1, when we vary λ_i we are changing amplifiers and then reoptimizing the source for use with this new amplifier and thereby obtaining a new source point.

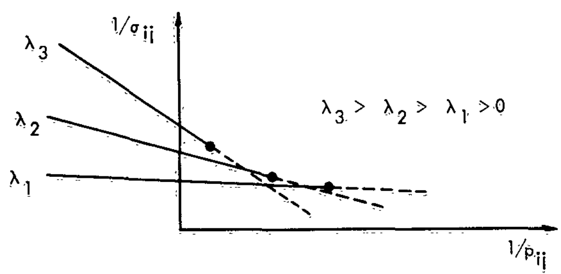

Fig. XII-2. Characteristic curves for $\lambda_i > 0$, $1/\mu_{i1}$.

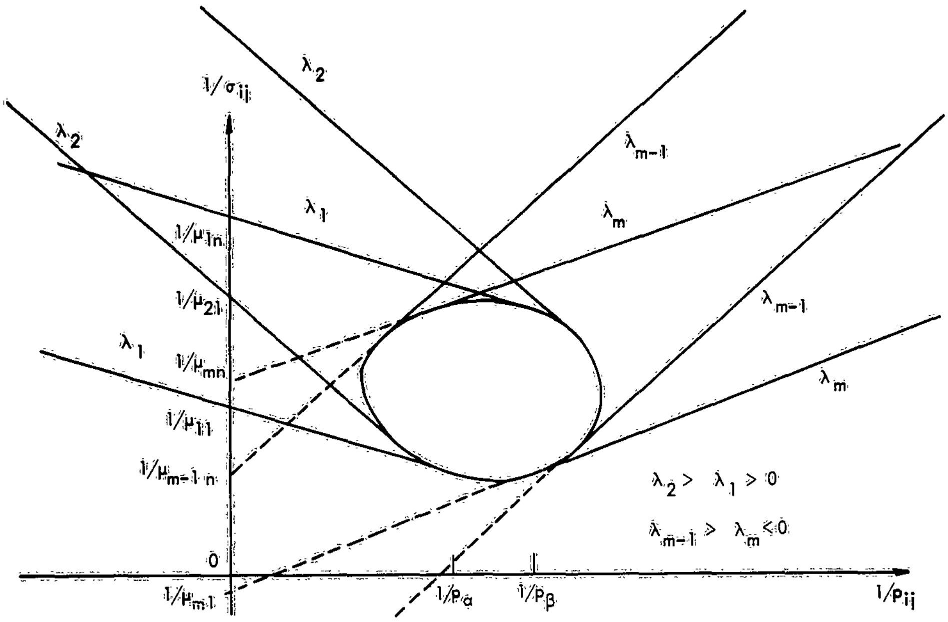

Fig. XII-3. Typical set of characteristic curves.

The closed curve generated is tangent to each of the characteristic lines. Physically, this curve represents the boundary of the region of values of the noise-to-signal ratio and the reciprocal of the exchangeable signal power that may be obtained at the output by imbedding only the source network, and not the amplifier, in an arbitrary lossless imbedding network.

In Fig. XII-3 we show a typical plot of characteristic curves for a positive definite source and an amplifier having both positive and negative eigenvalues. We have shown only those characteristics corresponding to extremal values of $1/\mu_i$ for four values of λ_i – the two smallest positive eigenvalues and the two smallest negative eigenvalues. (All solutions corresponding to intermediate eigenvalues of $1/\mu_i$ would give rise to characteristic curves that terminate at points inside the source region.) All of these characteristics may be interpreted. The line characterized by λ_1 and μ_{ij} is the true optimum-performance curve. It is the curve of the maximum signal-to-noise ratio as a function of exchangeable signal power for exchangeable signal power greater than p_a. The line characterized by λ_1 and μ_{1n} represents the worst way of increasing exchangeable signal power with the best reduction of the amplifier. The line characterized by λ_2 and μ_{21} is just a locus of points of stationary signal-to-noise ratio for fixed exchangeable signal powers. This same statement applies to all of the curves shown. The line characterized by λ_m and μ_{m1} represents the best way of reducing the exchangeable signal power below p_β. Since λ_m is negative here, we are using the amplifier as a positive resistor; for that matter, we are using the least noisy positive resistor appearing in the cannonic form of the amplifier.

W. D. Rummler

References

1. W. D. Rummler, Optimum noise performance of multiterminal amplifiers, Quarterly Progress Report No. 66, Research Laboratory of Electronics, M. I. T., July 15, 1962, pp. 71-77.

PLASMA DYNAMICS

This heading covers all of the work that is supported in part by the National Science Foundation and is under the over-all supervision of the Plasma Dynamics Committee of the Massachusetts Institute of Technology. The general objective is to combine the technical knowledge of several departments, in a broad attempt to understand electrical plasmas, to control them, and to apply them to the needs of communication, propulsion, power conversion, and thermonuclear processes.

(The members of the Plasma Dynamics Committee are: Prof. S. C. Brown (Chairman), Prof. D. J. Rose, Prof. A. H. Shapiro, Prof. L. D. Smullin, Prof. H. J. Zimmermann.)

XIII. PLASMA PHYSICS*

Prof. S. C. Brown
Prof. G. Bekefi
Prof. D. R. Whitehouse
M. L. Andrews
V. Arunasalam
J. F. Clarke
J. D. Coccoli
F. X. Crist
H. Fields
E. W. Fitzgerald, Jr.
W. H. Glenn, Jr.
E. B. Hooper, Jr.
J. C. Ingraham
P. W. Jameson
R. L. Kronquist
D. T. Llewellyn-Jones
J. J. McCarthy
W. J. Mulligan
J. J. Nolan, Jr.
G. L. Rogoff
F. Y-F. Tse
R. E. Whitney

RESEARCH OBJECTIVES

The aim of this group continues to be the study of the fundamental properties of plasmas with particular emphasis on plasmas in magnetic fields. In emphasizing our interest in high-density plasmas, we have spent a great deal of effort on production of plasmas of high-percentage ionization at low pressures under steady-state conditions, the achievement of which will allow us to carry on the fundamental studies in which we are most interested.

We are also studying ways of determining the characteristics of plasmas by means of microwaves and infrared optics. Along with these production and diagnostic studies, we are continuing measurements on the fundamental physics of loss and gain mechanisms of electrons in plasmas in magnetic fields. Emphasis is also being placed on the study of microwave radiation from plasmas, with and without magnetic fields, both as a tool for measuring the plasma temperature and thermal properties and as a means of understanding more about the motion of electrons and ions in magnetic fields.

Theoretical work has been concentrated on the study of waves in plasmas and of statistical theories of the nature of a plasma.

S. C. Brown

A. LOW-FREQUENCY PLASMA WAVES

A study has been initiated into the response of plasmas at frequencies much below the electron plasma frequency. Our object is to establish longitudinal ion plasma waves

*This work was supported in part by the U.S. Atomic Energy Commission (Contract AT(30-1)-1842); in part by the U.S. Air Force (Electronic Systems Division) under Contract AF19(604)-5992; and in part by the National Science Foundation (Grant G-24073).

in a plasma column and measure their propagation and attenuation characteristics. The experimental arrangement shown in Fig. XIII-1 has been built and is at present under test.

The fundamental idea behind the experiment is to produce a plasma column with cw microwave power into the TE_{111} mode of the cavity. The frequency is adjusted to the electron-cyclotron frequency for resonance heating at low gas pressures. A small modulation is then impressed on the microwave power to vary the electron heating within

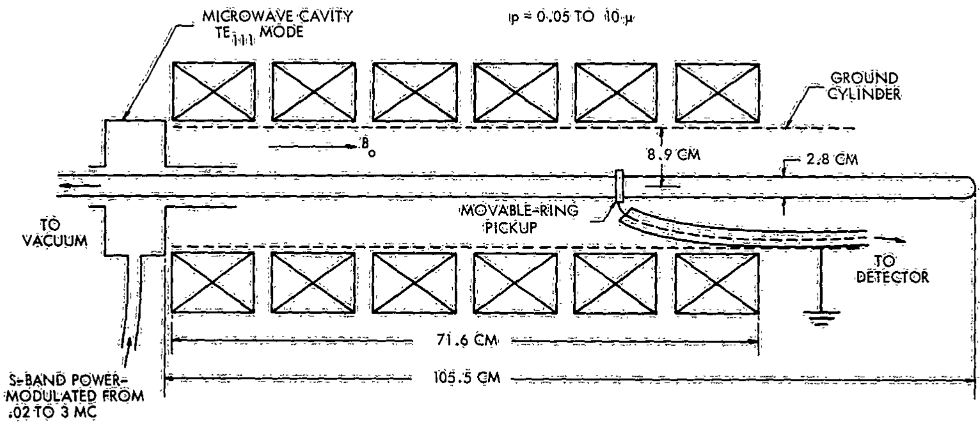

Fig. XIII-1. Experimental apparatus.

the cavity. As the electron energy is varied, the ionization frequency should also be modulated, and hence there will be a local modulation in the electron and ion density. Simple calculations of the ion plasma wave show that for frequencies of approximately 1 mc the wavelength of the ion (and electron) density perturbations can be made as small as a few centimeters, and we should observe a definite wave propagating down the column.

The presence of the wave is particularly easy to determine by measuring the potential that is external to the plasma column at the modulation frequency. Typical data are shown in Fig. XIII-2.

The appearance of the ac potential at the modulation frequency seems to be associated with the flow of charges in the body of the plasma, and because of the extremely long wavelength, it must be a flow of the hot electrons rather than the cold ions. Since the electron plasma wave is attenuated for frequencies below ω_p, we were encouraged to re-examine these waves with particular reference to the mechanism for transport of energy. The normal Boltzmann formulation for electron waves is solved for the perturbation of the distribution function away from some equilibrium distribution. Coupling

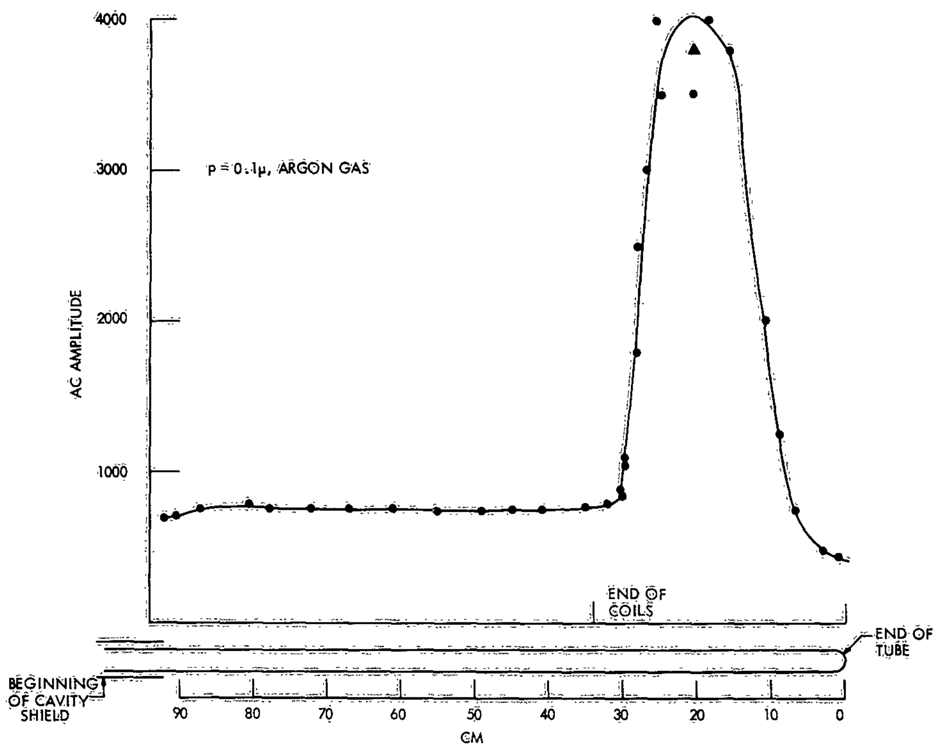

Fig. XIII-2. A-C amplitude of 1.1-mc signal on movable ring pickup when S-band power into cavity is modulated at 1.1 mc.

this result with Poisson's equation, we get the dispersion relation (assuming $\nu_c = 0$)

$$1 = \frac{\omega_p^2}{n_o} \int_{-\infty}^{\infty} \frac{f_o dv}{(\omega-k\cdot v)^2}. \tag{1}$$

The difficulties of this integral are associated with the pole at $v = \omega/k$ and lead to the phenomenon of Landau damping. If we approximate the denominator for small velocities, we get

$$\omega^2 = \omega_p^2 + 3k^2\langle v\rangle^2. \tag{2}$$

This steady-state dispersion, however, cannot be valid for the more complicated boundary-value problem in which the electron energy is periodically varied at some plane. The propagation characteristic will, in fact, depend on the particular variation of the distribution function, and also on the unperturbed distribution function.

At this point, therefore, we switch to a hydrodynamic approach that assuredly will miss Landau damping but, on the other hand, will show how momentum and energy are transported in this longitudinal wave. The derivation starts with the first four moments of the transport equation. For simplicity, we assume that electrons collide with neutrals and that it is possible to define a local temperature T associated with a Maxwellian distribution of velocities. This derivation thus differs from the Boltzmann approach, which actually tries to solve for the local distribution.

$$\frac{\partial n}{\partial t} + \bar{\nabla} \cdot \bar{\Gamma} = 0 \tag{3}$$

$$\frac{\partial \bar{\Gamma}}{\partial t} + \bar{\nabla}\left(\frac{ne\,T}{m}\right) + \frac{ne}{m}\,\bar{E} = -\nu_c \bar{\Gamma} \tag{4}$$

$$\frac{\partial}{\partial t}\frac{3}{2}(nT) + \bar{\nabla}\cdot\bar{H} + \bar{\Gamma}\cdot\bar{E} = -\,ng\,\nu_c\frac{3}{2}(T-T_{gas}) \tag{5}$$

$$\frac{\partial \bar{H}}{\partial t} + \bar{\nabla}\frac{5}{2}\,\frac{ne\,T^2}{m} + \frac{5}{2}\,\frac{ne\,T}{m}\,\bar{E} = -\,\nu_c\bar{H}, \tag{6}$$

where

n = particles/M^3 $\qquad$ ν_c = collisions/sec

$\bar{\Gamma}$ = particles/M^2 sec $\qquad$ g = energy-loss parameter

$\bar{H}$ = volts/M^2 sec $\qquad$ $\bar{E}$ = volts/M

T = volts

One can derive Eq. 2 from Eqs. 3 and 4 by making an assumption about the temperature variation in the longitudinal wave, that is, either assuming it to be isothermal or adiabatic, and linearizing the equations with small perturbations of the variables. A more complete analysis is made possible by assuming an arbitrary variation in the temperature, and by linearizing all four equations. For small-signal analysis, we assume that

$$\bar{H} = \underline{\bar{H}}e^{j(\omega t-kx)} \qquad T = T_o + \underline{T}e^{j(\omega t-kx)}$$

$$\bar{\Gamma} = \underline{\bar{\Gamma}}e^{j(\omega t-kx)} \qquad n = n_o + \underline{n}e^{j(\omega t-kx)}$$

$$\bar{E} = \underline{\bar{E}}e^{j(\omega t-kx)}$$

Now we set the collision frequency equal to zero, even though this is contrary to our assumption of a maintained local Maxwellian distribution. The character of the resulting waves will thus become evident, and we can add collisional damping later. The determinant of the linearized equations, although rather complex, results in a dispersion relation that, when written in nondimensional form, is

$$K^4 + (1-2W^2) K^2 + \frac{3}{5}(W^4-W^2) = 0, \tag{7}$$

where $W^2 = \omega^2/\omega_p^2$, and $K^2 = k^2(eT_o/m)^2/\omega_p^2$. There are two waves associated with Eq. 7, both of which are shown in Fig. XIII-3. Wave I is like the normal electron plasma wave, while wave II propagates down to zero frequency. The ratio of heat flow H to particle flow Γ for these waves is

$$\frac{H}{\Gamma T_o} = \frac{3}{2}\frac{W^2-1}{K^2}. \tag{8}$$

For wave II, the heat flow is zero at $\omega = \omega_p$, and the wavelength is finite. At very low frequencies, wave II has a large wavelength and phase velocity equal to the adiabatic electron sound velocity. This result seems to predict closer correlation with our experimental results than Eq. 2.

The presence of two electron waves is somewhat plausible, since we know that it is physically possible to excite independent variations in electron density and temperature at some plane in the plasma, and thus two waves will be needed to satisfy these boundary

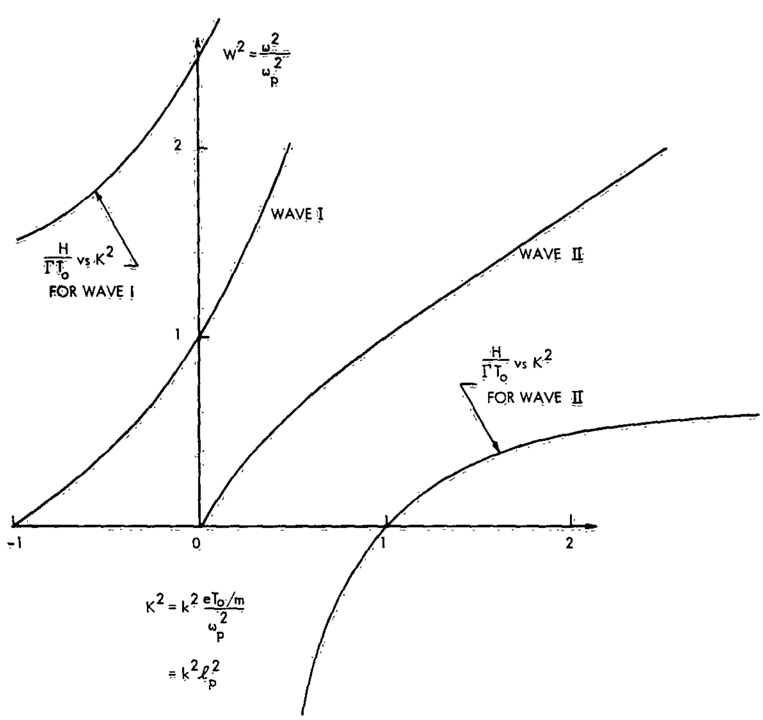

Fig. XIII-3. Waves associated with ω.

conditions. Experimental and theoretical work is continuing.

D. R. Whitehouse, P. W. Jameson

B. DECAMETER RADIATION FROM JUPITER

This report is a summary of a paper that has been submitted for publication to Nature.

The observed correlation between solar-flare activity and intense radio bursts from Jupiter in the 5-38 mc region has prompted several suggestions about the origins of this radiation.[1-3] With the premise that the radioactivity is brought on by sudden eruptions of fast solar electrons as they arrive at Jupiter, we have shown that an existing theory[4-6] for maserlike amplification of synchrotron radiation from electrons with a non-Maxwellian energy distribution orbiting in the Jovian magnetosphere can provide a quantitative model for the emission.

The theory predicts a narrow frequency band of amplification near the local electron gyrofrequency, but the intensity predicted for the second and higher harmonics is smaller than that of the fundamental by more than four orders of magnitude. Thus the appearance of a single band of radiation should not rule out the synchrotron mechanism, as has been suggested.[2]

G. Bekefi, J. L. Hirshfield

(Dr. J. L. Hirshfield is in the Department of Physics, Yale University.)

References

1. J. W. Warwick, Science 132, 1250 (1960).
2. L. Landovitz and Leona Marshall, Nature 195, 1186 (1962).
3. G. B. Field, J. Geophys. Research 65, 1661 (1960); also "Jupiter's Radio Emission," Princeton University Observatory Report (unpublished).
4. R. Q. Twiss, Australian J. Phys. 11, 564 (1958).
5. J. Schneider, Phys. Rev. Letters 2, 504 (1959); Z. Naturforsch. 15a, 484 (1960).
6. G. Bekefi, J. L. Hirshfield, and S. C. Brown, Phys. Fluids 4, 173 (1961); Phys. Rev. 122, 1037 (1961).

XIV. PLASMA ELECTRONICS*

Prof. L. D. Smullin	J. R. Cogdell	L. M. Petrie, Jr.
Prof. H. A. Haus	L. J. Donadieu	W. D. Rummler
Prof. A. Bers	S. A. Evans	A. J. Schneider
Prof. W. D. Getty	B. A. Hartenbaum	P. E. Serafim
Prof. D. J. Rose	W. G. Homeyer	P. S. Spangler
Prof. T. H. Dupree	H. Y. Hsieh	G. Theodoridis
Prof. L. M. Lidsky	A. J. Impink, Jr.	E. Thompson
Prof. E. P. Gyftopoulos	P. K. Karvellas	J. S. Tulenko
Dr. G. Fiocco	J. D. Levine	C. E. Wagner
F. Alvarez de Toledo	L. N. Lontai	S. Wilensky
W. L. Brassert	D. L. Morse	H. L. Witting
R. J. Briggs	R. T. Nowak	J. C. Woo

RESEARCH OBJECTIVES

1. Plasmas for Electrical Energy Conversion

The group working in plasma electronics is concerned with the synthesizing or design of particular plasma systems to perform specified functions. The research program described below is primarily concerned with the plasma as a component of a power generator: either controlled thermonuclear fusion or magnetohydrodynamic. To this end, we are studying several methods of producing and containing dense, hot plasmas. We are also concerned with the collective behavior of plasmas of finite dimensions, and are studying possible means of energy extraction. Thus we are led to the investigation of MHD waves on moving plasma streams, and of waves in plasma waveguides and their stability.

Beam-Plasma Discharge. During the past year we have shown that a relatively dense plasma can be produced by an electron beam injected into a low-pressure drift region. This phenomenon is basically a microwave discharge, in which the strong microwave fields are produced by the interaction between the beam and the plasma already present. With a 10-kv, 1-amp, 100-μsec pulsed beam, plasmas of $5 \times 10^{12}/\text{cm}^3$ density and very high electron temperatures have been produced.

During the coming year we shall extend this work, using more powerful beams (10-kv, 10-amps from a magnetron injection gun), and injected molecular beams. These techniques should allow us to approach 100 per cent ionization, and we should begin to see relatively high-temperature ions as a result of ohmic heating. We shall have four experiments running, devoted to the detailed study of various aspects of the beam-plasma discharge.

L. D. Smullin, W. D. Getty

Electron Cyclotron Resonant Discharge. Our preliminary experiments, using ~ 0.5 Mw of 10-cm power, have resulted in producing an intense discharge from which 2-Mev x-rays emanate. Because of lack of room for suitable shielding, the experiments were temporarily abandoned. We are now rebuilding our high-power experiment in another wing of the Research Laboratory of Electronics, where suitable shielding can

*This work was supported in part by the National Science Foundation (Grant G-24073); in part by the U.S. Navy (Office of Naval Research) under Contract Nonr-1841(78); and in part by Purchase Order DDL B-00368 with Lincoln Laboratory, a center for research operated by Massachusetts Institute of Technology with the joint support of the U.S. Army, Navy, and Air Force under Air Force Contract AF 19(604)-7400.

be installed; and, a low-power (~ 100 kw) system is also being assembled. An analog computer program is being developed for studying electron trajectories under the influence of an rf field and a mirror (nonuniform) magnetostatic field.

D. J. Rose, L. D. Smullin, G. Fiocco

Thomson Scattering of Light from Electrons. The first laboratory observation of light scattering by electrons was made in the Research Laboratory of Electronics in November 1962, by using a laser beam. During the coming year, we plan to develop this technique into a useful tool for plasma diagnostics.

G. Fiocco, E. Thompson

Theory of Active and Passive Anisotropic Waveguides. The work on this topic will proceed along two lines:

(i) Development of small-signal energy and momentum-conservation principles that are applicable to the linearized equations of anisotropic waveguides in the absence of loss. These are used to obtain criteria for the stability or amplifying nature of the waves in these systems.

(ii) Analysis of specific waveguides of current interest, and determination of their dispersion characteristics.

The dispersion characteristics may be also used to test the general criteria obtained from the conservation principles.

A. Bers, H. A. Haus

Magnetohydrodynamics Power Generation. We are studying the possibilities of energy extraction from moving fluids through coupling of circuit fields to the waves in the fluid. Both the linearized problem in two or three dimensions, and the nonlinear equations in a one-dimensional geometry are being studied; effects attributable to variation of geometric parameters are sought from the former, saturation effects and efficiences are studied through the latter.

H. A. Haus

2. Highly Ionized Plasma and Fusion Research

Plasma Kinetic Theory. Methods of solving the plasma kinetic equations, including the presence of self-generated and externally applied electromagnetic fields, are being successfully developed. This work, which leads to rigorous predictions of plasma properties, will be continued and extended.

T. H. Dupree

Charged-Particle Confinement by Nonadiabatic Motion. Injection of ions or electrons into a magnetic mirror or other confining structure by spatially resonant field perturbations is a continuing project. A 3-meter long experiment for trapping electrons in a mirror field (200 gauss central section) is being constructed, and the theories of initial trapping and eventual confinement time are being refined.

L. M. Lidsky, D. J. Rose

Superconducting Magnets. A large superconducting magnet (room-temperature working space, 0.05 m^3) will be completed early this year; engineering design principles that have been worked out for such systems have been reported, and the magnet itself is expected to be used for plasma-confinement experiments. Studies of field quenching, parasitic diamagnetic current generation, and general operating behavior of the magnet in various field configurations will be carried out.

D. J. Rose

Thermonuclear-Blanket Studies. Calculations carried out over the past year on neutron slowing down, neutron multiplication, tritium regeneration, heat transfer, and energy recovery are being extended to include other important effects. Principal effects are: addition of fissionable materials, gamma transport, and coil shielding. Experiments with 14 Mev neutrons from Van de Graaf D-T reactions on fusion blanket mock-up assemblies continue.

D. J. Rose, I. Kaplan

Cesium Plasmas. With a view to eventual electrical energy conversion from nuclear heat and other prime sources, the physical properties of the cesium plasma itself and a number of experimental devices are being studied.

E. P. Gyftopoulos

Arc-Plasma Studies. The hollow-cathode source previously developed and reported on will be used to generate plasmas in the density range $10^{15}/cm^3$, 90-95 per cent ionized by pulse techniques, to study plasma stability in long plasma columns, and to obtain a "standard" for comparison of diagnostic methods.

L. M. Lidsky

A. NONLINEAR ONE-DIMENSIONAL MAGNETOHYDRODYNAMIC MONOTRON

A linearized analysis of the one-dimensional magnetohydrodynamic (MHD) monotron has previously been carried out by Haus.[1] The present work involves a nonlinear analysis of the same device. The amplitude of the oscillations as limited by the nonlinearities can be determined, and, in particular, the efficiency of the device as an energy converter can be obtained. We have been able to solve the problem of the nonlinear one-dimensional MHD monotron of the same geometry as that of Haus[1] when the coil is terminated by a parallel combination of a load conductance and a sinusoidal current source (exciter), under the following assumed conditions: (a) the ratio of the specific heats of

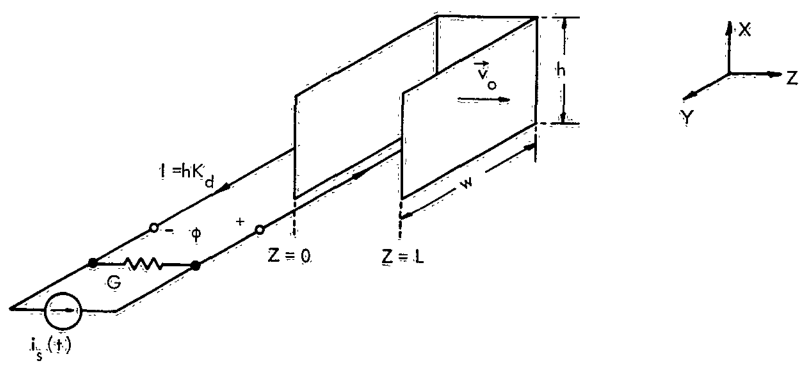

Fig. XIV-1. Monotron connected to external circuit.

the fluid is 2; (b) the flow remains supercritical throughout the entire flow field; and (c) the fluid is unperturbed at $t = 0$.

The monotron connected to the external circuit is shown in Fig. XIV-1. The sheets coupling to the fluid carry current of density K_d and the terminal current is thus $I = hK_d$.

For $\gamma = 2$, the normalized equations of motion for the fluid are

$$\frac{\partial V}{\partial T} + V\frac{\partial V}{\partial Z} + \bar{c}^2\frac{\partial R}{\partial Z} = J \tag{1}$$

$$\frac{\partial R}{\partial T} + \frac{\partial (VR)}{\partial Z} = 0, \tag{2}$$

in which the normalized variables are $Z = \frac{\omega}{v_o} z$, $T = \omega t$, $V(Z,T) = \frac{v}{v_o}$, $R(Z,T) = \frac{\rho}{\rho_o}$, $\bar{c} = \frac{c}{v_o}$, and $J = \frac{B_o}{\omega\rho_o v_o} J_d$ is the normalized driving current density. Here, v_o and ρ_o are the entry velocity and the entry density, respectively, c is the small-signal magnetoacoustic speed, and ω is the frequency of the source. Equations 1 and 2 can be obtained, for example, by combining Eqs. 1-6 of Haus and Schneider.[2]

A completely equivalent description of the fluid is provided by the so-called characteristic equations,[3] which are essentially linear combinations of Eqs. 1 and 2 arranged to place in evidence the fast- and slow-wave nature of the solution.

$$\frac{\partial}{\partial T}(V+2C) + (V+C)\frac{\partial}{\partial Z}(V+2C) = J \tag{3}$$

$$\frac{\partial}{\partial T}(V-2C) + (V-C)\frac{\partial}{\partial Z}(V-2C) = J \tag{4}$$

Here, $C = \bar{c}\sqrt{R}$ is the local magnetoacoustic speed. Except for the current terms on the right-hand side, these equations are identical with those describing the propagation of water (gravity) waves in shallow water. Indeed, our study of the special case $\gamma = 2$ was prompted in part by noting this similarity.

To obtain boundary conditions, we study the effect wrought on the fluid by the current sheets. When Eqs. 1 and 2 are integrated across each of the current sheets, we obtain

$$\left(\frac{V_2^2}{2} + \bar{c}^2 R_2\right) - \left(\frac{V_1^2}{2} + \bar{c}^2 R_1\right) = K \tag{5}$$

$$V_2 R_2 - V_1 R_1 = 0 \tag{6}$$

$$\left(\frac{V_4^2}{2} + \bar{c}^2 R_4\right) - \left(\frac{V_3^2}{2} + \bar{c}^2 R_3\right) = -K \tag{7}$$

$$V_4 R_4 - V_3 R_3 = 0. \tag{8}$$

The subscripts 1, 2, 3, and 4 indicate that the quantities are evaluated at $Z = 0-$, $Z = 0+$, $Z = L-$, and $Z = L+$, respectively. The normalized sheet current density is given by $K = \frac{B_o}{\rho_o v_o^2} K_d$.

Provided that both the fast and slow waves at $Z = 0+$ are forward waves, the fluid upstream from the current sheet is unaffected, and thus $V_1 = 1$ and $R_1 = 1$. The normalized terminal voltage $\Phi = \frac{\phi}{B_o v_o w}$ is given by

$$\Phi = 1 - V_3 R_3. \tag{9}$$

The circuit, a conductance G in parallel with an exciting current source $i_s(T) = I \sin T$, has the volt-ampere relation

$$I \sin T = hK_d + wv_o B_o G\Phi. \tag{10}$$

The combination of Eqs. 5, 6, 9, and 10 furnishes the relation that expresses the effect of the circuit upon the fluid:

$$V_2^2 + \left\{2P(1-V_3R_3)-(1+2\bar{c}^2)-2S \sin T\right\} V_2 + 2\bar{c}^2 = 0. \tag{11}$$

The fact that the fluid velocity at $Z = 0$ must be continuous in the limit of zero sheet current requires that the largest positive real root of the cubic equation for V_2 be chosen. The parameter $S = \frac{B_o}{\rho_o v^2 h} I$ expresses the strength of the source; $P = \left(\frac{w}{h}\right)\frac{B_o^2 G}{\rho_o v_o}$ expresses the magnitude of the load.

The behavior of the monotron is determined by either Eqs. 1 and 2, or Eqs. 3 and 4,

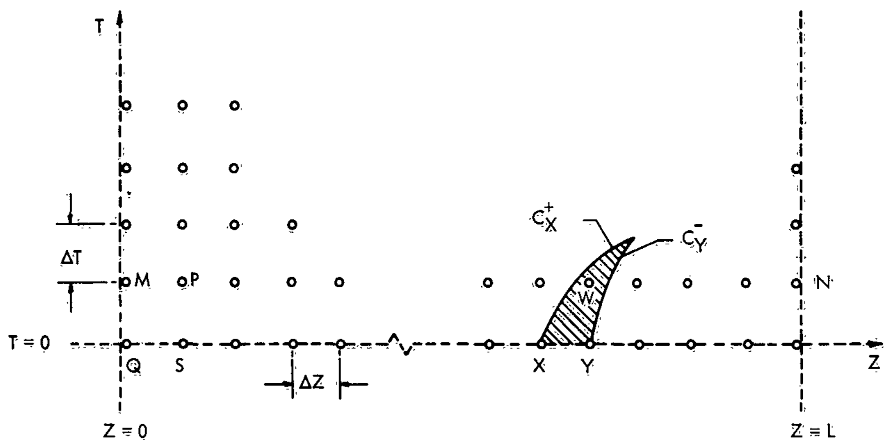

Fig. XIV-2. Lattice points that are pertinent to a numerical solution by finite differences of Eqs. 3 and 4.

with J set equal to zero, by Eq. 11, and by the initial conditions $V(Z,0) = R(Z,0) = 1$. The regime of operation is determined by the requirement that the flow be supercritical everywhere or, in other words, that the slow wave be a forward wave. The wave equation (4) indicates that the velocity of the slow wave is $V - \bar{c}\sqrt{R}$; we thus require that $(V-\bar{c}\sqrt{R})$ be greater than zero everywhere.

To obtain numerical solutions, we have replaced the partial derivatives in Eqs. 3 and 4 by difference quotients appropriate to a rectangular net of points spanning the region of interest $(0<Z<L, 0\leq T<\infty)$ in the Z-T plane (Fig. XIV-2). The resulting difference equations and Eq. 11 allow the computations to begin at $T = 0$ with the given initial conditions and progress into the region in the direction of increasing T.

With reference to Fig. XIV-2, the difference equations relate the values of V and R at point P, for example, to the values of V and R at points Q and S. Since V and R are each equal to unity along the entire bottom row $(T=0)$, the difference equations allow the values of V and R to be obtained for every lattice point of the second row, with the exception of the leftmost point, point M. The value at this point can be obtained, however, from the values at point N by means of the boundary condition, Eq. 11. With the second row completely determined, the values for the third row can be found, and so forth.

The lattice spacing in the Z-direction is fixed; the lattice spacing in the T-direction is adjusted at each stage as the computations proceed in order to ensure that the lattice point at which the values of V and R are to be found lies within the region of determinacy of the lattice points used in the calculation. Again, with reference to Fig. XIV-2, ΔT must be chosen small enough so that the lattice point W, for example, whose values of V and R are to be found from those at lattice points X and Y, lies in the shaded region defined by the fast-wave characteristic C_X^+ emanating from point X and the slow-wave characteristic C_Y^- emanating from point Y. This has been shown to be the condition

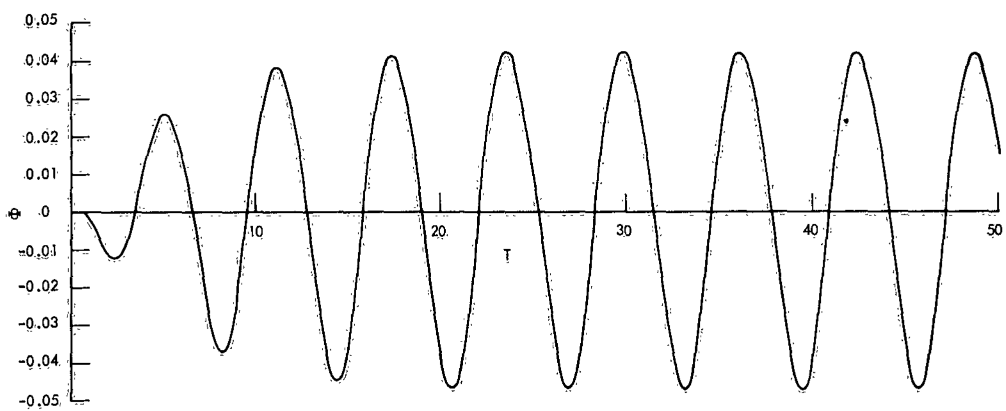

Fig. XIV-3. Typical terminal voltage waveform.

for which the solution of the difference equations converges to the solution of the differential equations in the limit of zero mesh spacing.[4,5] It is apparent that for this scheme to work, the flow must be supercritical so that the slope of the C_Y^- characteristic is positive.

In order to provide the most favorable conditions for energy conversion, the coil span L was chosen so that the terminal impedance of the monotron, as determined by small-signal analysis,[1] was negative real.

A typical terminal voltage waveform is shown in Fig. XIV-3. For this case the entry velocity was taken to be twice the magnetoacoustic speed ($c=0.5$), $S = 0.01$, $P = 0.5$ and $\omega L/v_o = 3\pi/8$. If an efficiency of energy conversion is defined as the ratio of the average electric power extracted from the fluid to the mechanical power incident on the monotron at $Z = 0$, the efficiency for the case illustrated is found to be 0.1 per cent, a very low value indeed. Note, too, the almost sinusoidal shape of the steady-state waveform. Indeed, for all allowed values of S and P, that is, all values that lead to solutions satisfying assumption (b), the steady-state output waveforms are sinusoidal in appearance and yield very low values of efficiency. We conclude that the regime studied is still essentially a linear one. In further work we shall attempt to remove the restriction that the flow be supercritical everywhere. This will undoubtedly lead to more distorted waveforms accompanied, we trust, by higher efficiencies.

The numerical calculations for the work described here were performed on the IBM 7090 computer of the Computation Center, M.I.T.

A. J. Schneider

References

1. H. A. Haus, Magnetohydrodynamic Monotrons, Internal Memorandum, Research Laboratory of Electronics, M.I.T., April 1961.

2. H. A. Haus and A. J. Schneider, A large-signal, steady-state solution for a one-dimensional plasma coupled to a traveling-wave circuit, Quarterly Progress Report No. 64, Research Laboratory of Electronics, M.I.T., January 15, 1962, pp. 90-92.

3. J. J. Stoker, Water Waves (Interscience Publishers, New York, 1957), p. 469 ff.

4. Ibid., p. 474 ff.

5. R. Courant, E. Isaacson, and M. Rees, On the solution of nonlinear hyperbolic differential equations by finite differences, Communs. Pure and Appl. Math. 5, 243 (1952).

B. AN ALTERNATIVE PROOF OF STABILITY FOR THE MAGNETOHYDRODYNAMIC WAVEGUIDE

It was shown in an earlier report[1] that the magnetohydrodynamic (MHD) waveguide is stable for all geometric configurations and for all values of the parameters describing the MHD beam. The proof given there involved an investigation of the two types of modes that can exist in such a waveguide. It was shown that the dispersion relation for one set of modes and the boundary conditions for the other set admit of only stable solutions. It can be shown that these results follow more simply from an investigation of the form of the power theorem that all solutions must satisfy. In this report we present the simpler stability proof to confirm the earlier one and to show again the importance of small-signal power theorems.

In the equations and boundary conditions relevant to the MHD waveguide, the frequency ω and the dc beam velocity v_o appear only in the combination $\omega_r = \omega - \beta v_o$, which is the frequency in a coordinate system moving with beam velocity. We can, therefore, always transform the equations into a coordinate system in which the beam is stationary without changing their form. A system is stable if the energy term in its small-signal power theorem (provided that it satisfies a power theorem) is positive definite[2] since, in that case, all real values of β require real values of ω_r. The energy term in the MHD power theorem[3] is

$$w = w_m + w_k = \frac{1}{2\mu_o} \overline{B} \cdot \overline{B} + \frac{1}{2} \rho_o \overline{v} \cdot \overline{v} + (\overline{v}_o \cdot \overline{v})\rho + \frac{p\rho}{2\rho_o} + \frac{\rho_o v_o}{B_o} \overline{B} \cdot \overline{v},$$

which is positive definite when v_o is set equal to zero. (Note that in Quarterly Progress Report No. 66 (page 125), Eq. 9 and the equations for S_K and w_k are in error. The term $(v_o/B_o)\overline{B} \cdot \overline{v}$ should be $\rho_o(v_o/B_o)\overline{B} \cdot \overline{v}$.) Thus, ω_r (and, therefore, ω) is real for all real β, and according to Sturrock[4] this is a sufficient condition for stability.

J. R. Cogdell

References

1. J. R. Cogdell, A stability proof for magnetohydrodynamic waveguides, Quarterly Progress Report No. 67, Research Laboratory of Electronics, M.I.T., October 15, 1962, pp. 76-79.

2. For a discussion of this application of the small-signal power theorem, see H. A. Haus, Small Signal Conservation Theorems, a paper presented at the Symposium on Plasma Physics, Faculté des Sciences, Orsay, France, September 10-21, 1962.

3. J. R. Cogdell, A magnetohydrodynamic small-signal power theorem, Quarterly Progress Report No. 66, Research Laboratory of Electronics, M.I.T., July 15, 1962, pp. 123-129.

4. P. A. Sturrock, Kinematics of growing waves, Phys. Rev. 112, 1488-1503 (1958).

C. SCATTERING OF LIGHT FROM ELECTRONS II

Using the apparatus indicated in Fig. XIV-4, we have observed scattering of optical radiation from an electron beam. Light from a ruby laser was focused to intersect an electron beam at right angles and the scattered radiation was observed at an angle $\theta = 65°$

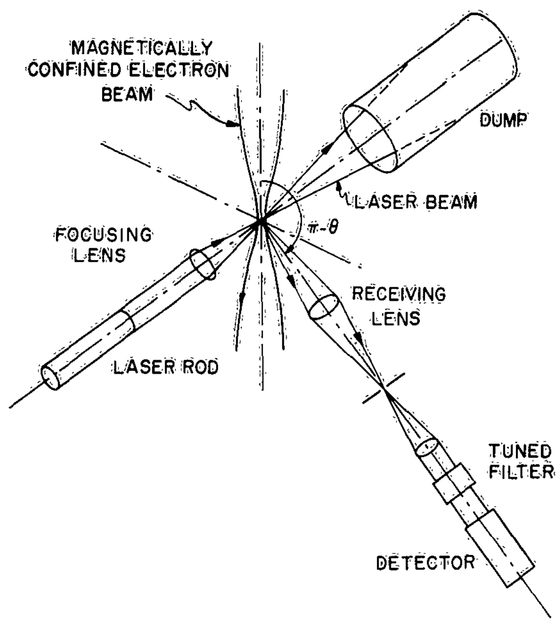

Fig. XIV-4. Simplified diagram of the apparatus.

with respect to this beam. The laser produced bursts of light at 6934 Å of approximately 20 joules and 800-μsec duration. An electron density estimated at $\sim 5 \times 10^9$ cm^{-3} was produced by magnetically focusing a 2-kv 75-ma electron beam. The polarization of the incident light was adjusted to be parallel to the magnetic field.

The scattered radiation from a volume ~2 mm in diameter was collected by the receiving lens, 20-mm in diameter, at a distance of 80 mm. After passage through an iris (to limit the field of view) and a system of filters, this radiation was detected by a photomultiplier with an S20 response, cooled to liquid-nitrogen temperature. The interference filters enabled us to reject the laser light scattered from the walls of the vacuum system, and to accept only the scattered radiation that was Doppler-shifted 259 Å. The bandwidth was limited to approximately 10 Å in order to reduce the background illumination from the electron gun. Oscilloscope traces of 2-msec duration of the photomultiplier output were obtained for the three cases:

(a) signal plus noise, i.e., the laser beam impinging on the electron beam;

(b) electron-beam noise, i.e., light from the filament plus possible excitation of residual gas by the beam.

(c) laser noise, i.e., the laser light scattered into the receiver in the absence of the electron beam.

As the photomultiplier dark current can be ignored, the sum of the photoelectron counts in (b) and (c) gives the total noise. Hence the difference between (a) and [(b) plus (c)] is a measure of the signal that is due to Thomson scattering. Many such groups of oscillograms were taken. The average value of this difference and its standard deviation are tabulated here for three series of trials.

Number of Trials	Average Thomson Photoelectrons	Standard Deviation
15	3.4	1.14
21	1.85	0.90
22	5.8	1.85

The variation in the average count for the three series is thought to be caused by changes in alignment. Also, in the last series there was a 20 per cent increase in the laser output, and the focusing of the electron beam was improved.

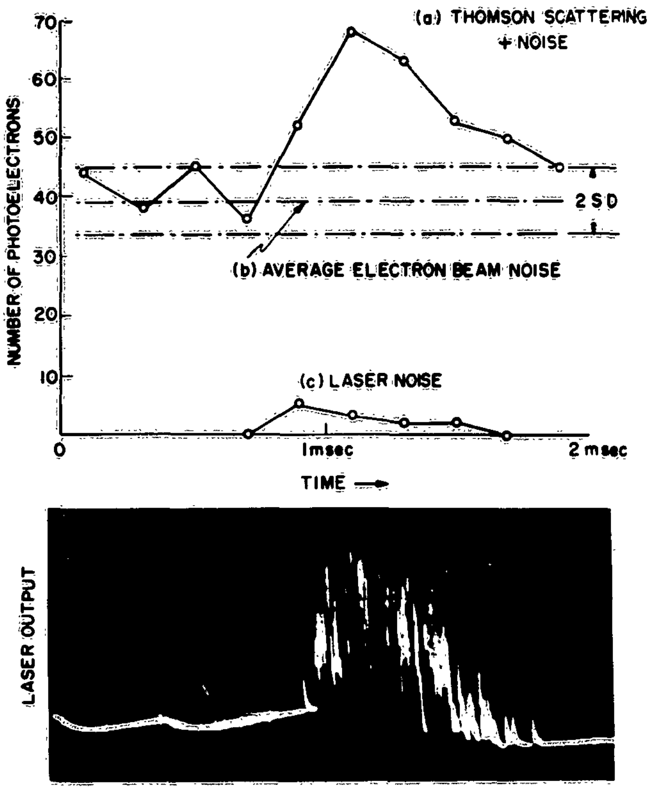

(d)

Fig. XIV-5. Number of photoelectrons in successive 0.2 msec intervals (summed over 36 successive trials) resulting from (a) Thomson scattering plus noise and (c) laser light scattered into the receiver in the absence of the electron beam. (b) Average electron beam noise and (d) oscillogram of the laser output.

Figure XIV-5 shows for the first two series of trials: (a) the total number of photoelectrons observed in successive 0.2-msec intervals; (b) the average noise level that is due to the electron beam and its standard deviation; (c) the contribution from the "laser noise"; and (d) an oscilloscope trace of the laser output.

The signal-to-noise ratio that we obtained could undoubtedly be improved by providing better trapping for the light from the electron-gun cathode and/or by using a dark emitter instead of the tantalum cathode that we used in our experiment. Also, higher beam current and better focusing should not be too difficult to obtain. Larger laser output would, of course, be beneficial because even in this initial experiment the isolation between the two optical paths, input and detector, was sufficiently good that the laser noise was almost negligible. By using this technique, it should be possible to study the profiles of high-density electron beams used, for example, in klystrons and traveling-wave tubes, and as these beams are usually of fairly high voltage, the large transverse Doppler shift will enable observations to be made at right angles to the electron beams.

G. Fiocco, E. Thompson

D. USE OF FISSILE NUCLIDES IN FUSION REACTOR BLANKETS

The investigation of the problem of the fusion reactor blanket with fissile nuclides discussed in Quarterly Progress Report No. 67 (page 91) has been continued. Most of the neutron multiplication and tritium breeding calculations have been finished, and the study of heating in the blanket is in progress. The calculations were made for slab blanket configurations with a diffuse plane neutron source.

1. Blanket Assembly with Th^{232} First Wall

In checking the calculations for the case of the metallic thorium first wall, an error was discovered in the thorium (n, 3n) reaction cross sections, and thus the results reported in Quarterly Progress Report No. 67 (page 92; see Table VIII-2) are incorrect. The results of the calculations based on the corrected cross-section data appear in Table XIV-1; the increase in tritium regeneration is approximately 8 per cent.

Calculations for a blanket assembly with a Th^{232} first wall (Table XIV-2) indicate that increasing the concentration of the lithium 6 isotope in the fused-salt coolant effectively reduces the neutron absorption in the first wall. A change in Li^6 concentration from its natural abundance (7.4 per cent) to 50 per cent increases the tritium production from 1.135 to 1.263 tritons per incident neutron for a 2.0-cm thick Th^{232} first-wall configuration. This rise in the regeneration ratio should be sufficient to ensure a self-sustaining tritium cycle for the fusion reactor.

To reduce the heat removal problems that arise because of the large amount of fission energy produced in the thorium, it is desirable to make the first wall as thin as structural and neutronic considerations will permit. Results were obtained for a 1.0-cm

Table XIV-1. Results of thorium first-wall calculations.

Th^{232} first-wall thickness	2.00 cm	1.00 cm	1.50 cm	2.00 cm
Li^6 concentration in both fused-salt regions	natural	50%	50%	50%
Fission rate	0.033	0.018	0.026	0.033
First-wall multiplication	0.372	0.206	0.294	0.373
First-wall absorption	0.261	0.055	0.093	0.134
Total neutron leakage	0.056	0.031	0.029	0.028
Tritium regeneration ratio	1.135	1.183	1.229	1.263

All results are per unit primary source neutron.

Table XIV-2. The three basic blanket configurations considered in this report.

Th^{232} First Wall

Vacuum	First wall	First-wall coolant	Primary attenuator	Thermal shield
	Th^{232}	$66LiF$-$34BeF_2$	$21C$-$79(66LiF$-$34BeF_2)$	
	A	6.25 cm	56.0 cm	

Data pertaining to individual calculations are given in Table XIV-1.

U^{238} Fused-Salt First-Wall Coolant

Vacuum	First wall	First-wall coolant	Primary attenuator	Thermal shield
	Mo	LiF-BeF_2-UF_4	$21C$-$79(66LiF$-$34BeF_2)$	
	1.0 cm	6.25 cm	49.0 cm	

Data pertaining to individual calculations are given in Tables XIV-3 and XIV-4.

U^{238} Fused-Salt Primary Attenuator Coolant

Vacuum	First wall	First-wall coolant	Primary attenuator	Thermal shield
	Mo	$66LiF$-$34BeF_2$	$21C$-$79(73LiF$-$27UF_4)$	
	1.0 cm	1.5 cm	49.0 cm	

Data pertaining to individual calculations are given in Table XIV-5.

All compositions are given in mole fraction percentages.

and a 1.5-cm thick first wall with a Li^6 concentration of 50 per cent; the minimum thickness is approximately 1.0 cm. The thickness of the first wall may be reduced further if the loss in the thorium neutron multiplication is compensated for by the addition of metallic beryllium to the attenuator region. (This possibility is discussed below in connection with the uranium fused-salt systems.) But, if the multiplication in thorium is so low that beryllium is needed to supplement it, then the use of thorium in the blanket seems purposeless.

2. Blanket Assembly with UF_4 Fused Salts

The plasma blanket system containing a lithium-beryllium-uranium fluoride fused salt in the first-wall coolant region has been studied for three salt compositions. The effects of increasing the isotopic concentration of Li^6 in the fluoride salt, and of adding metallic beryllium to the primary attenuator have been investigated. A system that contains the uranium-bearing fused salt in the attenuator (third) region also has been explored.

The three salts considered are $73LiF\text{-}27UF_4$, $60LiF\text{-}30BeF_2\text{-}10UF_4$, and $71LiF\text{-}16BeF_2\text{-}13UF_4$. The first two salts have been described previously[1]; the third mixture is the eutectic composition for a melting point of approximately 450°C.

Calculations indicate that for a first-wall coolant that is approximately 6.25 cm thick and contains uranium (Table XIV-2), a Li^6 concentration of 15-20 per cent is needed in both the first-wall coolant and the primary attenuator to give a tritium regeneration ratio of 1.15. Neutron capture is reduced in both the molybdenum first wall and the uranium in the coolant by the competing $Li^6(n,t)$ reaction; also, a large percentage of the leakage neutrons are utilized for tritium production by this reaction. The maximum tritium regeneration obtained was 1.271 for the $73LiF\text{-}27UF_4$ system, with a Li^6 concentration of 50 per cent in both fused-salt regions. The results of these calculations are summarized in Table XIV-3.

In the uranium-containing fused-salt blanket, the production of Pu^{239} for fission reactor fuel may be worth considering.[1] A favorable economic balance between tritium regeneration and plutonium production may be achieved by proper choice of the Li^6 concentration.

The tritium production in the blankets discussed above may be increased by including a region of metallic beryllium between the first-wall coolant and the primary attenuator. Calculations were made for the equivalent of a 5.0-cm thick slab of beryllium homogenized throughout the attenuator region; the results show a gain in the tritium breeding ratio of approximately 5 per cent. This homogeneous treatment was made necessary by the use of the three-region code,[2,3] and the results are conservative. The results are given in Table XIV-4.

The third blanket assembly shown in Table XIV-2 was investigated. Placing the

Table XIV-3. The effect of the Li^6 concentration in the fused salts on the tritium regeneration.

First-wall coolant composition (LiF-BeF_2-UF_4)	60-30-10	60-30-10	71-16-13	71-16-13	73-00-27[a]	73-00-27	73-00-27
Li^6 concentration in both fused-salt regions	natural	20%	natural	20%	natural	20%	50%
Fission rate	0.027	0.027	0.036	0.036	0.066	0.063	0.063
U^{238} multiplication	0.120	0.120	0.159	0.159	0.291	0.278	0.278
U^{238} absorption	0.101	0.062	0.122	0.076	0.231	0.144	0.084
Total neutron leakage	0.093	0.066	0.092	0.065	0.088	0.064	0.046
Tritium regeneration ratio	1.070	1.152	1.082	1.172	1.077	1.197	1.271

All results are per unit primary source neutron.

All compositions are given in mole fraction percentages.

[a]These calculations were made with a 6.68-cm thick first-wall coolant region.

Table XIV-4. The effect of adding metallic beryllium to the attenuator region on the tritium regeneration.[a]

First-wall coolant fused-salt composition (LiF-BeF_2-UF_4)	60-30-10	73-00-27
First-wall coolant thickness	6.25 cm	6.25 cm
Li^6 concentration in both fused-salt regions	natural	50%
Fission rate	0.027	0.063
U^{238} multiplication	0.120	0.278
U^{238} absorption	0.105	0.088
Total neutron leakage	0.086	0.048
Tritium regeneration ratio	1.141	1.332

The equivalent of 5 cm of beryllium metal is homogenized throughout the primary attenuator.

All results are per unit primary source neutron.

All compositions are given in mole fraction percentages.

[a] Compare with results in Table XIV-3.

Table XIV-5. The results for the calculations with $73LiF$-$27UF_4$ in the attenuator region.

Li^6 concentration in both fused-salt regions	natural	50%	50%
Beryllium enrichment in third region	0	0	~5.0 cm
Fission rate	0.110	0.109	0.100
U^{238} multiplication	0.449	0.444	0.403
U^{238} absorption	0.655	0.222	0.221
Total neutron leakage	0.120	0.062	0.063
Tritium regeneration ratio	0.751	1.248	1.303

All results are per unit primary source neutron.

$73LiF-27UF_4$ fused salt in the third region gave a tritium production of only 0.751 with natural lithium in the salt; a Li^6 concentration of 50 per cent increased this value to 1.248, and the further addition of the equivalent of 5.0 cm of beryllium to the attenuator region raised the tritium regeneration ratio to 1.303. This configuration has the advantage of distributing the fission energy over a large volume, thus reducing the peak fused-salt temperature and the resultant heat-removal problems. The fission and neutron capture rates are also increased over the corresponding rates in the systems discussed above. Thus, the total power output of the fusion reactor is raised, and a greater amount of Pu^{239} is produced. Table XIV-5 contains the results of the calculations for this blanket system.

3. Discussion

It is possible to obtain sufficient neutron multiplication with both a metallic Th^{232} first wall and a U^{238} fused-salt coolant blanket assembly to support a self-sustaining tritium cycle. Of the systems considered, the thorium first-wall configuration seems to be the least attractive because (a) the fission energy is liberated in a structural member that is already at a high temperature by virtue of its location, and thus the cooling problem is increased; (b) the build-up of fission products will decrease its effectiveness in neutron multiplication; and (c) radiation and fission damage may reduce its value as a structural support for the blanket assembly.

The uranium fused-salt systems seem practical and feasible because (a) the fission heat is deposited in the coolant itself; (b) fission products can be extracted continuously from the circulating fused salt; (c) the concentration of the uranium fluoride can be varied to control the power output; and (d) an economic balance between tritium regeneration and Pu^{239} production might be achieved by varying the Li^6 concentration in the fused salt.

L. N. Lontai, D. J. Rose, I. Kaplan

References

1. L. N. Lontai and A. J. Impink, Use of fissile nuclides in fusion reactor blankets, Quarterly Progress Report No. 67, Research Laboratory of Electronics, M.I.T., October 15, 1962, pp. 91-94.

2. W. G. Homeyer and A. J. Impink, Energy extraction blanket for a fusion reactor, Quarterly Progress Report No. 64, Research Laboratory of Electronics, M.I.T., January 15, 1962, pp. 128-131.

3. W. G. Homeyer, A. J. Impink, and D. J. Rose, Energy extraction blanket for a fusion reactor, Quarterly Progress Report No. 66, Research Laboratory of Electronics, M.I.T., July 15, 1962, pp. 142-150.

E. DESIGN AND CONSTRUCTION OF A LARGE PLASMA FACILITY

A facility whose design and construction was started by S. O. Dean (a former student) has now been completed. The machine provides a high-vacuum volume of 23 liters and has a pumping capacity of 500 μ-l/s in the pressure range $10^{-2} \div 10^{-3}$ Torr. Solenoid coils can produce a mirror region in the vacuum tank which measures 1.25 meters and 0.20 meter I.D. with mirror ratio $R \approx 5$ and mirror field ~3.2 kgauss at 200 amps. The mirror ratio can be varied by moving the two solenoids on rails. In the present use, the machine is arranged for a hollow-cathode discharge experiment running longitudinally in the mirror. (See Fig. XIV-6.) A special probe was designed for related measurements.

The high-vacuum tank consists of a central box (50 × 50 × 25 cm) and two cylindrical,

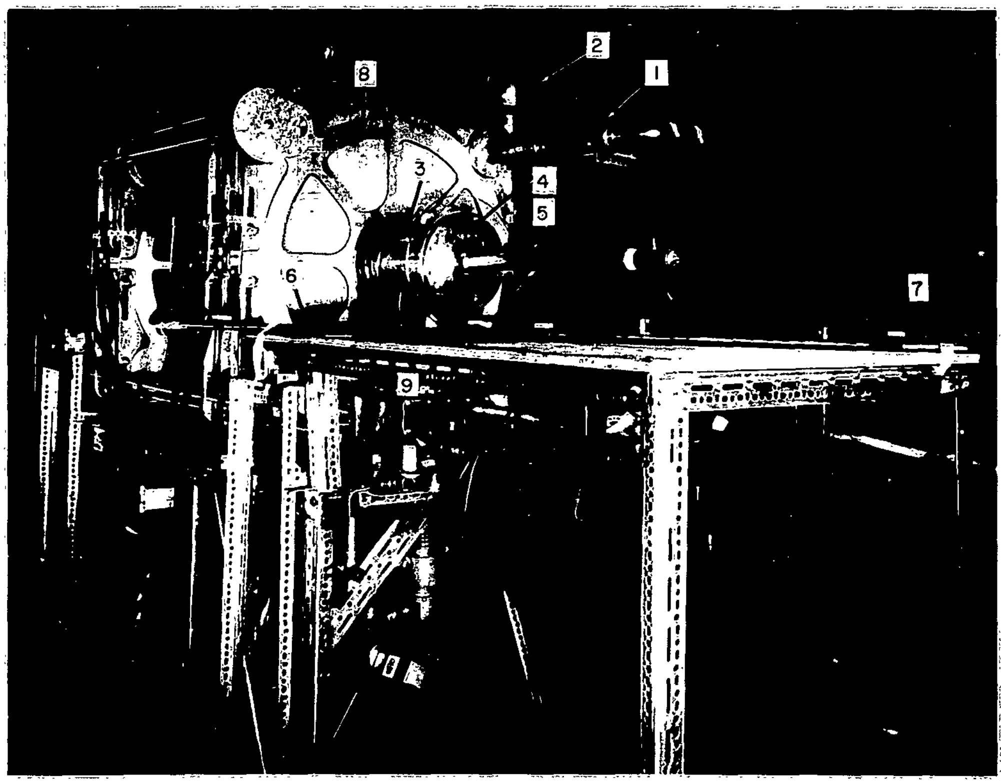

Fig. XIV-6. Plasma facility from anode end. (1) Magnet cooling-loop sliding seal. (2) Cooling-loop expansion tank. (3) High-vacuum tank extension. (4) Position of sliding seal for probe. (5) Anode electrode, inserted in tank through sliding seal. (6) and (7) Probe holder inside its coaxial rail; the four visible insulated supports fasten the rail to the vacuum tank's inside wall. (8) Magnet. (9) Baffle on top of one of three diffusion pumps.

20-cm I.D. arms, extending longitudinally through the mirror coils. Three extensions, 15-cm I.D., connect the tank to the diffusion pumps that are topped by water-cooled baffles and gate valves. Cooling of the side arms is achieved by water circulation (Fig. XIV-7).

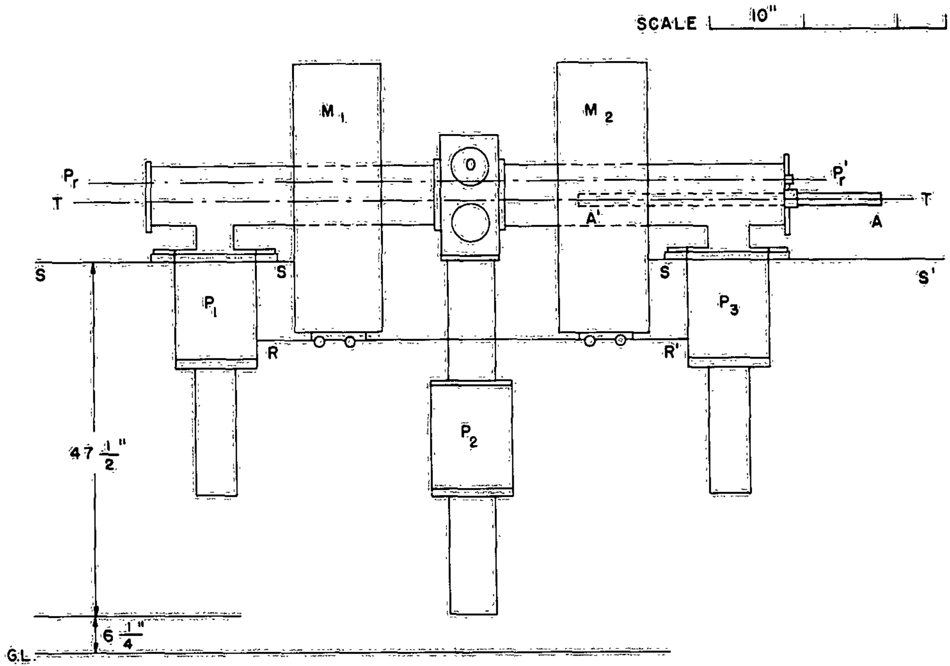

Fig. XIV-7. Assembly. AA', anode (cathode not shown); M_1M_2, magnet coils; O, observation ports; $P_1P_2P_3$, diffusion pumps and baffles; P_rP_r', probe-holder axis; TT', mirror axis; RR', magnet rails.

Each of the two solenoids consists of four aluminum double pancakes, 73-cm outside radius, and 5 cm thick. The pancakes are spaced 1.25 cm apart and are connected externally in series and are contained and supported along one diameter by a cast aluminum box (85 × 85 × 25 cm).

The coolant is circulated from the top to the bottom of the assembly and in direct contact with the coils. Pure distilled water or ethylene glycol is used. The circulation is in a closed loop, and a heat exchanger is installed in series with it; city water is used for heat removal. To enable movement of the magnets, sliding O-ring seals are installed in the cooling loop.

The electrodes for the hollow-cathode discharge are of standard design,[1] but more care than usual was taken in cooling the tips. These are almost entirely hollow and contain two rows of fins to improve the heat removal. Water is circulated in through a peripheral sleeve, and out axially. The electrodes can slide axially through O-ring seals in the end flanges of the side arms. The power supply consists of two AIRCO welding rectifiers in series, giving 200 amps at 80 volts under load. A spark-gap oscillator is included in the circuit as starter; a filter reduces the ripple to less than 1 per cent.

To probe the hollow-cathode discharge, whose maximum length can be 1.6 meters, Langmuir probes are used. Two of these, rigidly connected, are installed; they can be moved parallel to the mirror axis and rotated in a normal plane. The probe tip describes a circular path, 45° wide, through the mirror axis. The probes are placed 75 cm apart on a supporting arm 1.9 meters long. Each probe tip can span 80 cm of the arc; overlap of the two probe positions allows for reciprocal calibration. The movement is imposed from the outside through a sliding O-ring seal in the end flange. The stainless-steel holder arm contains and seals the probe leads; it is longitudinally supported in the tank by a coaxial cylindrical rail, 2.0 meters long. The rail also serves as screen against the sputtering from the arm.

F. Alvarez de Toledo

References

1. W. D. Getty, A low-pressure gas-arc discharge, Quarterly Progress Report No. 57, Research Laboratory of Electronics, M.I.T., April 15, 1960, pp. 27-29.

F. ENERGY EXTRACTION BLANKET FOR A FUSION REACTOR

Work on nonfissile systems has been completed and final reports are being prepared as theses[1,2] for submission to the Department of Nuclear Engineering, M.I.T.

Heating calculations have revealed that each 14.2 Mev D-T neutron will produce approximately 17.5 Mev of recoverable heat in the blanket. The maximum energy flux of 14.2 Mev neutrons that can be tolerated on a 2-cm molybdenum first wall is 4-5 Mw/m^2. Thermal stress and heat transfer to a fused Li_2BeF_4 coolant are both limiting at this power. The total blanket thickness necessary to shield superconducting coils is 110-120 cm.

W. G. Homeyer, A. J. Impink, Jr., D. J. Rose, I. Kaplan

References

1. W. G. Homeyer, Thermal and Chemical Aspects of the Thermonuclear Blanket Problem, Sc.D. Thesis, Department of Nuclear Engineering, M.I.T., December 1962.

2. A. J. Impink, Jr., Neutron Economy in Fusion Reactor Blanket Assemblies, Ph.D. Thesis, Department of Nuclear Engineering, M.I.T., January 1963.

G. SUPERCONDUCTING SOLENOID

1. Test of a Large Superconducting Coil

While the construction of the vessel and accessories of the large superconducting magnet[1] is progressing satisfactorily, we have proceeded to test a set of three coils in order to evaluate and choose the best design to be used for the remaining coils of the larger magnet. We have also developed an IBM 7090 computer program for the calculation of the magnetic field in any coil or set of coils.

The three coils have been tested in a vertical 14.00-in. liquid-helium dewar.[2] Figures XIV-8, XIV-9, and XIV-10 show close-up views of the coil X1 alone, the set of three coils, and the coil assembly with the dewar.

The specifications of the coils are given in Table XIV-6. Their differences are essentially in the winding, which for the coil X1 was made by using insulated Nb-Zr wire; some copper wire was wound inside and outside for the purpose of protection. For coil X2, the same insulated superconducting wire was used, but it was wound with bifilar copper magnet wire. Finally, coil X3 was made by using insulated copper-plated Nb-Zr, 0.0012 in. thick. No secondary copper winding was used. Figure XIV-11 shows the detail of the winding of coil X1.

Coil X1, which was ready first, underwent the most intensive testing, both alone and with the two other coils.

Intensive investigation of the quenching characteristics has been carried out in order to find the eventual training effect, deterioration of the critical current of the coil and energy balance in the various circuits, as well as the quenching current.

The listings in Table XIV-6 also indicate that the training effect was nonexistent for the three coils and, moreover, that the quenching current is not associated with the rate at which the current is increased (from 20 seconds to 5 minutes for a full increase). For coils X1 and X3 no deterioration of their properties was observed, although the energy involved became quite large (5 kilojoules with the three coils running). The recovery time after quenching is approximately 20 seconds. The deterioration of coil X2 has been found to be due to a kink in the wire which progresses up to a complete break.

The transient phenomena that occur at quenching have been recorded with an oscilloscope for coil X1 only. We have not been able to record the transient in coil X3, probably because of too small a rate of quenching. Figures XIV-12 and XIV-13 illustrate the basic process of quenching. For a single winding, the current decay is approximately 0.030 second. When two windings are separately driven, there is quite a big delay (0.260 sec) between the quenching of the two coils.

By integration of the transient curve of the copper coil, one can calculate the energy that has been dissipated in its external resistance (3 ohms). It appears that in our case only 2 per cent of the magnetic energy has been dissipated into the external resistance.

Table XIV-6. Coil data and results of the tests.

	X1			X2			X3	Notes
	inner	outer	total	inner (bifilar)	outer	total	total (copper-plated)	
I.D. (in.)	11.562	12.584	11.562	11.390	12.696	11.390	11.390	
Turn spacing	0.0124	0.0127	0.0126	0.0257	0.0116	(0.0190)	0.0144	( ) average value
Layer spacing	0.020	0.020	0.020	0.0172	0.022	(0.0202)	0.0242	
Space factor (%)	31.7	30.9	31.2	17.8	30.5	(20.4)	22.5	Length of each winding: 1.750 in.
Turns	1841	2740	4581	2580	1661	4241	4449	
Length of wire (ft)	5745	9363	15109	8419	5738	13757	14930	
Quenching current								
Minimum	20.0	16.0	15.1	15.1	16.0	11.5	20.0	
Maximum	22.7	19.0	16.7	18.5	18.5	15.5	22.0	
Average	22.0	18.0	16.0	(17.0)	(17.0)	(15.0)	21.5	
B av quench (kg) (central field)	0.818	1.880	2.880	1.080	1.780	2.500	3.750	
Number of quenches	46	10	57	8	10	10	10	
Training	No	No	No				No	
Deterioration	No	No	No			Yes	No	

Maximum field recorded with the three coils running together. 5,600 kgauss on the axis, that is, 11,000 gauss on the edge of the coil.

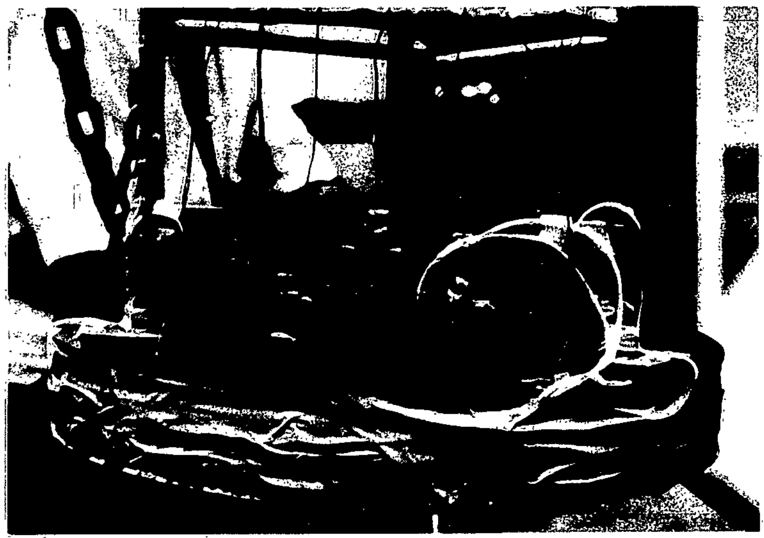

Fig. XIV-8. Coil X1 with its connections.

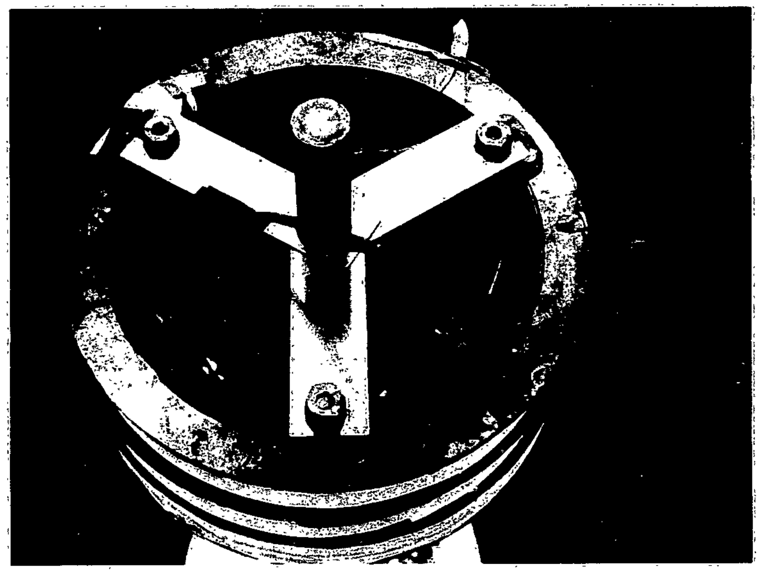

Fig. XIV-9. Three-coil arrangement with the terminal switches inside the coils.

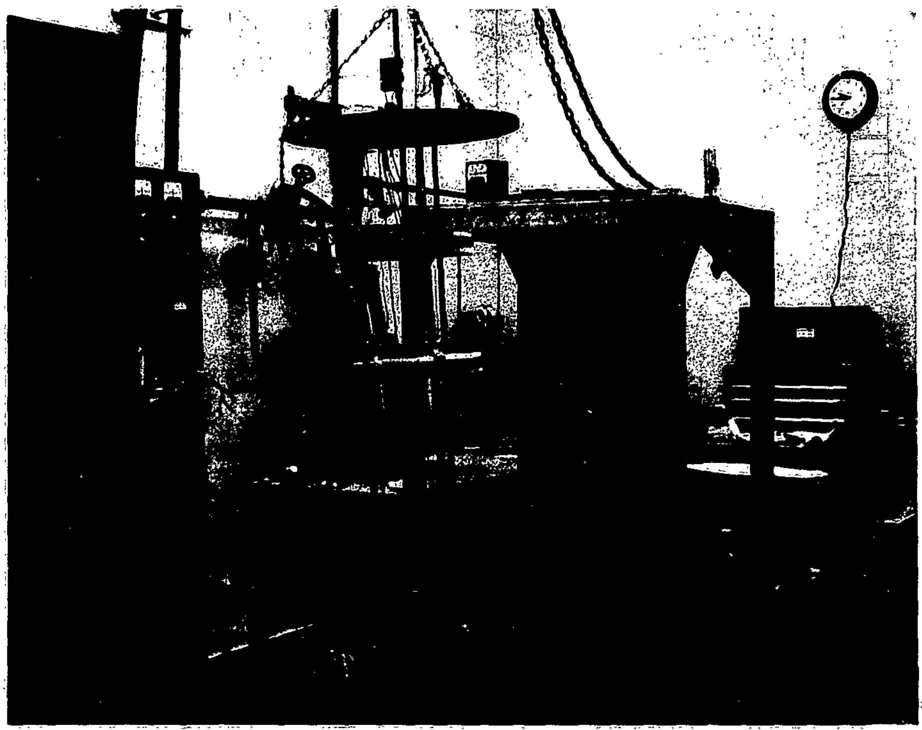

Fig. XIV-10. Coil X1 with its support, the 14-in. dewar.

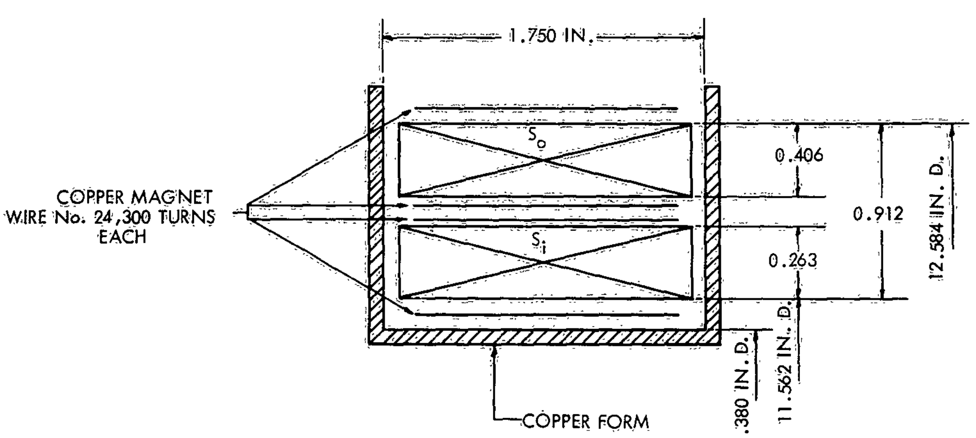

S_i INSIDE SUPERCONDUCTING WINDING - 1841 TURNS IN 13.13 LAYERS SEPARATED WITH 0.075 IN. MYLAR FOIL SPACE FACTOR 31.7%- 5745 FT., 1.681 LBS. OF Nb-Zr WIRE

S_o OUTSIDE SUPERCONDUCTING WINDING - 2740 TURNS IN 20.27 LAYERS SEPARATED WITY 0.075 MYLAR FOIL SPACE FACTOR 30.9%- 9363 FT., 2.816 LBS OF Nb-Zr WIRE

ALL THE WINDING IS ENCAPSULATED INTO AIR-DRY VARNISH (No. =301 OF PEDIGREE COMPANY)

Fig. XIV-11. Schematic cutaway of the winding of the X1 coil.

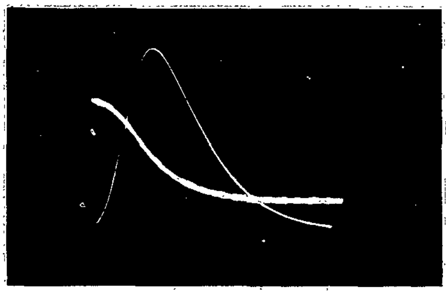

Fig. XIV-12. Quenching transient for inner coil. The bell-shaped curve is the voltage (across a 3-ohm resistor) of the current in the copper coil. Scale, 5 volts/cm. The other curve is the decay of the superconducting current, 5 amp/cm. Time scale, 5 msec/cm. Quenching time, 30 msec.

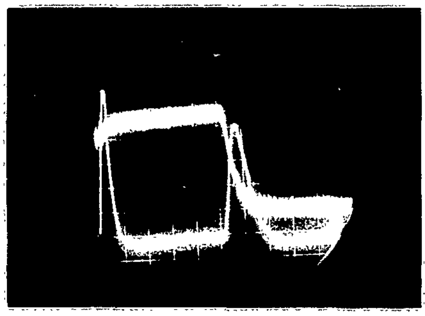

Fig. XIV-13. Quenching transient for the two windings in parallel. The curve with two peaks is for the copper coil (5 volts/cm across 3 ohms). Other curve is for the current in the inner coil (5 amps/cm). Time scale, 50 msec/cm. Quenching occurs in 2 steps: first, the outer coil quenches and current rises in the inner coil; second, after 0.260 sec the inner coil quenches. Each quenching takes approximately 30 msec.

This is due certainly to the large energy dissipation in the copper coil form, which was detected by a quick rise of its temperature.

The behavior of the copper-plated coil, X3, was found to be much more satisfactory than that of the two other coils in all respects. Its operation seems more stable, and it is possible to reach and maintain the current within a few per cent of the maximum value of the current. Moreover, its performances are approximately 30 per cent better than those of the other coils. Consequently, all of the remaining coils will be made of copper-plated wire similar to that used for coil X3.

The coils have been operated in the permanent current states, and differential

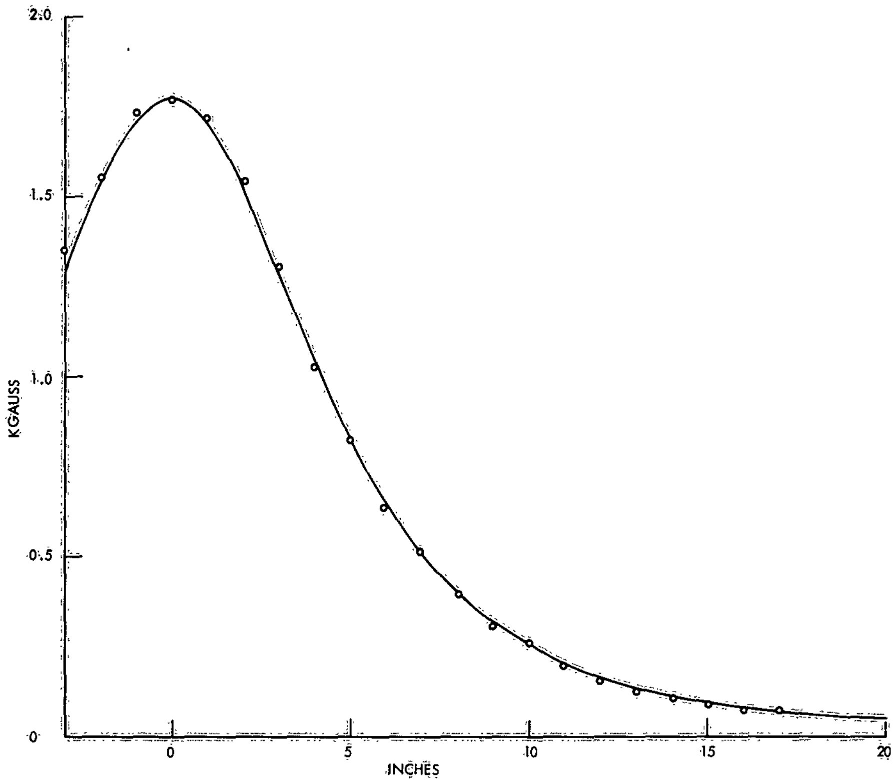

Fig. XIV-14. Field plot of coil X3 in permanent state. Current, 10 amps. The curve represents calculated values; measured values are plotted as o.

measurement of the magnetic field leads to the conclusion that there is no decay of the field (say, less than 10^{-4} per hour measured). The field plot measured in the permanent current state is shown in Fig. XIV-4 with the calculated value. The thermal switches operate very satisfactorily. Their power consumption is 0.150 watt for warming up the gate wire to the critical temperature, and their switching takes approximately 1 second.

We have been able to pump the field from the X3 coil to the X1 and X2 coils by using the proper switching sequence in and out of the permanent mode. The highest field produced has been achieved in this way.

The clamped contacts have shown a contact resistance of the order of 10^{-7} ohms, which is also quite satisfactory.

2. Magnetic Field Calculation

An IBM 7090 computer program has been developed[3] for the calculation of both components of the magnetic field at any location of a solenoid, including the winding interior.

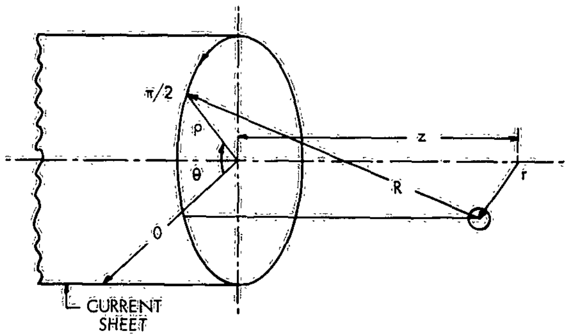

Fig. XIV-15. Coordinates used in calculation of the magnetic vector potential and magnetic field for a cylindrical geometry.

The program was then extended to calculate for a multicoil solenoid, for the reciprocal case of the determination of the current that will produce a given magnetic-field shape, and for the field of a uniformly distributed dipole in a solenoidal winding. All three cases are important for the evaluation of the performance of superconducting solenoids.

The principle of these field calculations is based on the splitting of the winding in several current sheets. We assume a uniform distribution on the current throughout the winding. It can be noted, then, that the program can be easily modified to fit any current distribution by weighting each current sheet accordingly.

The field is derived from the expression of the vector potential of a current loop[4-7]

$$A(r,z) = \frac{1}{2\pi}\int_0^{\pi} \frac{\cos\theta}{R}\, d\theta, \tag{1}$$

where R is the distance between the field point and the source point as shown in Fig. XIV-15:

$$R = [r^2-2r\cos\theta+1+z^2]^{1/2}. \tag{2}$$

The distances are normalized to the radius of the current sheet, and the vector potential (and subsequently the field) to the value of an infinitely long solenoid, that is, $\left(\mu\frac{NI}{L}\text{ in mks units or }\frac{4\pi}{10}\frac{NI}{L}\text{ in cgs units}\right)$.

For a current sheet extending from $z = S_1$ to $z = S_2$, the magnetic potential is

$$S(r,z) = \frac{1}{2\pi}\int_{S_1}^{S_2}\int_0^{\pi} \frac{\cos\theta}{R}\, d\theta ds. \tag{3}$$

If the order of integration is inverted, the integration with respect to S carried out, the angular integration modified by using the identity

$$\int_0^{\pi} F(\cos\theta)\, d\theta = \int_0^{\pi/2} F(\cos\theta)\, d\theta + F(-\cos\theta)\, d\theta, \tag{4}$$

and the origin S_1 extended to infinity, one obtains the vector potential of a semi-infinite current sheet:

$$A(r,z) = \frac{1}{2\pi}\int_0^{\pi/2} d\theta\, \cos\theta\, \ln\frac{z+\sqrt{z^2+r^2+1+2r\cos\theta}}{z+\sqrt{z^2+r^2+1-2r\cos\theta}} \tag{5}$$

The radial and axial magnetic fields are derived from the vector potential and are given by

$$H_r(r, z) = -\frac{\partial A(r, z)}{\partial z} \tag{6}$$

$$H_z(r, z) = \frac{1}{r}\frac{\partial}{\partial r}(rA(r, z)), \tag{7}$$

which, applied to Eq. 5, give

$$H_r(r, z) = \frac{2}{\pi} r \int_0^{\pi/2} \frac{\cos^2\theta \, d\theta}{Q_+Q_-(Q_++Q_-)} \tag{8}$$

and

$$H_z(r, z) = \frac{1}{2\pi}\int_0^{\pi/2} d\theta \cos\theta \left[\frac{1}{r}\ln\frac{z+Q_+}{z+Q_-} + \frac{2\cos\theta}{(z+Q_+)(z+Q_-)(Q_++Q_-)} \times \left(\left(\frac{z^2+1-r^2}{Q_+Q_-}\right)(z+Q_++Q_-) + z\right)\right]. \tag{9}$$

Here,

$$Q_+ = \sqrt{z^2+r^2+1+2r\cos\theta} \tag{10}$$

$$Q_- = \sqrt{z^2+r^2+1-2r\cos\theta}. \tag{11}$$

The field of a finite current sheet is obtained by superposition of negative and positive semi-infinite sheets:

$$H_{sol}(r, z) = H_{(r, z)} - H_{(r, z+s)},$$

where s is the normalized length of the solenoid.

From the basic current sheet calculations, the field is obtained by summation of current sheets.

$$H(r, z) = \sum_{n=1}^{N} H(r_s(n), z)/N, \tag{12}$$

where $r_s(n)$ is the relative radial distance of the field point with respect to the particular current sheet.

$$r_s(n) = r/\rho(n). \tag{13}$$

Several problems arise in the evaluation of the integrals. For z negative and $\theta = 0$, $Q_- = |z|$, so that $(z+Q_-) = 0$ and the integrand of H_z becomes infinite. This inconvenience is solved by using the following identity proper to a semi-infinite current sheet

$$\left.\begin{array}{ll} r < 1.0 & H_z(r, -z) = -H_z(r, z) + 1.0 \\ r = 1.0 & H_z(r, -z) = -H_z(r, z) + 0.5 \\ r > 1.0 & H_z(r, -z) = -H_z(r, z) \end{array}\right\} \tag{14}$$

For $z = 0$

$$\left.\begin{array}{ll} r < 1.0 & H_z(r, 0) = 0.5 \\ r = 1.0 & H_z(r, 0) = 0.25 \\ r > 1.0 & H_z(r, 0) = 0.0 \end{array}\right\} \tag{15}$$

Also, $H_r(r, z) = H_r(r, -z)$.

When $|r-1|$ and z both approach zero, the integrands of both H_r and H_z become very large when θ is small; indeed $Q_- \to 0.0$ for $|r-1|$, z, and $\theta \to 0.0$. Therefore, in order to conserve accuracy in the numerical integration, it has been found necessary to split the integration with emphasis in the range of $\theta \approx 0.0$. Various test runs, comparing the calculated values with those of Alexander and Downing,[6] have shown that the best accuracy was obtained with a three-part splitting, that is,

$$\int_0^{\pi/2} = \int_0^{0.0625} + \int_{0.0625}^{0.250} + \int_{0.250}^{\pi/2}$$

and by calculating Q_- as

$$Q_- = \sqrt{z^2 + (r-1)^2 + 4r \sin^2 (\theta/2.0)} \tag{16}$$

In such a way, an accuracy of the order of 10^{-6}, or better, can be maintained for $|r-1.0|$ and $|z| \geq 0.0005$, that is, well below any dimension of the wire used. The change from the single integration to a triple integration must occur in the vicinity of $|r-1.0|$ and $|z| \approx 0.4$.

Nevertheless, for $r = 1.0$ and $z = 0.0$, $H_r(1.0, 0.0) = \infty$. However, this is a purely mathematical conclusion, since, by definition, the thickness of the current sheet is zero, and the corresponding current density is infinite, a situation that never arises physically. To avoid such improper physical results, we stop the current sheet a distance ϵ from the corner, ϵ being less than the physical dimension of the actual current carrier. The use of a Gaussian integration procedure achieves the same purpose, since the lowest value of θ employed is not zero.

Finally, for $r = 0.0$, and for any z, the integrand of $H_z(r, z)$ again behaves badly for computation. However, in that case the field is calculated directly by integration of the Biot-Savard law for a thick solenoid of uniform current density.

$$H_z(0, z) = \frac{1}{2.0(\alpha-1)} \left[(\beta-\gamma) \ln \frac{\alpha + \sqrt{\alpha^2 + (\beta-\gamma)^2}}{1 + \sqrt{1 + (\beta-\gamma)^2}} + (\beta+\gamma) \ln \frac{\alpha + \sqrt{\alpha^2 + (\beta+\gamma)^2}}{1 + \sqrt{1 + (\beta+\gamma)^2}} \right] \tag{17}$$

See Fig. XIV-16 for definitions of α, β, and γ.

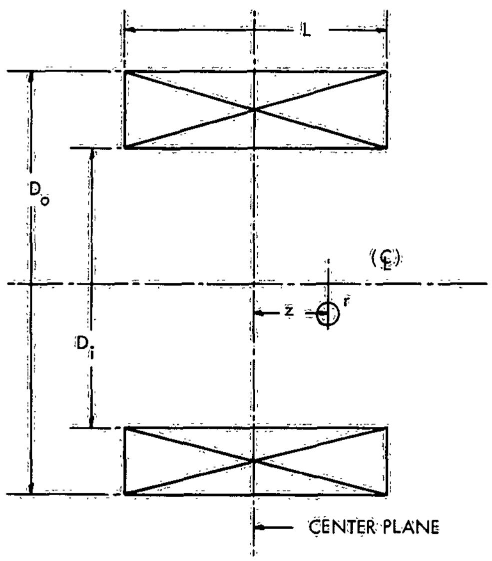

Fig. XIV-16. Configuration of a thick solenoid.

For a thin solenoid, $\alpha = 1.0$, and Eq. 17 becomes indeterminate. We replace it by the equation for the on-axis field of a current sheet

$$H_z(0,z) = \frac{1}{2.0}\left[\frac{\beta+\gamma}{\sqrt{1+(\beta+\gamma)^2}} + \frac{\beta-\gamma}{\sqrt{1+(\beta-\gamma)^2}}\right]. \tag{18}$$

Again, the field is normalized to the field of an infinitely long solenoid.

The program automatically provides selection between the various computation schemes so that the best accuracy and speed is obtained.

The numerical integration of Eqs. 2, 3, and 16 is carried out by a 10-point Gaussian quadrature. Test runs indicate that the accuracy is better than a 16-point Gaussian quadrature, probably because of less rounding-off error during the computation.

For a thick solenoid the accuracy may depend upon the number of current sheets in which the actual winding is split. When the field location is far away from the winding, fewer current sheets are required than when it is very close or inside the winding. There is no definite rule for selecting the optimum number of currents, and accuracy test runs must be made for each particular case. However, let us say that our results indicate that for a thin solenoid, that is, with thickness approximately 10 per cent of the radius, an accuracy of 10^{-5}, or better, is obtained with 5 current sheets for $r < 0.5$, and 10 current sheets for $r < 0.95$. Inside the winding, higher-order splitting is necessary, to approximately the same number as the physical number of layers, that is, from 20 to 30.

The results also have been compared with those obtained by spherical harmonic expansion.[8,9] We have found that using three terms of the expansion gives only 10^{-3} accuracy within 15 per cent of the radius for the z component, and very much less for the r component. The discrepancy between the two methods increases quickly when $r > 0.5$, and no comparison can be made for $r \geq 1.0$ because of nonconvergence of the harmonic expansion.

The basic computation is carried out in a subprogram that calculates H_z and H_r when called by a main program or subprogram. The input data of the subprogram are the inside diameter of the solenoid, the winding thickness, the solenoid length, the number of current sheets in which the winding is split, and the radial and axial field position with respect to the center of the solenoid.

The basic time to calculate the contribution of one current sheet to the H_r and H_z fields takes approximately 0.05 second on the IBM 7090 computer.

Consequently, for a field position that is far enough away from the winding so that

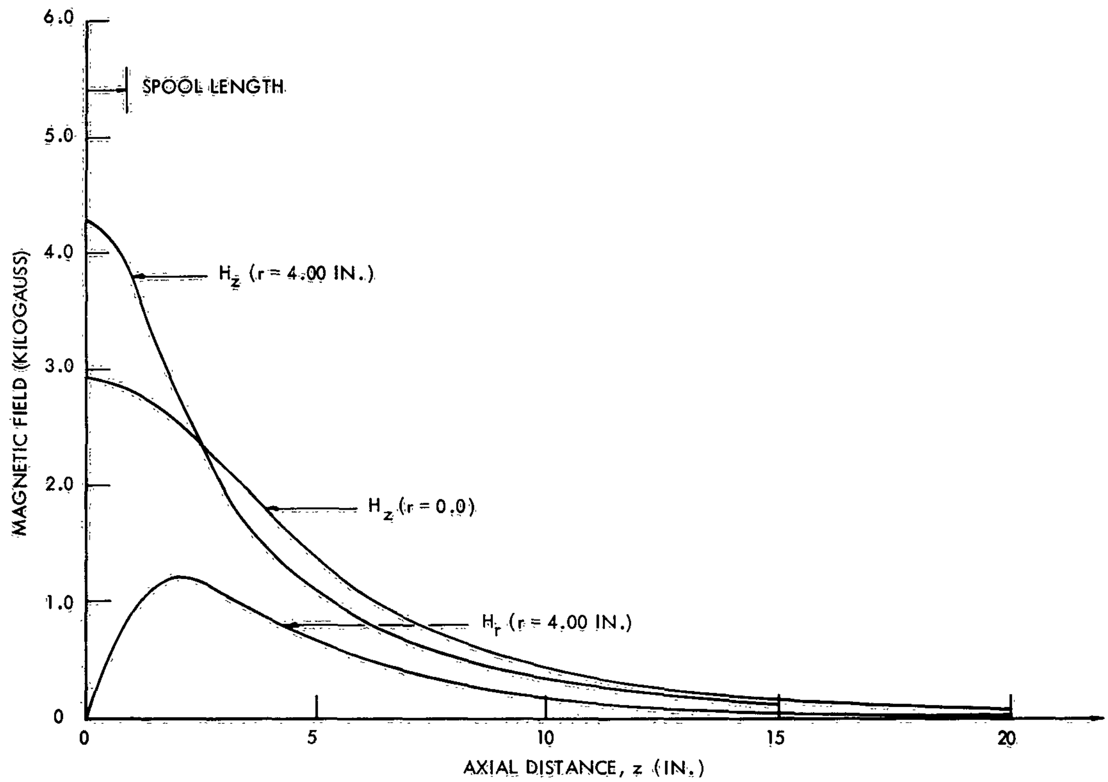

Fig. XIV-17. Field variation along the axis for coil X1.
$\alpha = 1.158$; $\beta = 0.151$.

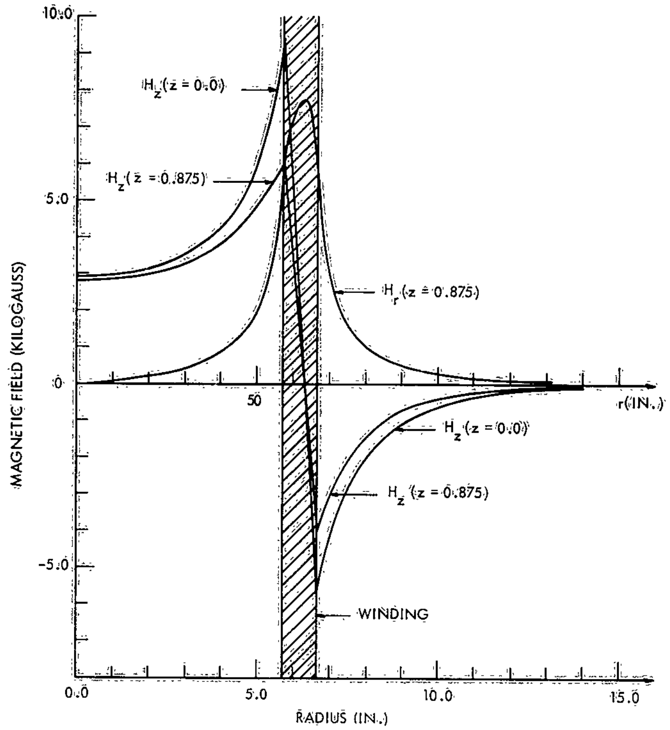

Fig. XIV-18. Field variation along the radius for coil X1. $\alpha = 1.158$; $\beta = 0.151$. $Z = 0.875$ is at the edge of the winding.

the integration is not split, that is, $|r-1|$ or $|z| > 0.4$, with the use of 5 current sheets, assumed the result is 0.25 second per point. If the field position is close to the edge of the winding, then the computation time is approximately three times longer. For any on-axis point, the use of Eq. 17 or Eq. 18 saves much more time and reduces the computation time to approximately 0.005 second.

We have applied the basic subprogram for the calculation of the field of a single solenoid and also for more complex problems.

For a multicoil solenoid, we simply used a summation of the two components of the field. Each coil is characterized independently.

$$H_{set}(r,z) = \sum_{i=1}^{P} H_{coil}(r, z_{(i)}) \times \frac{N_{(i)}J_{(i)}}{L_{(i)}}, \tag{19}$$

where $N_{(i)}$ is the number of turns, $J_{(i)}$ the current or current ratio, and $L_{(i)}$ the length of the i^{th} coil.

The inverse problem consists in the determination of $J_{(i)}$ so that the field satisfies

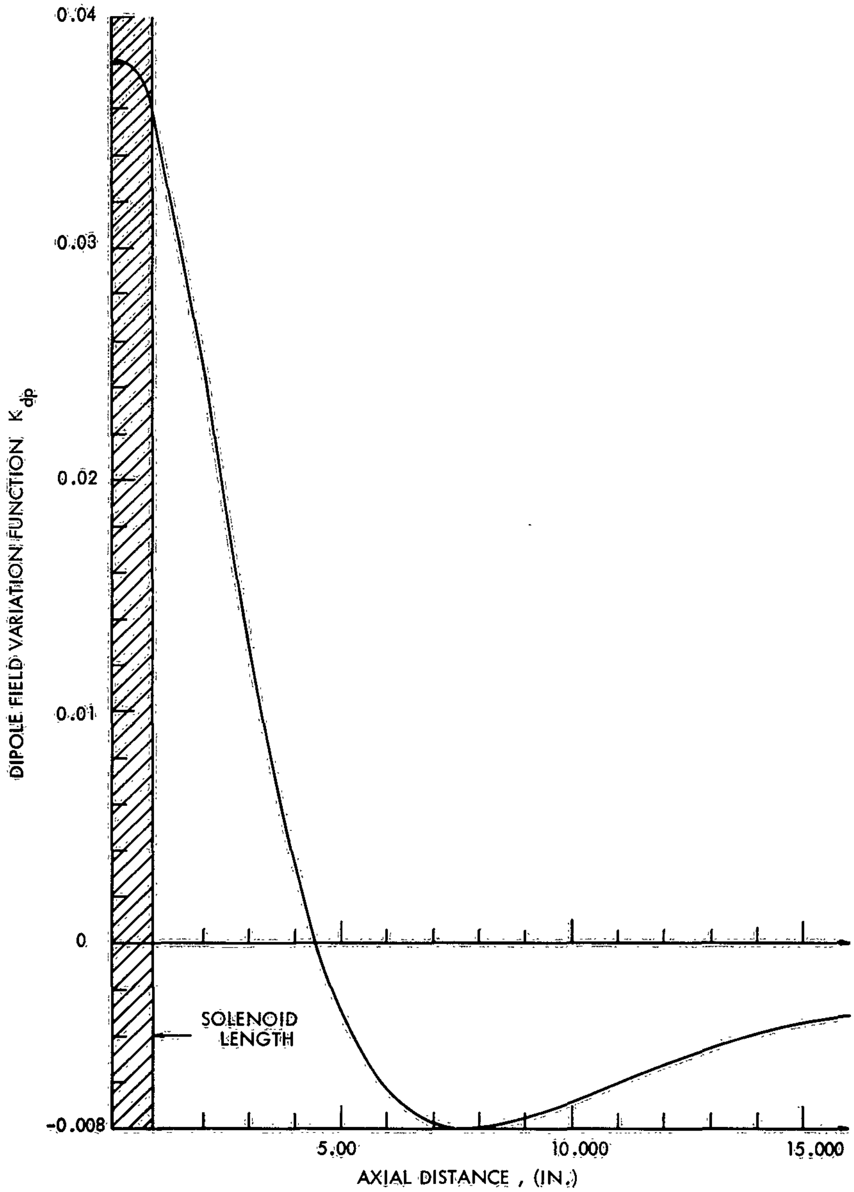

Fig. XIV-19. Axial dipole field of uniformly distributed dipoles in solenoid X1. $H_{gauss} = K_{dp} \times 19.3257 \times I_{amp}$. I_M = equivalent magnetization current.

a given value at P given positions. We have to solve the matrix equation

$$H_{(P)} = K_{(P,N)} J_{(N)};\tag{20}$$

thus

$$J_{(N)} = K^{-1}_{(P,N)} H_{(P)}. \tag{21}$$

This operation is easily carried out by the computer. Our program has been set to permit solving this problem when any series grouping of coils is devised.

Dipoles induced into a superconducting solenoid may be of prime importance for the limitation of the current into superconducting solenoids.[10] If we assume uniform distribution of dipoles throughout the winding, the magnetic field results from the superposition of two current sheets of equal strength of opposite direction, one along the inner diameter and the other along the outer diameter.

$$H_{dp} = H_{inner}(r,z) - H_{outer}(r,z) \tag{22}$$

The normalization factor of the field in that case is

$$K_{dp} = \mu \frac{I_M}{St} = \mu \frac{N_L}{L} I_M, \tag{23}$$

where St is turn spacing, N_L the number of turns per layer, L the length of the solenoid, and I_M the equivalent magnetization current.

For purposes of illustration we show in Figs. XIV-17, XIV-18, and XIV-19 the fields profiles and denote the field for the X1 coil which is described in the first part of this report.

L. J. Donadieu

References

1. L. J. Donadieu and D. J. Rose, Paper K4, International Conference on High Magnetic Fields, Massachusetts Institute of Technology, November 1-4, 1961.

2. We wish to thank Dr. Z. J. J. Stekly of the AVCO Everett Research Laboratories for the use of the dewar.

3. This work was partly done at the Computation Center, M.I.T.

4. W. R. Smythe, Static and Dynamic Electricity (McGraw-Hill Book Company, Inc., New York, 1950), p. 270.

5. C. Snow, Magnetic Fields of Cylindrical Coils and Annular Coils, National Bureau of Standards, Applied Math. Series, Paper No. 38, 1953.

6. N. B. Alexander and C. P. Downing, Tables for a Semi-Infinite Circular Current Sheet, ORNL-2828, October 13, 1959.

7. E. Durand, Electrostatique et Magnetostatique (Masson Companie, Paris, 1953).

8. D. B. Montgomery and J. Terrell, Some Useful Information for the Design of Air-Core Solenoids, AFOSR-1525, November 1961.

9. M. W. Garrett, J. Appl. Phys. 22 (1951).

10. D. B. Montgomery, Current Carrying Capacity of Superconducting Nb-Zr Solenoids, AFOSR-3015, National Magnet Laboratory, M.I.T., July 1962.

XV. PLASMA MAGNETOHYDRODYNAMICS AND ENERGY CONVERSION*

Prof. G. A. Brown
Prof. E. N. Carabateas
Prof. S. I. Freedman
Prof. W. H. Heiser
Prof. M. A. Hoffman
Prof. W. D. Jackson
Prof. J. L. Kerrebrock
Prof. J. R. Melcher
Prof. G. C. Oates
Prof. J. P. Penhune
Prof. J. M. Reynolds III
Prof. A. H. Shapiro
Prof. R. E. Stickney
Prof. H. H. Woodson
M. T. Badrawi
A. N. Chandra
R. S. Cooper
J. M. Crowley
R. Dethlefsen
M. G. A. Drouet
D. A. East
J. R. Ellis, Jr.
F. W. Fraim IV
J. Gerstmann
N. Gothard
J. B. Heywood
H. D. Jordan
P. G. Katona
F. D. Ketterer
G. B. Kliman
A. G. F. Kniazzeh
M. F. Koskinen
W. H. Levison
A. T. Lewis
M. A. Lutz
H. C. McClees, Jr.
C. W. Marble
T. D. Masek
S. A. Okereke
J. H. Olsen
C. R. Phipps, Jr.
E. S. Pierson
D. H. Pruslin
M. H. Reid
C. W. Rook
A. W. Rowe
R. Toschi
M. R. Sarraquigne
A. Shavit
J. H. Sununu
R. G. Vanderweil
G. L. Wilson
B. M. Zuckerman

RESEARCH OBJECTIVES

1. Plasma Magnetohydrodynamics

Our group is pursuing the intermediate objectives of improving the reliability and capability of the existing magnetically driven shock tube, for the purpose of increasing the reproducibility of the resulting data, enlarging the amount of plasma generated by the shock wave, increasing the resulting shock-front velocity, and making possible examination of unusual shock transitions and properties of the shock layer.

The reliability and reproducibility seem to be related to the breakdown behavior of the drive current, so experiments are being conducted which should make this breakdown more uniform in spatial distribution and give the drive current a more advantageous time distribution.

The capability is now limited by failure of shocks to form at low initial pressures (less than 50 μ Hg of hydrogen) and by leakage of plasma past the drive current sheet through the boundary layer. Removal of these barriers is the key to achieving the experimental goals outlined above.

Simultaneously, efforts are being made to devise or improve methods for taking experimental data because existing methods are not adequate for the task of obtaining detailed flow information, and are often very costly to implement.

A. H. Shapiro, W. H. Heiser

2. Energy Conversion

(a) Magnetohydrodynamic Energy Conversion

(i) The objective of our research in magnetohydrodynamic energy conversion is to study theoretically and experimentally the properties of parametric and wave-type power generators to determine their ranges of applicability. Our

*This work was supported in part by the National Science Foundation under Grant G-24073, and in part by the U.S. Air Force (Aeronautical Systems Division) under Contract AF33(616)-7624 with the Aeronautical Accessories Laboratory, Wright-Patterson Air Force Base, Ohio.

interest is primarily in large-signal operation of the type that might be suitable for large-scale power generation.

During the past year, progress has been made in devising a mathematical model to describe the small-signal behavior of the parametric machine. This model was verified with a solid-conductor analog, and the model was used to predict the small-signal behavior of parametric machines with gaseous conductors.[1] Small-signal experiments were performed with a magnetically driven shock tube to verify the analysis of generator operation with a gaseous conductor. In these experiments net power was generated.[2]

During the past year, our research on wave-type power generators has been directed toward achieving in a modified homopolar experiment the plasma conditions (flow velocity and conductivity) necessary for studying the amplifying interaction between magneto-acoustic waves and distributed electric circuits. Thus far, we have obtained a uniform, flowing plasma, but the conductivity is too low for wave experiments. Modifications are being made to improve the plasma conductivity in the experiment.

H. H. Woodson

References

1. H. H. Woodson, G. L. Wilson, and A. T. Lewis, A Study of Magnetohydrodynamic Parametric Generators, Third Symposium on the Engineering Aspects of Magnetohydrodynamics, Rochester, New York, March 1962.

2. G. L. Wilson, A. T. Lewis, and H. H. Woodson, Half-cycle plasma parametric generator, Quarterly Progress Report No. 67, Research Laboratory of Electronics, M.I.T., October 15, 1962, pp. 96-106.

(ii) We are concerned with electrohydrodynamic surface interactions. Previous investigations have clarified the fundamental aspects of wave propagation and instability,[1,2] with some consideration given to the nonlinear aspects of the problem.[3,4] Our investigations are now devoted to understanding the ways in which growing field-coupled surface waves can be used to provide electromechanical energy conversion. We have been shown that the mechanical medium can be an ionized gas[5] or a fluid.[6] Our present concern is with the effects of external electrical coupling and internal mechanical losses.

J. R. Melcher

References

1. J. R. Melcher, Electrohydrodynamic and magnetohydrodynamic surface waves and instabilities, Phys. Fluids 4, 1348-1354 (1961).

2. J. R. Melcher, Electrohydrodynamic surface resonators, Phys. Fluids 5, 1130-1131 (1962).

3. J. R. Melcher, Electrohydrodynamic and magnetohydrodynamic nonlinear surface waves, Phys. Fluids 5, 1037-1043 (1962).

4. C. H. Childs, Electrohydrodynamic Shocks and Anti-Shocks, S.B. Thesis, Department of Electrical Engineering, M.I.T., 1962.

5. L. O. Hoppie, The Electrohydrodynamic Traveling-Wave Amplifier: An Application of Low Conductivity Plasma, S.B. Thesis, Department of Electrical Engineering, M.I.T., 1962.

6. J. R. Melcher, Field-Coupled Surface Waves (to be published as a monograph by The M.I.T. Press, Cambridge, Massachusetts).

(b) Thermionic Energy Conversion

The present research objectives of our group are oriented toward a better understanding of the mechanisms controlling the performance characteristics of cesium thermionic converters. Toward the achievement of this goal, the following areas are under investigation.

(i) Theoretical and experimental studies of the effect of crystallographic orientation on the electron emission properties of a material both in vacuum and in cesium.

(ii) Theoretical and experimental studies of the transport properties of the interelectrode gap in cesium thermionic converters.

(iii) Measurements of the thermal conductivity of the cesium vapor over a wide range of temperatures.

(iv) Experimental studies of the oscillations observed at low cesium pressures.

E. N. Carabateas

3. Alkali-Metal Magnetohydrodynamic Generators

The over-all objective of our program is to determine the electrical properties of both superheated and wet flowing alkali-metal vapors at temperatures near 2000°K. A small potassium boiler, superheater, and condenser are now being constructed.

During the coming year, we aim to complete and check out the plasma facility, and to measure the electrical conductivity of the plasma both with and without a magnetic field. Theoretical studies of the conductivity of the wet vapor will also be completed.

J. L. Kerrebrock, M. A. Hoffman, G. C. Oates

4. Magneto-Fluid Dynamics

This group is principally concerned with interactions between electromagnetic fields and those electrically conducting fluids that can be treated on a continuum basis. Our work includes theoretical and experimental aspects and involves both the investigation of magnetohydrodynamic phenomena and their utilization for engineering applications, particularly for electrical power generation. The following problems are receiving attention.

(a) Magnetohydrodynamic Wave Phenomena

One of our experiments is concerned with the excitation of Alfvén waves in a liquid metal (NaK alloy). Electrical excitation by means of a current sheet has proved to be markedly superior to the mechanical methods used in experiments reported previously. Efforts are, at present, directed toward a systematic study of the excitation, transmission, attenuation, and reflection of these waves in the frequency range up to approximately 10 kc.

A second waveguide study is concerned with MHD wave propagation in nonuniform plasmas. A high-density cesium glow discharge is being set up for the experimental part of this investigation.

W. D. Jackson, J. P. Penhune, G. B. Kliman, N. Gothard, C. W. Rook

(b) Moving Space-Charge Waves in a Plasma

The nature of certain macroscopic instabilities observed in the plasma of glow discharge tubes is being examined. Traveling waves of electron and ion density have been observed spontaneously arising within several noble gas plasmas. These waves have also been generated with sounding probes and with external excitation. A linearized theory has been developed and its predictions are now being correlated with our experimental observations.

W. D. Jackson, R. S. Cooper

(c) Magnetohydrodynamic Channel Flow and Turbulence

The flow characteristics of electrically conducting fluids in channels or ducts are of interest in connection with many engineering applications of magnetohydrodynamics. While these include both liquid and ionized gas flows, the use of liquid metals has advantages for a considerable range of laboratory investigations.

The major experimental effort at the present time involves the construction of an NaK flow loop that will be used for studies of pressure-drop versus flow-rate relations (including those for MHD power-conversion devices) and the characteristics of turbulence in the presence of magnetic fields.

The theoretical treatment of turbulent-flow problems, thus far, has had only partial success and the need for a rational method has long been evident. An attempt is being made to develop Weiner's "Calculus of Random Functionals" and to apply it to both sustained and decaying turbulent-flow situations.

W. D. Jackson, J. M. Reynolds III, J. R. Ellis, Jr., F. W. Fraim IV, H. D. Jordan

(d) Mathematical Methods in Continuum Magnetohydrodynamics

This research is concerned with mathematical methods for the analysis of the interactions occurring in magnetohydrodynamics. The present work has grown out of the investigation of MHD channel flows; particularly out of the analytical and numerical techniques that were used to obtain solutions to the nonlinear differential equation governing the interaction of a traveling ac magnetic field with an MHD channel flow.

Our research concerns the application of techniques, such as perturbation expansions and iterational and variational methods, to a variety of nonlinear continuum MHD problems. The purpose of this effort is twofold: First, to produce solutions to specific problems that are of practical interest; second, to obtain a better understanding of the broad classes of problems to which these techniques are applicable.

J. P. Penhune

(e) Local Fluid-Velocity Measurement in an Incompressible Magnetohydrodynamic Flow

The behavior of several different types of probes is being investigated to develop devices for measuring the local fluid veloctiy in an MHD flow for the case in which the applied magnetic field is perpendicular to the fluid velocity. The development of such probes will be important for experimental investigation of MHD flows, particularly those associated with MHD power-generation devices.

Three types of probe are being investigated experimentally. The first is the standard Pitot tube in which the $\overline{J} \times \overline{B}$ force raises the fluid pressure at the stagnation point above the usual stagnation pressure of the fluid. The velocity-pressure relation is being determined as a function of the magnetic field. A second approach is the investigation of a two-dimensional aerofoil aligned parallel to the magnetic field. The last probe is a miniaturized electromagnetic flowmeter for which the calibration depends on the fluid Reynolds and Hartmann numbers, as well as on the local velocity.

A. H. Shapiro, W. D. Jackson, D. A. East, J. H. Olsen

(f) Liquid-Metal Magnetohydrodynamic Power Systems

The generation of electrical power on space vehicles offers a potential application for MHD generators to operate on a closed-cycle system in which a nuclear reactor is the termal-energy source. An important feature of an MHD scheme is the absence of rotating parts and, to utilize this, a working fluid is required with a sufficiently high electric conductivity at the temperatures involved.

A scheme in which a liquid metal is used as the working fluid is under investigation. Kinetic energy is imparted to this flow by driving it with its own vapor in a condensing-ejector system. The operation of this system on alkali metals is being studied, and the relative merits of ac and dc generators for this application are being examined.

W. D. Jackson, G. A. Brown

(g) Magnetohydrodynamic Induction Generator

The MHD induction machine utilizes the interaction between a traveling magnetic field (such as that produced by a polyphase winding) and a channeled, flowing fluid that may be either a plasma or a liquid metal.

The theoretical analysis of this machine has been completed for the case of slug flow of an incompressible fluid. It is now being extended to include entrance and exit effects, velocity profiles, and compressible fluids.

A two-phase, linear traveling-field coil system is in the course of construction. It will be used to study the operating characteristics of the induction generator on both plasma and liquid-metal flows.

W. D. Jackson, E. S. Pierson, M. H. Reid

(h) A-C Properties of Superconductors

Recent intensive efforts to fabricate hard superconductors have opened up a wide range of possibilities for utilizing these materials in the production of high dc fields, particularly in situations for which these are required in large volumes. The advantages associated with reducing field-power dissipation also apply to the production of ac fields, but there is an additional problem in that reactive power has to be circulated. This problem implies essentially zero-loss capacitive energy-storage elements, in addition to essentially infinite Q inductors. It is thus of interest to investigate the behavior of superconducting materials carrying ac currents in the presence of ac magnetic fields. As well as establishing the merits of superconductivity materials in inductor and capacitor fabrication, such investigations provide an additional method of gaining insight into the mechanism of superconductivity.

Present investigations deal with superconducting materials in the form of wire or ribbon, and two experimental techniques are being pursued.

(i) The current-carrying capacities of short, straight lengths of superconducting wire or ribbon are being determined as a function of frequency in the range up to 10 kc.

(ii) A-C solenoids, fabricated to avoid electric eddy currents and insulated to accommodate electrical fields arising from $\partial B/\partial T$ effects, are being tested. In both cases, the ac current required for transition to normal conductivity is obtained and, in the case of solenoids, the measurement of Q is being attempted.

A third investigation is planned to obtain data on the behavior of superconductors in an externally applied ac field. These will be derived either from a rotating magnet system or from a separate copper-conductor ac solenoid.

The work is, at present, experimental in character, but future theoretical studies are envisaged.

W. D. Jackson, A. N. Chandra, C. R. Phipps, Jr.

(i) Blood-Flow Studies*

Another activity is concerned with medical engineering, and is being carried on in association with the Cardiovascular Laboratories of the Peter Bent Brigham Hospital, Boston. Since my own interest is primarily in the use of magnetohydrodynamic methods for blood-flow measurement, there is, in fact, a close relation to the field of magneto-fluid dynamics. The scope of the group, however, is rather broader than this topic alone would imply.

The aim of our work is to apply engineering methods to the study of the cardiovascular system, and we are engaged in this jointly with Dr. Dexter and his associates at the Peter Bent Brigham Hospital. At present, we are evaluating flow-measuring devices (electromagnetic or magnetohydrodynamic, ultrasonic and thermistor) as a preliminary approach to the study of the characteristics of blood flow. A second aspect of our work is the identification and analysis of the mechanisms responsible for the regulation of cardiovascular functions.

W. D. Jackson

A. WORK COMPLETED

1. THE EFFECT OF SWIRL ON THE ELECTROMAGNETIC FLOWMETER

This research has been completed by H. D. Meyer and the results have been accepted by the Department of Mechanical Engineering, M.I.T., as a thesis in partial fulfillment of the requirements for the degrees of Master of Science and Bachelor of Science, September 1962.

W. D. Jackson, J. M. Reynolds III

2. EXPERIMENTAL CHARACTERISTICS OF A PLASMA JET

This research has been completed by M. D. Leis and the results have been accepted by the Department of Electrical Engineering, M.I.T., as a thesis in partial fulfillment of the requirements for the degree of Bachelor of Science, June 1962.

W. D. Jackson

3. BLOOD-FLOW STUDIES*

The present phase of this work has been completed and the results have been accepted as theses by the Department of Electrical Engineering, M.I.T., in partial fulfillment of the requirements for the degrees indicated.

P. G. Katona, "Analysis of Blood-Pressure Regulation Using Correlation Techniques," S.M. Thesis, June 1962.

J. R. Ellis, Jr., "Relative Merits of Certain Channel Sections in Electromagnetic Flowmeters," S. B. Thesis, June 1962.

J. E. Thompson, "Thermistors as Blood Flow-Rate Transducers," S.B. Thesis, June 1962.

J. D. Cervenka, "Flow Measurement Using Point-Contact Electrodes," S.B. Thesis, June 1962.

W. D. Jackson

*This research was supported in part by the National Institutes of Health (Grant HTS-5550).

B. EXPERIMENTAL MEASUREMENT OF THE THERMAL CONDUCTIVITY OF CESIUM VAPOR

An experimental measurement of the thermal conductivity of cesium vapor was made by a variation of the hot-wire cell method.[1] The hot-wire cell was operated at 600°K. At this temperature level the heat transfer resulting from thermal radiation was considerably greater than that resulting from thermal conduction. Because of this unfavorable ratio of heat fluxes, slight uncertainties in the thermal emissivity of nickel covered with a surface layer of cesium can result in large errors in the observed value of the thermal conductivity of the cesium vapor. Two cells were therefore used to measure simultaneously the thermal conductivity of cesium vapor and the thermal emissivity of nickel in a moderate-temperature cesium gas. The two cells were constructed so that the heat fluxes resulting from radiation were identical. End corrections for the finite-length tubes were made initially by measuring the thermal conductivities of air at room temperature with each cell individually and with both cells simultaneously, as was done at higher temperatures with cesium.

The thermal conductivity cells consisted of nickel wires, which were used as both resistance heaters and resistance thermometers, placed along the axis of copper tubes. Nickel and copper were used because of their stability in a cesium atmosphere and their availability.

The heat transfer[2] by radiation between a wire and a surrounding tube is

$$\frac{q}{A_w} = \left(\frac{1}{\left(\frac{1}{\epsilon_w} - 1\right) + \frac{D_w}{D_t}\left(\frac{1}{\epsilon_t} - 1\right) + \frac{1}{\overline{F}_{tw}}}\right)\sigma\left(T_w^4 - T_t^4\right). \tag{1}$$

The wire and tube emissivities were anticipated to be approximately 0.1 (later verified). For a wire diameter of 0.010 inch and tube diameters of 3/8 inch and 1/2 inch

$$\frac{1}{\epsilon_w} - 1 \approx 9$$

$$\frac{D_w}{D_t}\left(\frac{1}{\epsilon_t} - 1\right) \approx 0.18 \text{ and } 0.24$$

and

$$\overline{F}_{tw} = 1.00.$$

Thus the difference in radiative heat transfer in the two apparatus operating at the same tube and wall temperatures was 0.6 per cent.

End corrections for axial conduction along the wires to the ends were the same for the two cells. The cells were operated at pressures low enough so that the effect of natural convection on the heat transfer rate was less than 0.1 per cent of that caused by conduction. Convection amounts to 1 per cent of conduction at a Grashoff number of 1570, and 25 per cent at a Grashoff number of 2200.[3] The Grashoff number in the present apparatus was approximately 12. The energy transferred by thermionically emitted electrons in the cell was computed to be approximately 2×10^{-10} watt, well below the range of accuracy of the other measurements. Errors attributed to misalignment of the heated wire were calculated to be less than 0.1 per cent.

The difference in heat transfer in the two cells was attributed only to the difference in the gas conduction. Thus,

$$\frac{\Delta q}{\Delta T} = 2\pi k\, L\left(\frac{1}{\ln\frac{r_{o1}}{r_i}} - \frac{1}{\ln\frac{r_{o2}}{r_i}}\right). \tag{2}$$

Two measurements of the thermal conductivity of cesium vapor were made with the apparatus. The values obtained were 0.003046 Btu/hr ft°F at 1085°R (603°K), and 0.002946 at 1080°R (600°K). The average of these values is 0.002996 ± 1.6 per cent (experimental scatter). For a Prandtl number of 0.7 and a specific heat that includes the change in dimerization with temperature, the viscosity of cesium vapor is calculated to be 0.0547 lbm/hr ft (4.72×10^{-6} lb_f sec/ft^2).

S. I. Freedman, J. H. Sununu

References

1. J. H. Sununu, An Experimental Measurement of the Thermal Conductivity of Cesium Vapor, S.M. Thesis, Department of Mechanical Engineering, M.I.T., February 1963.

2. W. H. McAdams, Heat Transmission (McGraw-Hill Book Company, New York, 3rd edition, 1954).

3. E. R. G. Eckert and R. M. Drake, Heat and Mass Transfer (McGraw-Hill Book Company, Inc., New York, 1959).

4. W. D. Weatherford, J. C. Tyler, and P. M. Ku, Properties of Inorganic Energy Conversion and Heat Transfer Fluids for Space Applications, WADD Technical Report 61-906, Southwest Research Institute, San Antonio, Texas, November 1961.

C. WORK FUNCTION OF A CONDUCTOR

Finding many descriptions of the electron emission process very unsatisfactory, the author presents a report that he hopes will resolve most of the problems, give a new insight into the emission process, and help in predicting emission properties of materials. Following is the author's concept of an electron emitting surface, which he is now attempting to correlate with the large amount of existing experimental data.

It is assumed that the total potential energy change in removing an electron from a crystal is made up of three parts that add in a linear fashion: monopole work, dipole work, and work against external electrostatic fields.

Monopole work is defined as the contribution to the potential energy change of an electron (which is removed from a conductor) arising from interactions with induced surface charges that are induced by the escaping electron itself and not by external sources. The monopole work is simply an extension of the concept of "image-force work" into the surface electron cloud and into the crystal. Monopole work is that contribution to the total potential energy change which depends on the square of the electronic charge. The name "monopole work" is given because these forces vary as the inverse square of the distance from the surface.

Dipole work is defined as the contribution to the potential energy change of an electron (which is removed from a conductor) arising from interactions with permanent surface electrostatic fields. To be precise, dipole work equals the charge on an electron times the difference in electrostatic potential between the average potential inside the conductor and the potential at infinity of a conductor of uniform surface characteristics. The name "dipole work" is given because these forces are caused by a surface dipole or double layer.

External electrostatic fields are those fields caused by external sources and by surface charges induced on the conductor in order to maintain a uniform average potential inside the conductor.

It is well established that monopole work contributes substantially to the total potential energy difference between an electron inside a conductor and the same electron outside the conductor (Schottky effect). The existence of dipole work is a subject of considerable debate and speculation, which the author hopes to resolve in part. Electrostatic fields are generally considered to exist around the conductor so as to make the electrostatic potential at the surface of the conductor vary as the work function divided by the electronic charge. This point will be proved rigorously in the proof of Theorem 1.

Work function, for the purpose of this report, means the difference in energy between an electron at the Fermi energy and an electron at rest just outside the conductor. High fields at the surface of the conductor will not be considered in this treatment so that questions of Schottky effect and the meaning of "just outside the conductor" are not difficult to answer.

THEOREM 1: The electrostatic fields that exist around an isolated conductor are such that the difference in electrostatic potential between any two points near the surface of the conductor equals the difference in work function between the two corresponding regions of the surface, divided by the charge on the electron.

PROOF 1: Consider a process in which an electron at the Fermi energy is removed from the interior of a conductor through a surface of work function ϕ_1, moved through an external electrostatic potential difference $\Delta\Psi_{12}$, and then returned to the metal at the

Fermi energy through a surface work function ϕ_2. The change in energy for this process is

$$\Delta E = \phi_1 + e\Delta\Psi_{12} - \phi_2.$$

But, if the Fermi energy is uniform throughout the metal, the energy change must equal zero. Therefore,

$$\Delta\Psi_{12} = \frac{\phi_2 - \phi_1}{e}.$$

Since the process can be carried out through any two regions of the surface, the proof is completed.

This result is not surprising if one remembers the thermodynamic definition of work function (which, incidently, agrees with the definition stated above when the definition of μ is chosen to agree with the statistical mechanical definition)

$$\phi = -e\Psi - \mu.$$

Here, Ψ is the electrostatic potential that exists just outside the surface in question, and μ is the chemical potential of the electrons in the conductor.

THEOREM 2: The variation of work function with the nature of a surface must be caused by a change in the surface double layer. The monopole work associated with any surface of a conducting material of uniform composition is independent of the details of the surface.

PROOF 2: In a conductor of uniform composition the average electrostatic potential in the interior is constant. Therefore, the net field from all external sources and surface charges, taken together, must be zero inside the conductor. However, in the proof of Theorem 1 it was shown that the electrostatic potential varies as the work function just outside the conductor. In order to satisfy Maxwell's equations, there must be a surface double layer whose strength varies as the work function. That is, the dipole work associated with a surface varies as the work function.

The work function equals the monopole work M, plus the dipole work D, minus the electron degeneracy energy ζ.

$$\phi_1 = M_1 + D_1 - \zeta$$

$$\phi_2 = M_2 + D_2 - \zeta.$$

Since the dipole work varies as the work function and the electron degeneracy energy is constant, the monopole work must be constant and therefore independent of the details of the surface, which was to be proved.

When an electron has first entered the electron cloud of the surface, and before it

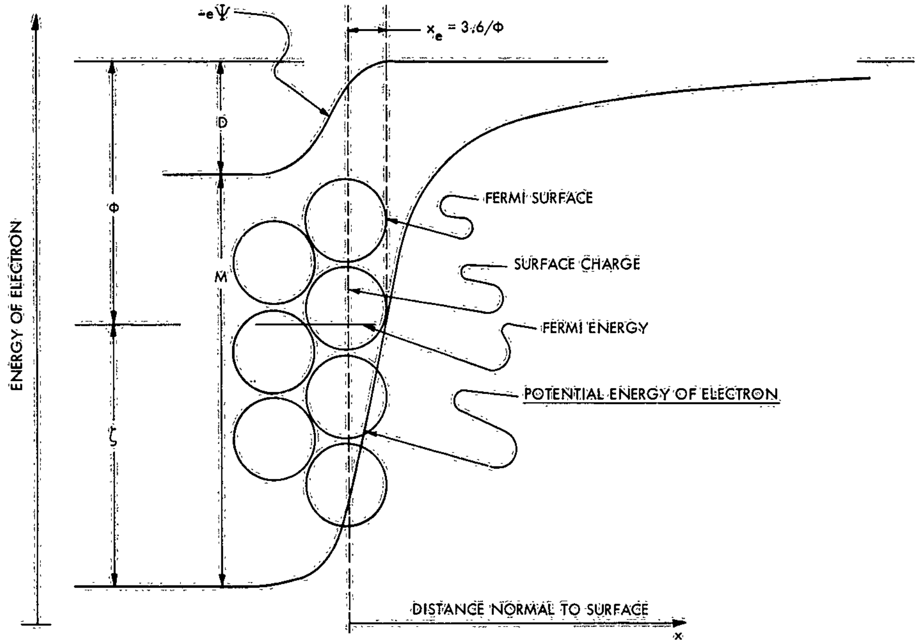

Fig. XV-1. Energy diagram of a surface.

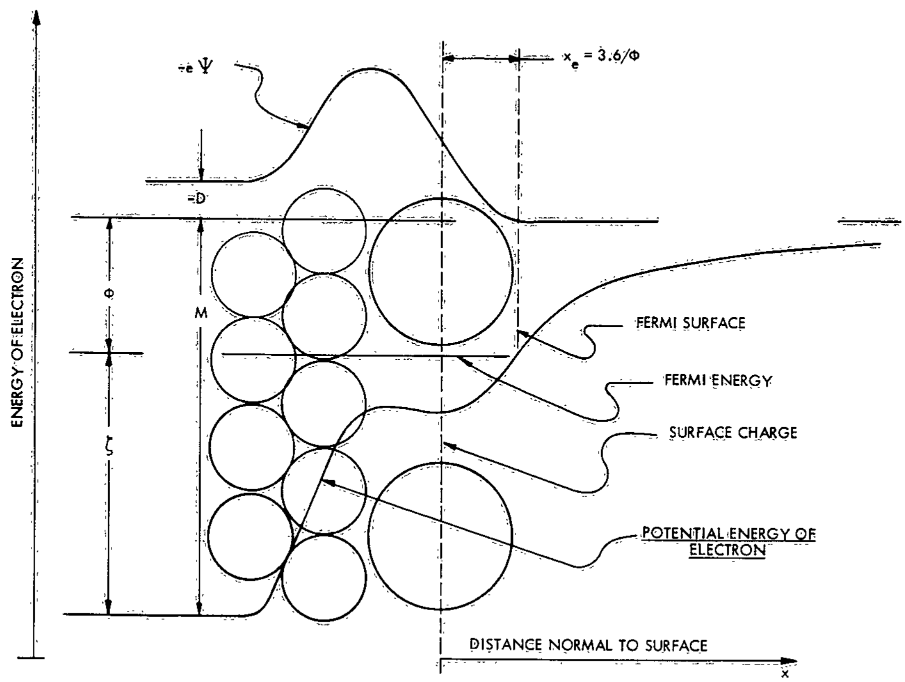

Fig. XV-2. Energy diagram of a surface with an adsorbed ionizible layer.

has reached the first plane of nuclei, it is repelled by the electron cloud and is attracted by the nuclei. This is the region of the surface dipole layer. The field of an electron is given by

$$\overline{E} = -\frac{14.4}{r^2} r,$$

where E is in volts per angstrom and r is in angstroms. Electronic separations are of the order of angstroms, as is the thickness of the dipole layer. This is adequate to provide the several electron volts of dipole work that is necessary to explain a work-function variation of an electron volt from one crystallographic surface to another.

Since electric fields exist outside the conductor, but not inside, there also must be a surface charge equal to the external field times the permittivity of free space. The surface charge is an induced charge and is dependent on the distribution of the work function over the surface of the conductor, as well as the presence of externally applied fields, whereas the double layer is permanent and determines the work function.

Theorem 2 rests heavily on the assumption that the work function is made up of two parts, that is, monopole work and dipole work. At the present time, it is not at all clear whether or not this assumption is warrented. Other terms may be important. However, any other terms that do prove to be important can be formally combined with the monopole work, and the important result of Theorem 2 is preserved: the variation of work function with the nature of a surface must be caused by a change in the surface double layer, alone.

It is generally recognized that a close-packed surface has a larger proportion of electrons outside the first plane of nuclei than a less densely packed surface, and thereby presumably has a stronger double layer (and therefore higher work function) than a less densely packed surface. Also, a close-packed surface has more nuclei per unit area to produce a stronger double layer. This prediction is in qualitative agreement with many experimental observations. Calculations are now being made to relate these ideas to the experimental data in a quantitative fashion.

The determination of the electron distribution near the surface of a conductor covered with an ionizable adsorbed film is a difficult problem. Some guess must be about the nature of the adsorbed particles. Are they atoms, ions or something in between? Rasor[1] assumes that surface particles are either atoms or ions in a number given by their thermal excitation probabilities. In effect, Rasor calculates the modification of the dipole work by the adsorbed particles. It is the author's belief that this is the reason for Rasor's striking success in computing the change in the work function as a function of surface coverage. The change in the dipole work equals the change in the work function.

Figures XV-1 and XV-2 show schematically the thermionic emitting surface described in this paper. Figure XV-1 shows a bare metal surface; Fig. XV-2 shows a surface partially covered with ionizable atoms (positive ions shown). A few surface atoms are shown; the conductor is to the left, free space to the right. The potential energy of an electron is plotted against the distance normal to the surface x, measured from the effective plane of the surface charge mentioned in the Schottky model. The potential energy, shown smooth inside the conductor, is the average potential energy used in the free-electron gas approximation. The electrostatic potential times the electronic charge is also shown plotted against the distance normal to the surface.

The Fermi energy is shown, as is the Fermi surface, that is, the surface on which Fermi electrons have their classical turning point. A physical interpretation is given of the Schottky cutoff distance x_e,

$$x_e = \frac{1}{4\pi\epsilon_o} \cdot \frac{e^2}{4\phi} = 3.6/\phi,$$

where x_e is in angstroms, and ϕ is in electron volts. The distance, x_e, is simply the distance between the effective plane of the surface charge and the Fermi surface.

The electron degeneracy energy ζ, and the monopole work M, both being functions of the substrate compostion alone, are shown. The work function ϕ and the dipole work D, which determines the work function, are also shown.

M. F. Koskinen

References

1. N. S. Rasor, First Summary Report of Basic Research in Thermionic Energy Conversion Processes, Paper B-3., Atomics International, November 1961.

D. POWER FLOW IN THE MAGNETOHYDRODYNAMIC INDUCTION MACHINE

The magnetohydrodynamic (MHD) induction machine, shown schematically in Fig.XV-3 for the flat linear version, utilizes the interaction between a traveling magnetic field and a channeled electrically conducting fluid to convert energy between mechanical and electrical forms. In principle, this type of machine is analogous to conventional rotating induction machines, and accordingly the well-established features of asynchronous operation apply to it. This report presents a generalization of previous work[1,2] to a magnet core of arbitrary permeability and conductivity.

1. The Model

The model to be analyzed is shown in Fig. XV-4. The fluid flows in the x direction between two parallel exciting plates of infinite extent in the x and z directions, a distance 2a apart. The fluid velocity is assumed to be constant and in the x direction (slug flow) to uncouple the electromagnetic and fluid equations and thus allow an analytical solution to be obtained. The region outside the plates is filled with a core of permeability μ_c and conductivity σ_c. The exciting plates, separated from the fluid and core by insulators of infinitesimal thickness to prevent current flow in the y direction, are assumed thin so that they can be replaced by current sheets with a surface conductivity $\sigma_s = \sigma_e b$, where b is the plate thickness and σ_e the material conductivity. The plates are driven by a current source that gives a symmetric surface current density

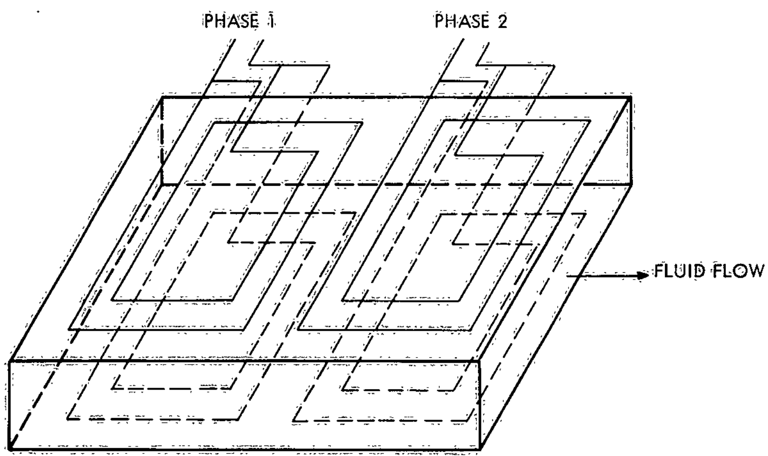

Fig. XV-3. The MHD induction machine.

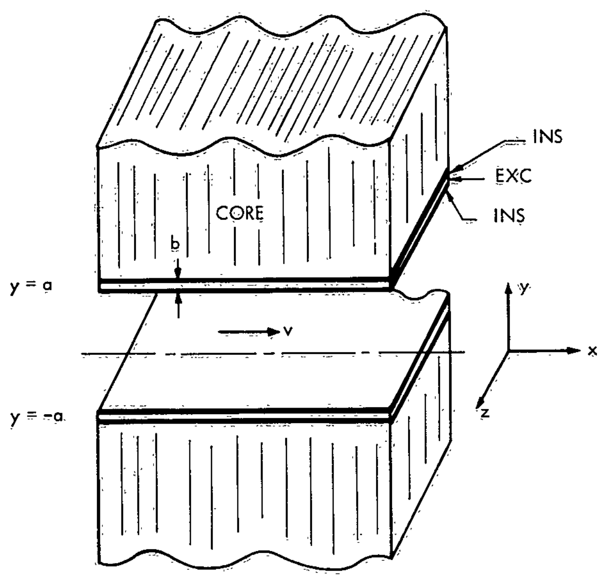

Fig. XV-4. The model.

$$\vec{K} = \vec{i}_z NI \cos(\omega t - kx), \tag{1}$$

which represents a traveling current wave of amplitude NI, frequency ω, wavelength $\lambda = 2\pi/k$, and velocity $v_s = \omega/k$. The surface current is considered to be produced by a balanced two-phase system with sinusoidally distributed windings of maximum turns density N and peak current I. Only two-phase excitation is considered, since, as shown by White and Woodson,[3] an n-phase system can be reduced to a two-phase equivalent.

2. Electromagnetic Fields

The electromagnetic fields are determined from Maxwell's equations with the usual magnetohydrodynamic approximation of neglecting displacement currents. Assuming constant velocity eliminates the need for the fluid equations. The analysis is simplified by the use of a vector potential $\vec{A}$ and a scalar potential ϕ defined by

$$\vec{B} = \vec{\nabla} \times \vec{A} \tag{2}$$

$$\vec{E} = -\vec{\nabla}\phi - \frac{\partial \vec{A}}{\partial t}. \tag{3}$$

Noting that Ohm's law in a moving fluid is $\vec{J} = \sigma(\vec{E}+\vec{v}\times\vec{B})$ and substituting Eqs. 2 and 3 in Maxwell's equations gives

$$\nabla^2\vec{A} - \mu\sigma\frac{\partial \vec{A}}{\partial t} + \mu\sigma(\vec{v}\times\vec{\nabla}\times\vec{A}) = 0 \tag{4}$$

$$\nabla^2\phi - \mu\sigma\frac{\partial\phi}{\partial t} = 0. \tag{5}$$

Here,

$$\vec{\nabla}\cdot\vec{A} + \mu\sigma\phi = 0 \tag{6}$$

has been chosen to uncouple Eqs. 4 and 5. The x- and t-dependence of all quantities must be as $e^{j(\omega t - kx)}$ from the excitation and boundary conditions. This will not be indicated explicitly. $\vec{A}$ is due solely to currents, so that it, as well as $\vec{J}$, is in the z direction and independent of z. The inclusion of all components of $\vec{A}$ will not affect the fields obtained.

The vector potentials in the fluid and core, from Eq. 4 with the conditions that the normal magnetic field is continuous across the boundary and the tangential magnetic field is discontinuous by the surface current, are

$$\vec{A}_f = \vec{i}_z \frac{\mu_f NI \cosh \gamma y}{\gamma \sinh \gamma a + \alpha\delta \cosh \gamma a} \tag{7}$$

$$\vec{A}_c = \frac{\vec{i}_z \mu_f NI\, e^{-\delta(y-a)}}{\gamma \tanh \gamma a + \alpha\delta}\ ;\ y \geq a \tag{8}$$

where

$$\gamma^2 = k^2(1+jsR_M) \tag{9}$$

$$\delta^2 = k^2(1+jR_{Mc}) \tag{10}$$

$$a = \frac{\mu_f}{\mu_c} \tag{11}$$

$$s = \frac{v_s - v}{v_s} \tag{12}$$

$$R_M = \frac{\mu_f \sigma_f v_s}{k} \tag{13}$$

$$R_{Mc} = \frac{\mu_c \sigma_c v_s}{k}. \tag{14}$$

The subscripts f, c, and e are used to denote fluid, core, and exciting plate quantities, respectively. s is the slip in terms of synchronous speed v_s, R_M and R_{Mc} the fluid and core magnetic Reynolds numbers. sR_M indicates the magnitude of the field-fluid interaction.

In the exciting plates $E_{ez} = NI/\sigma_s$. The scalar potential in the sheets, from Eq. 3, is

$$\phi_e = \frac{-NIz}{\sigma_s} - \frac{j\omega\mu_f NIz}{\gamma \tanh \gamma a + a\delta} \tag{15}$$

The scalar potential is zero outside the exciting plates. Note that the tangential electric field is not continuous across the boundary. Its discontinuity, however, serves only to determine the dipole charge layer on the insulating strips.[4]

3. Electrical Impedance

The electrical characteristics of the MHD induction machine are conveniently expressed in terms of the impedance observed at the terminals of an exciting coil. The impedance may be obtained from the voltage measured between the coil terminals

$$V = 2\int_x^{x+\lambda} (\Delta V)\, N \cos kx dx, \tag{16}$$

where $\Delta V = \phi_e(z) - \phi_e(z+c)$ is the voltage across a single wire and the integral represents the sum of ΔV over a coil that is considered to be a wavelength long and of depth c in the z direction. V is twice the integral because each coil is made up of two sections located above and below the channel, as shown in Fig. XV-4. The equivalent resistance and inductance are

$$R = \frac{2\pi N^2 c}{k\sigma_s} - R_o \operatorname{Im}\left\{\frac{k}{\gamma \tanh \gamma a + a\delta}\right\} \tag{17}$$

$$L = L_o \operatorname{Re}\left\{\frac{k}{\gamma \tanh \gamma a + a\delta}\right\}, \tag{18}$$

where

$$R_o = \omega L_o = \frac{2\pi\mu_f N^2 \omega c}{k^2} \tag{19}$$

and Re and Im stand for the real and imaginary part of the quantity in the brackets. If Eqs. 9 and 10 are substituted in Eqs. 17 and 18, it is seen that, excluding the term depending on σ_s, the normalized ratios R/R_o and L/L_o depend on only five dimensionless parameters: s, R_M, R_{Mc}, a, and ak. Since δ appears everywhere multiplied by a, and since $\mu_c \gg \mu_o$ for a good core, the effect of core loss is small.

For a slit channel, $\gamma a \ll 1$, and by assuming a lossless core and exciting coils ($\sigma_c=0$, $\sigma_e=\infty$), the equations can be written approximately as

$$\frac{R}{R_o} = \left(\frac{1}{a+ak}\right) \frac{sR_{Ma}}{1+s^2R_{Ma}^2} \tag{20}$$

$$\frac{L}{L_o} = \left(\frac{1}{a+ak}\right) \frac{1}{1+s^2R_{Ma}^2} \tag{21}$$

where

$$R_{Ma} = \frac{\mu_f\sigma_f v_s a}{(a+ak)} = \frac{R_M ak}{(a+ak)} \tag{22}$$

is the pertinent magnetic Reynolds number. The functional dependance is the same as for the ideal core slit-channel case[2] except for the replacement of R_M by R_{Ma}. The difficulty with a nonideal core is that it is much harder to obtain a large R_{Ma}, $R_{Ma} \leq R_M$, and this results in poorer performance.

4. Power Flow

Relations are obtained for the time-average real power flow in an MHD induction machine of dimensions ℓ and c in the x and z directions, respectively. The power supplied by the exciting windings to the fluid, the real part of the surface integral of Poynting's vestor over the fluid, is

$$P_s = \frac{P_o \operatorname{Im}\{k\gamma \tanh \gamma a\}}{(\gamma \tanh \gamma a+a\delta)(\gamma^* \tanh \gamma^* a+a\delta^*)}, \tag{23}$$

where

$$P_o = \frac{\mu_f \omega N^2 I^2 c\ell}{k} . \tag{24}$$

The mechanical power output, P_m, and the power dissipated in the fluid, P_r, are

$$P_m = \int_{-a}^{a} \int_{x}^{x+\ell} \left\langle \frac{\partial p}{\partial x} \right\rangle v \, dx dy = (1-s) \, P_s \tag{25}$$

$$P_r = \oint_{Vol} \frac{\overline{J} \cdot \overline{J}^*}{2\sigma_f} \, dv = sP_s, \tag{26}$$

where $\left\langle \frac{\partial p}{\partial x} \right\rangle$ denotes the time-average pressure gradient. These are identical with the power relations obtained for rotating induction machines when P_s is identified as the "gap power".

The power dissipated in the core because of its finite conductivity, P_c, is found in the same manner as for P_s to be

$$P_c = \frac{P_o \, \mathrm{Im} \, \{\alpha \ k\delta\}}{(\gamma \ \tanh \gamma a + \alpha\delta)(\gamma^* \ \tanh \gamma^* a + \alpha\delta^*)} . \tag{27}$$

The power dissipated in the exciting coil, analogous to P_r, is

$$P_e = \int_{x}^{x+\ell} \frac{KK^*}{\sigma_s} \, c \, dx = \frac{N^2 I^2 c\ell}{\sigma_s} \tag{28}$$

Note that for $\ell = \lambda$, $P_o = I^2 R_o$ and $P_s + P_c + P_e = I^2 R$, as expected.

The efficiency of the induction generator, power out divided by power in, is $\frac{P_s + P_c + P_e}{P_m}$, where P_s and P_m are negative for generator operation $(s \leq 0)$, while P_c and P_e, power losses, are always positive. For a lossless coil the efficiency is

$$\eta_g = \frac{1}{1-s} \left\{ 1 + \frac{\mathrm{Im} \ (\alpha\delta)}{\mathrm{Im}(\gamma \ \tanh \gamma a)} \right\}; \ s \leq 0 \tag{29}$$

in which the term in brackets is less than or equal to 1. For a lossless core, δ real, this reduces to the efficiency found previously for a slit-channel machine with an ideal core.[2]

E. S. Pierson

References

1. I. B. Berstein, J. B. Fanucci, K. H. Fishbeck, J. Jarem, N. I. Koram, R. M. Kulsrud, M. Lessen, and N. Ness, An electrodeless MHD generator, Second Symposium on the Engineering Aspects of Magnetohydrodynamics, University of Pennsylvania, Philadelphia, March 9-10, 1961, edited by C. Mannal and N. W. Mather (Columbia University Press, New York, 1962), p. 260.

2. W. D. Jackson and E. S. Pierson, Operating characteristics of the MHD induction generator, Symposium on Magnetoplasmadynamic Electrical Power Generator, King's College, University of Durham, Newcastle-on-Tyne, England, September 6-8, 1962.

3. D. C. White and H. H. Woodson, Electromechanical Energy Conversion, (John Wiley and Sons, Inc., New York, 1959), Chapter 10.

4. E. S. Pierson, Continuity of the tangential electric field in magnetohydrodynamic machines, Quarterly Progress Report No. 67, Research Laboratory of Electronics, M.I.T., October 15, 1962, pp. 106-109.

COMMUNICATION SCIENCES AND ENGINEERING

XVI. STATISTICAL COMMUNICATION THEORY*

Prof. Y. W. Lee
Prof. A. G. Bose
Prof. D. J. Sakrison
Prof. M. Schetzen
Prof. H. L. Van Trees, Jr.
V. R. Algazi
R. Alter
D. S. Arnstein
M. E. Austin
R. F. Bauer
E. M. Bregstone
J. D. Bruce
A. M. Bush
J. K. Clemens
A. G. Gann
C. E. Gray
W. F. Kelly
T. G. Kincaid
P. L. Konop
A. J. Kramer
D. E. Nelsen
J. K. Omura
A. V. Oppenheim
R. B. Parente
W. S. Smith
D. W. Steele
W. S. Widnall

RESEARCH OBJECTIVES

This group is interested in a variety of problems in statistical communication theory. Our current research is concerned primarily with the following problems:

1. A simple two-state modulation system has been designed and is under study. We are making a theoretical investigation of the linearity of the system and of its noise performance. The system will be applied to the problems of high-efficiency power amplification and regulation, multiplication, and low-frequency tape recordings.

2. The study of factors that influence the recording and reproduction of sound continues. The relative rôles of the normal modes of the reproducing room and of the transducer are under investigation.

3. In the Wiener theory of nonlinear systems, a nonlinear system is characterized by a set of kernels. A method for the determination of these kernels was reported in Quarterly Progress Report No. 60 (pages 118-130). Work on the method, both theoretical and experimental, is being continued.

4. The central idea in the Wiener theory of nonlinear systems is to represent the output of a system by a series of orthogonal functionals with the input of the system being a white Gaussian process. An attempt is being made to extend the orthogonal representation to other types of inputs that may have advantages in the practical application of the theory.

5. A study is being made of the various aspects of error in filtering when the noise is additive and statistically independent of the signal. Emphasis is placed on nonlinear no-memory filters.

6. Noise sources in space can be located by means of higher order correlation functions. A study is being made of the errors, caused by finite observation time, incurred in locating sources by this method.

7. Many physical processes can be phenomenologically described in terms of a large number of interacting oscillators. An experimental investigation is being made of some theoretical results that have been obtained.

8. A nonlinear system can be characterized by a set of kernels. The synthesis of a nonlinear system involves the synthesis of these kernels. A study is being made of efficient methods for synthesizing these kernels.

9. The advantages of pseudo-noise carrier systems are well known. One disadvantage is the large bandwidth requirement. This disadvantage can be compensated for in multiplex systems by using a large number of carriers in the same frequency band. If one uses a simple demodulation scheme for a particular channel, the other carriers act as additive noise. By using a more sophisticated demodulation scheme, this interference can be reduced. An experimental system is being constructed.

*This work was supported in part by the National Institutes of Health (Grant MH-04737-02).

10. A reasonably simple adaptive, coherent, binary communication system has been developed and analyzed. Theoretical results indicate that even in channels with reasonably fast fading there is an appreciable improvement over a conventional incoherent system.

11. Experimental work on threshold effects in phase-locked loop discriminators continues.

12. Interesting results pertaining to the analysis of nonlinear, randomly time-variant systems have been obtained. Work in this area continues and some experimental verification on typical systems is planned.

Y. W. Lee

A. THE SYNTHESIS OF A CLASS OF NONLINEAR SYSTEMS

In the Wiener theory of nonlinear systems,[1] a nonlinear system is characterized by a set of kernels, h_n. For a Gaussian input, the kernels can be determined by crosscorrelation.[2,3] If only N kernels are used to characterize the nonlinear system, then the resulting representation can be expressed in the form of a Volterra series

$$y(t) = \sum_{n=1}^{N} \int_0^{\infty} \cdots \int_0^{\infty} k_n(\tau_1, \ldots, \tau_n)\, x(t-\tau_1) \ldots x(t-\tau_n)\, d\tau_1 \ldots d\tau_n \tag{1}$$

in which y(t) is the response of the nonlinear system for the input x(t). If the system is realizable, then

$$k_n(\tau_1, \ldots, \tau_n) = 0 \quad \text{for any } \tau_j < 0,\ j = 1, 2, \ldots, n. \tag{2}$$

A problem in the practical application of these results is the synthesis of systems whose kernels are the kernels, k_n, of the Volterra series. If an n^{th}-order kernel of a system is separable, so that it can be written in the form

$$k_n(\tau_1, \ldots, \tau_n) = k_{a_1}(\tau_1)\, k_{a_2}(\tau_2) \ldots k_{a_n}(\tau_n), \tag{3}$$

then the system can be synthesized in the form depicted in Fig. XVI-1. The system is one in which the outputs of the n linear systems with impulse responses $k_{a_j}(t)$ are

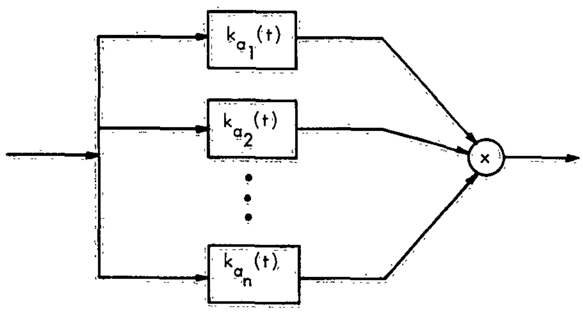

Fig. XVI-1. Synthesis of an n^{th}-order separable kernel.

multiplied together. However, in general, a kernel is not separable. A method suggested by Wiener is to expand the kernels in terms of a set of orthogonal functions such as the Laguerre functions.[1] Thus, if $\{\ell_n(t)\}$ is the set of Laguerre functions, then

$$k_1(\tau_1) = \sum_{n=0}^{\infty} c_n \ell_n(\tau_1)$$

$$k_2(\tau_1,\tau_2) = \sum_{n_1=0}^{\infty} \sum_{n_2=0}^{\infty} c_{n_1,n_2} \ell_{n_1}(\tau_1) \ell_{n_2}(\tau_2) \tag{4}$$

$$\vdots$$

$$k_N(\tau_1,\ldots,\tau_N) = \sum_{n_1=0}^{\infty} \cdots \sum_{n_N=0}^{\infty} c_{n_1,\ldots,n_N} \ell_{n_1}(\tau_1) \ldots \ell_{n_N}(\tau_N),$$

in which

$$c_{n_1,\ldots,n_p} = \int_0^{\infty} \cdots \int_0^{\infty} k_p(\tau_1,\ldots,\tau_p) \ell_{n_1}(\tau_1) \ldots \ell_{n_p}(\tau_p) d\tau_1 \ldots d\tau_p. \tag{5}$$

The synthesis of a first- and a second-order kernel in terms of Eq. 4 is depicted in Fig. XVI-2. However, the synthesis of a given system by this procedure will, in general, require an infinite number of multipliers. In this report, we shall present a method of determining whether a system can be synthesized by using only a finite number of multipliers. We also shall present a method for the synthesis of such systems. To explain the method, the analysis of a system with only a second-order kernel will be presented. The extension to systems with higher-order kernels will then be given.

1. Second-order Systems with Only One Multiplier

We shall first discuss the class of second-order kernels that can be synthesized by means of only one multiplier. A system consisting of only one multiplier whose kernel is clearly the most general second-order kernel that can be obtained is depicted in Fig. XVI-3. The second-order kernel of this system is

$$k_2(\tau_1,\tau_2) = \int_0^{\infty} k_a(\tau_1-\sigma) k_b(\tau_2-\sigma) k_c(\sigma) d\sigma. \tag{6}$$

The kernel transform of this system is the two-dimensional Laplace transform of its kernel:

$$K_2(s_1,s_2) = \int_0^{\infty} \int_0^{\infty} k_2(\tau_1,\tau_2) e^{-s_1\tau_1-s_2\tau_2} d\tau_1 d\tau_2 = K_a(s_1) K_b(s_2) K_c(s_1+s_2), \tag{7}$$

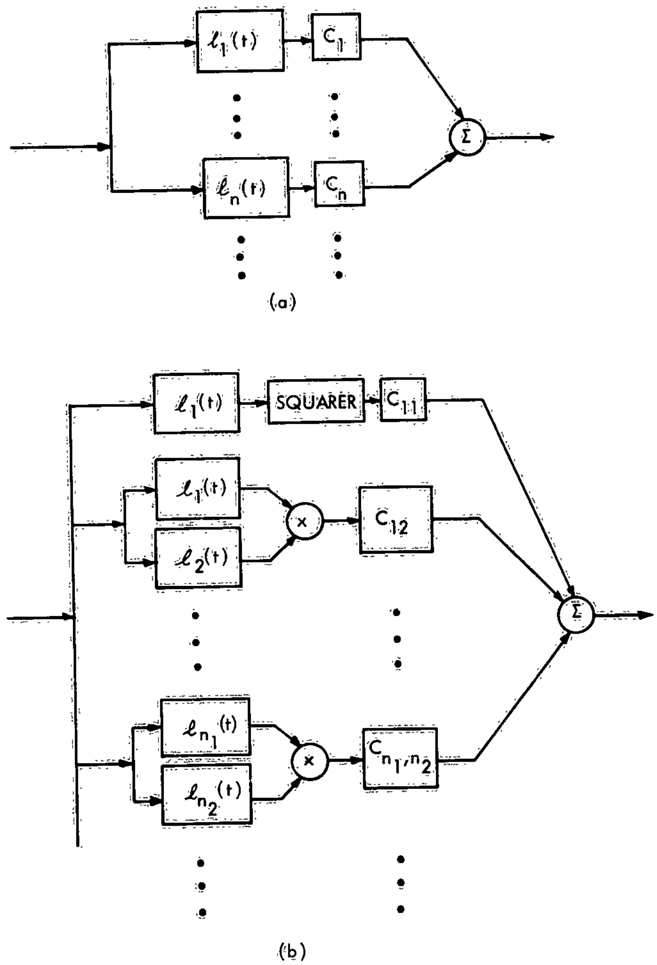

Fig. XVI-2. (a) Synthesis of a first-order kernel by means of Laguerre functions. (b) Synthesis of a second-order kernel by means of Laguerre functions.

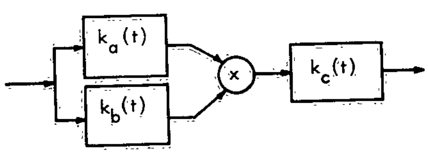

Fig. XVI-3. The most general second-order kernel with only one multiplier.

in which

$$K(s) = \int_0^{\infty} k(t)\, e^{-st}\, dt, \tag{8}$$

so that $K_a(s)$, $K_b(s)$, and $K_c(s)$ are the transfer functions of the linear systems with impulse responses $k_a(t)$, $k_b(t)$, and $k_c(t)$, respectively. To facilitate our discussion, we shall write the transfer function, $K(s)$, of a linear system in the form

$$K(s) = \frac{P(s)}{Q(s)}. \tag{9}$$

The zeros of $P(s)$ are the zeros of $K(s)$, and the zeros of $Q(s)$ are the poles of $K(s)$. Note, however, that $P(s)$ and $Q(s)$ are not necessarily polynomials in s. In terms of Eq. 9, we can write the kernel transform, $K_2(s_1,s_2)$, as given by Eq. 7, as

$$K_2(s_1,s_2) = \frac{P_a(s_1)\, P_b(s_2)\, P_c(s_1+s_2)}{Q_a(s_1)\, Q_b(s_2)\, Q_c(s_1+s_2)}. \tag{10}$$

2. Second-order Systems with N Multipliers

We now note that a system consisting of N multipliers, whose kernel is the most general second-order kernel that can be obtained, is one whose output

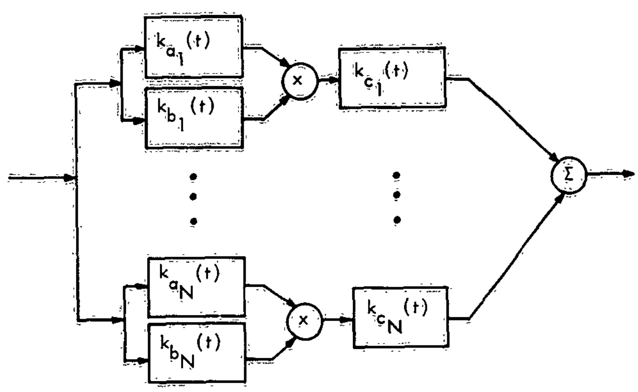

Fig. XVI-4. The most general second-order kernel with N multipliers.

is the sum of the outputs of N systems of the form depicted in Fig. XVI-3. Such a system is shown in Fig. XVI-4. By use of Eq. 6, the second-order kernel of this system is

$$k_2(\tau_1,\tau_2) = \sum_{n=1}^{N} \int_0^{\infty} k_{a_n}(\tau_1-\sigma)\, k_{b_n}(\tau_2-\sigma)\, k_{c_n}(\sigma)\, d\sigma, \tag{11}$$

and from Eq. 7, its kernel transform is

$$K_2(s_1,s_2) = \sum_{n=1}^{N} K_{a_n}(s_1)\, K_{b_n}(s_2)\, K_{c_n}(s_1+s_2). \tag{12}$$

By use of Eq. 10, the kernel transform can be written in the form

$$K_2(s_1,s_2) = \sum_{n=1}^{N} \frac{P_{a_n}(s_1)\, P_{b_n}(s_2)\, P_{c_n}(s_1+s_2)}{Q_{a_n}(s_1)\, Q_{b_n}(s_2)\, Q_{c_n}(s_1+s_2)}. \tag{13}$$

The sum of the series of Eq. 13 is of the form

$$K_2(s_1,s_2) = \frac{P_2(s_1,s_2)}{Q_2(s_1,s_2)}. \tag{14}$$

The zeros of $P_2(s_1,s_2)$ are the zeros of $K_2(s_1,s_2)$, and the zeros of $Q_2(s_1,s_2)$ are the poles of $K_2(s_1,s_2)$. From Eq. 13, we note that

$$P_2(s_1,s_2) = \sum_{n=1}^{N} R_{a_n}(s_1)\, R_{b_n}(s_2)\, R_{c_n}(s_1+s_2), \tag{15}$$

in which

$$R_{\alpha_n}(s) = P_{\alpha_n}(s) \prod_{\substack{j=1\\ j\neq n}}^{N} Q_{\alpha_j}(s) \qquad \alpha = a,\ b \text{ or } c \tag{16}$$

and

$$Q_2(s_1,s_2) = F_a(s_1)\, F_b(s_2)\, F_c(s_1+s_2) \tag{17}$$

in which

$$F_\alpha(s) = \prod_{n=1}^{N} Q_{\alpha_n}(s) \qquad \alpha = a,\ b \text{ or } c. \tag{18}$$

Thus $Q_2(s_1,s_2)$ is expressible as the product of three functions: a function of s_1, a function of s_2, and a function of (s_1+s_2); also, $P_2(s_1,s_2)$ is expressible as the sum of N such products.

We note that if N multipliers are used to synthesize a second-order kernel, then the second-order kernel transform must be of the form

$$K_2(s_1,s_2) = \frac{\sum_{n=1}^{N} R_{a_n}(s_1)\, R_{b_n}(s_2)\, R_{c_n}(s_1+s_2)}{F_a(s_1)\, F_b(s_2)\, F_c(s_1+s_2)}. \tag{19}$$

Furthermore, if a second-order kernel transform is expressible in the form of Eq. 19, then it can be synthesized by means of N multipliers.

3. Illustration of the Method of Synthesis

We shall illustrate, by means of two examples, a procedure by which this synthesis can be accomplished.

As our first example, we desire to synthesize the following second-order kernel transform:

$$K_2(s_1,s_2) = \frac{P_2(s_1,s_2)}{Q_2(s_1,s_2)}$$

$$= \frac{s_1^2s_2 + 4s_1^2 + 12s_1s_2 + s_1s_2^2 + 2s_2^2 + 12s_1 + 48}{s_1^2s_2 + 4s_1^2 + 12s_1s_2 + s_1s_2^2 + 2s_2^2 + 32s_1 + 20s_2 + 48}. \tag{20}$$

This kernel transform can be synthesized by means of a finite number of multipliers. Thus $Q_2(s_1,s_2)$ is expressible in the form $F_a(s_1)\,F_b(s_2)\,F_c(s_1+s_2)$. To determine these three functions, we first let $s_1 = 0$ and $s_2 = s$. Then the zeros of $Q_2(0,s)$ are the zeros of $F_a(0)\,F_b(s)\,F_c(s)$. Thus,

$$\begin{aligned} F_a(0)\,F_b(s)\,F_c(s) &= 2s^2 + 20s + 48 \\ &= 2(s+4)(s+6). \end{aligned} \tag{21}$$

Second, let $s_1 = s$ and $s_2 = 0$. Then the zeros of $Q_2(s,0)$ are the zeros of $F_a(s)\,F_b(0)\,F_c(s)$. Thus,

$$\begin{aligned} F_a(s)\,F_b(0)\,F_c(s) &= 4s^2 + 32s + 48 \\ &= 4(s+2)(s+6). \end{aligned} \tag{22}$$

Third, let $s_1 = s$ and $s_2 = -s$. Then the zeros of $Q_2(s,-s)$ are the zeros of $F_a(s)\,F_b(-s)\,F_c(0)$. Thus,

$$\begin{aligned} F_a(s)\,F_b(-s)\,F_c(0) &= -6s^2 + 12s + 48 \\ &= 6(s+2)(-s+4). \end{aligned} \tag{23}$$

By comparing the common zeros of Eqs. 21-23, we note that

$$\begin{aligned} F_a(s) &= (s+2) \\ F_b(s) &= (s+4) \\ F_c(s) &= (s+6) \end{aligned} \tag{24}$$

so that

$$Q_2(s_1,s_2) = (s_1+2)(s_2+4)(s_1+s_2+6). \tag{25}$$

By substituting Eq. 25 in Eq. 20 and expanding by partial fractions, we obtain

$$K_2(s_1,s_2) = 1 - \frac{20(s_1+s_2)}{(s_1+2)(s_2+4)(s_1+s_2+6)}. \tag{26}$$

Figure XVI-5 depicts the system whose second-order kernel transform is given by Eq. 26.

For our second example, we desire to synthesize a second-order system whose second-order kernel is

$$k_2(\tau_1,\tau_2) = \begin{cases} e^{-a\tau_1-b\tau_2} & \text{for } 0 \leq \tau_1 \leq c\tau_2 \\ 0 & \text{otherwise} \end{cases} \tag{27}$$

in which $a > 0$, $b > 0$, and $c > 0$. To accomplish this, we first must determine the second-order kernel transform, $K_2(s_1,s_2)$.

$$K_2(s_1,s_2) = \int_0^\infty d\tau_2 \int_0^{c\tau_2} d\tau_1\, e^{-a\tau_1-b\tau_2}\, e^{-s_1\tau_1-s_2\tau_2}$$

$$= \frac{-c}{[b+s_2][b+ac+cs_1+s_2]}. \tag{28}$$

We note that for $c \neq 1$, the second-order kernel transform cannot be synthesized with a finite number of multipliers. This can be seen by assuming that the denominator,

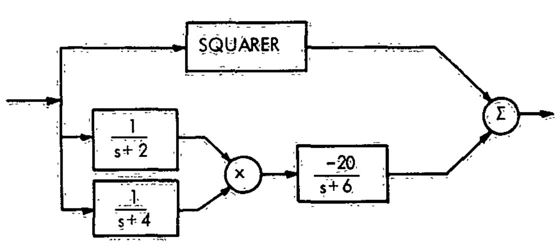

Fig. XVI-5. Second-order system whose kernel transform is given by Eq. 26.

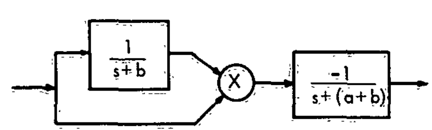

Fig. XVI-6. Second-order system whose kernel is given by Eq. 27 for c = 1.

$Q_2(s_1,s_2)$, can be expressed in the form $F_a(s_1)\, F_b(s_2)\, F_c(s_1+s_2)$. Then, by following the procedure used in our first example, we have

Furthermore, if a second-order kernel transform is expressible in the form of Eq. 19, then it can be synthesized by means of N multipliers.

3. Illustration of the Method of Synthesis

We shall illustrate, by means of two examples, a procedure by which this synthesis can be accomplished.

As our first example, we desire to synthesize the following second-order kernel transform:

$$K_2(s_1,s_2) = \frac{P_2(s_1,s_2)}{Q_2(s_1,s_2)}$$

$$= \frac{s_1^2s_2 + 4s_1^2 + 12s_1s_2 + s_1s_2^2 + 2s_2^2 + 12s_1 + 48}{s_1^2s_2 + 4s_1^2 + 12s_1s_2 + s_1s_2^2 + 2s_2^2 + 32s_1 + 20s_2 + 48}. \tag{20}$$

This kernel transform can be synthesized by means of a finite number of multipliers. Thus $Q_2(s_1,s_2)$ is expressible in the form $F_a(s_1)\, F_b(s_2)\, F_c(s_1+s_2)$. To determine these three functions, we first let $s_1 = 0$ and $s_2 = s$. Then the zeros of $Q_2(0,s)$ are the zeros of $F_a(0)\, F_b(s)\, F_c(s)$. Thus,

$$\begin{aligned} F_a(0)\, F_b(s)\, F_c(s) &= 2s^2 + 20s + 48 \\ &= 2(s+4)(s+6). \end{aligned} \tag{21}$$

Second, let $s_1 = s$ and $s_2 = 0$. Then the zeros of $Q_2(s,0)$ are the zeros of $F_a(s)\, F_b(0)\, F_c(s)$. Thus,

$$\begin{aligned} F_a(s)\, F_b(0)\, F_c(s) &= 4s^2 + 32s + 48 \\ &= 4(s+2)(s+6). \end{aligned} \tag{22}$$

Third, let $s_1 = s$ and $s_2 = -s$. Then the zeros of $Q_2(s,-s)$ are the zeros of $F_a(s)\, F_b(-s)\, F_c(0)$. Thus,

$$\begin{aligned} F_a(s)\, F_b(-s)\, F_c(0) &= -6s^2 + 12s + 48 \\ &= 6(s+2)(-s+4). \end{aligned} \tag{23}$$

By comparing the common zeros of Eqs. 21-23, we note that

$$\begin{aligned} F_a(s) &= (s+2) \\ F_b(s) &= (s+4) \\ F_c(s) &= (s+6) \end{aligned} \tag{24}$$

so that

$$Q_2(s_1,s_2) = (s_1+2)(s_2+4)(s_1+s_2+6). \tag{25}$$

By substituting Eq. 25 in Eq. 20 and expanding by partial fractions, we obtain

$$K_2(s_1,s_2) = 1 - \frac{20(s_1+s_2)}{(s_1+2)(s_2+4)(s_1+s_2+6)}. \tag{26}$$

Figure XVI-5 depicts the system whose second-order kernel transform is given by Eq. 26.

For our second example, we desire to synthesize a second-order system whose second-order kernel is

$$k_2(\tau_1,\tau_2) = \begin{cases} e^{-a\tau_1-b\tau_2} & \text{for } 0 \leqslant \tau_1 \leqslant c\tau_2 \\ 0 & \text{otherwise} \end{cases} \tag{27}$$

in which $a > 0$, $b > 0$, and $c > 0$. To accomplish this, we first must determine the second-order kernel transform, $K_2(s_1,s_2)$.

$$\begin{aligned} K_2(s_1,s_2) &= \int_0^\infty d\tau_2 \int_0^{c\tau_2} d\tau_1\, e^{-a\tau_1-b\tau_2}\, e^{-s_1\tau_1-s_2\tau_2} \\ &= \frac{-c}{[b+s_2][b+ac+cs_1+s_2]}. \end{aligned} \tag{28}$$

We note that for $c \neq 1$, the second-order kernel transform cannot be synthesized with a finite number of multipliers. This can be seen by assuming that the denominator,

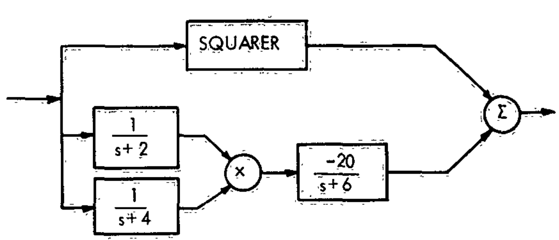

Fig. XVI-5. Second-order system whose kernel transform is given by Eq. 26.

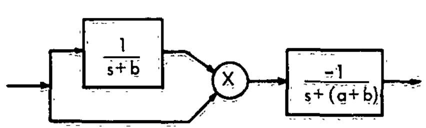

Fig. XVI-6. Second-order system whose kernel is given by Eq. 27 for c = 1.

$Q_2(s_1,s_2)$, can be expressed in the form $F_a(s_1)\,F_b(s_2)\,F_c(s_1+s_2)$. Then, by following the procedure used in our first example, we have

$$Q_2(s,0) = b(b+ac+cs)$$

$$Q_2(0,s) = (b+s)(b+ac+s) \tag{29}$$

$$Q_2(s,-s) = (b-s)(b+ac+cs-s).$$

For $c \neq 1$, the Eqs. 29 have no common zeros and thus the denominator, $Q_2(s_1,s_2)$, cannot be expressed in the form as given by Eq. 17.

However, for the special case in which $c = 1$, we have

$$K_2(s_1,s_2) = \frac{-1}{(b+s_2)(b+a+s_1+s_2)}. \tag{30}$$

This second-order kernel transform can be synthesized as shown in Fig. XVI-6.

4. Systems with Higher-Order Kernels

We now note that our results for second-order systems can be extended directly to higher-order systems. For example, a system consisting of only two multipliers whose kernel is clearly the most general third-order kernel that can be obtained is depicted in Fig. XVI-7. The third-order transfer function of this system is

$$K_3(s_1,s_2,s_3) = K_a(s_1)\,K_b(s_2)\,K_c(s_1+s_2)\,K_d(s_3)\,K_e(s_1+s_2+s_3). \tag{31}$$

Thus, if 2N multipliers are used to synthesize a third-order transfer function, then it must be of the form

$$K_3(s_1,s_2,s_3) = \frac{\sum_{n=1}^{N} R_{a_n}(s_1)\,R_{b_n}(s_2)\,R_{c_n}(s_1+s_2)\,R_{d_n}(s_3)\,R_{e_n}(s_1+s_2+s_3)}{F_a(s_1)\,F_b(s_2)\,F_c(s_1+s_2)\,F_d(s_3)\,F_e(s_1+s_2+s_3)}. \tag{32}$$

Furthermore, if a third-order transfer function is expressible in the form of Eq. 32, then it can be synthesized by means of 2N multipliers. A procedure

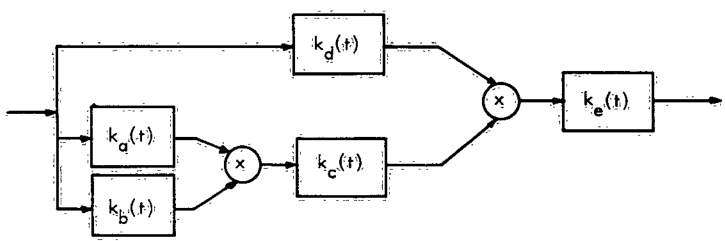

Fig. XVI-7. The most general third-order kernel with only two multipliers.

by which this can be accomplished is similar to the one described for the synthesis of second-order systems.

M. Schetzen

References

1. N. Wiener, Nonlinear Problems in Random Theory (The Technology Press of Massachusetts Institute of Technology, Cambridge, Mass., and John Wiley and Sons, Inc., New York, 1958).

2. Y. W. Lee and M. Schetzen, Measurement of the kernels of a nonlinear system by crosscorrelation, Quarterly Progress Report No. 60, Research Laboratory of Electronics, M.I.T., January 15, 1961, pp. 118-130.

3. M. Schetzen, Measurement of the kernels of a nonlinear system by crosscorrelation with Gaussian non-white inputs, Quarterly Progress Report No. 63, Research Laboratory of Electronics, M.I.T., October 15, 1961, pp. 113-117.

B. MAXIMA OF THE MEAN-SQUARE ERROR IN OPTIMUM NONLINEAR NO-MEMORY FILTERS

1. Introduction

In this report we are interested in the problem of mean-square filtering for the class of no-memory filters shown in Fig. XVI-8.

We consider the case

$$x(t) = m(t) + n(t)$$

$$z(t) = m(t),$$

in which m(t), the message, and n(t), the noise, are statistically independent. For this case we have obtained and reported previously[1] a relation between the amplitude probability density of the input and the characteristic of the optimum nonlinear no-memory filter. In the present report we use those results to derive a simple expression for the

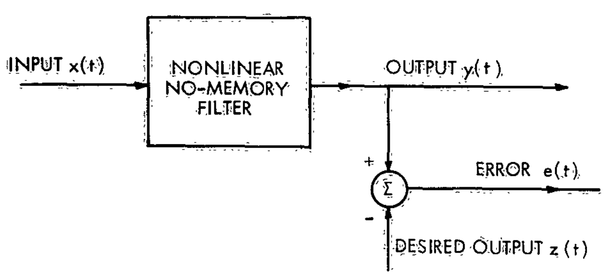

Fig. XVI-8. Filter operation considered in this report.

resulting mean-square error in the cases of Poisson noise and Gaussian noise. In the case of additive Gaussian noise, this expression involves only the amplitude probability density of the input and its first derivative. We take advantage of this characteristic to find the message probability density corresponding to the largest mean-square error in an optimum nonlinear no-memory filter under the constraint that the average message power be constant. The resulting message probability density is Gaussian.

2. Expression for the Mean-Square Error

The relation between the probability density of the input of the filter and the characteristic of the optimum nonlinear no-memory filter which we obtained previously is repeated here:

$$[x-g(x)]\, q(x) = \int q(x_1)\, f(x-x_1)\, dx_1.$$

Here, $q(x) = p_{m+n}(x)$ is the amplitude probability density of the input, $g(x)$ is the optimum nonlinear no-memory filter characteristic and

$$f(x) = \frac{1}{2\pi} \int F(t)\, e^{-jtx}\, dt$$

$$F(t) = \frac{d[\ln P_n(t)]}{d(jt)}$$

in which $P_n(t)$ is the characteristic function for the noise. Note that we use an integral sign without limits to indicate integration from $-\infty$ to $+\infty$. We can express $g(x)$ in terms of $q(x)$ by writing

$$g(x) = \frac{-\int q(x_1)\, f(x-x_1)\, dx_1}{q(x)} + x.$$

Whenever $f(x)$ is a singularity function, this relation for $g(x)$ leads to a simple expression for the mean-square error in terms of $q(x)$, the input probability density. The two well-known, nontrivial noise characteristics that give a singularity function for $f(x)$ are Gaussian noise and Poisson noise. We shall use the following expression for the mean-square error:

$$\overline{\mathcal{E}^2} = m^2 - \int g^2(x)\, q(x)\, dx,$$

in which m^2 is the mean-square value of the message. This expression is obtained without difficulty by using the known result that the error resulting from the optimum mean-square filter is uncorrelated with the output of all nonlinear no-memory filters with the same input.

a. Poisson Noise

$$P(x=k) = \frac{\lambda^k}{k!} e^{-\lambda}$$

$$P(t) = e^{\lambda(e^{jt}-1)}$$

hence

$$f(x) = \lambda u(x-1),$$

and

$$g(x) = -\lambda \frac{q(x-1)}{q(x)} + x.$$

$$\overline{\mathscr{E}^2} = m^2 - \int \left[-\lambda \frac{q(x-1)}{q(x)} + x\right]^2 q(x)\, dx$$

$$= m^2 - \int x^2 q(x)\, dx + 2\lambda \int xq(x-1)\, dx - \lambda^2 \int \frac{q^2(x-1)}{q(x)}\, dx$$

Since

$$\int xq(x-1)\, dx = \int (x+1)q(x)\, dx = \overline{m} + \lambda + 1$$

and

$$\int x^2 q(x)\, dx = m^2 + \lambda + \lambda^2 + 2\,\overline{m}\,\lambda,$$

then we have

$$\overline{\mathscr{E}^2} = \lambda + \lambda^2 - \lambda^2 \int \frac{q^2(x-1)}{q(x)}\, dx. \tag{1}$$

Equation 1 holds whether or not the message has zero mean.

b. Gaussian Noise

$$p_n(x) = \frac{1}{\sqrt{2\pi}\,\sigma} \exp\left(-\frac{x^2}{2\sigma^2}\right)$$

$$P_n(t) = \exp\left(-\frac{\sigma^2 t^2}{2}\right),$$

hence

$$f(x) = -\sigma^2 u_1(x)$$

and

$$g(x) = \sigma^2 \frac{q'(x)}{q(x)} + x.$$

$$\overline{\mathscr{E}^2} = m^2 - \int \left[\sigma^2 \frac{q'(x)}{q(x)} + x\right]^2 q(x)\, dx$$

Since

$$\int x^2 q(x)\, dx = m^2 + \sigma^2$$

and

$$\int x q'(x)\, dx = xq(x)\Big|_{-\infty}^{+\infty} - \int q(x)\, dx = -1,$$

then we have

$$\overline{\mathscr{E}^2} = \sigma^2 - \sigma^4 \int \frac{q'^2(x)}{q(x)}\, dx. \tag{2}$$

3. Maximum of the Error under Constraints for Additive Gaussian Noise

Since we have an expression for the mean-square error solely in terms of the input probability density, we can find extrema of the error under constraint by the method of calculus of variations. We shall consider, for the present, a power constraint on the input.

a. Power Constraint

We consider here a filtering problem characterized by additive Gaussian noise of known average power. We consider all possible messages of fixed average power, and in each case use the optimum nonlinear no-memory filter in the mean-square sense to separate the message from the noise. We now undertake to find the message probability density that gives an extremum of the mean-square error. Since the message and the noise are statistically independent, a constraint on the input average power is equivalent to a constraint on the message average power, and we write

$$\int x^2 q(x)\, dx = m^2 + \sigma^2.$$

Other constraints are

$$\int q(x)\, dx = 1$$

$$q(x) \geq 0 \qquad \text{for all } x$$

We take care of the last constraint by letting

$$y^2(x) \triangleq q(x),$$

and we have

$$\overline{\mathcal{E}^2} = \sigma^2 - 4\sigma^4 \int y'^2(x)\, dx. \tag{3}$$

Because $q(x)$ is the result of convolving a Gaussian probability density with the message probability density $p_m(x)$, we would need another constraint on $q(x)$ to ensure that $p_m(x)$ is positive. However, this constraint cannot be handled analytically, and we shall have to select among the solutions obtained for $q(x)$ those leading to an acceptable probability density. In terms of $y(x)$, using the Lagrange multiplier, we look for extrema of

$$J = \int \left[y'^2 + \lambda_1 x^2 y^2 + \lambda_2 y^2\right] dx,$$

in which λ_1 and λ_2 are Lagrange multipliers. This leads to the following Euler-Lagrange equation:

$$y'' + y\left[\lambda_1 x^2 + \lambda_2\right] = 0. \tag{4}$$

We have obtained here the Weber-Hermite differential equation. Since we are looking for solutions that are square integrable, we have the boundary conditions

$$y \to 0 \quad \text{for} \quad |x| \to \infty.$$

The differential equation has solutions that satisfy these boundary values[2] only if it is in the form

$$\frac{d^2y}{du^2} + y\left[n + \frac{1}{2} - \frac{u^2}{2}\right] = 0 \tag{5}$$

in which n, a non-negative integer, is the eigenvalue. The corresponding solutions or eigenfunctions are the Hermite functions

$$y_n(u) = D_n(u) \triangleq \exp\left(-\frac{u^2}{2}\right) 2^{-n/2}\, H_n\left(\frac{u}{\sqrt{2}}\right)$$

in which $H_n(v)$ is the Hermite polynomial.

$$H_n(v) \triangleq (-1)^n e^{v^2} \frac{d^n e^{-v^2}}{dv^n}$$

To put Eq. 4 in the form of Eq. 5, we let $x = cu$, in which c is a constant, and thus obtain the solution

$$y_n(x) = A\, D_n\left(\frac{x}{c}\right).$$

Here, A, an arbitrary constant, appears because the linear differential equation to be satisfied is an homogeneous equation. The solution for the amplitude probability density of the input becomes

$$q_n(x) = A^2 D_n^2\left(\frac{x}{c}\right).$$

It can be shown that the minimum of the integral $\int y'^2\, dx$ that appears with a minus sign in the expression for the mean-square error (Eq. 3) corresponds to the eigenvalue $n = 0$. For $n = 0$ we have

$$q(x) = A^2 \exp\left(-\frac{x^2}{2c^2}\right)$$

which is, therefore, the amplitude probability of the input giving the maximum mean-square error.

We satisfy the constraints by letting $A^2 = 1/\sqrt{2\pi}\, c$, and $c^2 = \sigma^2 + m^2$. Therefore,

$$q(x) = \frac{1}{\sqrt{2\pi}\sqrt{\sigma^2 + m^2}} \exp\left(-\frac{x^2}{2(\sigma^2+m^2)}\right).$$

The probability density of the message now is

$$p_m(x) = \frac{1}{\sqrt{2\pi}\, m} \exp\left(-\frac{x^2}{2m^2}\right).$$

Hence, when the noise is Gaussian and additive, and the message has a fixed average power, the maximum mean-square error is obtained whenever the message is also Gaussian. In such a case, the optimum no-memory filter reduces to an attenuator and

$$\overline{\mathscr{E}^2} = \sigma^2 - \sigma^4 \int \frac{q'^2(x)}{q(x)}\, dx = \frac{\sigma^2 m^2}{\sigma^2 + m^2}.$$

One might wonder if some interpretation can be given in the context to higher-order eigenvalues and eigenfunctions ($n = 1, 2$, etc.) which correspond to stationary values of the expression for mean-square error.

However, although $(q(x)=A^2D_n^2(x/c))$, the probability density of the input, is positive for all x, the corresponding message probability density $p_m(x)$ is not strictly positive for $n > 0$ and does not correspond to a physical situation.

Although we did not obtain it by the present formulation, an interesting result would be to find out whether a minimum of the optimum mean-square error exists under the same constraint. It is possible to show that an arbitrarily small error can be achieved unless additional constraints are used. Work is under way in this area.

V. R. Algazi

References

1. V. R. Algazi, Nonlinear no-memory filters of prescribed form, Quarterly Progress Report No. 66, Research Laboratory of Electronics, M.I.T., July 15, 1962, p. 201.

2. See, for instance, G. Birkhoff and G. C. Rota, Ordinary Differential Equations (Ginn and Company, Boston, 1962), p. 280.

XVII. PROCESS ANALYSIS AND SYNTHESIS

Dr. M. V. Cerrillo
Prof. H. J. Zimmermann
J. S. MacDonald
Rita K. Toebes

RESEARCH OBJECTIVES

The research of this group for the past several years has been concerned with a number of basic problems aimed at extending current concepts in communication theory. Theoretical concepts are being developed, and experimental verification is being sought for some of the "subjective" aspects of the communication problem. In general terms, these are problems that are routinely solved by the human brain. Without in any way implying an attempt to understand the functioning of the brain, the research seeks to establish explanations for some of these subjective effects. The theory of symmetry has been used as a basic tool in establishing orders in certain classes of subjectivity. Examples of the kinds of problem that are being studied are the characterization and transformation of style in music and paintings.

M. V. Cerrillo

XVIII. PROCESSING AND TRANSMISSION OF INFORMATION*

Prof. W. B. Davenport, Jr.	Dr. A. Wojnar	A. R. Hassan
Prof. P. Elias	T. Adcock	J. L. Holsinger
Prof. R. M. Fano	T. M. Anderson	T. S. Huang
Prof. R. G. Gallager	M. H. Bender	R. S. Kennedy
Prof. F. C. Hennie III	E. F. Berlekamp	L. Kleinrock
Prof. E. M. Hofstetter	J. E. Cunningham	A. H. Molin
Prof. D. A. Huffman	H. Dym	J. E. Savage
Prof. I. M. Jacobs	P. M. Ebert	J. R. Sklar
Prof. A. M. Manders	D. Ecklein	I. G. Stiglitz
Prof. B. Reiffen	D. D. Falconer	I. E. Sutherland
Prof. W. F. Schreiber	E. F. Ferretti	W. R. Sutherland
Prof. C. E. Shannon	G. D. Forney, Jr.	O. J. Tretiak
Prof. J. M. Wozencraft	U. F. Gronemann	W. J. Wilson
Dr. C. L. Liu	P. W. Hartman	H. L. Yudkin

RESEARCH OBJECTIVES

This group continues its investigation of sources that generate information, channels that transmit it, and machines that process it.

Work is continuing on the processing of pictures by means of computers. The broad objective of this work is to elucidate the fundamental properties of vision as they apply to image transmission and reproduction. Among the more specific objectives are the design of efficient image-transmission systems, and the development of devices capable of performing some "human" operations, such as noise reduction, image detection, and quality improvement.

The efficient transmission of speech by digital means is also receiving some attention. The objective of this work is the early exploitation for speech communication of digital transmission systems employing encoding and decoding.

During the past year, significant new results have been obtained on the properties of sequential encoding and decoding, and on feedback strategies for noisy two-way channels. Increased emphasis is being placed on the exploitation of these techniques in conjunction with physical channels, and on the design of the necessary encoding and decoding equipment. Plans for the future include the development of acoustic channels capable of simulating multipath and scattering phenomena of practical interest, and of encoding and decoding equipment sufficiently flexible to permit experimentation in real time in conjunction with these channels.

An effort is being made to bring into sharper focus the relation between the newer encoding techniques and older modulation schemes. For this purpose, the behavior near threshold of frequency modulation and pulse-position modulation are being investigated by experimental, as well as analytical, means.

Work continues, also, on the structural characteristics of digital machines. A prime objective of this work is the establishment of relations among the reaction time of machine, the complexity of the data processing to be performed, the number of storage elements, and the speed of the elementary components.

R. M. Fano, D. A. Huffman, W. F. Schreiber, J. M. Wozencraft

*This research was supported in part by Purchase Order DDL B-00368 with Lincoln Laboratory, a center for research operated by Massachusetts Institute of Technology, with the joint support of the U.S. Army, Navy, and Air Force under Air Force Contract AF19(604)-7400; and in part by the National Institutes of Health (Grant MH-04737-02).

A. PICTURE PROCESSING

1. A STUDY OF THE PICTURE-SAMPLING PROCESS

Every picture-transmitting system involves a stage in which an electric signal is abstracted from a source image, and a stage in which the electric signal is converted to another image. The first of the above-mentioned stages may be thought of as a sampling process, and the second as a filtering operation.

If the picture-transmitting system is one that sends a sequence of signal values (sampled data), the over-all system may be modeled as the block diagram shown in Fig. XVIII-1. While this block diagram is not a good description of all possible image-transmission systems, many systems do fit our model. Note that the input function is a function of two dimensions (space) if the picture is a photograph, and of two spatial dimensions and time for a real image. The present study is restricted t. still pictures; thus the filters and functions are defined on two variables — they are two dimensional.

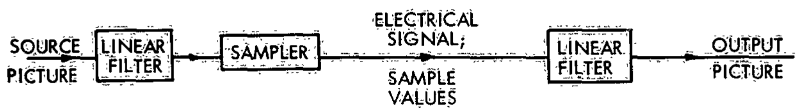

Fig. XVIII-1. Diagram of image-transmission system.

The purpose of this study is to investigate the effect of the impulse responses of the two linear filters in Fig. XVIII-1 on the quality of the transmitted picture. The experiments will be performed with the digital television equipment built by our group.[1] The filter used before sampling is synthesized by defocusing the scanner lens, and placing a transparency on the lens. The impulse response of such an optical system is just the transmittance distribution of the transparency on the lens. The linear filter that converts the sample values into the final picture is a similar combination of defocused lens and transparency in the recording camera.

O. J. Tretiak

References

1. J. W. Pan, U. F. Gronemann, T. S. Huang, J. E. Cunningham, and W. F. Schreiber, Picture Processing Research, Quarterly Progress Report No. 61, Research Laboratory of Electronics, M. I. T., April 15, 1961, p. 133.

2. THE MATHEMATICAL FOUNDATION OF THE SYNTHETIC HIGHS SYSTEM

The Synthetic Highs[1] system is a channel-capacity reduction technique that is useful for efficient coding of television signals. Figure XVIII-2 illustrates the logic used, and Figure XVIII-3 shows waveforms illustrating the underlying principle. Figure XVIII-3a

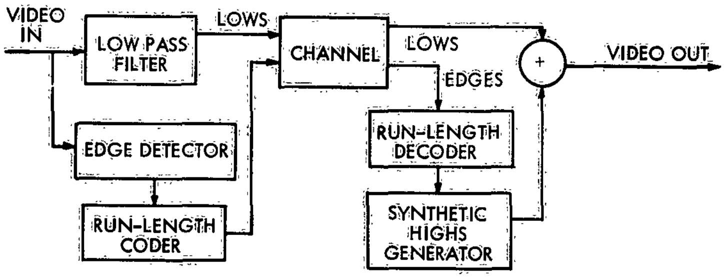

Fig. XVIII-2. Diagram of Synthetic Highs system.

is an exemplary video signal. The low-frequency component (Fig. XVIII-3b) is transmitted conventionally. The edge detector is essentially a differentiator, giving the output, (Fig. XVIII-3c). This signal is transmitted by some form of run-length coding, put back in real time by the decoder, and applied to the synthetic highs generator (a linear filter) to produce the waveform (Fig. XVIII-3d). This waveform is added to the transmitted lows to produce the output video.

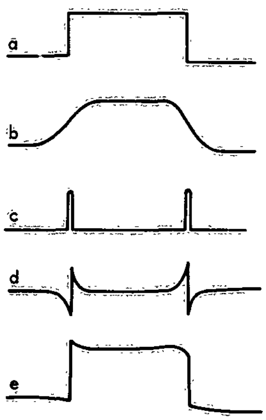

Fig. XVIII-3. Waveforms of Synthetic Highs system.

It has always been evident from qualitative considerations that if the edge detection (differentiation), coding, and decoding were error-free, then a linear filter could be found to generate a high-frequency component to produce a video output identical with the input.[2] This has been confirmed by experiment, but never proved mathematically. The purpose of this note is to present a proof and to extend the theory to two- and three-dimensional coding.

a. One-dimensional Case

Consider a picture whose brightness as a function of position is called B(x). If the spatial impulse response of the lowpass filter is M(x), and the output of the edge detector is dB/dx, then we have the problem of finding a filter whose impulse response $H(x)$ satisfies the following equation:

$$\int \frac{dB(x')}{dx} H(x-x')\, dx' = B(x) - \int B(x')\, M(x'-x)\, dx'. \tag{1}$$

Put into words, the edge signal dB/dx is applied to the filter H, and the output is to be the high-frequency component of the original video, expressed as the entire signal minus the low-frequency component. This equation is solved by taking transforms of both sides. sides. Thus

$$j\omega\, b(\omega)\, h(\omega) = b(\omega) - b(\omega)\, m(\omega). \tag{2}$$

As long as $b(\omega) \neq 0$,

$$j\omega\, h(\omega) = 1 - m(\omega). \tag{3}$$

Taking inverse transforms, we obtain

$$\frac{dH}{dx} = u_o(x) - M(x) \tag{4}$$

$$H(x) = u_{-1}(x) - \int_{-\infty}^{x} M(x')\, dx' \tag{5}$$

which is precisely the result that was obtained experimentally.

b. Two-Dimensional Case

Since the correlation between vertically disposed picture elements is fully as great as that between horizontally disposed elements, it is clear that increased savings are available by extending the technique to two dimensions. The first successful attempt to do this was reported by a member of our group recently.[3] In his work, John W. Pan detected both horizontal and vertical edges and transmitted them to the receiver by fitting a series of straight lines to the outlines of objects in the picture. The high-frequency signal was synthesized in terms of either a vertical or horizontal edge, whichever was closer to the fitted line segment. Artifacts occurred at the corners of objects and along contours of approximately 45°, the former being partially eliminated by a special "rounding" routine.

An alternative procedure suggests itself in connection with the preceding mathematical derivation. Suppose that we use a system very similar to that in Fig. XVIII-2, but in which the filters are two-dimensional, the edge detector is a contour detector, and the run-length coder is some form of contour tracer and coder. The question then arises about whether there is a two-dimensional filter into which one can put data on the contours of an image (such data being efficiently codable) and out of which one might obtain the two-dimensional high-frequency component of the image. The filter should be invariant with the image so that all possible images might be handled without introducing spurious artifacts in special cases such as at corners of objects. It has been found possible to solve this problem if the gradient of the image, ∇B is used as an edge detector, and if the filter is specified by its vector impulse response.

The output of the filter, which is the scalar high-frequency component, is then defined as the dot product convolution of the input ∇B and the response H. Thus we have a relation analogous to (1) to define H.

$$\nabla B \odot \overline{H} = B - B \otimes M, \tag{6}$$

where $\otimes$ is the conventional scalar convolution, and $\odot$ is the dot product convolution. Taking the transform of both sides, we have

$$[j\overline{\omega}\, b(\overline{\omega})] \cdot \overline{h}(\omega) = b(\overline{\omega}) - b(\overline{\omega})\, m(\overline{\omega}). \tag{7}$$

For $b \neq 0$,

$$j\overline{\omega} \cdot \overline{h} = 1 - m(\overline{\omega}) \tag{8}$$

which, by rule (A-5) in the Appendix, can now be retransformed into the space domain to yield

$$\nabla \cdot \overline{\overline{H}} = u_0(\overline{r}) - M(\overline{r}). \tag{9}$$

We solve for $\overline{H}$ by integrating throughout the circle of radius r.

$$\int_0^{2\pi}\int_0^{r} \nabla \cdot \overline{H}\, r\, dr d\theta = \int_0^{2\pi}\int_0^{r} [u_0(\overline{r}) - M(\overline{r})]\, r\, dr d\theta = 1 - \int_0^{2\pi}\int_0^{r} M(\overline{r})\, r\, dr d\theta \tag{10}$$

We simplify this equation by assuming radial symmetry and by applying the divergence theorem to the left-hand side.

$$\begin{aligned} \oint_r \overline{H} \cdot \hat{n}\, r\, d\theta &= 1 - 2\pi \int_0^r L(\overline{r})\, r dr \\ \overline{H} \cdot \hat{r}\, 2\pi r &= 1 - 2\pi \int_0^r L(\overline{r})\, r dr \end{aligned} \tag{11}$$

$$\overline{H} = \hat{r}\left[\frac{1}{2\pi r} - \frac{1}{r}\int_0^r L(\overline{r})\, r dr\right] \tag{12}$$

This general result indicates that it is possible to implement the system of Fig. XVIII-2 in two dimensions. The reconstructed picture should be identical to the original if the gradient field is transmitted without error. Previous experience with the tolerance of human vision to errors caused by nonexact gradient transmission in one dimension indicate that quite high efficiency; that is, more than ten-to-one reduction in data rate should be possible with quite small quality impairment. To achieve this, it will be necessary to fit curves of at least second degree to the detected gradient points, so that discontinuous second derivatives of the outlines may be avoided.

c. Three-Dimensional Case

The relation (9) is valid for any number of dimensions, since it was derived in vector form, the only restriction being the transformability of the function involved. We may thus solve for $\bar{H}$ in three dimensions, assuming radial symmetry,

$$\int_r \nabla \cdot \bar{H}\, dV = 1 - \int_r L(\bar{r})\, dV, \tag{13}$$

where $\int_r dV$ signifies a volume integral within the sphere of radius r. Again using the divergence theorem, we obtain

$$\int_r \bar{H} \cdot \hat{n}\, dS = 1 - \int_r M(\bar{r})\, dV \tag{14}$$

$$\bar{H} \cdot \hat{r}\, 4\pi r^2 = 1 - \int_r M(\bar{r})\, dV \tag{15}$$

$$\bar{H} = \frac{\hat{r}}{4\pi r^2}\left[1 - \int_r M(\bar{r})\, dV\right]. \tag{16}$$

The three-dimensional situation arises when we deal with images that change in time. The input is then B(x, y, t). From our analysis, it appears possible to reconstruct B(x, y, t) at the receiver by combining a low-frequency component (that is, a low-definition, low frame-rate picture) with a synthetic highs component. The last component is found from the dot product convolution of the transmitted gradient and a spatio-temporal filter $\bar{H}$.

To economize on the transmission of the gradient data, presumable it would be possible to perform a contour-tracing operation and then transmit a few parameters of the contours. In this case, the "contours" would be surfaces rather than curves.

It is evident that the restriction to radially symmetrical three-dimensional filters means that the errors introduced into the space and time domains of the moving image which are due to quantizing errors, will be similar. Since the spatial and temporal frequency responses of human vision, as deduced from threshold measurements, are similar in shape (some worker believe they are physiologically related) it is to be expected that similar distortions will be similarly acceptable.

APPENDIX

FOURIER TRANSFORMS IN VECTOR NOTATION

1. Introduction

Using capitals to represent functions in the space domain and lower case letters for their corresponding transforms, we have

$$\bar{r} = x\hat{i} + y\hat{j}$$

$$\bar{\omega} = \omega_x\hat{i} + \omega_y\hat{j}$$

$$\bar{H}(r) = \bar{H}(x, y) = H_x\hat{i} + H_y\hat{j}.$$

(Do not confuse $j = \sqrt{-1}$ with $\hat{j}$, the unit vector in the y or ω_y direction.)

We define the two-dimensional transform

$$\bar{m}(\omega) = \iint M(\bar{r})\, e^{-j\bar{\omega}\cdot\bar{r}}\, dA.$$

Here, dA is the area element in the space domain. On this basis, and using the linearity properties of Fourier transforms, we have

$$\bar{h}(\bar{\omega}) = h_x(\bar{\omega})\hat{i} + h_y(\bar{\omega})\hat{j}$$

$$= \hat{i} \iint H_x(\bar{r})\, e^{-j\bar{\omega}\cdot\bar{r}}\, dA + \hat{j} \iint H_y(\bar{r})\, e^{-j\bar{\omega}\cdot\bar{r}}\, dA$$

$$\bar{h}(\bar{\omega}) = \iint \bar{H}(\bar{r})\, e^{-j\bar{\omega}\cdot\bar{r}}\, dA$$

which we write

$$\bar{h}(\bar{\omega}) \Longleftrightarrow \bar{H}(\bar{r}) \tag{A-1}$$

$$h_x(\bar{\omega}) \Longleftrightarrow H_x(\bar{r}) \tag{A-2}$$

$$h_y(\bar{\omega}) \Longleftrightarrow H_y(\bar{r}). \tag{A-3}$$

2. Differential Operators

Since $h(\bar{\omega}) = \iint H(\bar{r})\, e^{-j\bar{\omega}\cdot\bar{r}}\, dA$, it can be shown for reasonable H's that

$$H(\bar{r}) = \iint h(\bar{\omega})\, e^{j\bar{\omega}\cdot\bar{r}}\, \frac{d\Omega}{(2\pi)^2},$$

where $d\Omega$ is the area element in the frequency domain. Thus

$$\frac{\partial H}{\partial x} = \iint j\omega_x h(\bar{\omega})\, e^{j\bar{\omega}\cdot\bar{r}}\, \frac{d\Omega}{(2\pi)^2}$$

$$\frac{\partial H}{\partial y} = \iint j\omega_y h(\bar{\omega})\, e^{j\bar{\omega}\cdot\bar{r}}\, \frac{d\Omega}{(2\pi)^2}.$$

Since $\nabla H = \hat{i}\frac{\partial H}{\partial x} + \hat{j}\frac{\partial H}{\partial y}$, we have

$$\nabla H = \iint j\bar{\omega} h(\bar{\omega})\, e^{j\bar{\omega}\cdot\bar{r}}\, \frac{d\Omega}{(2\pi)^2}$$

$$\boxed{\nabla H \Longleftrightarrow j\bar{\omega} h} \tag{A-4}$$

If $\bar{H}$ is a vector, so that $H_x \Longleftrightarrow h_x$, then $\frac{\partial H_x}{\partial x} \Longleftrightarrow j\omega_x h_x$, and so on.

Since $\nabla \cdot \bar{H} = \frac{\partial H_x}{\partial x} + \frac{\partial H_y}{\partial y} = \iint j(\omega_x h_x + \omega_y h_y)\, e^{j\bar{\omega}\cdot\bar{r}}\, \frac{d\Omega}{(2\pi)^2}$

$$\boxed{\nabla \cdot \bar{H} \Longleftrightarrow j\bar{\omega}\cdot\bar{h}} \tag{A-5}$$

3. Convolutions

In multidimensional space, we can take convolutions among vectors, scalars or vectors and scalars. It is of interest to find the equivalent operation in the frequency domain to these various convolutions in the space domain. By strict analogy with the one-dimensional use, we have

$$P \otimes Q \Longleftrightarrow pq \tag{A-6}$$

$$\bar{P} \otimes Q \Longleftrightarrow \bar{p}q, \text{ where } \otimes \equiv \text{scalar convolution.} \tag{A-7}$$

Since $\bar{P} \cdot \bar{Q} = P_x Q_x + P_y Q_y$,

$$\bar{P} \odot \bar{Q} \Longleftrightarrow \bar{p}\cdot\bar{q}, \tag{A-8}$$

where $\odot$ ≡ scalar product convolution.

W. F. Schrieber

References

1. W. F. Schreiber, C. F. Knapp, and N. D. Kay, Synthetic Highs — an experimental TV bandwidth reduction system, SMPTE J. 68, 525 (1959)

2. In practice, the motivation for using this technique is that for statistical and psychophysical reasons, it is possible to make substantial economies in the transmission of the edge signal without serious image degradation. These economies involve, among other things, the introduction of quantizing errors into the edge transmission.

3. J. W. Pan, Picture processing, Quarterly Progress Report No. 66, Research Laboratory of Electronics, M. I. T., July 15, 1962, p. 229.

B. FREQUENCY-COMPRESSIVE FEEDBACK SYSTEMS

1. Introduction

The main purpose of this research project is to extend the analysis of a signal-tracking FM system[1] which has recently been applied successfully in space communication. A system with a frequency-compressive feedback loop around the frequency demodulator was devised[2] as early as 1939, but its applications did not appear until the late 1950's, and, in fact, a careful analysis was not begun until the appearance of Enloe's paper,[3] in 1962. Enloe's prediction of the second threshold in the closed loop seems to be qualitatively correct; the purpose of the present research is to provide a quantitative verification.

In order to extend the analysis of threshold phenomena in FM systems, an attempt has been made to develop new formulas for determining the input and output signal-to-noise ratios at the "threshold of full improvement." Thus, we seek to bridge the gap between exact analysis (leading to complex nondiscussible expressions) and elementary approximations with limited validity.

Our final aim is to prescribe the synthesis procedure for optimum FM reception filters and to determine the power-bandwidth "trade-off" relations.

2. Threshold in the Conventional System

Threshold in an FM system is the transition region between linear and nonlinear input-output behavior, as well as between Gaussian and non-Gaussian output noise domains. Early progress in analyzing the FM threshold phenomena has been achieved mainly by the very complex computations of Rice[4,5] and Stumpers.[6] Rice's results were exploited by Skinner,[3] who produced the threshold curves of the conventional FM system with ideal filters and an ideal demodulator.

Skinner's plot[3] clearly shows that the carrier-to-noise power ratio (CNR) producing the threshold (of full improvement[7]) depends on filter bandwidths and can hardly be considered constant. The widely assumed existence of a fixed threshold CNR leads inevitably to errors of approximately 5 db, or more.

To facilitate the analysis of the real, sliding threshold, we propose a new simple expression:

$$r_t' = \frac{B_{IF}}{B_{LF}},$$

where r_t' is the demodulator input CNR at the threshold (in the if band), B_{IF} is the equivalent two-sided noise bandwidth of the predemodulator filter, and B_{LF} is the equivalent noise bandwidth of the postdemodulator filter.

Comparison of this formula with the Skinner-Replogle[8] exact threshold curves shows

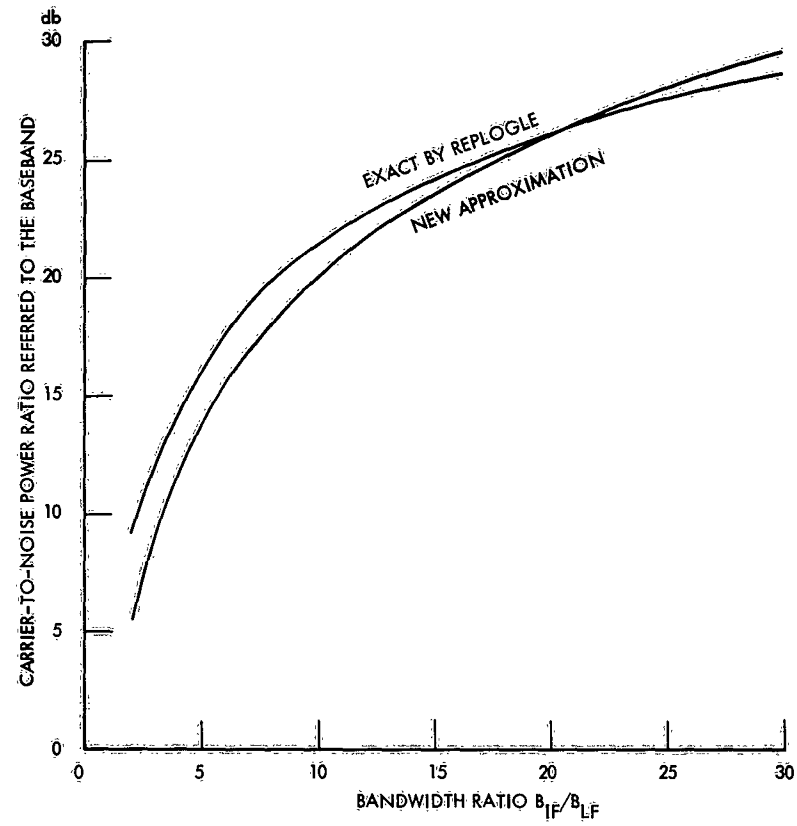

Fig. XVIII-4. Comparison of the new expression for threshold carrier-to-noise power ratio in the baseband with the Skinner-Replogle exact threshold curve.

that now the errors do not exceed 2 db in the very wide range

$$\frac{B_{IF}}{B_{LF}} = 3 \div 30.$$

(See Fig. XVIII-4.)

The well-established expression for output signal-to-noise power ratio at and above the threshold of full improvement is

$$R = \frac{3}{2} m^2 r,$$

where both the input CNR, denoted r, and the output SNR, denoted R, are determined in a bandwidth that is equal to the baseband; m denotes the modulation index of an FM signal. Hence, we obtain a new formula for SNR at threshold:

$$R_t = \frac{3}{2} m^2 r_t = \frac{3}{2} m^2 \left(\frac{B_{IF}}{B_{LF}}\right)^2.$$

Let us also assume that the if filter of nearly rectangular shape has a noise bandwidth equal to the approximate bandwidth of the FM signal:

$$B_{IF} = B_S \cong 2f_m(1+m),$$

where f_m denotes the baseband width or the maximum modulating frequency. Then, with the postdemodulator filter also matched to the baseband ($B_{LF}=f_m$), we obtain

$$r_t \approx 4(1+m)^2$$

$$R_t \approx 6m^2 (1+m)^2.$$

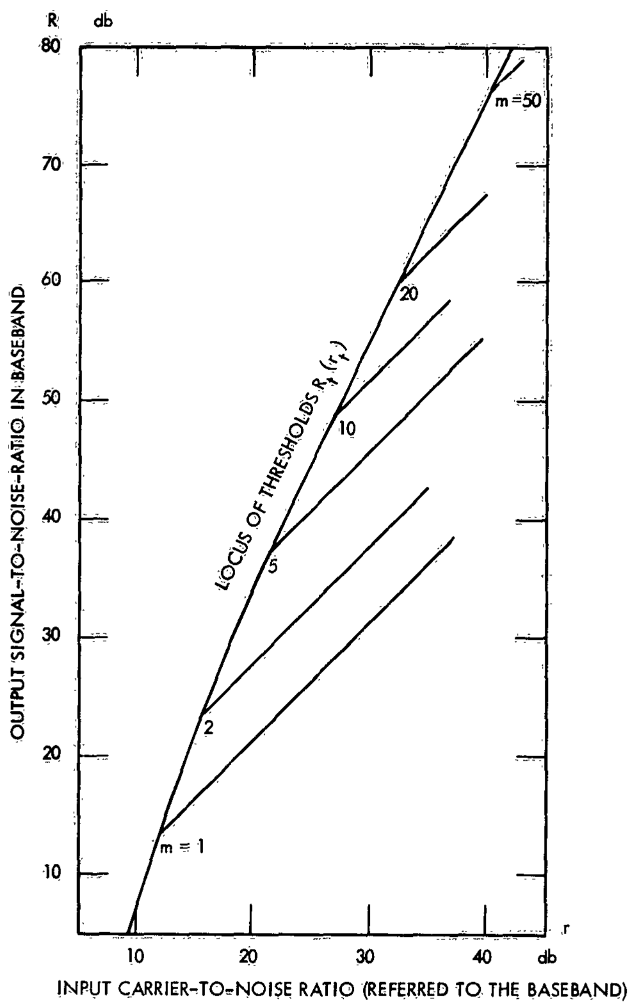

Fig. XVIII-5. Optimum conventional FM systems.

This set of simple but fairly accurate formulas can be used to analyze quantitatively the threshold behavior in a conventional FM system. Note, for instance, that if the signal power, the noise power spectral density, and the baseband remain fixed, there exists a unique minimum value of the signal modulation index

$$m_{min} = \sqrt{\sqrt{\frac{R_t}{6} + \frac{1}{4}} - \frac{1}{2}},$$

which will yield the required system output performance R_t with minimum signal-bandwidth consumption.

Since r_t and R_t are strictly interrelated in an optimal fashion, we can represent all optimal conventional systems by a single locus (Fig. XVIII-5)

$$R_t = \frac{3}{2} r_t \left(\frac{r_t}{4} - \sqrt{r_t} + 1\right).$$

Each point on the locus graph corresponds to one value of the signal characteristic

$$m = \frac{1}{2} \sqrt{r_t} - 1.$$

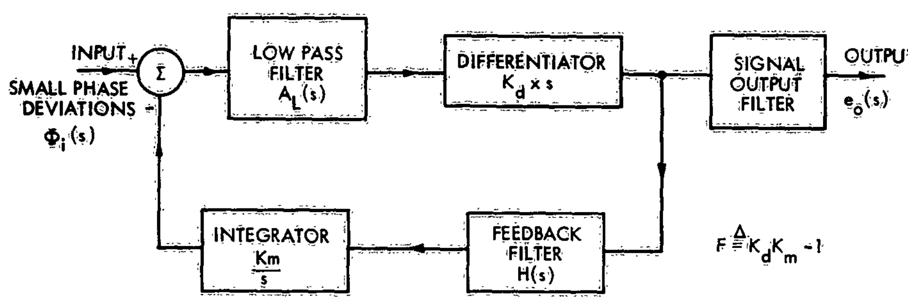

Fig. XVIII-6. Linearized baseband analog for a frequency-compressive FM system.

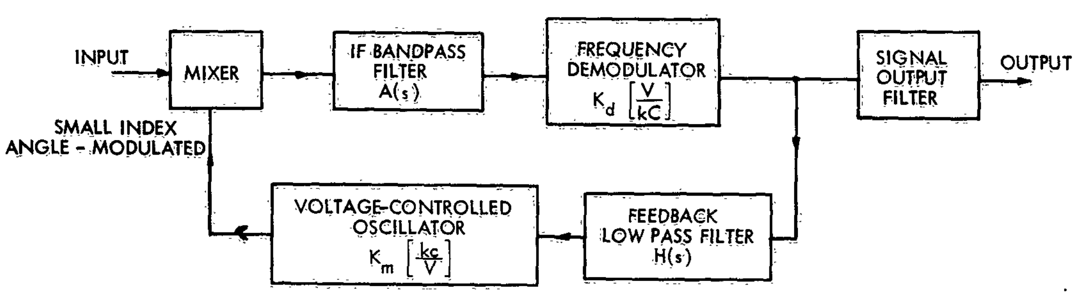

Fig. XVIII-7. Block diagram for a frequency-compressive feedback FM system.

3. Thresholds in the Frequency-Compressive Feedback System

In order to analyze the threshold behavior in the frequency-compressive feedback loop, we adopt Enloe's reasoning and results.[3,8] In particular, the fundamental limitation in exchanging power and bandwidth is believed to occur because of the so-called closed-loop feedback threshold.

When using the linearized baseband analog (Fig. XVIII-6) of the actual system (Fig. XVIII-7) note that a variety of feedback filter structures is possible, but for the if filter the single-pole bandpass structure is imposed by stability requirements. Enloe has found that the input noise in quadrature with the carrier produces angle noise modulation of the variable oscillator. If the rms phase deviation of this noise modulation is no longer small compared with unity, a new (feedback) threshold occurs.

As a measure for the location of this feedback threshold, Enloe suggested the input carrier-to-noise ratio ρ_c in the closed-loop noise bandwidth B_c, and evaluated it as

$$\rho_c = 5\left(\frac{F-1}{F}\right)^2,$$

where F is the feedback factor, which equals the frequency deviation compression ratio. Noise bandwidth B_c must be defined for the transfer from signal input to the oscillator input of the mixer.

The last formula may easily be translated to the customary baseband width f_m, and it becomes

$$\rho = 5\left(\frac{F-1}{F}\right)^2 \times \frac{B_c}{f_m}.$$

This threshold CNR can now be directly compared with the conventional (so-called open-loop) threshold r_t that occurs in the usual way in the frequency demodulator, preceded by a narrow-band if filter. Since both thresholds are independent, it is obvious that maximum system sensitivity occurs with $\rho = r_t$. This condition can be met by proper location of transfer poles around the feedback loop.

When positioning the pole of the if filter the compression of the signal modulation index, which is now m/F in the if path, should be implemented. Thanks to the reduction of nonlinear distortion in the feedback loop, it is no longer necessary that the signal bandwidth equal the filter noise bandwidth.[8] It is now sufficient to make the analog single-pole filter natural frequency, $a/2\pi$, equal to the if signal-frequency deviation, mf_m/F. Hence

$$\frac{a}{2\pi} = f_m \frac{m}{F}$$

and with the if filter noise bandwidth $B_{IF} = \frac{a}{2}$, we find

$$\left.\frac{B_{IF}}{f_m}\right| = \pi \frac{m}{F},$$

so that for the conventional threshold,

$$r_t = \left(\frac{B_{IF}}{f_m}\right)^2 \approx 10\left(\frac{m}{F}\right)^2.$$

The closed-loop noise bandwidth B_c depends for the most part on the structure and parameters of the feedback filter. With certain simple structures, however, a proportional relation of the type $B_c \approx 2\, f_m F$ is approximately valid. In this case we have

$$\rho \approx 10 \frac{(F-1)^2}{F}.$$

To fulfill the condition of maximum sensitivity, $\rho = r_t$, we then require

$$10\left(\frac{m}{F}\right)^2 = 10 \frac{(F-1)^2}{F}.$$

From this equation, we obtain the optimum signal index

$$m_{opt} = (F-1)\sqrt{F}$$

for a most sensitive feedback system with the compression ratio F. If the output performance R_t is prescribed, there is then no choice for F except

$$F_{opt} = 1 + \sqrt[4]{\frac{R_t}{15}} = 1 + 0.51\sqrt[4]{R_t},$$

and algebraically we can find

$$\rho = \frac{5.1\ \sqrt{R_t}}{1.97 + \sqrt[4]{R_t}}.$$

Now, a power comparison of the threshold r_t of a conventional FM system with that of a feedback system (ρ) is straightforward. Of course, equal performance R_t of both systems at the threshold should be assumed:

$$R_t = \frac{3}{2} m^2 r_t = \frac{3}{2} m_F^2 \rho,$$

where the subscript F pertains to the feedback system. Since for the conventional system, then, we have

$$r_t = \left(1 + \sqrt{1 + 2\sqrt{\frac{2}{3} R_2}}\right)^2$$

the extension of threshold amounts to

$$\frac{r_t}{\rho} = \frac{\left(1 + \sqrt{1 + 2\sqrt{\frac{2}{3} R_t}}\right)^2}{5.1 R_t / \left(1.97 + \sqrt[4]{R_t}\right)}.$$

Assuming, for example, that $R_t = 10^4$, or 40 db, we obtain the following feedback system parameters.

$$F_{opt} = 1 + 5.1 \sqrt[4]{10^4} = 6.1$$

$$m_{F_{opt}} = 5.1 \sqrt{6.1} = 12.6.$$

The power saving, in comparison with the standard system is, then

$$\frac{r_t}{\rho} = 4.5, \text{ or } 6.5 \text{ db}.$$

Note that there is actually a trade-off between bandwidth and power, since the signal bandwidth increases proportionally as $1 + m_F$. This leads to

$$\frac{B_{S_F}}{B_S} = \frac{1 + m_F}{1 + m} = \frac{1 + (F-1)\sqrt{F}}{\sqrt{\sqrt{\frac{R_t}{6}} + \frac{1}{4}} + \frac{1}{2}}.$$

In our example, it amounts to

$$\frac{B_{S_F}}{B_S} = \frac{13.6}{6.9} = 1.97,$$

that is, the 6.5-db power saving will require a 97 per cent increase in spectrum occupancy. It is, however, not the best trade-off obtainable with an optimally designed feedback filter.

4. Optimization of the Feedback Loop

For the feedback loop to be stable and to have finite noise bandwidth, it is necessary to interrelate the number of poles and the number of zeros in the open-loop transfer function. Two choices are possible: the number of poles exceeds the number of zeros by 1 (this gives a better stability margin), or the number of poles exceeds the number of zeros by 2 (this is still stable, although with a smaller margin).

Practical tests have shown that three poles in the open loop, excluding the chain of broadband if amplifiers, is the upper limit. It is known, also, that only one pole is allowed in the narrow-band if filter for stability reasons. Therefore one need only consider the following structures for the feedback filter: 1p; 1p and 1z; 2p and 1z; 2p and 2z.

In this list, the class with one zero can be subdivided into two groups: the zero cancels the if filter pole, and the zero does not cancel the if filter pole. The latter will subsequently be called a stabilizing zero. It is obvious that in the "2p and 2z" filter, one zero is of the cancelling type and the other of the stabilizing type.

The main requirements for the optimum feedback loop synthesis are: (a) open-loop transfer function should be reasonably <u>uniform</u> over the baseband (in order to have the if frequency deviation compressed for all modulation frequencies); and (b) closed-loop noise bandwidth should be <u>minimized</u> by a judicious choice of the feedback filter structure and of the location of its stabilizing zero.

It is important to note again that the closed-loop transfer and bandwidth are defined between the two inputs of the mixer (Fig. XVIII-7). The closed-loop transfer function $H_c(s)$ is uniquely determined by the open-loop transfer function $H_o(s)$.

$$H_c(s) = \frac{H_o(s)}{1 + H_o(s)}.$$

The definition of the closed-loop noise bandwidth that has been adopted is

$$B_c = \frac{1/2\pi j}{[H_c(0)]^2} \int_{-j\infty}^{j\infty} H_c(s)\, H_c(-s)\, ds$$

and the integration can easily be performed for rational transfer functions.[9]

In particular, the open-loop transfer function of the highest permitted order has the form

$$H_o(s) = \frac{a}{s+a} \times \frac{b}{s+b} \times \frac{s+c}{c} \times (F-1),$$

which directly corresponds to the most general "2p and 2z" case, and also to the "1p and 1z" (stabilizing) case. Then the closed-loop transfer function is

$$H_c(s) = \frac{ab(F-1)(s+c)/c}{s^2 + [a+b+ab(F-1)/c]\, s + abF},$$

and the closed-loop noise bandwidth can be shown to be

$$B_c = \frac{abF}{2(a+b)} \times \frac{c^2 + abF}{c^2 + abc(F-1)/(a+b)}$$

It is now possible to prove that there is only one choice of value for c to minimize B_c:

$$c_{opt} = \frac{F}{F-1}\left[(a+b)+\sqrt{(a^2+b^2)+ab(F+1/F)}\right].$$

After tedious algebraic manipulations, we obtain the minimum noise bandwidth of the closed-loop with an optimum stabilizing zero

$$B_{c_{min}} = \frac{abF^2}{c_{opt}(F-1)} = \frac{abF}{a+b+\sqrt{a^2+b^2+ab\left(F+\frac{1}{F}\right)}}.$$

This is a quite general result of considerable interest for the system design.

In the apparently best "2p and 2z" class of feedback filters, there are two special cases of particularly advantageous performance. The following simple expressions hold true for the binomial filter with two cascaded real poles, $a = b$,

$$c_{opt} = b\,\frac{F+\sqrt{F}}{\sqrt{F}-1}; \qquad B_{c_{min}} = b\,\frac{F\sqrt{F}}{(1+\sqrt{F})^2}$$

For the Butterworth filter, with two conjugate poles, we denote

$$a = \frac{A}{\sqrt{2}}(1+j) \qquad b = \frac{A}{\sqrt{2}}(1-j) = -aj$$

and it follows that

$$c_{opt} = \frac{AF}{F-1}\left(\sqrt{2}+\sqrt{F+\frac{1}{F}}\right)$$

$$B_{c_{min}} = \frac{AF\sqrt{F}}{\sqrt{F^2+1}+\sqrt{2F}}$$

Other possible filter structures have been catalogued during this work together with their noise bandwidths. The determination of the feedback-filter parameters with regard to the baseband width will be the subject of further study.

In order to prepare an orientation for the expected results, we shall continue with the example given above for the optimum Butterworth filter. If we assume that half-power bandwidth of the open-loop transfer function coincides with the highest modulation frequency f_m, we must set $A = 2\pi f_m$. Consequently,

$$\frac{B_{c_{min}}}{f_m} = \frac{2\pi F}{\sqrt{F + \frac{1}{F} + \sqrt{2}}}$$

and

$$r_{t_F} = \rho = \frac{10\pi(F-1)^2/F}{\sqrt{F + \frac{1}{F} + \sqrt{2}}}.$$

Furthermore, it can be found that

$$R_t = \frac{150(F-1)^4}{\left(\sqrt{F + \frac{1}{F} + \sqrt{2}}\right)^2}.$$

Solving this for F, with $R_t = 10^4$ as before, we obtain

$$F_{opt} = 6.74$$

wherefrom

$$m_{F_{opt}} = 13.2 \quad \text{and} \quad \rho = 38.0.$$

Finally, the power saving is evaluated as 7 db at the expense of a 106 per cent increase in signal bandwidth. Note that the efficiency of power-bandwidth exchange remains virtually unaffected by the optimization of the feedback filter.

5. Direction of Further Study

After the final choice of the best filter structure, the design procedure for the feedback filter will be formulated. Then the optimization problem of the feedback system will be resolved. The analytical results will be summarized in a general chart in which the optimum system parameters m_F, F will be indicated, as well as the system performance at threshold in terms of r_t and R_t. The expected threshold extension will also be obtainable from the chart.

Preliminary measurements have resulted in qualitative agreement with the analysis. The principal analytical conclusions will undergo a comprehensive experimental verification.

The author gratefully acknowledges the aid and encouragement of Professor John M. Wozencraft. Many helpful suggestions from Professor L. A. Gould and Professor E. M. Hofstetter are also appreciated. This part of the research project was performed while the author was working under a Ford Foundation Postdoctoral Fellowship.

A. Wojnar

References

1. C. L. Ruthroff, Project Echo: FM demodulators with negative feedback, Bell System Tech. J. 40, 1149 (1961).

2. J. G. Chaffee, The application of negative feedback to frequency-modulation systems, Bell System Tech. J. 18, 404 (1939).

3. L. H. Enloe, Decreasing the threshold in FM by frequency feedback, Proc. IRE 50, 18 (1962).

4. S. O. Rice, Mathematical Analysis of random noise, Bell System Tech. J. 24, 46 (1945).

5. S. O. Rice, Properties of sine wave plus noise, Bell System Tech. J. 27, 109 (1948).

6. F. L. H. M. Stumpers, Theory of frequency-modulation noise, Proc. IRE 36, 1081 (1948).

7. M. Schwartz, Signal-to-noise effects and threshold effects in FM, Proc. National Electronic Conference, Vol. 18, p. 59, 1962.

8. L. H. Enloe, The synthesis of frequency feedback demodulators, Proc. National Electronic Conference, Vol. 18, p. 477, 1962.

9. G. C. Newton, L. A. Gould, and J. F. Kaiser, Analytical Design of Linear Feedback Controls (John Wiley and Sons, Inc., New York, 1957).

XIX. ARTIFICIAL INTELLIGENCE*†

Prof. M. L. Minsky
Prof. C. E. Shannon
P. W. Abrahams
D. G. Bobrow
D. J. Edwards
T. P. Hart
D. C. Luckham
L. G. Roberts
I. E. Sutherland

RESEARCH OBJECTIVES

The purpose of our work is to investigate ways of making machines solve problems that are usually considered to require intelligence. Our procedure is to attack the problems by programming a computer to deal directly with the necessary abstractions, rather than by simulating hypothetical physiological structures. When a method for solving a problem is not known, searches over spaces of potential solutions of the problem, or of parts of the problem, are necessary. The space of potential solutions of interesting problems is ordinarily so enormous that it is necessary to devise heuristic methods[1-3] to replace the searching of this space by a hierarchy of searches over simpler spaces. The major difficulty, at present, is the excessive length of time required for building machinery or even for writing programs to test heuristic procedures. For this reason, a major part of our effort is going into the development of ways of communicating with a computer more effectively than we can now communicate. This work has two aspects: development of a system for instructing the computer in declarative, as well as imperative, sentences, called the advice-taker,[4] and development of a programming language called LISP[5-7] for manipulating symbolic expressions that will be used for programming the advice-taker system and will also be of more general use.[8] We are embarking on a major effort to integrate this work into the new M.I.T. time-shared real-time computer system.

Maintenance and further development of LISP will be continued by Professor J. McCarthy, who is now at Stanford University. We plan to continue close association with his group.

It is our belief that the field of artificial intelligence is limited only by the amount of qualified effort that can be put into it, and by the machine limitations that still prohibit more ambitious experiments. Our group is working in the following areas.

1. Differential Equations Solved by Symbolic Methods

Dr. J. Slagle has completed his program, SAINT, for "first-year calculus" and is working on more powerful methods for symbolic solution of ordinary differential equations.

2. Resource Allocation Heuristics

B. Bloom, D. J. Edwards, and others are working on the problems of conflicting goals that arise in the chess problem. T. P. Hart is working on related problems in the more tractable game of Kalah. Thesis students have been assigned problems in working out techniques for other games.

*This work is supported in part by the National Science Foundation (Grant G-16526); in part by the National Institutes of Health (Grant MH-04737-02); and in part by the Computation Center, M.I.T.

†Several members of this group, working at the Computation Center, are not members of the Research Laboratory of Electronics: Prof. H. Rogers, Jr. (Department of Mathematics, M.I.T.), Dr. O. G. Selfridge (Lincoln Laboratory, M.I.T.), Dr. J. Slagle (Lincoln Laboratory, M.I.T.), and the following graduate students: B. Bloom, T. Evans, T. Jones, D. M. R. Park, B. Raphael, W. Teitelman.

3. Pattern Recognition and other Problems in Visual Images

Professor Minsky and Dr. Selfridge are working on the general theory; the results will appear in a series of papers, two of which are completed. T. Evans has almost completed his study of pictorial-verbal analogies, which will appear in his doctoral thesis. I. E. Sutherland has completed his superb "Sketchpad" picture-description system, which will appear in his dissertation. D. J. Edwards and M. Minsky have started a study of relative merits of Bayes and matched-filter approximations for recognition. We are beginning work on programmed description of motion and animation. L. G. Roberts is exploring problems in description of three-dimensional forms.

4. Heuristic Reasoning about Bodies of Verbal Description Data

Work on systems related to the advice-taker is finally becoming concretely realized. T. Jones and M. Minsky are running preliminary versions of an advice-taker system. J. Slagle's differential-equations system will also be designed along these lines. B. Raphael is working on related systems concerned with interpreting language statements relevant to the state of an internal pictorial model. D. G. Bobrow is concerned with detailed interpretation of ordinary language statements concerning a mathematical domain: "word-problems" in a system for High School algebra.

5. Mathematical Aids and Models

P. W. Abrahams is completing his dissertation research on a symbolic proof-checking system, which expands relatively informal meta-statements about theorem proofs into detailed applications of the rules of inference from assorted logical subsystems, thereby providing a mechanization of the expression "the reader will easily verify." D. C. Luckham is working on a theory of program equivalence and simplification. M. Minsky is completing a book on computer-oriented theory of recursive functions, Turing machines, and Post systems.

6. Mechanical Hand

H. Ernst's work on his TX-0 mechanical hand was completed a year ago, and we are planning to continue such work, this time, in association with the M.I.T. time-sharing system. We hope also to work toward a computer-operated micromanipulation system under computer-sensed visual control.

7. Neural Nets

M. L. Minsky and O. G. Selfridge are working on theories of neural nets. They have completed an analysis of certain synaptic learning processes in loop-free nets, and plan to study the formation of certain kinds of assemblies in nets with cycles.

8. Time Sharing and the Mathematical Laboratory

We have an ambitious design for a laboratory in which mathematicians and physicists can apply new techniques for solving problems involving equations that are impractically cumbersome for hand-manipulation by ordinary mathematical techniques. What is needed is a control language for describing and executing the processes ordinarily carried out by a working research mathematician, implemented by a heuristic program. This system as now envisioned would be a new national research facility, for visits by scientists with appropriate problems. It is awaiting the development of a control language that involves new man-machine interaction problems, for the appropriate time-shared visual consoles that are necessary.

M. L. Minsky

References

1. M. L. Minsky, Some Methods of Artificial Intelligence and Heuristic Programming, Proc. Symposium on the Mechanisation of Thought Processes, National Physical Laboratory, Teddington, England, November 24-27, 1958 (H.M. Stationery Office, London, 1959).

2. M. L. Minsky, Steps toward artificial intelligence, Proc. IRE 49, 8-30 (1961).

3. M. L. Minsky, A selected, descriptor-indexed bibliography to the literature on artificial intelligence, Trans. IRE, Vol. HFE-2, No. 1, pp. 39-55, March 1961.

4. J. McCarthy, Programs with Common Sense, Proc. Symposium on the Mechanisation of Thought Processes, National Physical Laboratory, Teddington, England, November 24-27, 1958 (H.M. Stationery Office, London, 1959).

5. J. McCarthy, Recursive functions of symbolic expressions in computation by machine, Part I, Commun. Assoc. Computing Machinery 3, 184-195 (April 1960).

6. J. McCarthy, A Basis for a Mathematical Theory of Communication, Proc. Western Joint Computer Conference, Los Angeles, California, May 1961.

7. J. McCarthy, Computer Programs for Checking Mathematical Proofs, a paper presented at the Symposium on Recursive Function Theory, New York, April 1961.

8. J. McCarthy, Time-Sharing Computer Systems (lecture, M.I.T., May 1961); Management and the Computer of the Future (The M.I.T. Press, Cambridge, Mass., and John Wiley and Sons, Inc., New York, 1962).

XX. SPEECH COMMUNICATION*

Prof. K. N. Stevens
Prof. M. Halle
Prof. J. B. Dennis
Dr. A. S. House
Dr. T. T. Sandel
Jane B. Arnold
J. M. Heinz
W. L. Henke
A. P. Paul
J. R. Sussex
E. C. Whitman

RESEARCH OBJECTIVES

The objectives of our work are to further our understanding of: (a) the process whereby human listeners decode an acoustic speech signal into a sequence of discrete linguistic symbols such as phonemes; and (b) the process whereby human talkers encode a sequence of discrete linguistic symbols into an acoustic signal.

Current research activities related to these objectives include experiments on the generation of speech by electrical analog speech synthesizers, development of means for controlling analog speech synthesizers by a digital computer, measurements of movements of the speech-generating structures during speech production, studies of methods of speech analysis, accumulation of data on the acoustic characteristics of utterances corresponding to phonemes in various linguistic contexts, and studies of the perception of speechlike sounds.

K. N. Stevens, A. S. House, M. Halle

A. A COMPUTER PROGRAM FOR CONTROLLING THE DYNAMIC VOCAL-TRACT ANALOG (DAVO)

A program for the TX-0 computer has been prepared to allow flexible operation of the dynamic analog speech synthesizer constructed by Rosen.[1] The development of this control program has been the subject of a Master of Science thesis.[2] The objective of this work is to replace the control system originally incorporated into DAVO by a more versatile one involving the TX-0 computer and interconnection equipment consisting mainly of digital-to-analog converters.[3]

Control of the vocal-tract analog is accomplished through 24 analog voltages that specify cross-section area as a function of distance along the tract, and 3 voltages that control amplitude of buzz and noise excitation, and coupling between the oral tract and an analog of the nasal cavity. Voicing frequency is controlled through the timing of glottal pulses supplied to the vocal-tract model. The original control system for DAVO employed trapezoidal waveform generators as sources for the control voltages, and was limited to essentially monosyllabic utterances without resort to tape-splicing.

In using the control program to operate DAVO, a number of control signals are specified as sequences of piecewise quadratic segments. The control voltages for the vocal-tract area function are represented as a linear combination of up to three area functions selected from a library of vocal-tract configurations. The coefficients of the linear combination are provided by control signals. One control signal is used within

*This research was supported in part by the U. S. Air Force (Electronic Systems Division) under Contract AF 19(604)-6102; in part by the National Science Foundation (Grant G-16526); and in part by the National Institutes of Health (Grant MH-04737-02).

the program to generate glottal pulses at a corresponding rate, and three others become control voltages for excitation and nasal coupling. The input to the control program is a time-ordered list containing the parameters of each quadratic control-signal segment, the assignment of configurations from the library, and other functions. The input list is processed by the control program, and gives a series of digital samples representing the motion of the control voltages with time. The samples are stored, then read out later to perform the synthesis in real time. The size of the magnetic core memory in the TX-0 computer limits the length of an utterance to approximately 1 sec; however, this will be greatly extended through the use of the digital tape unit that is now available. Initial experiments with the program show that the processing time is approximately 50 times real time when the samples are computed at 1-msec intervals. When the interval is increased to 6 msec, the processing-to-real-time ratio is improved, and is 25 times. New instructions added to the TX-0 computer and some improvements in the program might possibly reduce the ratio to 10.

The internal structure of the program has been designed so that changes and additions to its function can be easily accomplished. It should be pointed out that the program will not become really useful for general speech-synthesis work until a compiler is available to simplify the preparation of input lists and make on-line changes in the utterance conveniently possible. Such a compiler is now being developed.

The control program also employs stored correction curves to correct for irregularities in the characteristics of some components of the analog. At present, a method of automatically calibrating the vocal-tract analog is being investigated. This involves obtaining the correction curves through the observation of available variables in the system, and without having to dismantle or isolate any of its parts.

J. R. Sussex, J. B. Dennis

References

1. G. Rosen, Dynamic Analog Speech Synthesizer, Technical Report 353, Research Laboratory of Electronics, M. I. T., February 10, 1960.

2. J. R. Sussex, Computer Control of a Dynamic Analog Speech Synthesizer, S. M. Thesis, Department of Electrical Engineering, M. I. T., September 1962.

3. J. B. Dennis, Speech synthesis, Quarterly Progress Report No. 67, Research Laboratory of Electronics, M. I. T., October 15, 1962, pp. 157-162.

B. A TRANSISTORIZED ARTICULATORY SPEECH SYNTHESIZER

Work is progressing on the design of an improved dynamic analog of the vocal organs to replace the vacuum tube analog (DAVO) constructed by Rosen.[1]

Like Rosen's device, the new analog will represent the acoustical system of the vocal tract as a lumped-element transmission line in the electrical domain. The theory of such analogs is treated by Kasowski,[2] Fant,[3] and Stevens, Kasowski, and Fant.[4] Essentially, the vocal tract is considered a cascade of cylindrical segments of common length but variable areas. In the electrical system, in which voltage is analogous to pressure, and current to acoustic volume velocity, each segment is represented by a series inductance and a shunt capacitance, and a cascade of such sections forms an artificial line (Fig. XX-1). It can be shown that

$$A = \frac{\rho c}{k}\left(\frac{C}{L}\right)^{1/2} \quad \text{and} \quad \ell = c(LC)^{1/2}, \tag{1}$$

where A is the area of the section, ℓ its length, ρ the density of air, c the sound speed, and k an arbitrary constant of the transmission line, depending upon the choice of units and the impedance level.

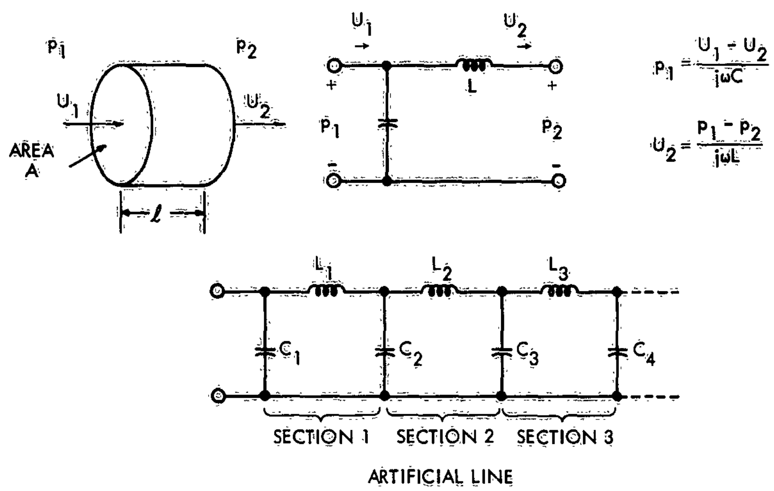

Fig. XX-1. Electrical analog of a short lossless tube.

In the static analog of Stevens, Kasowski, and Fant,[4] each inductance and capacitance was set manually and could not be changed during the course of an utterance. In Rosen's device, each L and C is electrically controlled by an elaborate timing system, and it thus can be used to synthesize speech sounds and transitions that depend upon a gross motion of the articulatory mechanism for their performance.

In the existing DAVO, the tract configuration represented by the analog is controlled by a set of analog voltages supplied to each LC section by a potentiometer matrix that must be set by the operator. In each section, the product of L and C is constrained to be constant and independent of the area represented, thus keeping the section length invariant (by Eq. 1). Recent attempts to control DAVO from the TX-0 computer have

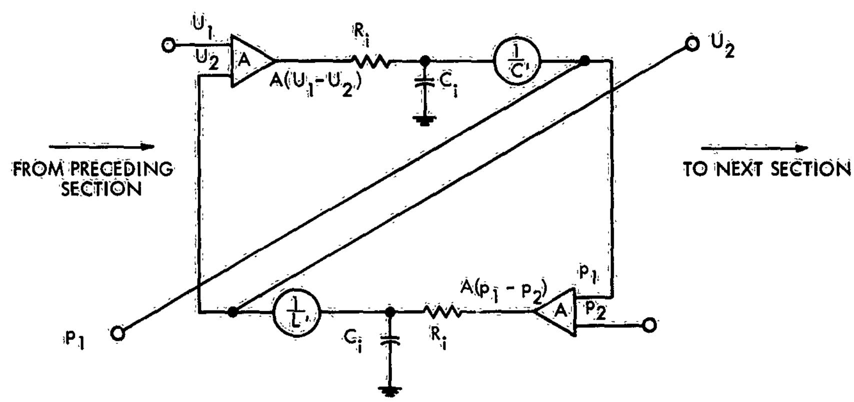

$$\frac{1}{j\omega C} \approx \frac{A}{C'R_iC_ij\omega}; \quad \frac{1}{j\omega L} \approx \frac{A}{L'R_iC_ij\omega}$$

Fig. XX-2. Proposed analog section.

demonstrated that the present device is poorly suited to digital control. The instability of the vacuum tube circuitry employed and the analog nature of the control system have caused great difficulty.

The new analog will be completely transistorized and designed for operation by a digital computer. Hence the control signals will be in digital form. The LC constraint can then be included in the computer program or discarded to allow small changes in the tract length during phonation. This eliminates from the system a complex piece of hardware, which in Rosen's DAVO serves as a frequent source of trouble in calibration and maintenance.

But the greatest difference between the existing DAVO and that which is proposed here is the very manner in which the inductance and capacitance are obtained. For the former, Rosen uses a saturable reactor; for the latter, the input impedance of a variable-gain Miller amplifier – in both cases a physical element. In the proposed design (Fig. XX-2), each section is constructed as a self-contained analog computer that receives as inputs two signal voltages representing the volume velocity at the input of the section and the pressure at the input of the next section. It performs on these the mathematical operations associated with a series inductance and shunt capacitance and delivers two output voltages, again representing pressure and volume velocity, to be used as inputs by the adjoining sections in which the process is repeated. As shown in Fig. XX-2, both integrations required are performed by simple RC circuits following differential amplifiers. Thus,

$$\frac{1}{L} \approx \frac{1}{R_iC_i} \cdot \frac{1}{L'} \cdot A \qquad \frac{1}{C} \approx \frac{1}{R_iC_i} \cdot \frac{1}{C'} \cdot A. \tag{2}$$

Here, $1/L'$ and $1/C'$ represent two step attenuators, controlled by digital signals and capable of attenuating from 1 db to 64 db in steps of 1 db. The degree of attenuation effectively varies the value of L and C and thus sets the desired area for the section. This area will be variable over a range 15-0.01 sq cm, and a complete closure of the tract will be available for the first time.

It is also possible to implement this approach with RC differentiating circuits in the loop. This approach has the advantage of requiring a much smaller gain A for the differential amplifiers, but leads to stability problems. Experiments have been conducted with both circuits, but still no decision has emerged as to which will prevail.

The design and successful testing of the digital attenuators, differential amplifiers, and simplified models of a single section have been completed. At present, a detailed study is being carried through to determine how the effects of acoustical losses should be accounted for in the system. It appears at this stage that the nonideal integration (or differentiation) of the RC circuits introduces damping that closely approximates the acoustical situation; that is, that the exact equations of the analog of Fig. XX-2 are practically identical with those of an RLC circuit with a Q of approximately 20.

Considerable work must be expended in several areas to complete the project. First, an analytical study must be made of the section design and a cascade of such sections to determine the nature and extent of errors arising in this approximation of the vocal tract. Also, the details of combining the hardware components into a compact and stable system have not been settled, and no consideration whatever has been given to the representation of the glottal source and radiation impedance at the lips.

E. C. Whitman

References

1. G. Rosen, Dynamic Analog Speech Synthesizer, Technical Report 353, Research Laboratory of Electronics, M.I.T., February 10, 1960.

2. S. E. Kasowski, A Speech Sound Synthesizer, S.M. Thesis, Department of Electrical Engineering, M.I.T., January 1952.

3. C. G. M. Fant, Acoustic Theory of Speech Production (Mouton and Company, 's-Gravenhage, 1960).

4. K. N. Stevens, S. Kasowski, and C. G. M. Fant, An electric analog of the vocal tract, J. Acoust. Soc. Am. 22, 734-742 (1953).

C. COMPUTER CONTROL OF A TERMINAL ANALOG SPEECH SYNTHESIZER

A system has been developed for the control of a terminal analog (or resonance) type of speech synthesizer by the TX-0 digital computer, which is similar to the application of a computer to the control of an articulatory analog speech synthesizer recently described by Dennis.[1] The system includes the necessary equipment for the coupling of the computer to the synthesizer and a program for the computer which effects the desired operation of the synthesis system.

The synthesizer consists of a cascaded series of electrically variable resonators. An electrical signal that is an analog of the glottal excitation to the human vocal tract is generated and then passed through the synthesizer. Each of the variable resonators impresses one formant on the signal. By varying the formant frequencies, as well as the amplitude and fundamental frequency of the source generator, sounds that closely approximate the voiced sounds of human speech can be produced.

The purpose of the new control system is to provide a means by which the parameters of the synthesizer may be independently and simultaneously varied as a function of time in a manner specified by input data in a numerical format. A computer program uses these input data to produce the necessary temporal sequence of digital outputs that, after being converted to analog form by a digital-to-analog converter, control the

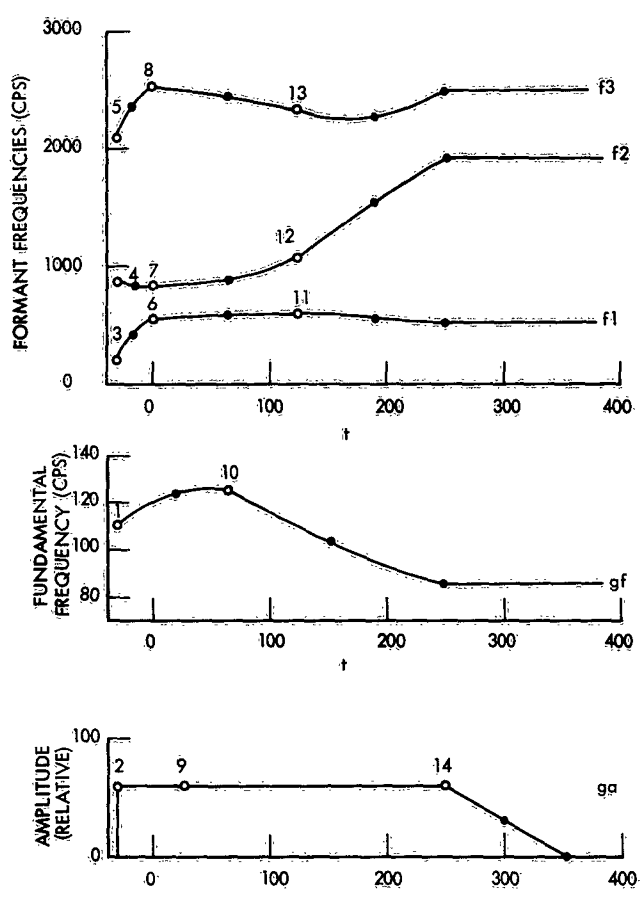

Fig. XX-3. Sample parameter specification.

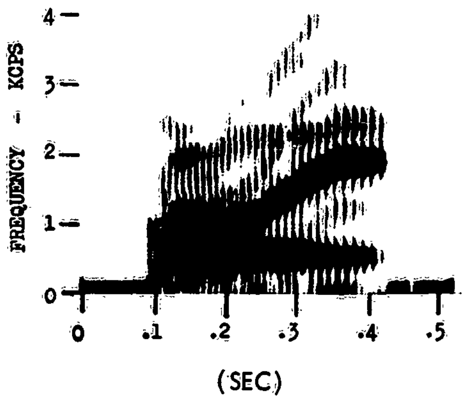

Fig. XX-4. Sound spectrogram of output produced by the synthesizer for the input data shown in Fig. XX-3.

synthesizer parameters.

Temporal variations for each of the parameters are described by a sequence of confluent segments of second-degree curves. The input data that specify each of these time segments include the value of the parameter at the initial, central, and final values of time of that segment. From these data the program calculates the parameter value for all intervening time on the basis of the quadratic function that the data uniquely determine. This scheme allows a high degree of flexibility, inasmuch as the segment density can be varied according to the complexity of the desired temporal variation. The specification of each time segment also includes data that identify the particular parameter being described, the duration of the time segment, and data that determine the time relationship between the segments of the various parameters.

The input data are first sketched graphically and then transcribed directly into the numerical format used by the computer. An example of this process is shown by Fig. XX-3. The small circles denote the beginning of a new time segment, and the numbers associated with each circle identify the time sequence in which they occur. This particular example produces a speech sample approximating the word boy. A sound spectrogram of the output of the synthesizer for this input is shown in Fig. XX-4.

Measurements of the acoustic output of the system have indicated satisfactory performance, and several speech samples have been synthesized.

Further details concerning the physical realization of the synthesis system and its use can be found in the author's thesis.[2]

W. L. Henke

References

1. J. B. Dennis, Speech synthesis, Quarterly Progress Report No. 67, Research Laboratory of Electronics, M. I. T., October 15, 1962, pp. 157-162.

2. W. L. Henke, Computer Control of a Terminal Analog Speech Synthesizer, S. M. Thesis, Department of Electrical Engineering, M. I. T., August 1962.

XXI. MECHANICAL TRANSLATION*

V. H. Yngve
Carol M. Bosche
Elinor K. Charney
Ann Congleton
J. L. Darlington
D. A. Dinneen
G. H. Harman
Muriel S. Kannel
E. S. Klima
Gisela Laurent
E. S. Lowry
J. D. McCawley
T. More, Jr.
W. K. Percival
A. C. Satterthwait

RESEARCH OBJECTIVES

The primary objective of our research program is to find out how languages can be meaningfully manipulated and translated by machine, and to evaluate the quality that can be achieved with different approaches, the usefulness of the results and their costs. A further objective is to achieve a basic understanding of human communication and language use, and to add to the general knowledge of noncomputational uses of digital computing machinery.

We have always stressed a basic, long-range approach to the problems of mechanical translation. We are placing emphasis on completeness, when completeness is possible, and on finding out how to do a complete job if one is not now possible. This emphasis has led us into the study of many of the fundamental questions of language and translation. We are not looking for short-cut methods that might yield partially adequate translations at an early date — an important goal that is being pursued by other groups. We are seeking definitive solutions that will be permanent advances in the field, rather than ad hoc or temporary solutions that may eventually have to be discarded because they are not compatible with improved systems.

A broad and basic program of research is being carried out. In linguistic theory, a computer model of linguistic behavior is being studied which has already provided insight into the reasons why human languages are complex. Linguistic descriptions are being prepared for English, German, French, and Arabic. An experimental Arabic to English translation program is under development. In the area of semantics, work is proceeding along several avenues in an attempt to program a machine to understand English. Language is also being studied from a logical point of view to clarify the semantic significance of certain difficult and crucial words. The nature of the translation relation is being given special emphasis. Computer programming languages are being studied. The group has developed and is improving COMIT, a convenient large-scale computer programming system which greatly reduces the effort required to write programs related to the research.

V. H. Yngve

A. GENERATIVE GRAMMARS WITHOUT TRANSFORMATION RULES

A phrase-structure grammar has been written which generates roughly the same set of sentences generated by the most comprehensive transformational grammar[1] of English with which we are acquainted.

Chomsky and others have argued that a grammar consisting of a set of phrase-structure generation rules, along with a very simple rule of interpretation, which assigns structural descriptions to sentences on the basis of the manner of generation,

*This work was supported in part by the National Science Foundation (Grant G-24047).

is inadequate for giving a full grammatical description of sentences in English. On the basis of these arguments, many grammarians have chosen to write grammars using transformational generation rules, rules of considerably more mathematical power than phrase-structure rules. However, as Chomsky would be the first to point out, the arguments that he has given do not show that no adequate grammar for English may be written which uses phrase-structure generation rules.

The argument against the use of phrase-structure grammars is threefold. First, such grammars will be quite long, complex, ad hoc, and therefore difficult to write. Second, grammatical description in terms of parsing alone is not complete.[2] Third, phrase-structure grammars cannot exploit or explain certain general features of particular languages.[3]

In order to circumvent these difficulties the following suggestion has been made by Chomsky[4]:

(1) To the phrase-structure rules of the generative grammar add rules that are essentially more powerful (transformational rules).

(2) Add interpretation rules to give added structural description where certain transformational rules have or have not been used.

We have found that it is not at all necessary to introduce transformational rules to circumvent these difficulties, and, in fact, there are certain advantages in not doing so. We restrict the generation rules to phrase-structure rewrite rules of the sort described by one of us.[5] We retain the parsing interpretation for these generation rules.[6] We augment this interpretation by using a notation for the abbreviation of the phrase-structure generation rules. This abbreviated notation makes use of subscripts of the kind that have been provided for the purpose in the COMIT computer programming language.[7] Grammatical relations beyond those disclosed through parsing analysis are explicated in terms of derivations in the abbreviated notation. Finally we introduce an "evaluation procedure" for choosing between equivalent sets of generation rules. Our evaluation procedure involves a criterion of simplicity which enables us to exploit (and thereby explain) grammatical regularities in a given language.

The phrase-structure grammar that has been written by one of us (Harman) has been written in the form of a computer program that can produce sentences chosen at random from the set generated by the grammar. Examination of the sentences that are produced aids in eliminating errors in the grammar. This grammar generates nearly the same set of sentences as does the transformational grammar on which it is based. The only differences involve a few points at which the transformational grammar appeared to be in error.

We are now in a position to compare the two grammars from the point of view of the threefold argument that has been given against phrase-structure grammars. We have compared the lengths of the two grammars and find them to be of approximately the same size: one reasonable method of comparison shows the transformational grammar to be shorter, another equally reasonable method shows the phrase-structure grammar to be shorter. As for complexity and ease of writing, it would appear that the phrase-structure grammar is easier to write because the rules, being unordered, are relatively more independent. Neither of the grammars can be said to be ad hoc.

The arguments that phrase-structure grammar would be incomplete and not able to exploit and explain certain general features of particular languages is not borne out in this case. Our phrase-structure grammar provides for and explains adequately all of the features of English provided for and explained adequately by the transformational grammar. It is able to do this by virtue of the additional interpretation provided by the subscript notation that also provides the compactness over an unabbreviated form of the rules.

In other words, arguments for the introduction of transformational generation rules, on the grounds that one type of grammar using phrase-structure generation rules lacks explanatory power, can be met.

Arguments that phrase-structure generation rules lack the mathematical power needed seem incoherent, at least at present. At any rate, the additional mathematical power of the transformation rules was not needed in the very sophisticated transformational grammar of English which we used for a comparison.

The result that a phrase-structure grammar appears to be adequate for English is also of great practical interest to those attempting to handle natural language by machine.

G. H. Harman, V. H. Yngve

References

1. An improved version of the transformational grammar given by R. B. Lees, The grammar of English nominalizations, Part II, Int. J. Am. Ling., Vol. 26, No. 3, July 1960.

2. N. Chomsky, Syntactic Structures (Mouton and Company, The Hague, second printing 1962), Chapter 5.

3. Ibid., Chapter 8.

4. N. Chomsky, Syntactic Structures, op. cit.

5. V. H. Yngve, A model and an hypothesis for language structure, Proc. Am. Phil. Soc. 104, 444-466 (1960).

6. These rules differ somewhat from those discussed by Chomsky, op. cit., p. 41, footnote. The exact form of these rules is unimportant as far as our argument here is concerned.

7. V. H. Yngve, A programming language for mechanical translation, Mechanical Translation 5, 24-41 (1958).

B. AN ORDINARY LANGUAGE INPUT FOR A COMIT PROOF-PROCEDURE PROGRAM

Work is in progress on a COMIT program for the translation of arguments from ordinary language into logical notation. This is conceived as an input device to a COMIT program, based on the Davis-Putnam proof-procedure algorithm, which tests quantified and nonquantified logical formulae for validity by the reductio ad absurdum method of attempting to deduce a contradiction from the negation of a formula.[1-3]

The translation program works essentially as follows.

(a) It divides the words of the input argument into two basic categories — the punctuative words, or "P-words," words like 'if', 'then', 'either', 'or', 'therefore', etc., which usually divide sentential clauses from one another, and the nonpunctuative words, or "W-words," which are all the rest and constitute the content of the sentential clauses. Accordingly, every word or punctuation mark in the input argument is subscripted, by means of a dictionary lookup, with either 'P' or 'W'. In the sentence

If it rains then it pours.

the P-words are 'if', 'then', and '.', and the W-words are 'it', 'rains', and 'pours'. A sentential clause is any finite sequence of W-words occurring between two P-words; in the example, 'it rains' and 'it pours' are the two sentential clauses.

(b) It performs some simplifications and expansions on the input sentences. All verbal forms are reduced to the infinitive, so that 'If it rains then it pours', 'If it will rain then it will pour', 'If it is raining then it is pouring', 'If it would rain then it would pour', etc. (all of which state basically the same implication) are all reduced to 'If it rain then it pour'. Sentences in which several subjects are attached to the same predicate, or in which several predicates are attached to the same subject, are expanded into their implicit sentential clauses. Thus, 'Jack and Jill went up the hill' is expanded into 'Jack went up the hill and Jill went up the hill'; and 'Jack both fell down and broke his crown' (the program requires the 'both' as the cue to activate the expansion subroutine) is expanded into 'Jack fell down and Jack broke his crown'. Sentences using 'either... or...' and 'neither...nor...' constructions are likewise expanded whenever possible. A fallacy would result if this type of expansion were applied, e.g., to 'Jack and Jill are cousins'; thus the input arguments must be stated without using relational sentences of this sort. Later, we hope to improve the program to handle them.

(c) It substitutes the letters 'A', 'B', 'C', etc., for the sentential clauses in the argument, by using the same symbol for the same sentential clause whenever it occurs.

(d) It parenthesizes the argument, on the basis of a set of 20 rules that make explicit the groupings that are implicit in the use of the P-words. Thus, 'If A then B or if C then D' is parenthesized (by using the arrow for implication and the wedge for disjunction) as '(((A)→(B)) V ((C)→(D)))'. In COMIT notation this formula appears as '*(+ *(+ *(+ A + *) + IMPLIES + *(+ B + *) + *) + OR + *(+ *(+ C + *) + IMPLIES + *(+ D + *) + *) + *)'. A logical argument is usually stated as a set of premises in the form of sentences separated by periods, which is followed by a conclusion introduced by a word like 'therefore' or 'hence'. Our program symbolizes an argument as one long sentence in the form of an implication, the 'therefore' (or 'hence', etc.) being replaced by 'implies', and the periods being replaced by 'and'.

The characteristics of the restricted English employed follow from the limitations on what the program can do. The restrictions fall into three general categories:

(i) Restrictions following from the fact that the program's only criterion of identity of two propositions or "ideas" is the identity of the sentences expressing them. Two propositions stated in different words, even though they may be synonymous, are symbolized with different letters, unless one or more of the subroutines mentioned in (b) above result in the sentences being expressed in the same wording and word order.

(ii) Restrictions on the use of the P-words and the C-words (which are a subset of the P-words and include the binary connectives 'and', 'or', etc.). The P-words that are at the same time C-words may be used only if a boundary is intended between two sentential clauses, so that a sentence like 'He implies that it will not rain' is ruled out, since the 'implies that' will fallaciously divide the sentence into two sentential clauses, 'He' and 'it will not rain', which are connected by an implication sign. Also, every intended division between two sentences must be made explicit, so that 'If it rains it pours' must have a 'then' inserted between 'rains' and 'it' before the program will correctly handle the sentence.

(iii) Restrictions on the vocabulary. The program employs no grammatical recognition routine to speak of; thus a fixed vocabulary must be selected in advance, with all of the nouns, verbs, and adjectives specified. A given word may not be used in more than one of these categories; e.g., if 'praise' is used in the set of arguments submitted, it must be used either as a noun or as a verb, but not both.

The program has been successfully tested on a variety of examples taken, with the required changes in wording, from Copi.[4] Some of the improvements contemplated for the program in the future include coupling the program with a more powerful grammar, and enabling it to perform the more subtle intraclause analyses required for quantificational and relational logic. The proof-procedure program, based on the Davis-Putnam algorithm, is finished and runs reasonably well. It will do propositional, quantificational, and relational logic. Other improvements in this program will have to await improvements in the theory of proof procedures. The ordinary language input program discussed in this report will, however, do only some of the analyses required for propositional logic.

J. L. Darlington

References

1. M. Davis and H. Putnam, A computing procedure for quantification theory, J. Assoc. Computing Machinery 7, 201-215 (1960).

2. J. Darlington, A COMIT program for the Davis-Putnam algorithm, Internal Memorandum, Mechanical Translation Group, Research Laboratory of Electronics, M.I.T., May 1962.

3. J. Darlington, A restricted English for the formulation of arguments in propositional logic, Internal Memorandum, Mechanical Translation Group, Research Laboratory of Electronics, M.I.T., November 1962.

4. I. M. Copi, Introduction to Logic (Macmillan and Company, New York, 1955).

C. SENTENCE-MEANING AND WORD-MEANING

In Quarterly Progress Report No. 66 (pages 289-293), I pointed out that it is necessary for an understanding of the semantical behavior of those morphemes that function as structural-constants[1] to distinguish between sentence synonymy and word synonymy. The principle underlying this view is that it is the particular configuration of structural-constants belonging to a well-formed grammatical string which gives rise to the fundamental sentence-meaning, the meaning of each individual structural-constant, as a morpheme, remaining constant - hence the term 'structural-constant' - but the meaning of each configuration varying, the variation depending upon both the structural properties of the configuration and the particular indispensable structural-constants that occur in it.

This semantical theory has been constructed to apply only to the analysis of the meanings of structural-constants and their interlocking relationships and does not attempt to cover the analysis of the meanings of lexical items that function as denotative terms. It is the author's opinion that different methods are required for the semantical analysis of those morphemes that function denotatively and those that function structurally. This method of analyzing the meaning of structural-constants and their various configurations departs quite radically from the methods proposed thus far which have been formulated primarily to handle denotative terms. In this theory, the denotative morphemes are treated as variables, only the class over which they range having structural significance. Thus, although it makes a great deal of difference to the total meaning of a sentence whether Jane or John is named as the subject or object of an action and whether the particular activity or relationship named by the verbal is of a certain kind, appropriate substitution of one member of a set for another does not alter the basic sentence-type, nor do such substitutions alter the fundamental sentence-meaning.

For an illustration of this theory, let us look at the following sentence:

(1a) If John is to be president, he must get his organization ready now.

In sentence (1a) the fundamental sentence-meaning is: John's getting his organization ready now is a necessary condition of his being president. The event denoted by the clause 'John is to be president' has not occurred nor does the sentence as a whole claim that it ever will, since the getting ready of the organization is not the sufficient condition of being president. Some sentences that are synonymous with sentence (1a) which are important in that they express the same fundamental meaning with a complete change of structural-constant, are

(1b) Unless John gets his organization ready now, he can not be president.

(1c) Only if John gets his organization ready now, can he be president.

It should be noted that the fundamental sentence-meaning of the above synonymous sentences, when it can be expressed through a symbolic notation, will be logical in form, not grammatical. Grammatically, the form of sentence (1a) has the shape that 'If John is to be president' is the dependent clause, whereas 'he must get his organization ready now' is the independent clause. In sentence (1b), 'Unless John gets his organization ready now' becomes the dependent clause, and in sentence (1c) 'Only if' subordinates that which in sentence (1a) was the independent clause to the dependent clause. Thus, from the point of view of grammatical form, either elementary sentence can be subordinated to the other without a change in fundamental sentence-meaning. Logically, however, the event denoted by the sentence 'he is to be president' is dependent for its existence upon the previous occurrence of the event denoted by the elementary sentence 'he gets his organization ready now'. The symbolic notation, formulating the fundamental sentence-meaning, must express this physical dependency. Thus far, no new notation expressing explicitly the relations of necessary and sufficient conditions has been introduced into the formal logical systems.[2] Expanding the logical notation of the formal systems will be a necessary step in establishing rules for coordinating sets of synonymous strings of one language system to sets of synonymous strings from another language system so that a sentence-by-sentence translation can be carried out.

Sentence (1a) can be expressed as a partially interpreted sentence-type, i.e., a sentence-type whose indispensable structural-constants that form the configuration expressing the fundamental sentence-meaning are explicitly indicated and whose denotative morphemes are indicated only by the class to which they belong.

(1d) If x is to be f, then x (or y) must g.

Sentences (1b) and (1c) can easily be put into abbreviated schematical forms. The combination of a partially interpreted sentence-type set up as equivalent to another represents a tautology whose major connective is an equivalence. Each tautology is a transformation law. It is to be noted that the transformation laws for every language are obtained by empirical observation; the sentences established as transforms of each other must be synonymous in actuality.

To show how vital to sentence-meaning the particular configuration of structural-constants is, let us alter sentence (1a) by affixing to it just one morpheme, the structural-constant, 'even', in prenex position.

(2a) Even if John is to be president, he must get his organization ready now.

The sentence-meaning of sentence (2a) is immediately seen to be quite different from sentence (1a) which expresses a relation of necessary condition. The fundamental meaning of sentence (2a) is that the accepted fact of John's being president in the future is unexpectedly not the sufficient condition of John's not having to get his organization ready now. When the structural-constant 'even' enters into the configuration of indispensable structural-constants belonging to sentence (1a), there is an immediate effect upon the 'meaning' of the individual morphemes: the event of John's being president is now known to take place in the future, 'is to be' thus becoming a simple future tense instead of being an indispensable structural configuration expressing necessary condition; the auxiliary 'must' represents no longer an indispensable structural feature. Sentence (2a) is synonymous with sentences of the following set:

(2b) Although John is to be president, he must get his organization ready now.

(2c) In spite of the fact that John is to be president, he still must get his organization ready now.

(2d) If John is to be president, he must get his organization ready now anyway.

Sentence (2d) shows very clearly that the listener must be aware of the total structural configuration of a sentence before he can determine the meaning of the sentence, since sentence (2d) is exactly like sentence (1a) in shape except for its very last morpheme 'anyway'. The morpheme, 'even', in prenex position, prepares us psychologically for a second clause denoting an unexpected event; 'anyway' psychologically springs the event denoted by the second clause as a surprise. The partially interpreted sentence-type to which sentence (2a) belongs is

(2e) Even if x f's, x (or y) must g.

The distinction between sentence-meaning and word-meaning is particularly important in clarifying the semantic nature of the free-variables 'any', 'ever', 'whatever', and other related morphemes. Only if the two concepts are carefully kept separate can one explain how it is that the meaning or the definition of the free-variable can remain constant but the sentence-meanings of the structural configurations in which the morpheme occurs can vary.[2]

Whereas it appeared at one time to me that free-variables were the only structural-constants that behave in this peculiar way of apparently shifting in meaning in different contexts, recent investigation has convinced me that this 'peculiar' behavior attends many of the structural-constants.[3]

This theory opens the way to a solution of linguistic problems that have plagued grammarians for a long time. I have recently proposed a solution[4] for determining the proper occurrence of free-variable morphemes in sentences whose import has been termed negative by grammarians, although their grammatical forms contain neither explicit nor implicit negative morphemes. One of the results was to show that this 'negative' import, ascribed by grammarians to morphemes such as 'few', 'little', 'only', 'too', and 'hardly' as opposed to their respective polar words 'many', 'much', 'all', 'enough', and 'almost' had been obtained by the replacement of the original non-negative sentence under discussion by a negative sentence synonymous to it. The negative sentence had been derived by an unformulated, intuitive recognition that sentences as wholes are related semantically as synonymous although the negative quality was erroneously assigned to a particular morpheme rather than to the sentence-meaning as a whole. However, by selecting only one negative grammatical string as representing the canonical grammatical form of the sentence under consideration, they failed to see that there are many synonymous sentences, some negative in form, some positive. Thus it was not possible for them to understand the real function of the structural-constant; they had considered as 'negative' a morpheme that is not itself negative because the selected structural-constant can occur in other configurations that do not give rise to a negative fundamental sentence-meaning. Furthermore, since, by the rules that transform one grammatical string into another grammatical string preserving the original sentence-meaning, one can always transform a string in which no negative morphemes appear into a synonymous string in which negative morphemes do appear, the explanation offered appears very arbitrary. One has only to look at sentence (1a) and the sentences synonymous to it to see this point. In sentence (1a) there is no explicit negation, but in sentence (2b) when 'unless' occurs in the first clause, an explicit negation 'not' must occur in the second clause, but if 'only if' occurs in the first clause, the negation must disappear if the fundamental sentence-meaning is to be preserved. It is this constant interplay of structural-constants that the early grammarians overlooked. They relied upon intuitive semantic paraphrasing only when they were forced into it by the need of explaining certain phenomena in the language under analysis. The author is writing a paper on the problem of the occurrence of free-variable morphemes within these so-called negative contexts.

Elinor K. Charney

References

1. For explanation of 'structural-constant', see Elinor K. Charney, On the Semantical Interpretation of Linguistic Entities That Function Structurally, paper presented at the First International Conference on Mechanical Translation of Languages and Applied Language Analysis, National Physical Laboratory, Teddington, England, September 5-8, 1961.

2. Elinor K. Charney, Linguistic analogues of the free-variable, Quarterly Progress Report No. 64, Research Laboratory of Electronics, M.I.T., January 15, 1962, pp. 208-211.

3. For examples of 'all' and 'only', see Elinor K. Charney, On the problem of sentence synonymy, Quarterly Progress Report No. 66, Research Laboratory of Electronics, M.I.T., July 15, 1962, pp. 289-293.

4. Elinor K. Charney, On the Occurrence of Free-Variables in Sentences of "Negative" Import, lecture presented at Linguistics Seminar, Research Laboratory of Electronics, M. I. T., November 9, 1962.

D. FINNISH NOUN MORPHOLOGY

This report gives a description of parts of a set of rules that I have written for the morphophonemics of Finnish nouns and adjectives.[1] The rules apply in a fixed order and are assumed to operate on the output of the syntactic part of a grammar of Finnish (this means that the rules may refer to the immediate constituent structure of, and the syntactic categories and syntactic boundary markers involved in, the forms on which they operate).[2] The complete set of rules takes care of the complete singular paradigm of all "regular" (I use this word in a rather broad sense) Finnish nouns.[3] It will be shown that the rules established for the "regular" nouns apply without change to several nouns and adjectives that are traditionally considered irregular. The complete set of rules has been tested by means of a computer program that executes the rules in sequence and prints out the results both in the form of a matrix of distinctive feature specifications and in a phonemic orthography.

The rules separate into two parts: a set of "morpheme-structure rules," which fill in feature specifications that are redundant by virtue of sequential constraints on the occurrence of the various segments, and a set of morphophonemic rules. The forms upon which the morphophonemic rules operate are called <u>base forms</u>. The dictionary part of the grammar of which these rules form a part will list forms in which only non-redundant feature specifications are made; these forms, which the morpheme-structure rules convert into base forms, are called <u>dictionary forms</u>. For example, in a 3-consonant sequence in Finnish, the last consonant must be a voiceless stop. The features relating to the manner of articulation of this consonant do not have to be listed in the dictionary, since only a stop can follow two consonants; one of the morpheme-structure rules will add the features of obstruent and noncontinuant to any consonant that is preceded by two consonants.

The rules thus operate according to the following scheme.

dictionary forms → | morpheme-structure rules | → base forms → | morphophonemic rules | → actual words

Consider the following paradigms:

	"eyelash"	"child"	"ski"	"door"	"name"	"snow"	"large"
Nominative	ripsi	lapsi	suksi	uksi	nimi	lumi	suuri
Genitive	ripsen	lapsen	suksen	uksen	nimen	lumen	suuren
Partitive	ripseä	lasta	suksea	usta	nimeä	lunta	suurta

These forms will be predicted corectly if one assumes that the words have base forms of ripse, laps, sukse, uks, nime, lum, and suur and supplies the grammar with rules whereby 1) e is added after certain consonants and clusters except in the partitive case; 2) the first of a sequence of three consonants formed at a morpheme boundary is eliminated (uks + ta → usta; I am assuming the traditional rule that the partitive ending is a/ä after a single vowel, and ta/tä elsewhere); 3) final e is raised to i in nouns and adjectives, and 4) nasals assimilate to the point of articulation of a following consonant.

Consider, for a moment, the rule that changes final e to i. This rule not only takes care of the alternation of i in the nominative with e in the oblique cases,[4] but also of certain other phenomena. Consider, for example, the forms with a possessive suffix: the rule given applies only when the e is final, so that e would remain e when no possessive suffix follows. This is in complete agreement with the facts:

ripsi, "eyelash";	ripseni, "my eyelash"
lapsi, "child";	lapseni, "my child"
suksi, "ski";	sukseni, "my ski"
lumi, "snow";	lumeni, "my snow"

Now consider situations in which an s in the nominative alternates with a t or d in the oblique cases.[5] It will be necessary to assume two separate morphophonemes t and c to represent those t's that do not and do alternate, respectively, with s; in many situations it is predictable whether or not the alternation will occur, but the existence of doublets, such as läksi/lähti (past tense of lähteä, "to leave"), means that there are environments in which this cannot be predicted.

In t/s alternations, the s occurs either before i (the i may be either an alternant of e in the nominative of nouns – see above – or the plural marker in nouns, or the past tense marker in verbs) or in final position in polysyllabic nouns. The first class of cases of t/s alternation thus requires a rule that states that c → s before i. Then paradigms such as

	"hand"	"one"
Nominative	käsi	yksi
Genitive	käden	yhden
Illative	käteen	yhteen

will be generated correctly if one assumes base forms of käc and yhc (a sequence of velar plus dental is subject to regressive assimilation of the feature of continuity: ht and ks occur, but hs and kt do not; this dissimilation rule will transform the underlying form yhsi into the correct form yksi).

What about the cases in which the s alternant of t is in final position and thus not followed by i? Example:

	"freedom"	"beauty"
Nominative	vapaus	kauneus
Genitive	vapauden	kauneuden
Illative	vapauteen	kauneuteen

To answer this question, let us return to the earlier examples of *ripsi*, etc. Note that these words are all disyllabic. Compare the examples above with the following paradigms:

	"gratitude"	"event"
Nominative	kiitos	tapaus
Genitive	kiitoksen	tapauksen
Partitive	kiitosta	tapausta
Illative	kiitokseen	tapaukseen

These paradigms differ from those of *lapsi* and *uksi* only in the nominative case, in which the final *i* is missing and the consonant cluster simplifies. The simplification of the final cluster is easily incorporated into the rules. The rule already required for simplifying clusters in the partitive now reads

$$C \rightarrow \emptyset \text{ (i.e., is deleted) in the environment } \_\_\_ C + C$$

(+ denotes morpheme boundary). All that is needed is to change the environment to read $\_\_\_ C \left\{ {+ C \atop \#} \right\}$ (# means word boundary); this would then transform *kiitoks* and *tapauks* into the desired forms *kiitos* and *tapaus*. With respect to the fact that these words lack a final *i*, suppose that I just added a somewhat ad hoc rule that deletes final *i* if it occurs beyond the second syllable, so that *kiitos* would be obtained through an intermediate stage *kiitoksi*. That is, one rule would add a final *i* and then another rule would delete it, which admittedly sounds a trifle hocus-pocus-ish; however, it is no more complicated than the other solutions that present themselves, and, moreover, it turns out that it automatically takes care of *vapaus* and *kauneus* if base forms of *vapauc* and *kauneuc* are assumed: the final *i* is inserted, $c \rightarrow s$ before *i*, and then the final *i* is eliminated. This, incidentally, is exactly what happened historically: *vapaus* < *vapausi*; *kiitos* < *kiitoksi*. However, historical considerations aside, the solution given here seems likely to be the simplest synchronic description of the presence vs absence of final *i* and the *t/s* alternation, since it requres only the addition of one simple rule (*i*-deletion in polysyllabic nouns), in addition to rules that already have to be in the grammar to take care of other phenomena.

Consider, now, such paradigms as

	"tooth"	"spring"	"billy goat"
Nominative	hammas[6]	kevät	kauris
Genitive	hampaan	kevään	kauriin
Partitive	hammasta	kevättä	kaurista
Inessive	hampaassa	keväässä	kauriissa

The phenomenon to be accounted for is the disappearance of the final consonant and the appearance of the long vowel in the oblique cases. To explain this, let me digress for a moment and treat the topic of the occurrence of vowel sequences in Finnish words.

The vowel sequences that can occur within a syllable are the long vowels, the high-to-mid diphthongs (ie, yö, uo), and diphthongs whose second member is a high vowel. The long mid-vowels are of somewhat limited distribution: outside of a handful of recent loanwords, they only occur where they are created by some morphological process such as the vowel lengthening that occurs in the third person singular of verbs, the illative case of nouns, and the oblique cases of the class of nouns mentioned in the last paragraph. This means that aside from the loanwords, to which special rules will have to apply anyway, there will be no base forms containing long mid-vowels. This means that it would be possible to represent the high-to-mid diphthongs in base forms as if they were the corresponding long mid-vowels ee, öö, oo, and then obtain the high-to-mid diphthongs by a rule that raises the first mora of a long mid-vowel. This decision, based purely on the desire to simplify the statement of the occurrences of vowel sequences within a syllable (instead of saying "long high or low vowel, high-to-mid diphthong, or vowel plus high vowel," it now suffices to say "long vowel or vowel plus high vowel"), automatically removes an exception to the rules relating to noun plurals and the past tense of verbs. The rule in question relates to sequences of vowels that precede the plural or past-tense marker i. Most Finnish texts state that the second vowel of the sequence is lost except in the case of the high-to-mid diphthongs, in which the first vowel is lost. If these diphthongs are represented as long mid-vowels, this exception disappears, provided that the rule for the diphthongization of long mid-vowels follows the vowel-elimination rule (which will now state simply that the second vowel is lost). Example:

	"eats"	"ate"	"to the road"	"to the roads"
Base form	söö	söö + i	tee + lle'	tee + i + lle'
Vowel elimination	söö	sö + i	tee + lle'	te + i + lle'
Diphthongization	syö	sö + i	tie + lle'	te + i + lle'
Final result:	syö	söi	tielle'	teille'

Incidentally, these rules that I have established here for a synchronic description of Finnish morphology exactly mirror the historical development: Modern Finnish ie, yö, uo develop from Old Finnish ee, öö, oo. The vowel sequences within a syllable (in base forms) can thus be restricted to geminate vowels and vowel plus high vowel. This means that the grammar will contain a morpheme-structure rule corresponding to this restriction; the simplest candidate for this rule is a rule according to which progressive assimilation takes place when a vowel is followed by a non-high vowel within the same syllable.

Let us now return to nouns of the hammas type. I will attempt to account for these with as little machinery as is absolutely necessary beyond the rules already in the grammar. I already have a rule that adds an *e* in certain still vaguely specified environments. Suppose that it also applies to nouns of the *hammas* type. This will not affect the nominative case, since the final vowel would be eliminated later according to the rule already established. Consider the underlying forms for the genitive which would then result:

A. hampase + n   keväte + n   kaurise + n

If the *s* or *t* is removed, then a vowel sequence *ae*, *äe*, *ie*, etc., will arise. If the vowel-assimilation "morpheme-structure" rule is moved into the morphophonemic part of the grammar, then nothing more is needed. The forms A would be transformed into

B. hampae + n   keväe + n   kaurie + n

by the consonant-elimination rule and then into the desired forms

C. hampaa + n   kevää + n   kaurii + n

by the vowel-assimilation rule.[7] All that needs to be done now is to formulate the consonant-elimination rule, provided, of course, that one can be formulated, something that I still have not established.

Nouns of the *hammas* type are all disyllabic. They can, indeed (assuming the obvious base forms of *hampas*, *kevät*, *kauris*), be characterized as those nouns whose base form ends in a single obstruent (i.e., a single consonant other than a liquid or nasal). Note that nouns of the *vapaus* type, in which the final consonant is preserved, are trisyllabic (va pa us; kau ne us).[8] This fact immediately suggests a possible rule: An intervocalic obstruent is eliminated when preceded by exactly two syllables. However, a somewhat simpler, neater, and more intuitive form of the rule can be obtained by taking into account the alternating stress of Finnish. As far as I can determine, excluding certain recent loans and foreign names, base forms are at most three syllables long, so that a form obtained by the *e*-addition rule is at most four syllables long; the four syllables would have the stress pattern / ∪ | ∪ (strong-minimal-low-minimal). The intervocalic obstruent is thus dropped if and only if it is preceded by a vowel with minimal stress.

The rules referred to here must apply in the following order:

(1) addition of *e* after a stem-final consonant,

(2) raising of a final *e* to *i* in nouns,

(3) deletion of final *i* from polysyllabic nouns,

(4) deletion of an intervocalic obstruent when preceded by a minimally stressed vowel,

(5) progressive assimilation of vowel segments within a syllable when the second is not high.

Note that these rules take care not only of the oblique forms of the *hammas* type of noun but also the forms with possessive suffixes. *Hammas*, *kevät*, and *kauris* have the following forms with a possessive suffix:

hampaani, "my tooth"
keväänì, "my spring"
kauriini, "my billy goat"

Starting from the forms

hampas + ni   kevät + ni   kauris + ni

rule (1) produces

hampase + ni   keväte + ni   kaurise + ni,

rules (2) and (3) do not apply (since the e added by rule (1) is not final), rule (4) yields

hampae + ni   keväe + ni   kaurie + ni,

and rule (5) yields the desired forms

hampaa + ni   kevää + ni   kaurii + ni.

On the other hand, if there is no possessive suffix in the nominative case, then the vowel added by rule (1) is deleted by rule (3), which means that the s or t is no longer intervocalic, so that rule (4) will not apply and the desired forms hammas, kevät, and kauris will not be obtained.

Further confirmation of the validity of these rules is given by the fact that the rules without any modification predict correctly not only the complete singular paradigms of all "regular" nouns and adjectives, which is what they were established to describe, but also the paradigms of several words that are usually regarded as "irregular." Three such examples are the nouns sydän and tuhat and the ordinal number words. Consider the following paradigms:

	"heart"	"thousand"	"third"
Nominative	sydän	tuhat	kolmas
Genitive	sydämmen[9]	tuhannen[10]	kolmannen
Partitive	sydäntä	tuhatta	kolmatta
Illative	sydämmeen	tuhanteen	kolmanteen

The appropriate base forms are sydämm, tuhant, and kolmanc. The nominative case forms are generated as follows (for the other cases the derivations are obvious):

	sydämm	tuhant	kolmanc
e-addition	sydämme	tuhante	kolmance
vowel raising	sydämmi	tuhanti	kolmanci
$c \rightarrow s$	sydämmi	tuhanti	kolmansi
$i \rightarrow \emptyset$	sydämm	tuhant	kolmans
cluster simplification	sydäm	tuhat	kolmas
final $\rightarrow$ dental	sydän	tuhat	kolmas

J. D. McCawley

References

1. A paper that contains the complete set of rules, of which this is an abbreviated version, will be available soon in duplicated form from the Mechanical Translation Group, Research Laboratory of Electronics, M.I.T. Some of the rules are given here in a slightly simplified (and thus incorrect) form in the interests of simplicity; the differences are slight and affect only certain minor phenomena that are not treated here.

2. The descriptive model that I use is described in detail by Halle, The Sound Pattern of Russian (Mouton and Company, The Hague, 1959).

3. All statements that I make here for nouns also hold for adjectives; adjective morphology differs in no way from noun morphology in Finnish.

4. I use the term "oblique cases" to refer to all cases except the nominative and partitive.

5. The d is the result of consonant mutation, a process by which voiceless stops at the beginning of short closed syllables are modified. The larger version of this report contains a full treatment of consonant mutation rules.

6. The mp/mm alternation is a result of consonant mutation.

7. In order for the vowel-assimilation rule to be able to apply, not only the consonant but also the syllable boundary preceding it will have to be removed. Note that it is possible for the second and third syllables to be separated by a syllable boundary but no consonant: kor ke a; ta pa us. Vowel assimilation does not occur in such cases. Syllable boundary is, of course, nondistinctive: it is inserted according to rules that correctly predict its occurrence.

8. The au diphthong can occur in only the first syllable. In au sequences beyond the first syllable, both vowels are syllabic, i.e., they are separated by a syllable boundary, as in vapaus.

9. The oblique case forms of sydän are written with a single m in standard orthography; however, a double m is actually pronounced.

10. nn is the alternant of nt under consonant mutation.

XXII. LINGUISTICS*

Prof. R. Jakobson
Prof. A. N. Chomsky
Prof. M. Halle
Dr. G. H. Matthews
Dr. Paula Menyuk
T. G. Bever
S. K. Ghosh
Barbara C. Hall
Y. Isami
J. J. Katz
R. P. V. Kiparsky
D. T. Langendoen
T. M. Lightner
P. M. Postal
C. B. Qualls
J. J. Viertel
K. Wu

RESEARCH OBJECTIVES

This group sees as its central task the development of a general theory of language. The theory will attempt to integrate all that is known about language and to reveal the lawful interrelations among the structural properties of different languages as well as of the separate aspects of a given language, such as its syntax, morphology, and phonology. The search for linguistic universals and the development of a comprehensive typology of languages are primary research objectives.

Work now in progress deals with specific problems in phonology, morphology, syntax, language learning and language disturbances, linguistic change, semantics, as well as with the logical foundations of the general theory of language. The development of the theory influences the various special studies and, at the same time, is influenced by the results of these studies. Several of the studies are parts of complete linguistic descriptions of particular languages (English, Russian, Siouan) that are now in preparation.

Since many of the problems of language lie in the area in which several disciplines overlap, an adequate and exhaustive treatment of language demands close cooperation of linguistics with other sciences. The inquiry into the structural principles of human language suggests a comparison of these principles with those of other sign systems, which, in turn, leads naturally to the elaboration of a general theory of signs, semiotics. Here linguistics touches upon problems that have been studied by modern logic. Other problems of interest to logicians – and also to mathematicians – are touched upon in the studies devoted to the formal features of a general theory of language. The study of language in its poetic function brings linguistics into contact with the theory and history of literature. The social function of language cannot be properly illuminated without the help of anthropologists and sociologists. The problems that are common to linguistics and the theory of communication, the psychology of language, the acoustics and physiology of speech, and the study of language disturbances are too well known to need further comment here. The exploration of these interdisciplinary problems, a major objective of this group, will be of benefit not only to linguistics; it is certain to provide workers in the other fields with stimulating insight and new methods of attack, as well as to suggest to them new problems for investigation and fruitful reformulations of questions that have been asked for a long time.

R. Jakobson, A. N. Chomsky, M. Halle

A. A NOTE ON THE FORMULATION OF PHONOLOGICAL RULES

This report deals with a restriction that must be imposed on phonological rules of the type

(1) $A \rightarrow B$ in env: $X \underset{Z}{\underline{\quad}} Y$

*This work was supported in part by the National Science Foundation (Grant G-16526) and in part by the National Institutes of Health (Grant MH-04737-02).

where the capital letters represent distinctive-feature specifications and X, Y, Z may be null (i.e., the rule may apply in all environments).

Following Halle[1] and Chomsky,[2] we shall define segments $\{\alpha\}$ and $\{\beta\}$ to be phonemically distinct (i.e., nonrepetitions) if and only if at least one feature has a different value in $\{\alpha\}$ than in $\{\beta\}$. Thus segments $\{\alpha\}$ and $\{\beta\}$ below are phonemically distinct because $\{\alpha\}$ is specified [+feature A] whereas $\{\beta\}$ is specified [-feature A]; segment $\{\gamma\}$, however, is phonemically distinct neither from $\{\alpha\}$ nor from $\{\beta\}$ because there is not one feature in $\{\gamma\}$ that has a different value either in $\{\alpha\}$ or $\{\beta\}$:

segment:	$\{\alpha\}$	$\{\beta\}$	$\{\gamma\}$
feature A:	+	-	0
feature B:	+	+	+

We discuss possible interpretations of how rules of type (1) should be applied to segments of type $\{\gamma\}$.

In particular, we want to determine how rule (2) should be applied to segment $\{\gamma\}$:

(2) [+feature A] → [-feature B].

Let us assume first, that rule (2) applies to segment $\{\gamma\}$ and thus specifies $\{\gamma\}$ as [-feature B]. Application of (2) to $\{\beta\}$ and $\{\gamma\}$ will then produce the following distinctive-feature matrix:

segment:	$\{\beta\}$	$\{\gamma\}$
feature A:	-	0
feature B:	+	-

Since segments $\{\beta\}$ and $\{\gamma\}$ were not phonemically distinct to begin with and since they are phonemically distinct after application of rule (2), we conclude that

> No rule may be applied to any segment if a feature to the left of the arrow has not already been specified for that segment.

Now let us assume that rules of type (2) do not apply to segments of type $\{\gamma\}$. We begin with segments $\{\alpha\}$ and $\{\gamma\}$. Application of rule (2) to these segments results in the following matrix:

segment:	$\{\alpha\}$	$\{\gamma\}$
feature A:	+	0
feature B:	-	+

Once again we have succeeded in producing two phonemically distinct segments from segments that initially were not phonemically distinct. We therefore conclude that

> No rule may not be applied to any segment if a feature to the left of the arrow has not already been specified for that segment.

The application of this restriction to specifications in the environment is obvious.

T. M. Lightner

References

1. M. Halle, The Sound Pattern of Russian (Mouton and Company, The Hague, 1959), p. 32.

2. N. Chomsky, Review of Jakobson and Halle, Fundamentals of Language, Int. J. Am. Ling. 23, 234-235 (1957).

B. VOWEL HARMONY IN CLASSICAL (LITERARY) MONGOLIAN

In Classical Mongolian (CM), vowels in a word must be either all grave or all acute, in agreement with the gravity of the first vowel in the word. The vowel i, however, may occur either with grave vowels or with acute vowels.

The CM vowel phones are as follows:

segment:	u	o	ü	ö	i	a	e
flat:	+	+	+	+	−	−	−
diffuse:	+	−	+	−	+	−	−
grave:	+	+	−	−	0	+	−

We would like to account for CM vowel harmony in essentially the same way that Halle accounts for Finnish vowel harmony.[1] We would require the following two ordered rules:

(1) $\begin{bmatrix}+\text{voc}\\-\text{cns}\end{bmatrix} \rightarrow [\alpha\text{grv}]$ in env: $\left(\begin{bmatrix}+\text{voc}\\-\text{cns}\\\alpha\text{grv}\end{bmatrix}X\right)_1$ ———

where X may be any number of nonvowel segments and may contain + boundaries or juncture symbols but may not contain a pair of #'s (i.e., may not contain a word boundary).

(2) $\begin{bmatrix}+\text{voc}\\-\text{cns}\\-\text{flt}\\+\text{dif}\end{bmatrix} \rightarrow [-\text{grv}]$

In the examples below capital letters represent archiphonemes not specified for gravity; thus U represents {u, ü}, etc. We omit boundary markers, since they play no role in vowel harmony.

(a) emA →1→ eme 'woman'
(b) barsUn →1→ barsun 'tiger (gen. sg.)'
(c) barsI →1→ barsï →2→ barsi 'tiger (acc. sg.)'

The difficulty with this analysis lies in the existence of words that have i for their first vowel phoneme (nigen 'one,' e.g.). Since the first vowel of these stems is unspecified for gravity, it may be objected that one may not formulate rule (1).

At first glance this seems to be a serious objection: either one must discard the intuitively correct analysis above or else one must specify i for gravity in these words – and thus violate Halle's simplicity criterion.[2]

Closer examination reveals that an objection of this type is ill-formed.

Given a word whose first vowel is i, there is no way to tell whether the other vowels in the word should be back vowels or front vowels. In actual fact, the other vowels may be either front or back, depending on the particular morpheme in question. The i in these words must, therefore, be specified for gravity.

In short, the phonemic CM vowel system contains one more vowel than the phonetic CM vowel system[3]:

segment:	u	o	ü	ö	ĭ	i	a	e
flat:	+	+	+	+	-	-	-	-
diffuse:	+	-	+	-	+	+	-	-
grave:	+	+	-	-	+	-	+	-

Examples of application of rules (1)-(3) to words whose first vowel phoneme is i or ĭ are the following:

(d) bidAnU →1→ bidenü (→2→ bidenü) 'of us (inclusive)'
(e) ĭnAdU →1→ ĭnadu →2→ inadu 'on this side'

T. M. Lightner

References

1. M. Halle, Questions of linguistics, Nuovo cimento 13, 513-514 (1959).

2. M. Halle, On the role of simplicity in linguistic descriptions, Proc. Symposia in Applied Mathematics, Vol. 12 (American Mathematical Society, New York, 1961), pp. 89-94.

3. It may be of interest to note that in Proto-Mongolian there were phonetically two nonflat diffuse vowels – an i that occurred only in words with front vowels, and an ĭ that occurred only in words with back vowels. The two phonetic vowels i and ĭ subsequently merged into one phonetically front vowel i, but phonemically we must retain both i and ĭ. See K. Grønbech and J. Krueger, An Introduction to Classical (Literary) Mongolian (Otto Harrassowitz, Wiesbaden, 1955), p. 18, and N. Poppe, Grammar of Written Mongolian (Otto Harrassowitz, Wiesbaden, 1954), p. 11.

C. ON THE PRESENT TENSE THEME o/e IN RUSSIAN

Most North Russian (R) dialects and a few South R dialects are commonly considered to have the present tense theme o for verbs with stems in a consonant or in a back vowel (the so-called first conjugation). The remaining North R dialects and most South R dialects are considered to have the present tense theme e. There are also a few dialects that are considered to have both e and o: e before soft consonants and o before hard consonants.[1]

Thus, for example, the 2 Sg, 3 Sg, 1 Pl, 2 Pl present tense forms of the stem pas-, may occur in any of the following phonetic forms, depending on the particular dialect in question:

A:	pas, óš	pas, ót	pas, óm	pas, ót, e
B:	pas, éš	pas, ét	pas, ém	pas, ét, e
C:	pas, óš	{pas, ót / pas, ét,}	pas, óm	pas, ét, e

We cannot accept any analysis that postulates that the underlying present tense theme is either e or o for any R dialect (in fact, for any East Slavic language).

Let us first look at type A (the contemporary standard literary dialect is of this type). If the present tense theme is postulated as o, then the rules of the transformational cycle will read, in part (we omit rules that are irrelevant here), as follows[2]:

C-1: Transitive softening occurs in env: $\_\_\_\_ + \begin{bmatrix}+\text{voc}\\-\text{cns}\\-\text{flt}\end{bmatrix} + \begin{bmatrix}+\text{voc}\\-\text{cns}\\+\text{flt}\end{bmatrix}$

C-2: $\begin{bmatrix}+\text{voc}\\-\text{cns}\end{bmatrix} \rightarrow \emptyset$ in env: $\_\_\_\_ (+) \begin{bmatrix}+\text{voc}\\-\text{cns}\end{bmatrix}$

C-3: $[+\text{cns}] \rightarrow [+\text{sharp}]$ in env: $\_\_\_\_ + \begin{Bmatrix}\underline{i}\\\underline{e}\\\underline{o}\end{Bmatrix} + X$ where X may not be null.

C-4: Erase parentheses and return to C-1.

We note that the specification of the environment in C-3 will be rather complex because i, e, and o do not form a natural class of vowels.

Our suggestion is to postulate a front, rounded vowel, ö, as the present tense theme. Rule C-3 will then read:

C-3': $[+\text{cns}] \rightarrow [+\text{sharp}]$ in env: $\_\_\_\_ + \begin{bmatrix}+\text{voc}\\-\text{cns}\\-\text{grv}\end{bmatrix} + X$

After all of the rules of the transformational cycle have been applied, the forms of pas- listed above will be as follows:

A': pas, öš   pas, öt   pas, öm   pas, öt, e

We require now only the following phonetic rule:

P-A: [+flat] → [+grave]

Application of rule P-A to the forms above will give the correct final phonetic forms.

A": pas, óš pas, ót pas, óm pas, ót, e

We must prefer this analysis to an analysis that uses the present tense theme o because our analysis requires fewer distinctive feature specifications.

Now let us examine type B. The postulation of a present tense theme e for this type would involve a considerable increase in the complexity of the grammar because rule C-1 would have to be changed drastically. We would have to find some environment that causes transitive softening in forms like ((p, is+a + e) + t), ((xod+i + i) + u) – ultimately p, íšet and xóžu – and prevents transitive softening in forms like ((xod+i + i) + at), ((smotr+e + i) + at), ((pas + e) + u) – ultimately xód, at, smótr, at, pasú. Such an environment cannot be of the simple form shown in rule C-1.

If, however, we were to postulate that the present tense theme for type B were ö, then we could use rule C-1 as it stands. We would now need only to have the following phonetic rule in place of P-A:

P-B: [-grave] → [-flat]

This rule will ensure that ö → e and the final phonetic form of the examples given above will have the (correct) vowel e.

At this point it should be clear that we want to postulate ö as the present tense theme for type C also. For these dialects we will require, not one, but two phonetic rules:

P-C1: $[+\text{flat}] \rightarrow [+\text{grave}]$ in env: $\underline{\quad\quad} \begin{bmatrix} +\text{cons} \\ -\text{shrp} \end{bmatrix}$

P-C2: [-grave] → [-flat]

We must point out that the present analysis clearly brings forth the underlying unity of R conjugation; the particular dialectal variations find their explication in low-level phonetic rules, i.e., at a late stage of phonetic specification rather than at an earlier stage.

Although we leave Ukrainian (U) and Byelorussian (BR) conjugation for later studies, we would like to mention the inherent plausibility that the present theme in these languages is also ö.

In U the late phonetic rule will be P-B; rule C-3 does not apply in U. Thus the present rules will generate the following U forms:

stem	2 Sg	3 Sg	1 Pl	2 Pl
pas-	paséš	pasé(t,)	pasemó	paseté
pis+a-	píšeš	píše(t,)	píšemo	písete

In BR the late phonetic rules will be P-C1 and P-C2. Thus the present rules will generate the following BR forms[3]:

n, os- n, as, éš n, as, é(c,) n, as, óm n, as, ac, ó

G. H. Matthews, T. M. Lightner

References

1. See N. Durnovo, Očerk Istorii Russkogo Jazyka (Gosudarstvennoe izdatel'stvo, Moscow-Leningrad, 1924), Sec. 512, p. 333.

2. For more information on the transformational cycle in Russian, see M. Halle, Note on cyclically ordered rules in the Russian conjugation, Quarterly Progress Report No. 63, Research Laboratory of Electronics, M.I.T., October 15, 1961, pp. 149-155, and T. M. Lightner, On pon, át, and obrazovát, type verbs in Russian, Quarterly Progress Report No. 67, Research Laboratory of Electronics, M.I.T., October 15, 1962, pp. 177-180.

3. In BR there will be a late phonetic rule š, → š. Furthermore, pretonic e in BR is pronounced [a]. See any elementary BR grammar, for example, R. G. A. deBray, Guide to the Slavonic Languages (E. P. Dutton Company, Inc., New York, 1951), p. 139.

D. DISCONTINUOUS ONE-WAY GRAMMARS

Chomsky[1] defines a class of grammars each of which contains a finite number of rules of the form $\chi_1 A \chi_2 \rightarrow \chi_1 \omega \chi_2$, where A is a single symbol, and $\omega \neq I$. Such grammars are called context-sensitive phrase structure (CS) grammars. Context-free phrase structure (CF) grammars are a subclass of CS grammars for which all of the rules are of the form $A \rightarrow \omega$, i.e., χ_1 and χ_2 are always null. A sequence of strings $(\phi_1, \phi_2, \ldots, \phi_n)$ is called a ϕ-derivation of a grammar G if $\phi = \phi_1$, and for each i $(1 \leq i < n)$ there are strings $A, \chi_1, \chi_2, \psi_1, \psi_2$ which are such that $\phi_i = \psi_1 \chi_1 A \chi_2 \psi_2$, $\phi_{i+1} = \psi_1 \chi_1 \omega \chi_2 \psi_2$, and $\chi_1 A \chi_2 \rightarrow \chi_1 \omega \chi_2$ is a rule of G. The language L_G is the set of strings that do not contain nonterminal symbols and conclude S-derivations of the grammar G. Such a string is called a sentence of L_G.

CONVENTION 1: By $\omega^{(n)}$ is meant a string ω that is n symbols in length, or that is initial and/or final in a string, i.e., follows and/or precedes #, and not greater than n symbols in length.

DEFINITION 1: (a) A left-to-right (L-R) ϕ-derivation is a ϕ-derivation in which ψ_1 and χ_1 given above are always strings of terminal symbols, i.e., $\phi_i = yxA\chi\psi$, $\phi_{i+1} = yx\omega\chi\psi$, and $xA\chi \rightarrow x\omega\chi$ is a rule of the grammar.

(b) A right-to-left (R-L) ϕ-derivation is a ϕ-derivation in which χ_2 and ψ_2 given above are always strings of terminal symbols, i.e., $\phi_i = \psi\chi Axy$, $\phi_{i+1} = \psi\chi\omega xy$, and $\chi Ax \rightarrow \chi\omega x$ is a rule.

DEFINITION 2: (a) An L-R grammar is one whose rule applications are restricted so that all of its derivations are L-R derivations.

(b) An R-L grammar is one whose rule applications are restricted so that all of its derivations are R-L derivations.

(c) A one-way grammar is either an L-R grammar or an R-L grammar.

DEFINITION 3: (a) A right discontinuous (RD) rule is one of the form $\chi_1 A \chi_2 \to \chi_1 \overset{n_1}{\text{—}} a_1 \overset{n_2}{\text{—}} a_2 \ldots a_{m-1} \overset{n_m}{\text{—}} a_m \chi_2$, where $m \geq 1$ and $n_i \geq 0$ $(1 \leq i \leq m)$. A rule of this type rewrites a string of the form $\psi_1 \chi_1 A \omega \chi_2$ as $\psi_1 \chi_1 \omega_1 a_1 \omega_2 a_2 \ldots a_{m-1} \omega_m a_m \psi_2$, where $\omega_i^{(n_i)}$ $(1 \leq i \leq m)$, and for some τ, $\omega \psi_2 = \omega_1 \omega_2 \ldots \omega_m \psi_2 = \chi_2 \tau$.

(b) A left discontinuous (LD) rule is one of the form $\chi_1 A \chi_2 \to \chi_1 a_m \overset{n_m}{\text{—}} a_{m-1} \overset{n_{m-1}}{\text{—}} \ldots \overset{n_2}{\text{—}} a_1 \overset{n_1}{\text{—}} \chi_2$, where $m \geq 1$ and $n_i \geq 0$ $(1 \leq i \leq m)$. An LD rule rewrites a string of the form $\psi_1 \omega A \chi_2 \psi_2$ as $\psi_1 a_m \omega_m a_{m-1} \omega_{m-1} \ldots \omega_2 a_2 \omega_1 \chi_2 \psi_2$, where $\omega_i^{(n_i)}$ $(1 \leq i \leq m)$, and for some τ, $\psi_1 \omega = \psi_1 \omega_m \omega_{m-1} \ldots \omega_1 = \tau \chi_1$.

Note that the rules defined by Chomsky[1] are special cases, both of RD rules and of LD rules, i.e., those in which $n_i = 0$ $(1 \leq i \leq m)$.

DEFINITION 4: (a) An RD grammar is a phrase structure grammar that contains just RD rules.

(b) An LD grammar is one that contains just LD rules.

(c) A discontinuous grammar is either an RD grammar or an LD grammar.

DEFINITION 5: A discontinuous one-way grammar is either an L-R RD grammar or an R-L LD grammar.

The following theorems and corollaries have been proved.

THEOREM 1: For each discontinuous one-way grammar there is an equivalent CF grammar.

Proof is by reduction to a push-down storage automaton (PDS).[2]

COROLLARY 1: For each CF grammar – and thus for each PDS – there is an equivalent nondeterministic PDS containing just three types of instructions in addition to a single initial and a single final instruction. For each terminal symbol $\underline{a}$ of the grammar the PDS has the instruction $(a, S_1, a) \to (S_1, \sigma)$; for each nonterminal symbol A the PDS has the instruction $(e, S_1, A) \to (S^A, \sigma)$, and for each rule of the grammar $A \to \omega$ the PDS has the instruction $(e, S^A, e) \to (S_1, \omega)$. The initial and final instructions are $(e, S_0, \sigma) \to (S_1, S)$ and $(e, S_1, \sigma) \to (S_0, \sigma)$, respectively.

COROLLARY 2: Given any discontinuous one-way grammar, there is an algorithm for constructing an equivalent CF grammar.

THEOREM 2: For each discontinuous grammar there is an equivalent CS grammar.

G. H. Matthews

References

1. N. Chomsky, On certain formal properties of grammars, Information and Control 2, 137-167 (1959).

2. N. Chomsky, Formal properties of grammars, Handbook of Mathematical Psychology, Vol. 2, edited by R. R. Bush, E. H. Galanter, and R. D. Luce (John Wiley and Sons, Inc., New York, in press).

E. CHILDREN'S GRAMMAR

In describing children's grammar there are three objectives that seem most important. The first of these is to be able to examine language at particular times in its development as a self-contained system. The second is to be able to describe the changing processes of this system as the child matures. The third and most important is to gain some insight into the basic capacities of the child to understand and produce language.

Most studies of children's grammar have measured the percentage and proporation of what has been termed 'adult usage' in the child's language.[1] Such aspects as completeness of sentence structure and sentence length were the focus of these studies. I felt that such an approach would not contribute to reaching the objectives stated above. For these reasons, in this research program a transformational model of grammar was used to describe a children's grammar.[2] This technique allows us to describe the rules or categories from which the child may generate the sentences in his language. This grammar is analogous to a categorization theory of learning. The rules formulated for generating possible sentences in a language are the categories of grammatical structure in the language (the negative sentence, the imperative sentence, etc.). It is hypothesized that the attributes of a given category are memorized and the child can then produce new instances of the category.

1. Method

The language of 159 children ranging in age from 2 years, 10 months to 7 years, 1 month was elicited and recorded in various stimulous situations: (a) responses to a projective test, (b) conversation with an adult, and (c) conversation with peers. The last two situations took place both in controlled and in free (classroom) environments. The language sample produced by each child was analyzed by using the transformational model. A grammar was written which contained rules to produce all of the sentences in the total language sample.[3]

2. Results

It was found that all of the basic structures that generated all of the sentences obtained could be described within the framework of the transformational grammar.

Almost all of the structures used by adults to generate their sentences were found in the grammar of the youngest children (youngest 4-month age range). Structures that are nonconsistent with adult use of rules occurred infrequently. These were termed structures restricted to a children's grammar. There were few significant differences in the usage of all structures by males and females or by children whose I.Q. is above or below the mean I.Q. of the sample population.

It was also found that most of the structures were used at an early age and used consistently. Most of the structures that were still in the process of being acquired by the youngest group were also still in the process of being acquired by the oldest group (first-grade children).[4] There was a steady increase in the percentage of children using the various structures as they matured.

A subsample of the population was presented with sentence examples of the various syntactic structures taken from their own language sample and asked to repeat these sentences after the experimenter.

These examples consisted of a set of sentences exemplifying transformations found in both children's and adults' grammar and a set of sentences exemplifying structures restricted to a children's grammar. This study was undertaken to determine the differences, if any, between the production of language and innate capacity. It was found that success in repetition was not correlated with sentence length at all but, rather, with the specific structure of the sentence. Also, it was found that although these children produced the restricted structures in their spontaneous language, they corrected these forms when asked to repeat. Significantly more of the youngest children corrected these structures.

3. Additional Data

One developmental trend observed in this analysis of children's grammar was the use of alternate rules by the same child. That is, the children generate their sentence from rules that conform with adult use of rules, and, simultaneously, from rules that are restricted to a children's grammar. For example, some children under 3 years of age use the rule:

> pronoun + singular + first person in the context subject or object becomes <u>me</u>.
> ("Me have this one.")

Simultaneously, they use the rule:

> pronoun + singular + first person in the context subject becomes <u>I</u>.
> ("I like that.")

It was found that the use of alternate rules, on the whole, gradually declines from the beginning age range of the sample population to its end. However, the specific rules that are alternated change through this age period as the children mature. For example, contraction deletion ("I going to the movies.") accounts for a significant number of the restricted forms at the youngest age level but not at the oldest. On the other hand, tense restriction in conjunction ("They get mad and then they pushed him.") accounts for a significant number of the restricted forms at the oldest age level but not at the youngest. These data may give us further insight into the notions of simplicity or complexity of children's grammar and the concepts of differentiation and integration in language learning.

Paula Menyuk

References

1. D. McCarthy, Language development in children, Manual of Child Psychology, edited by L. Carmichael (John Wiley and Sons, Inc., New York, 1954).

2. N. Chomsky, Syntactic Structures (Mouton and Company, The Hague, 1957).

3. P. Menyuk, A Descriptive Study of Syntactic Structures in the Language of Children: Nursery School and First Grade, D. Ed. Thesis, School of Education, Boston University, 1961.

4. P. Menyuk, Syntactic structures in the language of children, J. Child Develop. (accepted for publication).

F. THEORETICAL IMPLICATIONS OF BLOOMFIELD'S "MENOMINI MORPHOPHONEMICS"

At least two publications written during the final decade of Leonard Bloomfield's career contain extensive use of ordered descriptive rules: "Menomini Morphophonemics"[1] and the first four chapters of "Eastern Ojibwa."[2]

"Menomini Morphophonemics" (MM) is a well-known example of experimentation with synchronic morphophonemic rules. Bloomfield emphasizes that the rules occur in a purely descriptive order, but the form of the rules and their application demonstrate a limited notion of the concept "rule," and unavoidably reflect his comprehensive understanding of historical Algonquian.[3]

1. The Form of the Rules and the Order

The morphemes are written in morphophonemes and constitute the "basic forms" of the language, the input to the morphophonemic system. These basic forms are combined and then transformed to phonemes by the morphophonemic rules.

The rules are of the form:

(1) $A \rightarrow B$ in the environment C

and are generally classed according to the environment C, not according to the process

$A \rightarrow B$ or to the units that interact in that process, A, B. In other words, rule (1) can be combined only with a rule

(2) $P \rightarrow Q$ in the environment C

Thus a numbered rule consists of many processes or subrules that all occur in the same environment:

(3) Rule N:

$$\left.\begin{array}{l} \text{a)}\ A \rightarrow B \\ \text{b)}\ P \rightarrow Q \\ \ \vdots \quad \vdots \quad\ \ \vdots \\ \text{n)}\ X \rightarrow Y \end{array}\right. \quad \text{in environment } C$$

It can be shown that the subrules of N, (a...n) often must apply simultaneously, i.e., if applied in any order, the output is incorrect. In the only case in which different processes must be ordered, even though they occur in the same environment, they are written as two separate numbered rules.

The general conclusion drawn from these characteristics of the rules is that Bloomfield was working with a series of <u>ordered environments</u>. For instance, the same process is written in two separate rules only because the rules have different environments. Rules (4) and (5) are presented as disjoint because the environments are disjoint, although it is just that characteristic that should allow them to be combined:

(4) $R \rightarrow S$ in env. X

(5) $R \rightarrow S$ in env. Y

A rule of the form (4+5) was not an alternative for Bloomfield.

(4+5) $R \rightarrow S$ in env. $\begin{Bmatrix} X \\ Y \end{Bmatrix}$

The constraint that does not allow rules of the type (4+5) limits the power of any simplicity criterion. Since rules are combined by common environments only, the goal of descriptive simplicity in MM would have the effect of minimizing the number of environmental statements, but the number and ordering of the processes within the ordered environments would be immaterial to the grammar. The resulting system is redundant because environments often cannot be ordered when the processes occurring within those environments might be ordered to great advantage.

In spite of these limitations, Bloomfield presented ordering depths of at least five rules, apparently operating with the goal of minimizing the total of numbered rules, that is, the number of environments. Efforts to reduce this number by reordering the MM rules have very little effect.

2. Simplification of the MM System

The Menomini morphophonemic system as presented in MM can be significantly simplified if different environments with processes in common may be combined. For example, if rules of the type (4+5), as well as of the type (3), are allowed, the original MM vowel assimilation subsystem can be reduced from 33 process statements to 24 without the invention of any new statements. Reordering and combinations make the existing system redundant so that 9 statements may be deleted, and no new ones need be added. If new rules of the same type are devised (still by using phonemic notation) the assimilation system can be further reduced to 13 statements.

The general application of these synchronic methods to the entire MM morphophonemic system halves the number of process statements, decreases the number of morphophonemes from 26 to 18, and leaves the total number of different environment statements unchanged. These simplifications of the MM system are based entirely on considerations that are internal to the synchronic description of the Menomini language.

Certain problems with general implications for the construction of morphophonemic systems are raised by Menomini. A general high-vowel assimilation system is described:

$$
(6)\qquad
\begin{array}{lcl}
 & \mathrm{I} & \\
y+\bar{e} & \rightarrow & \bar{e} \\
w+\bar{e} & \rightarrow & \bar{o} \\
y+æ & \rightarrow & e \\
w+æ & \rightarrow & o
\end{array}
\qquad\qquad
\begin{array}{lcl}
 & \mathrm{II} & \\
y+e & \rightarrow & i \\
w+e & \rightarrow & i \\
y+\bar{æ} & \rightarrow & \bar{i} \\
w+\bar{æ} & \rightarrow & \bar{i}
\end{array}
$$

all in environment C ____

Here, column I shows progressive assimilation with respect to gravity, column II progressive assimilation with respect to diffuseness. These facts would be easily describable were it not for the fact that the affected vowels in column I are /æ, ē/ and in column II /ǣ, e/. Short /æ/ acts with long /ē/ and long /ǣ/ with short /e/. This grouping can be described in features (the Menomini vowel system is a quadrangle):

$$
(7)\qquad
\begin{bmatrix} \alpha\text{long} \\ \beta\text{compact} \\ -\text{grave} \end{bmatrix}
\qquad\qquad
\begin{array}{l}
\text{column I: } \alpha = \sim\beta \\
\text{column II: } \alpha = \beta
\end{array}
$$

But there is no way to differentially describe the processes in columns I and II, except by writing two separate rules, one for the case $\alpha = \sim\beta$ and the other for the case $\alpha = \beta$. At best, this would introduce a new technique into the system. If /e/ and /æ/ are first <u>exchanged</u> in this environment, the system would become

$$
(8)\qquad
\begin{array}{lcl}
 & \mathrm{I'} & \\
y+\bar{e} & \rightarrow & \bar{e} \\
w+\bar{e} & \rightarrow & \bar{o} \\
y+e & \rightarrow & e \\
w+o & \rightarrow & o
\end{array}
\qquad\qquad
\begin{array}{lcl}
 & \mathrm{II'} & \\
y+\bar{æ} & \rightarrow & \bar{i} \\
w+\bar{æ} & \rightarrow & \bar{i} \\
y+æ & \rightarrow & i \\
w+æ & \rightarrow & i
\end{array}
$$

The descriptive rules would be

$$(9)\quad \left.\begin{array}{lccc} \mathrm{I}' & [-\text{compact}] & \rightarrow & [\alpha\ \text{grave}] \\ \mathrm{II}' & [+\text{compact}] & \rightarrow & [+\text{diffuse}] \end{array}\right\} \text{ in env. } \begin{bmatrix} -\text{voc} \\ -\text{cons} \\ \alpha\text{grave} \end{bmatrix} \quad [-\overline{\text{grave}}]$$

(a later general rule deletes the semivowels).

To exchange /e/ and /æ/ in phonemic notation would be extremely cumbersome, although possible if it were required that all subrules of a numbered rule apply simultaneously. Since Bloomfield's system must have that requirement, he could have written a rule:

$$(10)\quad \begin{array}{lcc} \text{a) e} & \rightarrow & \text{æ} \\ \text{b) æ} & \rightarrow & \text{e} \end{array} \quad \text{in env.} \quad C\begin{Bmatrix} y \\ w \end{Bmatrix}$$

As long as (10a) and (10b) apply simultaneously, there will be an exchange between /e/ and /æ/. But if the rules are ordered, then both /e/ and /æ/ will end up either as /e/ (order: a, b) or as /æ/ (order: b, a). A third element B that is discrete from all of the elements at this point in the system must be introduced.

$$(11)\quad \begin{array}{lcc} \text{a) e} & \rightarrow & \text{B} \\ \text{b) æ} & \rightarrow & \text{e} \\ \text{c) B} & \rightarrow & \text{æ} \end{array} \quad \text{in env.} \quad C\begin{Bmatrix} y \\ w \end{Bmatrix}$$

In distinctive features (10a) and (10b) would be

$$(12)\quad \begin{array}{lccc} \text{a)} & [-\text{compact}] & \rightarrow & [+\text{compact}] \\ \text{b)} & [+\text{compact}] & \rightarrow & [-\text{compact}] \end{array} \quad \text{in env.} \quad [+\text{cons}] \begin{bmatrix} -\text{voc} \\ -\text{cons} \end{bmatrix} \begin{bmatrix} +\overline{\overline{\text{voc}}} \\ -\text{grave} \end{bmatrix}$$

This would produce the same problem as (10), but, by using the variable β, rules (12a) and (12b) may be combined so that effectively they occur simultaneously.

$$(13)\quad [\beta\ \text{compact}] \rightarrow [\sim\beta\ \text{compact}] \quad \text{in env. (12)}$$

This has made use of the existing convention that $\sim + = -$ and $\sim - = +$, also used for some cases of assimilation.[4]

For correct syllable syncope in the lengthening of vowels and for correct vowel raising, in certain positions glottal stop must be interpreted as V?V. After the vowel length and height rules are applied, the introduced vowels surrounding the glottal stop are deleted. Thus there are two rules

$$(14)\quad \begin{array}{lccc} \text{m)} & ? & \rightarrow & \text{V?V} \\ \text{n)} & \text{V?V} & \rightarrow & ? \end{array}$$

which dramatically simplify the length and height systems intervening between (14m) and

(14n). Unless a more thorough examination of Menomini shows this to be unnecessary, it will remain an example of the addition and exact deletion of segments within the morphophonemic grammar.

3. Evaluation of the Simplifications

Is it possible to motivate the simplifications discussed above other than by the criterion of orthographic efficiency? The simplifications are in accord with the principle of descriptive simplicity but this is, at best, only an indication of the efficacy of the simplifications. It is important to show that the new simplified system satisfies criteria other than that of simplicity itself.

Although no criterion is formally proposed, there are certain comments by Bloomfield which imply (perhaps unintentionally) an indicator of the accuracy and usefulness of any descriptive system of ordered rules. This indicator is the similarity of the morphophonemes and early rules of the synchronic description of a language to the corresponding forms in the reconstructed proto-language.[5]

Bloomfield divides the morphophonemic system into two parts, (a) the morphophonemes and the first 18 rules, and (b) the last 17 rules. He points out that the rules of the latter subsystem "approximate the historical development from Proto-Algonquian to present-day Menomini." Expanded as a general statement, this suggests that the mechanism of diachronic linguistic change is simply the orderly addition of new rules to the grammar. Bloomfield confirms this implication by noting that the early subsystem of MM resembles the early subsystem of the ancestor language, reconstructed Proto-Algonquian. The rules added to describe diachronic change must be affixed to the end of the grammar, and the morphophonemes and the rules at the beginning of the morphophonemic system should remain unaffected over long periods of time. Thus the correct description of a language, based only on synchronic data, according to this view, should incidentally display morphophonemes and early rules identical with those of the parent language.

4. Comparison of MM and the Simplified System with Proto-Algonquian

The morphophonemes and early rules presented in MM "bear some resemblance" to the corresponding systems of Proto-Algonquian, and indicate that this early subsystem has remained fairly constant. If the synchronic simplifications of MM are correct improvements, then the early subsystem of the simplified description should show an improved resemblance to the corresponding Proto-Algonquian forms and rules. Consider the following comparisons of the forms and rules of Proto-Algonquian and the Menomini system, as presented in MM and also as simplified by synchronic descriptive techniques.

The short vowel and semivowel system of Proto-Algonquian analyzed by Bloomfield from four Algonquian languages has four vowels:

(15) i o

e a

This system in MM is much more complicated:

(16) e o, u w, y

ə æ a

A measure of the complication is that the transformation of (15) to (16) would require extremely intricate correspondence rules. But the simplifications of (16) based only on synchronic considerations reduce it to a new four-vowel system:

(17) e o

æ a

This system is essentially the same as the Proto-Algonquian system. System (16) can be transformed to system (17) by the addition of one simple rule:

(18) $\begin{bmatrix} -\text{ grave} \\ \alpha \text{ diffuse} \end{bmatrix} \rightarrow \begin{bmatrix} -\text{ diffuse} \\ \sim\alpha \text{ compact} \end{bmatrix}$

which demonstrates that the morphophonemes of the improved system are much more similar to the Proto-Algonquian forms than are those presented in MM.

Now observe the correspondences among some early rules. Proto-Algonquian has the rule:

(19) a) $t \rightarrow \check{c}$ in environment __ i
b) $\theta \rightarrow \check{s}$

The reflex of this rule in MM is

(20) a) $t \rightarrow \check{c}$ in environment $\_\_\begin{Bmatrix} e \\ \bar{e} \\ y \end{Bmatrix}$
b) $n \rightarrow \check{s}$

where (19a) and (20a) correspond, but (19b) and (20b) and the environment are dissimilar. A correspondence rule would have to change /θ/ to /n/ and /i/ to /e, ē, y/. In the simplified Menomini system the rule is interpreted as

(21) a) $t \rightarrow \check{c}$ in environment __ e
b) $\theta \rightarrow \check{s}$

If rule (18) is applied to the Proto-Algonquian system (19), it becomes identical with (21).

The morphophonemes and early rules of the simplified synchronic description of MM resemble the corresponding forms of Proto-Algonquian more closely than do those of the unsimplified system in MM. Thus the application of the synchronic methods resulted in a description of Menomini which is implied but not fully realized by Bloomfield.

T. G. Bever

References

1. L. Bloomfield, Menomini Morphophonemics, Problemes de la Phonologie Synchronique; in Travaux du cercle linguistique de Prague 8, 105-115 (1939).

2. L. Bloomfield, Eastern Ojibwa, edited by C. Hockett (University of Michigan, Ann Arbor, 1956), pp. 3-30.

3. L. Bloomfield, Algonquian, Linguistic Structures of Native America, Vol.6 (1946).

4. M. Halle, On the reality of generative grammars, Word 18, 54-72 (1962).

5. M. Halle, A descriptive convention for treating assimilation and dissimilation, Quarterly Progress Report No. 66, Research Laboratory of Electronics, M.I.T., July 15, 1962, pp. 295-296.

XXIII. COMMUNICATIONS BIOPHYSICS*

Prof. W. A. Rosenblith
Prof. M. A. B. Brazier†
Prof. M. Eden
Prof. M. H. Goldstein, Jr.
Prof. W. T. Peake
Prof. W. M. Siebert
Dr. J. S. Barlow‡
Dr. A. Cavaggioni**
W. A. Clark††
Dr. B. G. Farley††
Dr. G. L. Gerstein
Dr. François Grémy‡‡
Dr. E. Giberman***
Dr. R. D. Hall
Dr. N. Y-S. Kiang†††
Dr. T. T. Sandel††
Dr. Eda Berger Vidale
J. A. Aldrich
R. M. Brown
S. K. Burns
R. R. Capranica
Eleanor K. Chance
R. J. Clayton
A. H. Crist
P. R. Gray
J. L. Hall II
F. T. Hambrecht
J. G. Krishnayya
R. G. Mark
P. Mermelstein
C. E. Molnar‡‡‡
Donna A. Molnar
R. R. Pfeiffer†††
Cynthia M. Pyle
D. M. Snodderly, Jr.
G. F. Svihula
Aurice V. Weiss
T. F. Weiss
J. R. Welch
M. L. Wiederhold
G. R. Wilde

RESEARCH OBJECTIVES AND SUMMARY OF RESEARCH

Our basic objective is a better understanding of the communication senses. Hearing, in particular, will continue to receive our major attention.

A number of experimental studies are aimed at increasing our knowledge of the neural coding of sensory stimuli. These include: recording from single nerve cells located in the accessory olive of the cat under conditions of binaural stimulation; patterns of single-unit activity in the cochlear nucleus of cat in relation to the sound stimulus and anatomical location of the unit; unit responses from the lateral geniculate body of the rat to patterns of light and shadow in the visual field. Studies of "ongoing" activity also continue to be of interest. A study of conditioning of the bullfrog's heart rate by sound stimuli is aimed at determining which sounds get coded into this animal's auditory system and at his behavioral responses to natural and unnatural sounds.

In a number of electrophysiological studies we are attempting to correlate neuroelectric activity with physiological state. These include: behavioral studies of rats with gross electrodes recording from locations on and in their sensory pathways; studies of neuroelectric activity recorded from cats in different stages of sleep and wakefulness; studies in unanesthetized cats with brain stem sections of cortical responses to shocks delivered to the sensory pathways; and studies of the olivocochlear bundle.

The development of mathematical models closely related to neurophysiological mechanisms is a major effort of the group. In this category are the following modeling studies: coding of auditory signals as patterns of neural impulses in the eighth nerve; mechanisms of some features of binaural localization; some limitations on auditory discrimination

---

*This work was supported in part by the National Science Foundation (Grant G-16526); and in part by the National Institutes of Health (Grant MH-04737-02).

†Visiting Professor in Communication Sciences from the Brain Research Institute, University of California at Los Angeles.

‡Research Associate in Communication Sciences from the Neurophysiological Laboratory of the Neurology Service of the Massachusetts General Hospital.

**From the Istituto di Fisiologia, Università di Pisa.

††Staff Member, Lincoln Laboratory, M.I.T.

‡‡(Maître de Conferences, Laboratoire de Physique) Visitor from Faculté de Medecine (Paris).

***From the Department of Physics, Weizmann Institute of Science, Israel.

†††Also at Massachusetts Eye and Ear Infirmary.

‡‡‡Staff Associate, Lincoln Laboratory, M.I.T.

implied by the nature of peripheral coding; and "ongoing" activity of single units.

Psychophysical studies form an important adjunct to the physiological and modeling work. These include studies of judgments of various binaural patterns, and of discriminability of noiselike signals.

Considerable instrumentation is involved in our experimental work, in presentation of stimuli, recording and processing of neuroelectrical signals, and physiological monitoring of the animals. Design of instruments ranging from telemetering systems to mixer-amplifiers, from real-time correlators to heart-rate meters, from digital devices for generating precisely controlled sounds to sacks for restraining cats are an important and indispensible part of our effort.

Close cooperation with the Eaton-Peabody Laboratory of the Massachusetts Eye and Ear Infirmary and with various groups at Lincoln Laboratory, M.I.T., continues to play a crucial role in our work. In particular, we anticipate a number of important applications for the LINC, a Laboratory Instrument Computer of considerable generality and utility, developed at Lincoln Laboratory under the leadership of Wesley A. Clark and with the collaboration of several Lincoln Laboratory staff members, the engineering assistance of Lt. Charles E. Molnar of Air Force Cambridge Research Laboratories, and the aid of members of the Research Laboratory of Electronics.

M. H. Goldstein, Jr., W. M. Siebert, W. A. Rosenblith

References

1. C. D. Geisler and W. A. Rosenblith, Average responses to clicks recorded from the human scalp, J. Acoust. Soc. Am. 34, 125-127 (1962).

2. M. H. Goldstein, Jr., L. S. Frishkopf, and C. D. Geisler, Representation of sounds by responses of single units in the eighth nerve of the bullfrog, J. Acoust. Soc. Am. 34, 734 (1962).

3. N. Y-S. Kiang, M. H. Goldstein, Jr., and W. T. Peake, Temporal coding of neural responses to acoustic stimuli, Trans. IRE, Vol. IT-8, pp. 113-119, 1962.

4. N. Y-S. Kiang, T. Watanabe, Eleanor C. Thomas, and Louise F. Clark, Stimulus coding in the auditory nervous system and its implications for otology, Trans. Am. Otol. Soc. 50, 264-283 (1962).

5. W. T. Peake, M. H. Goldstein, Jr., and N. Y-S. Kiang, Responses of the auditory nerve to repetitive acoustic stimuli, J. Acoust. Soc. Am. 34, 562-570 (1962).

6. W. T. Peake, N. Y-S. Kiang, and M. H. Goldstein, Jr., Rate function for auditory nerve responses to bursts of noise: Effect of changes in stimulus parameters, J. Acoust. Soc. Am. 34, 571-575 (1962).

7. M. A. B. Brazier, The analysis of brain waves, Sci. American 206, 142-153 (1962).

8. M. A. B. Brazier, The problem of periodicity in the electroencephalogram: Studies in the cat, EEG Clin. Neurophysiol. 14, 943-949 (1962).

9. J. S. Barlow, Simulation of normal and abnormal electroencephalograms, Quarterly Progress Report No. 65, Research Laboratory of Electronics, M.I.T., April 15, 1962, pp. 221-228.

10. S. K. Burns, The electroencephalogram of fraternal twins, S. B. Thesis, Department of Electrical Engineering, M.I.T., June 1962.

11. B. G. Farley, Some results of computer simulation of neuron-like nets, Fed. Proc. 21, 92-96 (1962).

12. B. G. Farley, Problems in the study of the nervous system, Proceedings of the 1962 Spring Joint Computer Conference (National Press, Palo Alto, Calif., 1962), pp. 147-152.

13. B. G. Farley, Some similarities between the behavior of a neural network model and the electrophysiological experiments, Self-Organizing Systems, edited by M. C. Yovits, G. T. Jacobi, and G. D. Goldstein (Spartan Books, Washington, D.C., 1962), pp. 535-550.

14. R. J. Clayton, Cortical activity correlated with behavior in the rat, S.B. Thesis, Department of Electrical Engineering, M.I.T., June 1962.

15. A. K. Ream, EEG correlates of behavioral states in the rat, S.B. Thesis, Department of Electrical Engineering, M.I.T., June 1962.

16. R. W. Rodieck, N. Y-S. Kiang, and G. L. Gerstein, Some quantitative methods for the study of spontaneous activity of single neurons, Biophys. J. 2, 351-368 (1962).

17. G. L. Gerstein, Mathematical models for the all-or-none activity of some neurons, Trans. IRE, Vol. IT-8, pp. 137-143, 1962.

18. J. S. Barlow, A phase-comparator model for the diurnal rhythm of emergence of Drosophila, Ann. N.Y. Acad. Sci. 98, Art. 4, pp. 788-805, 1962.

19. M. Eden, Pattern recognition and handwriting, Trans. IRE, Vol. IT-8, pp. 160-166, 1962.

20. W. A. Rosenblith (Ed.), Processing Neuroelectric Data (The M.I.T. Press, Cambridge, Mass., 2d printing, 1962); see pp. ix-xxvii.

21. W. A. Rosenblith, Contribution to discussion on "What Computers Should Be Doing" in Management and the Computer of the Future, edited by M. Greenberger (The M.I.T. Press, Cambridge, Mass., and John Wiley and Sons, Inc., New York, 1962), pp. 311-315; 320-321.

22. W. A. Rosenblith, Computers and Brains. To be published in the volume based on the Brown University Lecture Series on "Applications of Digital Computers" (1961-1962).

23. W. A. Rosenblith, Introduction to Symposium on Mathematical Models of Biophysical Mechanisms, Biophys. J. 2, 99-100 (1962). (Part 2, No. 2, Proc. Symposia, International Biophysics Congress, Stockholm, July 31-August 4, 1961).

A. BINAURAL INTERACTION IN SINGLE UNITS OF THE ACCESSORY SUPERIOR OLIVARY NUCLEUS IN CAT

There has been conjecture as to the physiological mechanisms associated with the localization of sounds in space, and a number of models have been proposed.[1-3] However, there were meager electrophysiological data on the behavior of single units until the work of Galambos, Schwartzkopff, and Rupert,[4] and even that study was far from exhaustive. Psychophysical experiments with humans indicate that the difference in time of arrival of the stimuli at the two ears, the difference in intensity of the stimuli at the two ears, and the average intensity (average of intensity at left and right ears expressed in decibels) are all influential in determining the apparent position of a sound source.[5-7] Also, these experiments indicate that human observers are capable of detecting extremely small interaural time differences (of a few microseconds),[8] and extremely small interaural intensity differences (of a few tenths of a decibel).[9]

In an attempt to obtain electrophysiological data that are pertinent to a better understanding of the neurophysiology of binaural localization, we are investigating the electrical activity of single nerve cells in the accessory nucleus of the superior olive in cats under conditions of binaural stimulation. Anatomical and electrophysiological considerations indicate that this is a reasonable place in which to look. As far as is known, the accessory nucleus is the most peripheral station in the classical ascending auditory pathway to receive inputs from both ears.[10] Previous electrophysiological studies have demonstrated the existence of neurons in the accessory nucleus which are extremely sensitive to small changes in interaural time difference.[4] We have recorded from several hundred cells in the accessory nucleus, giving major attention to the question of binaural interaction. A summary of our present results is given here. A model is suggested which is in agreement with some aspects of binaural localization of sounds in both cats and humans.

1. Methods

We have used as stimuli clicks presented through earphones. Clicks have the desirable feature of being punctate in time. Earphones provide independent control of interaural time and intensity differences, which is not possible with free-field stimulation. Clicks are produced by applying 100-μsec rectangular voltage pulses to PDR-10 earphones.

We have tried several kinds of microelectrodes and have settled on an etched stainless-steel electrode. The etching and insulating procedure is essentially the same as that described by Brown and Tasaki,[11] but we also plate the tip of the electrode, first with copper and then with platinum black.

An anesthetized (Dial) cat is in a soundproof, electrically shielded chamber. We position the electrode on the ventral surface of the medulla, using the rack and pinion controls of a stereotaxic instrument. The electrode is advanced by means of a hydraulic micromanipulation system from outside the soundproof chamber. As the electrode is advanced, we present the cat with a stimulus consisting of clicks at approximately -50 db relative to 4 volts across the earphones (approximately 50 db relative to visual detection level of the slow potential observed in the accessory nucleus) with an interaural time interval of 25 msec and an over-all repetition period of approximately 300 msec. At the same time, we monitor on an oscilloscope the electrical activity picked up by the electrode.

The position of the electrode tip relative to the accessory nucleus is determined by one or more of the following methods: (a) We measure the depth of penetration of the electrode from the surface. (b) We measure the position of the electrode relative to the depth at which the slow-wave potential reverses polarity (see below). (c) In some cases we have marked the electrode position by passing a current through the electrode, with subsequent histological control. As far as we have been able to determine, the nerve cells that exhibit binaural interaction are located in or near the accessory nucleus.

We have taken as a measure of unit activity the percentage of stimulus presentations to which the unit responds at least once. We determine this by presenting a given number of stimuli (usually 50) and counting the number of stimulus presentations to which the unit responds. In most of the cases this has been on-line by means of a level discriminator and electronic counter. In a few cases we have recorded the responses on magnetic tape.

2. Results

As the electrode is advanced, we see two distinct kinds of electrical activity. One is what Galambos and his co-workers have termed the "slow-wave" potential[4]; the other is spike responses from individual nerve cells. The slow-wave potential follows the pattern described by Galambos, and others. Ventromedial to the accessory nucleus, stimulation of the contralateral ear evokes a negative-going slow wave, and stimulation of the ipsilateral ear evokes a positive-going slow wave. Dorsolateral to the accessory nucleus, the polarities are reversed. While this slow wave may, in some sense, represent the excitation for cells in the accessory nucleus, we have not attempted to study in detail the interaction between slow wave and unit activity. We have been interested in the slow wave only insofar as it provides an indication of the position of the electrode relative to the accessory nucleus.

We have observed firing patterns of cells showing many sorts of binaural interaction. We shall mention briefly two kinds of interaction. Some cells show summation, in that

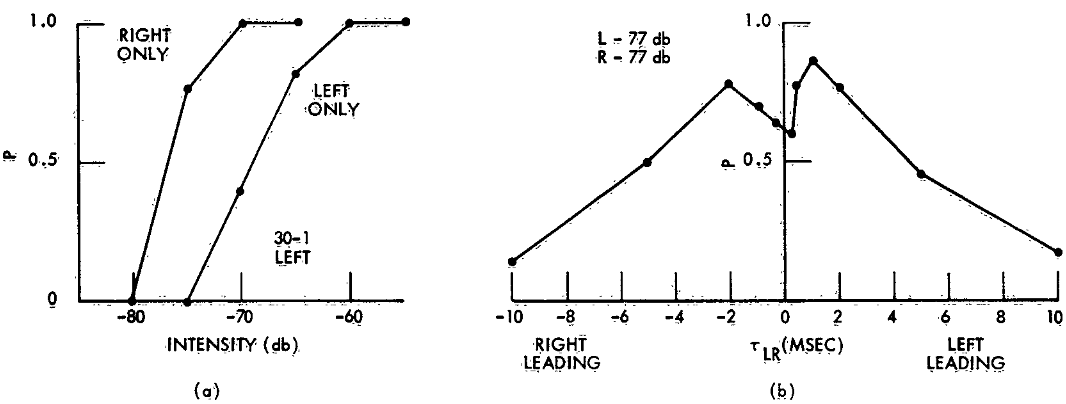

Fig. XXIII-1. Cell showing summation of stimuli to two ears. (a) Monaural intensity series. (b) Effect of interaural time difference. P is relative frequency of firing measured over 50 stimulus presentations at a rate of ~3 per second; τ_{LR} is time difference between clicks in left and right ears.

if the stimuli are presented simultaneously to the two ears they respond more than they respond to stimulation of either ear alone. This summation may extend over several milliseconds, as shown in Fig. XXIII-1, or over a few hundred microseconds, as in Fig. XXIII-2. This property has been observed in approximately 20 cells.

Other cells have the cyclic behavior shown in Fig. XXIII-3. As the interval between the clicks to the two ears is varied, the unit shows several successive peaks of excitability. We have seen three such cells, all with a time between adjacent peaks of approximately 1 msec.

The group of cells in which we are most interested shows the properties summarized in Fig. XXIII-4. These cells respond to monaural stimulation of the contralateral ear,

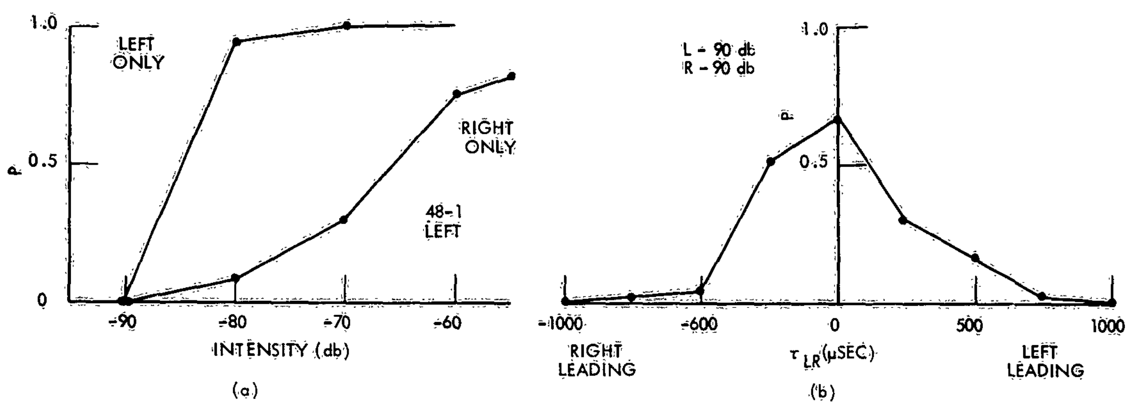

Fig. XXIII-2. Cell showing summation of stimuli to two ears. (a) Monaural intensity series. (b) Effect of interaural time difference.

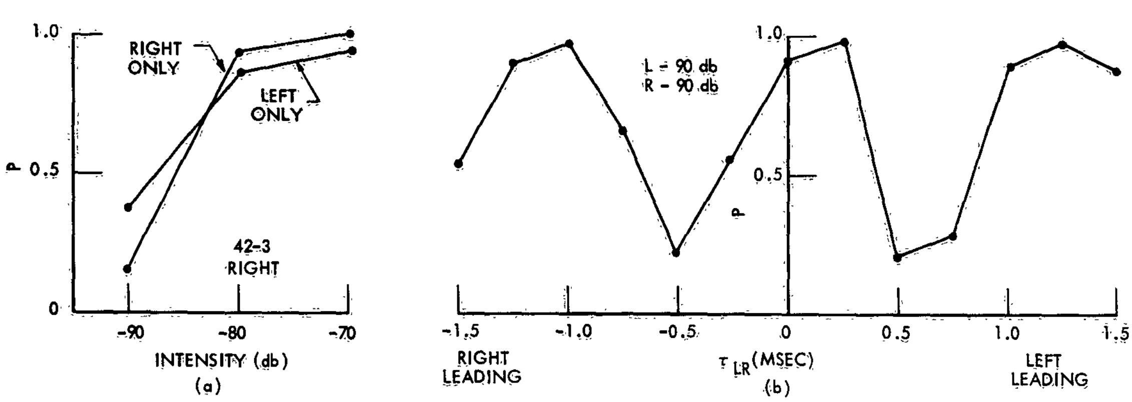

Fig. XXIII-3. Cell showing cyclic interaction of stimuli to two ears. (a) Monaural intensity series. (b) Effect of interaural time difference.

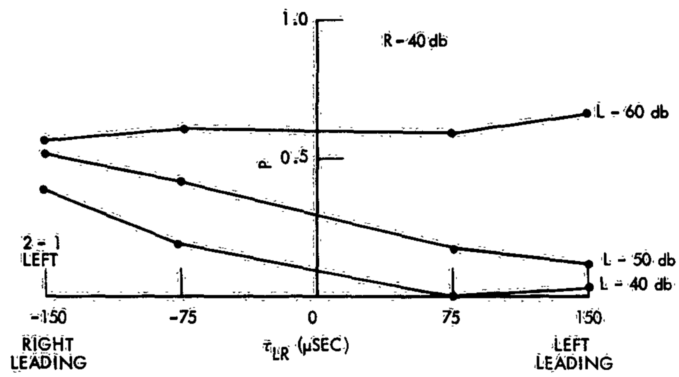

Fig. XXIII-4. Effect of interaural time difference, interaural intensity difference. Cell on left side.

but not to monaural stimulation of the ipsilateral ear. For all of these cells, the percentage of stimulus presentations to which the unit responds can be decreased either by making the stimulus to the ipsilateral ear more intense while holding interaural time difference constant or by making the stimulus to the ipsilateral ear arrive earlier while holding interaural intensity difference constant.

There is a striking parallel between the properties of cells of the type shown in Fig. XXIII-4 and results of psychophysical experimentation in humans. The responsiveness of these cells (we have recorded from approximately 50 of them) is a function of interaural time difference, interaural intensity difference, and average intensity. These parameters are also involved in determining the apparent location of a sound source with humans. This parallel of physiological and psychophysical data has led us to suggest the following model for the process of binaural localization: Binaural stimuli excite cells in the left and right accessory nuclei. If the stimulus at the left ear is more intense or arrives earlier than that at the right, more cells will be excited in the right accessory nucleus, and vice versa. Because of the sensitivity of these cells to both interaural time and intensity difference, time and intensity differences can be made to offset each other at the level of the individual cell. The psychophysical judgment of sidedness comes about as a result of any imbalance of the number of cells excited at the left and right accessory nuclei. This schema is similar to one proposed recently by van Bergeijk,[3] and, as pointed out by van Bergeijk, it has a great deal in common with a model proposed in 1930 by von Békésy.[1] A simplified diagrammatic representation of our model is shown in Fig. XXIII-5.

In our model we assume that each cell that we observe is representative of a population of cells, and that the system is symmetrical; that is, there are similar populations of cells in the left and right accessory nuclei. Although we are restricted to

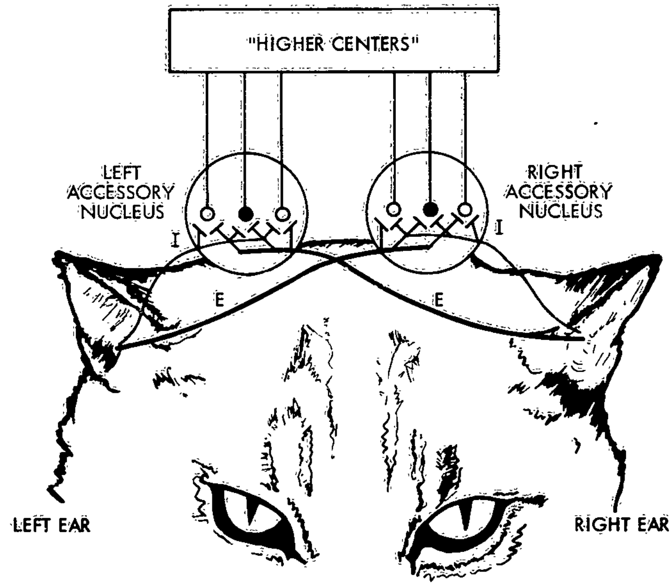

Fig. XXIII-5. Cells in both left and right accessory nuclei are innervated by excitatory inputs from the contralateral ear and inhibitory inputs from the ipsilateral ear. Ascending fibers from both accessory nuclei go to hypothetical "higher centers." The psychophysical judgment of sidedness is related to the relative number of cells responding at the two sides. The two solid cells are intended to indicate that the system is symmetrical, that is, in the model each cell on one side has its counterpart on the other.

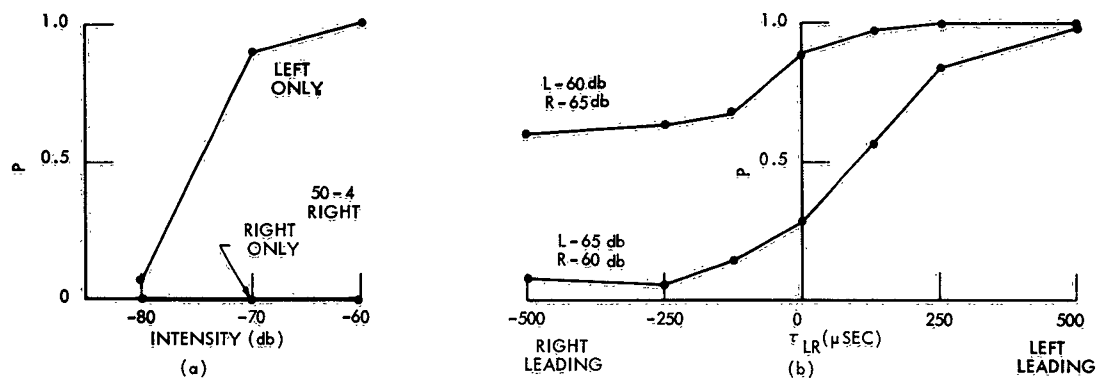

Fig. XXIII-6. (a) Monaural intensity series. (b) Effect of interaural time difference and interaural intensity difference. Cell on right side.

observing cells on only one side at a time, we can infer the behavior of corresponding cells on the opposite side by this assumption. A typical example is shown in Fig. XXIII-6. This cell was situated on the right-hand side of the cat. We observed the activity of the cell over a range of interaural time differences from plus to minus 500 μsec, where positive numbers indicate that the stimulus to the left ear is leading, and negative numbers indicate that the stimulus to the right ear is leading. Two intensity conditions are illustrated: left −60 db, right −65 db; and left −65 db, right −60 db. In order to infer the behavior of a hypothetical symmetrical cell on the left side, we interchange "left" and "right," both for time difference and for intensity difference, for one of these two curves. The resulting plot for the condition left −60 db, right −65 db is shown in Fig. XXIII-7.

For purposes of the model, we are interested in the relative number of cells firing at the two sides. We have taken as a measure of this $\mathcal{R}_L = P_L/(P_L+P_R)$, where P_R is the probability that the cell on the right will fire to a given stimulus presentation, and P_L is the probability that the hypothetical cell on the left will fire to a given stimulus presentation. This measure is bounded between 0 (corresponding to activity on the right and no activity on the left) and 1 (corresponding to activity on the left and no activity on the right), and is symmetrical about 0.5. That is, since $\mathcal{R}_L = 1 - \mathcal{R}_R$, where $\mathcal{R}_R = P_R/(P_L+P_R)$, the curve of $\mathcal{R}_R$ is the curve of $\mathcal{R}_L$ reflected about the 0.5 level.

If we had a homogeneous population of cells, we would be able to generalize directly from the behavior of a single cell to the total number of cells responding. Although we do not have a homogeneous population, it is still possible to set bounds on over-all activity from our data. As an example, consider the situation in which the stimulus to the left ear is more intense than the stimulus to the right ear, and the two stimuli are

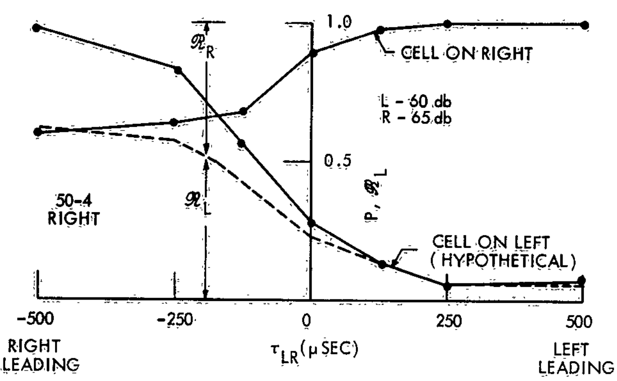

Fig. XXIII-7. Same cell as in Fig. XXIII-6, with "left" and "right" interchanged for original condition (left, −65 db; right, −60 db). Dashed line shows $P_L/(P_L+P_R) = \mathcal{R}_L$.

presented simultaneously. While $\mathcal{R}_L$ is not necessarily the same for any two cells, $\mathcal{R}_L$ is less than 0.5 for all cells that we have observed. Therefore we are justified in saying that, on the average, more cells respond to this particular stimulus configuration in the right population than in the left population.

Figure XXIII-8 summarizes the behavior of a typical cell. In this plot, $\mathcal{R}_L$ is shown on the ordinate and interaural time difference is shown on the abscissa. Interaural intensity difference is held constant at 5 db, and average intensity is the parameter. Keeping in mind that (a) the data are from cats and (b) the model is highly simplified, we can compare predictions of the model and psychophysical results from humans. The effects of interaural time and interaural intensity difference are in qualitative agreement. With zero interaural time difference and the stimulus to the left ear more intense, we have $0 \leq \mathcal{R}_L < 0.5$, corresponding to "image to the left." If interaural intensity difference and average intensity are held constant and the stimulus to the left ear is made to arrive earlier, $\mathcal{R}_L$ decreases, corresponding to movement of the image to the left.

Interaural time difference can offset the effect of interaural intensity difference for individual cells in terms of the model, just as it can in human centering experiments.[5, 6] At point A in Fig. XXIII-8, for example, the stimulus to the left ear is 5 db more intense but lags the stimulus to the right ear by 120 μsec, and $\mathcal{R}_L = 0.5$, corresponding to equal firing probabilities at the two sides. In this sense an interaural intensity difference can be said to be "equivalent" to an interaural time difference, and we can define a time-intensity trading ratio in microseconds per decibel. The time-intensity trading ratio for point A would be 120 μsec per 5 db, or 24 μsec per db.

In Fig. XXIII-9, this time-intensity trading ratio is plotted as a function of average intensity for 12 cells that we have observed. The dashed lines indicate the range of time-intensity trading ratios obtained from human subjects presented with clicks with

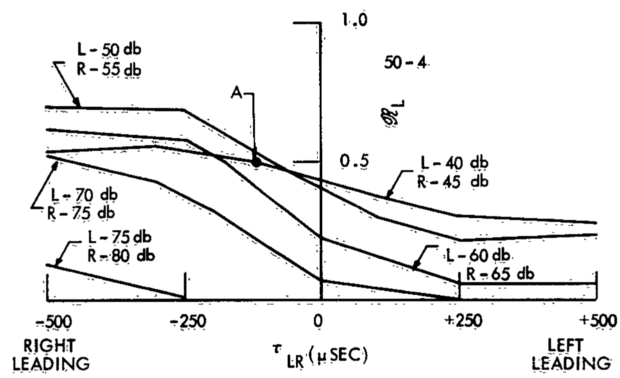

Fig. XXIII-8. Effect of interaural time difference and average intensity on $\mathcal{R}_L$. Interaural intensity difference, 5 db.

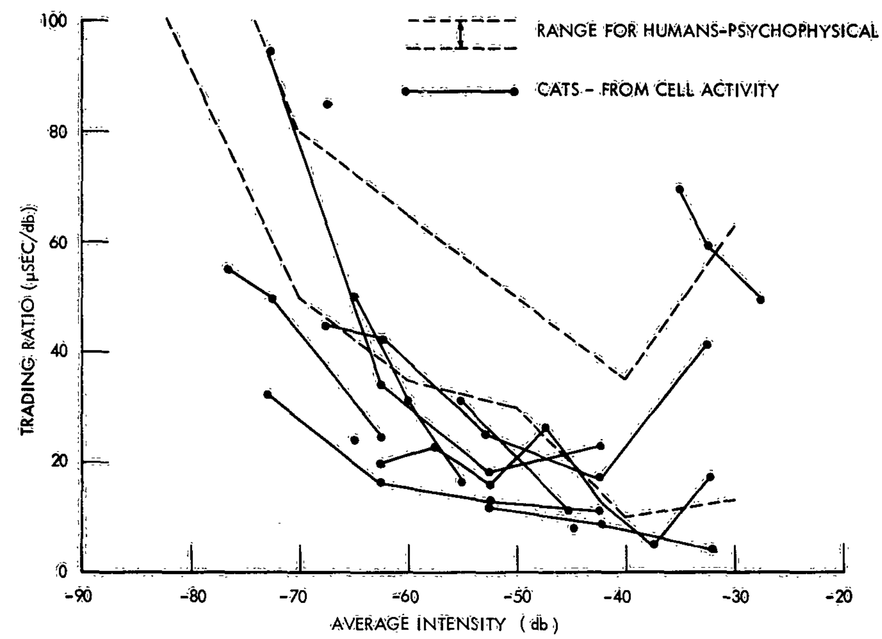

Fig. XXIII-9. Time-intensity trading ratio for human beings compared with that computed on the basis of the model. The dashed lines indicate the range of time-intensity trading ratios for humans (see E. E. David et al.[6]). Solid points represent time-intensity trading ratios computed from single units on the basis of the model. Points from the same cell at different intensities are joined by a solid line. Not shown on this graph are two points computed from a single low-threshold cell: -99.5 db, 430 μsec/db; -101.5 db, 330 μsec/db.

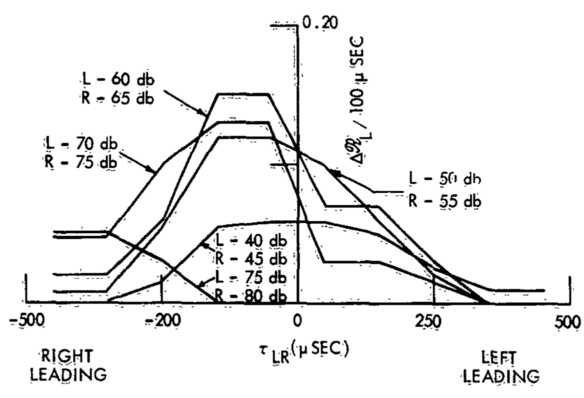

Fig. XXIII-10. Slope of curves in Fig. XXIII-8. Ordinate is the change in $\mathcal{R}_L$ resulting from a 100-μsec change in interaural time difference.

a given interaural intensity difference and asked to obtain a centered image by adjusting the interaural time difference (see David et al.,[6] Fig. 5, impulse). The two sets of results are in close agreement, considering that they refer to two different species, etc., and they both show a trend downward with increasing intensity.

The range of interaural time differences over which a change in interaural time difference produces a change in unit activity is consistent with reasonable assumptions about the cat's localization behavior. The sensitivity of a unit to changes in interaural time difference as measured by the slope of the curves in Fig. XXIII-8 is greatest for values of interaural time difference near zero, and it shows a sharp decrease for values of interaural time difference greater than 200-300 μsec. The slope of the curves in Fig. XXIII-8 is plotted as a function of interaural time difference in Fig. XXIII-10. The slopes are not symmetrical about zero interaural time difference because of the presence of an interaural intensity difference.

These curves can be related to a psychophysical parameter known as the Hornbostel-Wertheimer constant. This parameter is defined as the interaural time difference beyond which change in interaural time difference produces little change in position of the sound image. In humans this is approximately 500 μsec.[1] Since the distance between the ears is smaller for cats than it is for humans, and therefore the maximum interaural time difference that could occur in free-field stimulation is smaller, it is perhaps not unreasonable to assume that the Hornbostel-Wertheimer constant for cats, if such a thing could be measured, would also be smaller.

A particularly interesting feature of the model is that the minimum interaural time difference that can be discriminated in terms of the model compares favorably with the minimum interaural time difference that the cat is capable of discriminating behaviorally. We can obtain an estimate of the precision afforded by the model by making the following assumptions: (a) There is in each accessory nucleus a homogeneous population of n cells. (b) Each cell on the left fires to a given stimulus presentation with probability P_L and does not fire with probability $Q_L = 1 - P_L$. Similarly, each cell on the right fires with probability P_R. (c) Firings of individual cells are mutually independent.

We define random variables X_L and X_R as the number of cells on the left and right sides, respectively, which respond to a given stimulus presentation. From our assumptions, the means and variances of these random variables are

$$E(X_L) = m_L = nP_L, \quad \sigma^2(X_L) = \sigma_L^2 = nP_LQ_L \tag{1}$$

$$E(X_R) = m_R = nP_R, \quad \sigma^2(X_R) = \sigma_R^2 = nP_RQ_R. \tag{2}$$

We define a third random variable, X_D, as the difference between X_L and X_R.

$$X_D = X_L - X_R. \tag{3}$$

It follows that

$$E(X_D) = m_D = m_L - m_R = n(P_L - P_R), \tag{4}$$

and from the assumption of independence that

$$\sigma^2(X_D) = \sigma_D^2 = \sigma_L^2 + \sigma_R^2 = n(P_L Q_L + P_R Q_R). \tag{5}$$

We now ask the question, For a given number of cells n, what is the smallest difference ΔP between P_L and P_R which will result in X_D being greater than zero with probability at least 0.75? (If the higher centers in our model made a "forced-choice" decision of right or left of center based simply on whether X_L was greater than or less than X_R, the choice of 0.75 probability would mean that three out of four stimulus presentations would result in the judgment "right of center." The choice of 0.75 is arbitrary. It is chosen as a convenient level midway between 0.5, corresponding to pure chance, and the asymptotic value 1.0. While it is chosen on much the same basis as the 0.75 level is chosen in psychophysical experiments, it should not be construed as corresponding to a behavioral just-noticeable difference.) If n is large, we can use the normal approximation to the binomial, so that X_D can be approximated by a normal distribution, and from a tabulation of the normal distribution we find that

$$P(X_D > 0) > 0.75 \text{ if } m_D > 0.7\sigma_D. \tag{6}$$

Setting $m_D = 0.7\sigma_D$ and substituting from Eqs. 4 and 5, we have

$$n(P_L - P_R) = 0.7 \sqrt{n(P_L Q_L + P_R Q_R)} \tag{7}$$

$$P_L - P_R = \Delta P = 0.7 \sqrt{(P_L Q_L + P_R Q_R)/n}. \tag{8}$$

Since we are interested in small differences between P_L and P_R, we can set $P_L Q_L + P_R Q_R = 2(P_L Q_L)$. Finally, we have

$$\Delta P = \sqrt{(P_L Q_L)/n}. \tag{9}$$

Let us, for the moment, set n = 5000. This estimate is based on the density of cells in the accessory nucleus and the size of the accessory nucleus[3] and on the assumption that one-fourth to one-half of the cells in the accessory nucleus are of the type that can be included in the model. It is probably conservative. Referring to Fig. XXIII-7, we see for this particular cell and this particular stimulus configuration that $P_L = 0.7$, $Q_L = 0.3$, when P_L and P_R are equal. Substituting these numbers in Eq. 9, we have

$\Delta P = \sqrt{(0.7 \times 0.3)/5000} = 0.006.$

In order to determine the change in interaural time difference to which this corresponds, we observe from Fig. XXIII-7 that a change in interaural time difference of 50 μsec results in a difference between P_L and P_R of ~0.12. Therefore $\Delta P = 0.006$ corresponds to a change in interaural time difference of $0.006/0.12 \times 50$ μsec, or 2.5 μsec. This value is typical of the cells that we have observed and is of the same order of magnitude as the minimum change in interaural time difference that the cat is capable of discriminating behaviorally.[12]

While our assumptions of homogeneity and independence are gross simplifications, we have an indication that the model potentially may be capable of discriminations of the right order of magnitude.

J. L. Hall II, Cynthia M. Pyle

References

1. G. von Békésy, Experiments in Hearing, translated and edited by E.G. Wever (McGraw-Hill Book Company, Inc., New York, 1960), Chapter 8.

2. L. A. Jeffress, A place theory of sound localization, J. Comp. Physiol. Psychol. 41, 35-39 (1948).

3. W. A. van Bergeijk, Variations on a theme of Békésy: A model of binaural interaction, J. Acoust. Soc. Am. 34, 1431-1437 (1962).

4. R. Galambos, J. Schwartzkopff, and A. Rupert, Microelectrode study of superior olivary nuclei, Am. J. Physiol. 197, 527-536 (1959).

5. B. H. Deatherage and I. J. Hirsh, Auditory localization of clicks, J. Acoust. Soc. Am. 31, 486-492 (1959).

6. E. E. David, Jr., N. Guttman, and W. A. van Bergeijk, Binaural interaction of high-frequency complex stimuli, J. Acoust. Soc. Am. 31, 774-782 (1959).

7. G. Moushegian and L. A. Jeffress, Role of interaural time and intensity differences in the lateralization of low-frequency tones, J. Acoust. Soc. Am. 31, 1441-1445 (1959).

8. R. G. Klumpp and H. R. Eady, Some measurements of interaural time difference thresholds, J. Acoust. Soc. Am. 28, 859-860 (1956).

9. A. W. Mills, Lateralization of high-frequency tones, J. Acoust. Soc. Am. 32, 132-134 (1960).

10. W. A. Stotler, An experimental study of the cells and connections of the superior olivary complex of the cat, J. Comp. Neurol. 28, 401-431 (1953).

11. K. T. Brown and K. Tasaki, Localization of electrical activity in the cat retina by an electrode marking method, J. Physiol. 158, 281-295 (1961).

12. D. Katz, Animals and Men: Studies in Comparative Psychology (Longmans, Green, New York, 1937).

B. POSTAURICULAR ELECTRIC RESPONSE TO ACOUSTIC STIMULI IN HUMANS

Many investigators have reported that acoustic stimuli alter the electric activity recorded from the scalp of humans. Several of these reports describe evoked responses

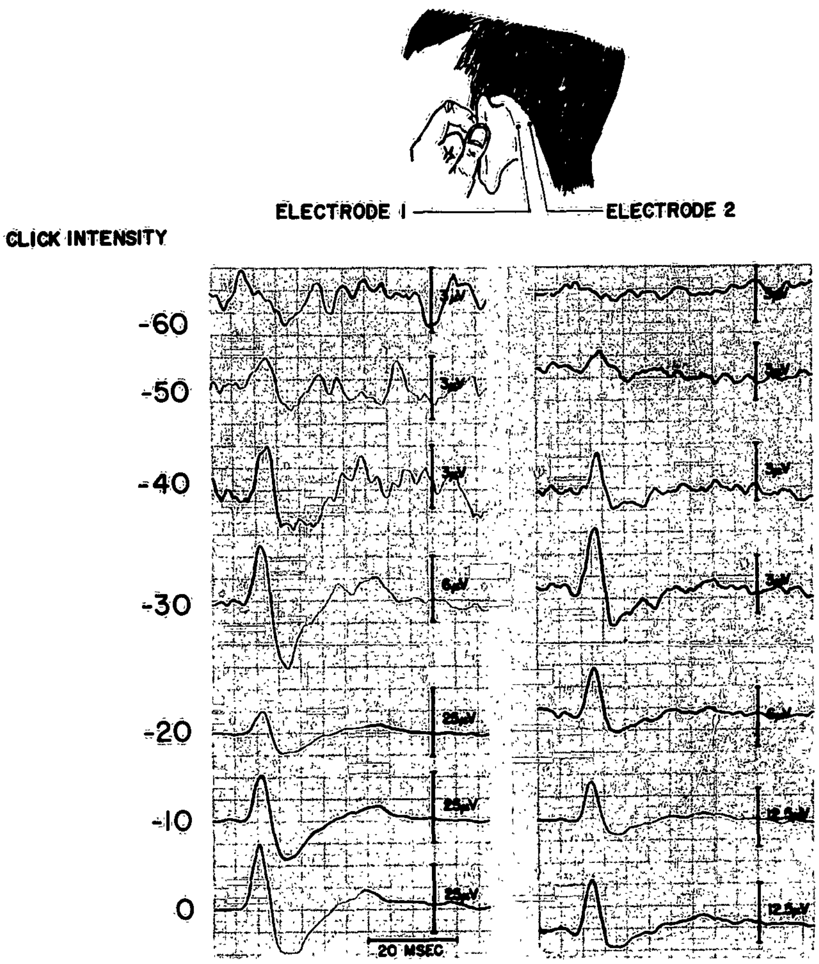

Fig. XXIII-11. Averaged responses to clicks for two electrode locations behind the left ear. The electrodes were stainless-steel needles. The reference electrode was clipped to a saline-moistened cotton pad on the right earlobe. Negative polarity for the active electrodes is plotted upward. Responses are shown for 7 stimulus intensities. Clicks were produced by applying a 10-μsec rectangular pulse to the terminals of an Altec 1-755A loud-speaker that was located ~4 feet in front of the subject seated in a soundproof room. Clicks were presented at a 10/sec rate; reference level (0 db) = 13 volts into the speaker. With this stimulus arrangement the psychophysical threshold was approximately -65 db for this subject. (The beginning of each trace in this and subsequent figures marks the instant at which a monitoring microphone placed near the ear detects the arrival of the click.) Number of responses averaged for each trace, N = 1000. Recording session 1 on this subject (N. Y-S. K., 1/12/62).

with latencies of less than 70 msec.[1-6] We have recently found a short latency response localized behind the external ear (auricle) which does not appear to have been previously reported. Some of the characteristics of this response are sufficiently unusual to warrant a brief report.

The postauricular response has been recorded both from needle electrodes thrust into the skin posterior to the attachment of the ear (Fig. XXIII-11) and from wick electrodes curled over the attachment of the ear. Since the responses are not visually detectable in single traces except at high stimulus intensities, it was necessary to compute[7] averaged responses on the ARC.

Figure XXIII-11 shows responses recorded from two electrodes located behind the ear. The distance between the electrodes was 1.5 cm. The responses from electrode 1 show a peak approximately 11 msec after the acoustic stimulus arrives at the ear. This

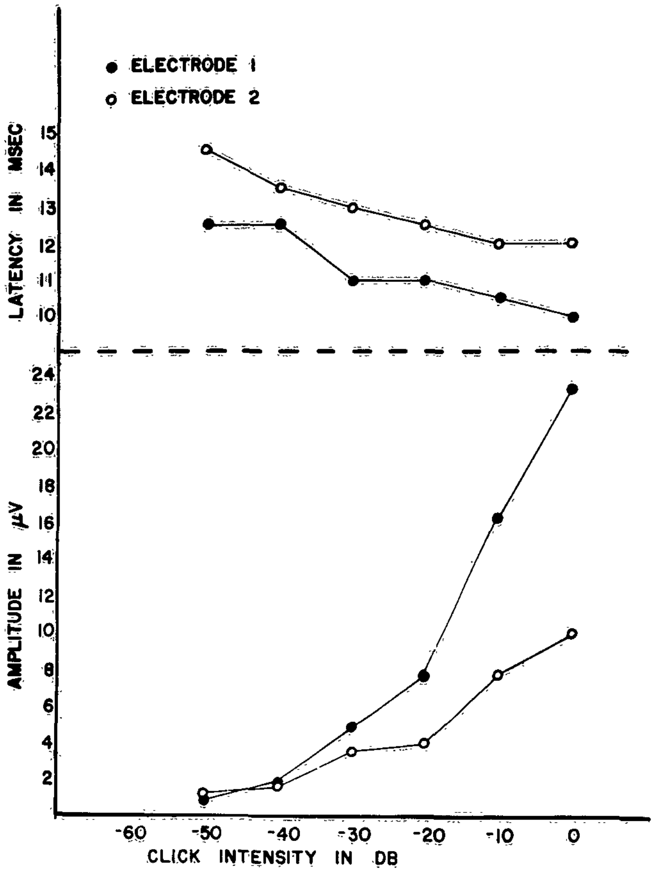

Fig. XXIII-12. Latencies and amplitudes of the negative peaks in the traces of Fig. XXIII-11 as functions of click intensity. Latencies are measured from the beginning of each trace; amplitudes are measured from base line to peak.

negative peak is followed approximately 7 msec later by a positive peak that is less prominent in the recordings from electrode 2. In general, the waveform of the responses can vary considerably with location of the electrode, although the most prominent deflections occur with latencies in the 10-20 msec range. For a specific location on any one subject, the response waveform seems to be quite repeatable except as noted below.

Figure XXIII-12 shows that the latency of the negative peak decreases and its amplitude increases with increasing click intensity. There is a relatively constant difference of approximately 2 msec between the latencies of the responses from the two electrodes. Note also that the amplitude of responses is smaller for electrode 2. This is consistent with our observation that the responses are largest in the region near the attachment of the external ear.

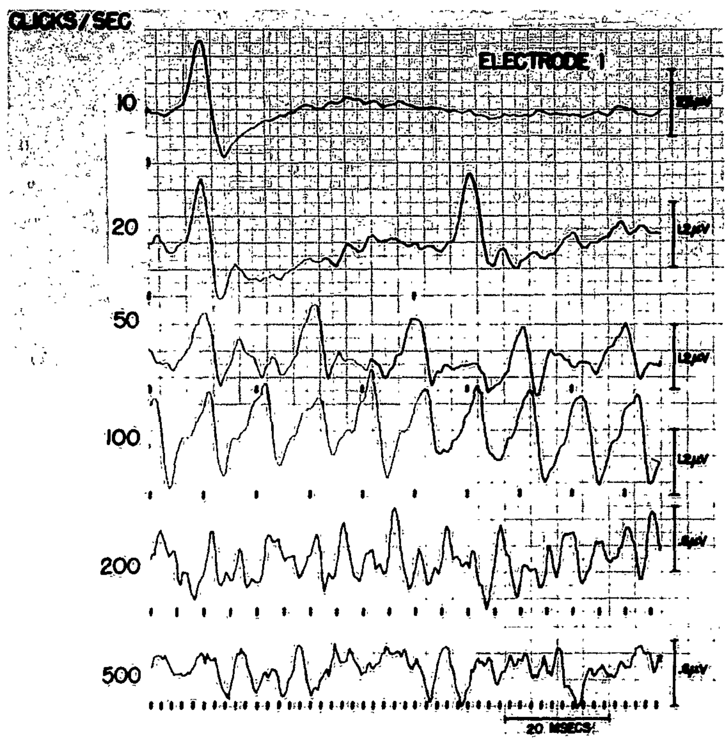

Fig. XXIII-13. Averaged postauricular responses for several click rates. The marks under each trace denote the times of arrival of the clicks at the ear. The electrode was placed in the same location as electrode 1 of Fig. XXIII-11. The reference electrode was on the right earlobe. Clicks were produced by 10-μsec rectangular pulses delivered to the loud-speaker terminals. Click intensity, -10 db re 7 volts into loud-speaker; N = 1000. Recording session 2 on this subject (N. Y-S. K., 1/24/62).

Figure XXIII-13 shows the postauricular response for six different click rates. The responses at 200 clicks/sec and 500 clicks/sec are complicated by the overlap of responses to successive clicks. However, it is clear that some responses are synchronized with clicks, even at the 200/sec rate.

These results might seem to suggest that the relationship of these responses to the stimulus parameters can be easily described. However, this appears to be so only for the first few recording sessions. One of the exasperating aspects of working with this

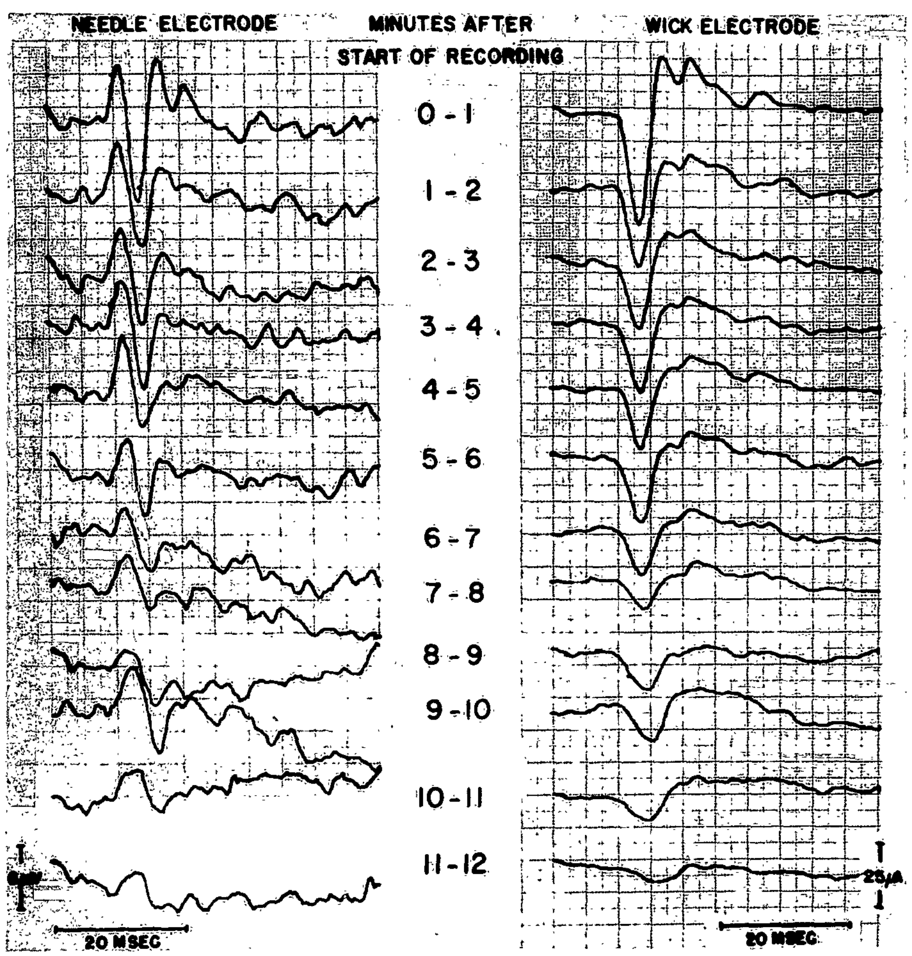

Fig. XXIII-14. Averaged postauricular responses as a function of time after the start of stimulation. Averages of responses recorded simultaneously from both a needle electrode and a wick electrode. Reference electrode on nose. Clicks were produced by 100-µsec rectangular pulses. Click intensity, −20 db re 17 volts; repetition rate, 10/sec; N = 500. Recording session 4 on this subject (N. Y-S. K., 3/20/62).

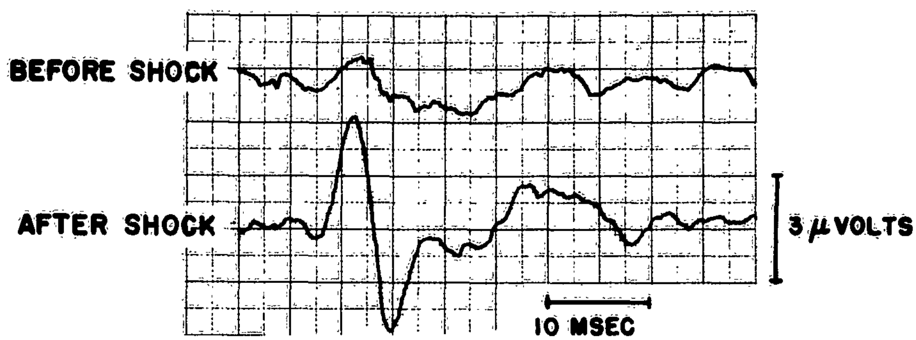

Fig. XXIII-15. Averaged postauricular responses from a subject before and after the delivery of electric shock to the bare feet. The responses of the subject to steady clicks had decreased steadily with time from the start of the session. After the responses had declined to the level shown in the trace marked "before shock," the shock was delivered. The first 100 seconds of response activity were then processed to give the trace labeled "after shock." Responses recorded between a wick electrode and reference on nose. Stimulus conditions identical with those of Fig. XXIII-14; N = 1000. Session 5 for this subject (E.C.T., 4/5/62).

particular response is illustrated in Fig. XXIII-14. On the fourth recording session for this subject, responses were recorded for more than 12 minutes during which time click stimuli were delivered at the rate of 10/sec. Both needle and wick electrodes were used for this run. The wick electrode was in contact with almost the entire posterior line of attachment of the external ear. The responses recorded by the needle electrode are smaller than those in Fig. XXIII-11 because the needle could not be placed in the same locations with the wick in place. The waveforms of the responses from the two electrodes are quite different, particularly in that the initial negative peak is absent in the wick recordings. The later components in the responses recorded by the two electrodes seem to be comparable in latency, and they decline in amplitude in a similar way. This gradual decrease in response amplitude does not occur in initial recording sessions and occurs more rapidly in later recording sessions. For some of our more "experienced" subjects, responses that had been stable in the initial sessions decreased rapidly in amplitude after the first few responses in later sessions. In sessions in which the amplitude had become small, various instructions to the subjects, such as "count the clicks," "relax," and "read," did not result in an increase in amplitude. Also, changes in room illumination or click intensity and repetition rate did not bring back the response. One instance in which the responses did become large again momentarily is shown in Fig. XXIII-15. Electric shocks to several of our subjects resulted in a spectacular increase in response amplitude with subsequent rapid decrease. After the shocks were repeated several times they, too, ceased to have significant effects.

The position of the head also seems to be a factor in the appearance of the

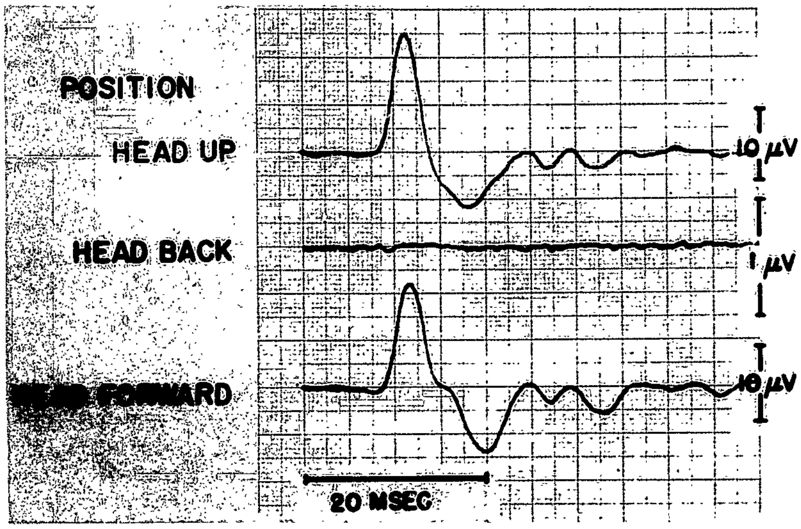

Fig. XXIII-16. Postauricular responses influenced by head position. The head was first oriented in an upright position. Then the head was allowed to fall back until it rested comfortably on a support. Finally, the head was brought forward in a bending position. Changes in head position often had dramatic effects on the responses, but at other times did not. Checks of the recording arrangement were always made to ensure that no electrical connections were disturbed as a result of head movements. Stimulus conditions are identical with those of Fig. XXIII-14. N = 1000 for the top and bottom traces; N = 500 for the middle trace. A needle electrode behind the left ear was used in these recordings with the reference electrode on the right earlobe. Session 4 for this subject (E.C.T., 3/26/62).

postauricular response. For most of our subjects an upright position or forward bend of the head resulted in larger responses than tilting the head back. The effect is not always as dramatic as that illustrated in Fig. XXIII-16, even for the same subject. A similar phenomenon has been previously reported for a longer latency response to auditory stimuli.[8]

A few miscellaneous facts can also be noted. The postauricular responses are obtainable with other transient stimuli, such as bursts of tone or bursts of noise. They are obtainable bilaterally, even by using earphones to stimulate only one ear. Clear responses were obtained from 8 of 10 subjects. Of these eight, four were male and four female. All subjects were less than 40 years of age and healthy. No responses could be detected in records obtained from two subjects with severe hearing losses.

The ease of recording postauricular responses invites further experimentation to determine their origin. The lability of the response challenges the ingenuity of the experimenter. This lability resembles the behavior of certain responses recorded from the brains of unanesthetized cats.[9] In particular, a decrease in amplitude with prolonged stimulation is characteristic of some components of the cortical responses in cats. It is difficult, however, to make direct comparisons between these two sets of data recorded in different ways from different species.

Despite the synchrony of the postauricular responses with stimuli at high rates (Fig. XXIII-13), it is possible that the response arises from activity of either ear or neck muscles. The sensitivity of the response to changes in electrode location and the effects of head position support such a view. The response is unlikely to be the result of stapedius muscle activity in the middle ear, since a clear response was obtained in a subject who had undergone stapes surgery with resultant severing of the muscle.

N. Y-S. Kiang, A. H. Crist, M. A. French, A. G. Edwards

(Dr. A. G. Edwards is a Resident at the Massachusetts Eye and Ear Infirmary.)

References

1. J. Calvert, H-P. Cathala, F. Contamin, J. Hirsch, and J. Sherrer, Potentials évoqués corticaux chez l'homme, Rev. Neurol. 95, 445-454 (1956).

2. C. D. Geisler, L. S. Frishkopf, and W. A. Rosenblith, Extracranial responses to acoustic clicks in man, Science 128, 1210-1211 (1958).

3. N. Y-S. Kiang, The use of computers in studies of auditory neurophysiology, Trans. Am. Acad. Ophthalmol. Otolaryngol. 65, 735-747 (1961).

4. E. L. Lowell, C. T. Williams, R. M. Ballinger, and D. P. Alvig, Measurements of auditory threshold with a special purpose analog computer, J. Speech Hearing Res. 4, 105-112 (1961).

5. T. Suzuki and I. Asawa, Evoked potential of waking human brain to acoustic stimuli, Acta Oto-laryngol. 48, 508-515 (1958).

6. H. L. Williams, D. I. Tepas, and H. C. Morlock, Jr., Evoked responses to clicks and electroencephalographic stages of sleep in man, Science 138, 685-686 (1962).

7. W.A. Clark, R.M. Brown, M.H. Goldstein, Jr., C.E. Molnar, D.F. O'Brien, and H. E. Zieman, The average response computer (ARC): A digital device for computing averages and amplitude and time histograms of electrophysiological response, Trans. IRE, Vol. BME-8, No. 1, pp. 46-51, 1961.

8. C.D. Geisler, Average Responses to Clicks in Man Recorded by Scalp Electrodes, Technical Report 380, Research Laboratory of Electronics, M.I.T., November 4, 1960, see p. 124.

9. D. C. Teas and N. Y-S. Kiang, Evoked cortical responses as a function of 'state variables,' Quarterly Progress Report No. 63, Research Laboratory of Electronics, M.I.T., October 15, 1961, pp. 171-176.

C. RESPONSES OF A NEURONLIKE NET TO PAIRED STIMULI

We have reported previously that the response to the second of a pair of stimuli to a neuronlike net goes through damped "cycles" of alternate "enhancement" and "depression" as a function of the length of the interval between the two stimuli.[1] Other work on such "recovery curves" has confirmed and extended this result.

The variance of these recovery curves was found to be considerable, seldom being less than 20-30 per cent of the amplitude of the cyclic oscillation, and sometimes exceeding it. The explanation for this variability lies in the fact that the stimulus pair never re-encounters identical conditions, since the net is spontaneously active.

We found that the intervals between the peaks in the recovery curves increase when the time constant that represents the refractory property of the neuronlike elements is increased. This effect was expected, since the periods for spontaneous oscillations show a similar dependence.

Finally, we found that the "enhancement-depression" cycle varies in prominence as a function of the intensity of the stimuli. If the two stimuli are of equal intensity, there is one intensity level that produces the effect with greatest prominence. At high intensities (for which a large proportion of the elements is stimulated), the activity of the net dies, or nearly dies, after the first stimulus, since most of the elements are simultaneously refractory: the cycle vanishes under these conditions. At low stimulus intensities, "spontaneous" firings occur so frequently that the responses are small compared with the total activity; thus the effect vanishes into the noise level.

A detailed account of these results has been given in R. B. Keim's thesis.[2]

R. B. Keim, B. G. Farley

References

1. B. G. Farley, Some results of computer simulation of neuronlike nets, Quarterly Progress Report No. 64, Research Laboratory of Electronics, M.I.T., January 15, 1962, pp. 258-267; N.B. p. 265.

2. R. B. Keim, Paired Stimuli Response of a Neural Net Model, S.B. Thesis, Department of Biology, M.I.T., September 1962.

XXIV. NEUROPHYSIOLOGY*

W. S. McCulloch
M. A. Arbib
F. S. Axelrod
M. Blum
J. E. Brown
R. C. Gesteland
M. C. Goodall
W. L. Kilmer
K. Kornacker
J. Y. Lettvin
Diane Major
L. M. Mendell
N. M. Onesto
W. H. Pitts
J. A. Rojas
A. Taub
P. D. Wall

RESEARCH OBJECTIVES

The aims of this group can be stated best under three main headings:

1. Basic Theory

Our purpose is to develop the necessary logical and mathematical theory for an understanding of computation such as the brain performs, and thus lay foundations for an attack on the problem of decision making in the presence of a redundancy of potential command such as that encountered in the reticular formation.

M. A. Arbib, M. Blum, N. M. Onesto,
W. L. Kilmer, W. S. McCulloch

2. Project Plans

(a) Olfactory Physiology. We expect to go to the second-order neurons now in an attempt to unravel the categories of the first order.

R. C. Gesteland, W. H. Pitts, J. Y. Lettvin

(b) Electrodes. We shall prosecute the study of specifically sensitive O_2, pH, and other sorts of electrodes, partly for oceanographic application, partly for biological application.

W. H. Pitts, R. C. Gesteland, J. Y. Lettvin

(c) Instrumentation. Various electronic devices will be built as the need arises.

J. Y. Lettvin, R. C. Gesteland

(d) Visual Processes. We are branching into the study of form-function relations and color vision, as well as into further octopus work.

H. R. Maturana, J. Y. Lettvin

(e) Visual Processes of the Rat. We plan to study the organization of receptive fields in rodents.

J. E. Brown, J. A. Rojas

(f) Physiological Optics. We are working on schemes to track the position and focus of an eye from a distance.

B. H. Howland, R. C. Gesteland, J. Y. Lettvin

*This work was supported in part by Bell Telephone Laboratories, Inc.; The Teagle Foundation, Inc.; the National Institutes of Health (Grant NB-01865-05 and Grant MH-04737-02); and in part by the U.S. Air Force (Aeronautical Systems Division) under Contract AF33(616)-7783.

3. Problems of Sensory Projection Pathways

During the past year, we have concentrated on two major lines of approach to the problems of cutaneous sensory mechanisms. The first has dealt with the control system situated about the first central synapse where nerve fibers from the skin converge on cells in the dorsal part of the spinal cord. We have shown that the very small cells scattered throughout the region of these synapses and which make up the substantia gelatinosa are involved in modulating the transmission of impulses across this first junction. This censorship of arriving nerve impulses is affected by previous activity in the same pathway, by activity in neighboring areas of skin, by intense activity in distant areas, particularly in paws and face, and by stimulation of the cerebellum, mid-brain, pons, and medulla. The censorship mechanism seems to be in continuous action, and we believe that it is best studied by steady stimuli, rather than by sudden brief changes in the environment. The mechanisms that we have seen in the cat would predict interactions between various types of skin stimuli, and we have carried out concomitant experiments on man to examine these hypotheses. These psychological experiments have shown that there is a most interesting interaction in man between light-pressure stimuli and electrical stimulation. We have published some of this work in Brain and in the Journal of Physiology, and two other papers will appear, in 1963, in Experimental Neurology. In the coming year, we shall pursue the study of the censorship mechanism in an attempt to find something of its role in the normal functioning of the animal.

Our second line of approach is an attempt to discover the language used by the skin in telling the brain about the location of the stimulus. We are studying two reflexes that require the motor mechanisms to know the exact location of the stimulus. The first is the scratch or swipe reflex, and the second is the eye blink. We are studying the pathways over which the information is carried both in normal animals and in frogs and salamanders who have been operated on in their youth. If dorsal and ventral skin are reversed in the tadpole, the scratch reflex of the adult frog is aimed at the embryological position of the skin, and not at its actual position, so that it is evident that some message is going from skin to central nervous system which tells the nature of the skin rather than its position. We hope to discover the nature of this message by microelectrode studies of the cord. Similar work is being done on amphibia in which an additional eye is implanted on the head. The extra eye will generate a blink reflex in the normal eye if it is touched, and so we know that nerves are somehow capable of telling the brain that they are in cornea and not in ordinary skin. This problem has been studied in normal frogs, a paper will soon appear in Experimental Neurology, and this work will be pushed vigorously during the next year.

A. Taub, K. Kornacker, Diane Major, P. D. Wall

XXV. NEUROLOGY*

L. Stark	A. A. Sandberg	I. H. Thomae
F. H. Baker	Susanne Shuman	A. Troelstra
R. W. Cornew	J. L. Simpson	E. C. Van Horn, Jr.
H. T. Hermann	Gabriella W. Smith	P. A. Willis
J. C. Houk, Jr.	I. Sobel	S. Yasui
E. L. Mudama	S. F. Stanten	L. R. Young
F. Naves		B. L. Zuber

RESEARCH OBJECTIVES

The aim of our work is to apply the concept of communication and control theory to our analyses of neurological and biological mechanisms. The group is composed of neurologists, mathematicians, and electrical engineers. Our research endeavors to span a wide field that includes experiments on human control mechanisms, mathematical methods for analysis of nonlinear systems, including simulation, clinical studies with on-line digital-computer techniques employed, neurophsiology of simple invertebrate receptors, and adaptive pattern-recognition techniques with the use of computers.

L. Stark

A. WORK COMPLETED

Short summaries follow of theses accepted by the departments, and in partial fulfillment of the requirements for the degrees, indicated.

1. A Sampled Data Model for Eye-Tracking Movements, Sc.D. Thesis, Department of Aeronautics and Astronautics, M.I.T., May 1962.

A sampled-data model has been developed, based on the following principles: 1) the predictability of the target signal has a profound effect on the system's ability of track continuous and discontinuous target motion; 2) the saccadic and pursuit systems function separately; and 3) the eye-movement tracking characteristics are of a discrete nature.

L. R. Young

2. A Convenient Eye Position and Pupil Size Meter, S.M. Thesis, Department of Electrical Engineering, M.I.T., June 1962.

A specialized television system, in which a technique of circular track scanning is employed, takes continuous readings of eye pupil size and position. The ac components of scanning deflection signals are proportional to the eye pupil diameter, and the dc components are proportional to the coordinates of eye pupil position.

C. A. Finnila

*This research is supported in part by the U.S. Public Health Service (B-3055, B-3090), the Office of Naval Research (Nonr-1841 (70)), the Air Force (AF33(616)-7588, AF49(638)-1130, AFAFOSR-155-63), and the Army Chemical Corps (DA-18-108-405-Cml-942); and in part by the National Science Foundation (Grant G-16526).

3. The Design and Construction of a Motor Coordination Testing Servomechanism, Department of Electrical Engineering, M.I.T., June 1962.

An instrument consisting of two electrically identical dc servomechanisms with concentric output shafts was designed to test the dynamic behavior of human motor coordination in the lower arm and wrist.

G. L. Gottlieb

4. Effects of Alcohol and Barbiturates on Rotational Mechanical Responses, S.B. Thesis, Department of Electrical Engineering, M.I.T., June 1962.

The effect of alcohol and barbiturates on the response of subjects following a light spot with a pointer was found to depend on the frequency at which the input light moved on the screen.

W. G. Henrikson

5. Head-Position Indicator, S.B. Thesis, Department of Electrical Engineering, M.I.T., June 1962.

A gyroscope-demodular system was used to indicate head position, so that the place where a subject looks in a given situation can be determined.

H. R. Howland

6. Computer Analysis of Handwriting Applied to Cancer Detection, S.B. Thesis, Department of Electrical Engineering, M.I.T., June 1962.

The Kaufer Neuromuscular Test was programmed on the TX-0 computer, the results analyzed, and improvements suggested.

R. G. Kurkjian

7. A Semiconductor Regulated DC Power Supply, S.B. Thesis, Department of Electrical Engineering, M.I.T., June 1962.

An efficient power supply for application to a servomechanism system is obtained by cascading a transistorized filter and a transistor dc regulator.

K. D. Labaugh

8. A Measuring Device for the Tremor of the Human Finger, S.B. Thesis, Department of Electrical Engineering, M.I.T., June 1962.

With a transducer that employs the change in capacitance of two plates, caused by varying the distance between them, a signal can be detected which indicates finger tremor.

G. Segal

9. The Pupil Light Reflex in the Owl, S.B. Thesis, Department of Biology, M.I.T., May 1962.

The pupil reflex of an owl to light was found to contain nonlinearities that contribute to the variability of the gain results.

G. H. Northrop

10. Linear Light Source for Eye Stimulation, Department of Electrical Engineering, M.I.T., June 1962.

A television screen is used as a light source to stimulate the eye, and thus enable one to observe the pupil under various stimulation conditions.

G. Sever

11. The Effects of Drugs on the Transfer Function of the Human Pupil System, Department of Biology, M.I.T., May 1962.

Using physostignine and hydroxyamphetamine hydrobromide together, we found that the minimum phase lag was increased, and the gain of the transfer function decreased.

J. W. Stark

12. Effect of Operating Conditions on Noise in Human Pupil Servomechanism, S.B. Thesis, Department of Electrical Engineering, M.I.T., June 1962.

The mean-square value of noise was found to be a monotonically increasing function of light intensity: the noise has stationary components from 0.08 cps to 2 cps, and the spectrum contained a relative maximum at 15 cycles per minute which corresponded to the respiration rate.

B. P. Tunstall

13. Transient Adaptation in the Human Pupil Servomechanism, S.B. Thesis, Department of Biology, M.I.T., June 1962.

The rapid rise in visual threshold is concomitant, but not simultaneous, with a rapid rise in pupil response when the steady light input to the pupil is decreased.

W. M. Zapol

B. EYE CONVERGENCE

An apparatus similar to that described by Rashbass and Westheimer[1] (Fig. XXV-1) has been used to present a convergence-divergence stimulus to human subjects.

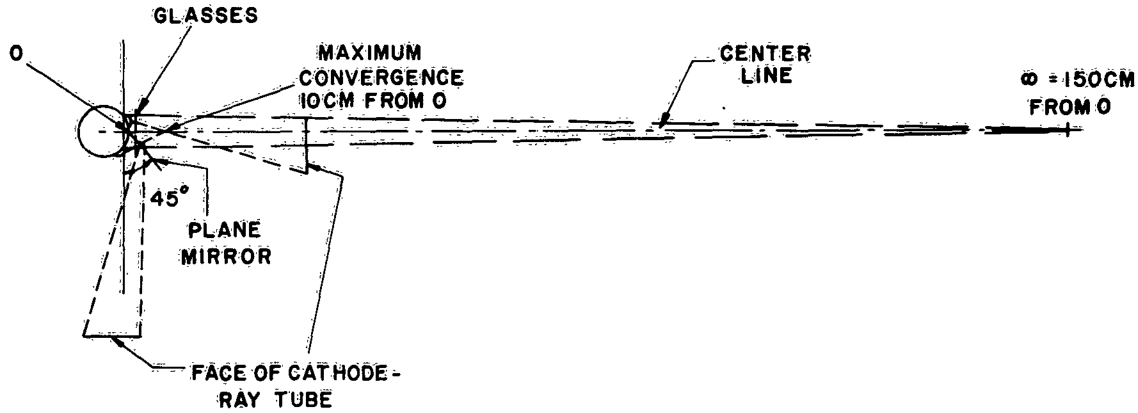

Fig. XXV-1. Eye-convergence apparatus.

The electrical apparatus used is shown in Fig. XXV-2. Eye movements are recorded from photocells mounted on eyeglass frames.[2] The variable measured

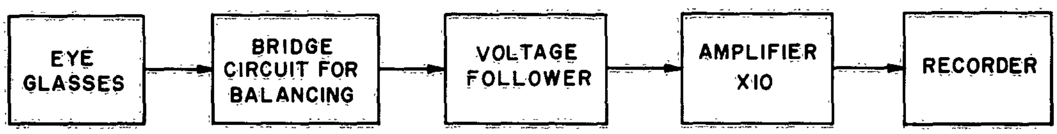

Fig. XXV-2. Electrical circuit for eye-convergence apparatus.

thus far, the angle of convergence-divergence (α_r), is defined as the angle between the line of sight when the eye is focused at infinity and the line passing through the target and the center of the eye. Calibration of eye movements (Fig. XXV-3) is accomplished by having the subject focus on a light appearing at infinity and then on a light that is a known distance from the first. Thus a known α_r is subtended. Subjects have been presented with sinusoidal and step stimuli. Records of stimuli and responses appear in Fig. XXV-3. Future investigations will include closed-loop predictable and unpredictable frequency responses with single and

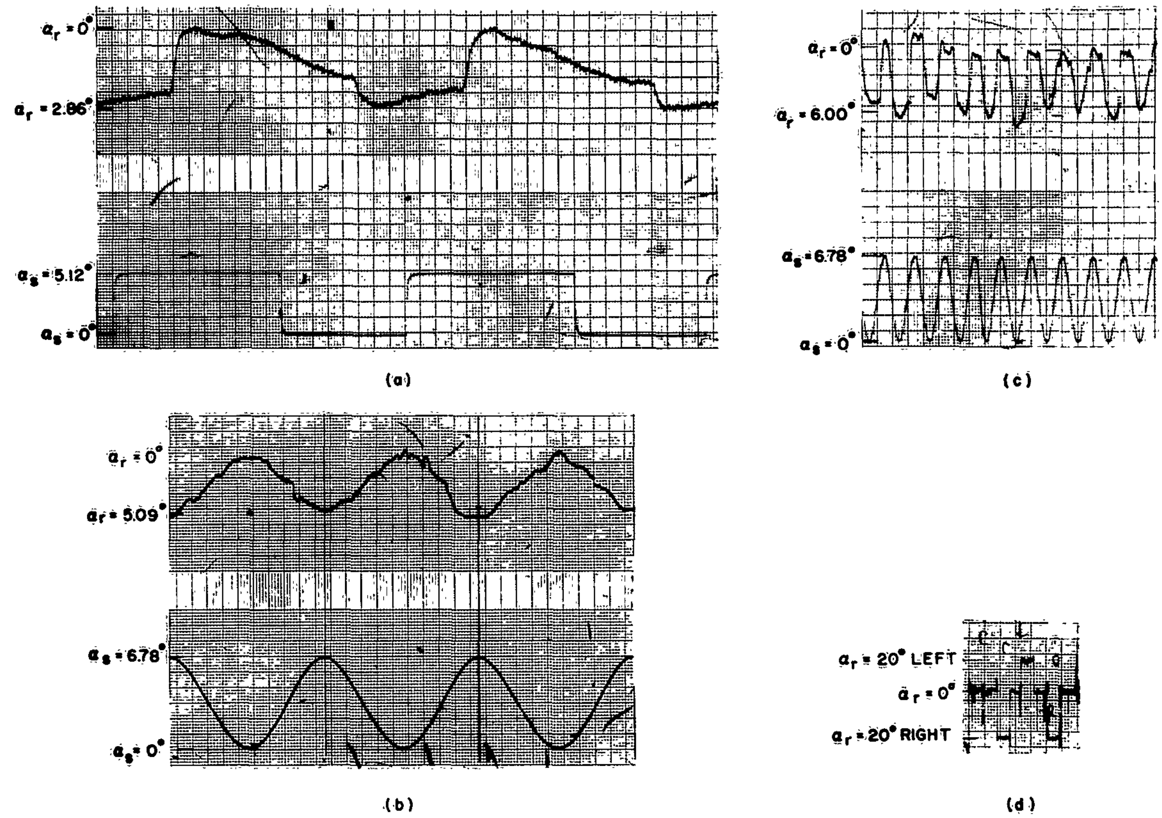

Fig. XXV-3. (a) Step response, f = 1.0 cps.
(b) Sinusoidal response, f = 0.1 cps.
(c) Sinusoidal response, f = 1.0 cps.
(d) Typical calibration, α_s = stimulus angle; α_r = response angle (average value shown).

mixed computer-produced sinusoidal stimuli used. Finally, the dynamics of the system when the feedback loop has been opened will be investigated.

B. L. Zuber, L. Stark

References

1. C. Rashbass and G. Westheimer, Disjunctive eye movements, J. Physiol. 159, 339-360 (1961).

2. G. P. Nelson, L. Stark, and L. R. Young, Phototube glasses for measuring eye movements, Quarterly Progress Report No. 67, Research Laboratory of Electronics, M.I.T., October 15, 1962, pp. 214-216.

C. PUPILLARY NOISE

In an attempt to discover possible sources of pupillary unrest (noise), a crosscorrelation program has been written for the GE 225 computer. With the aid of this program

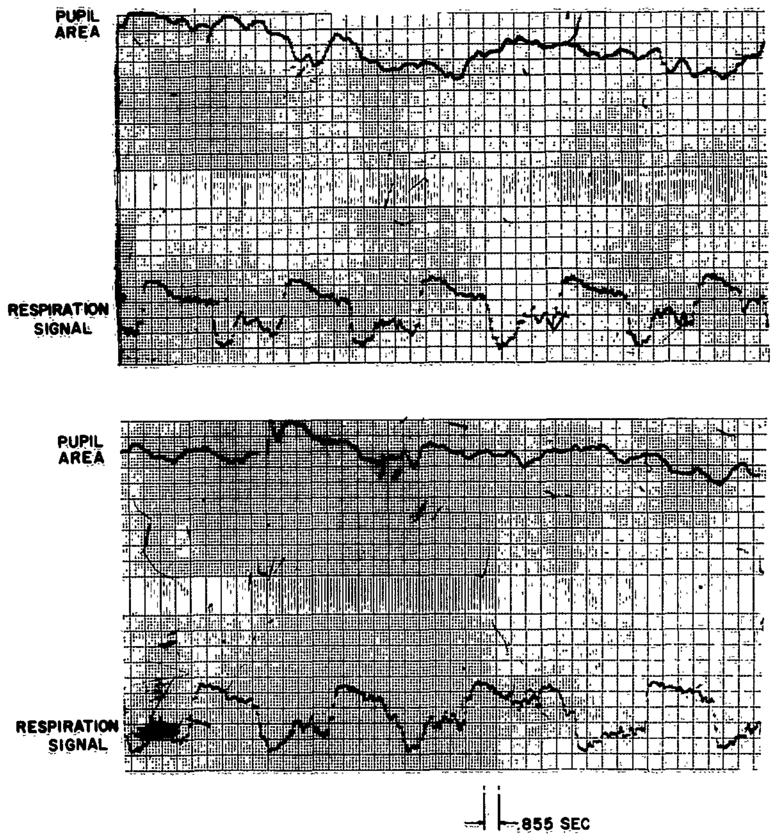

Fig. XXV-4. Digitalized records of pupil area and respiration signal.

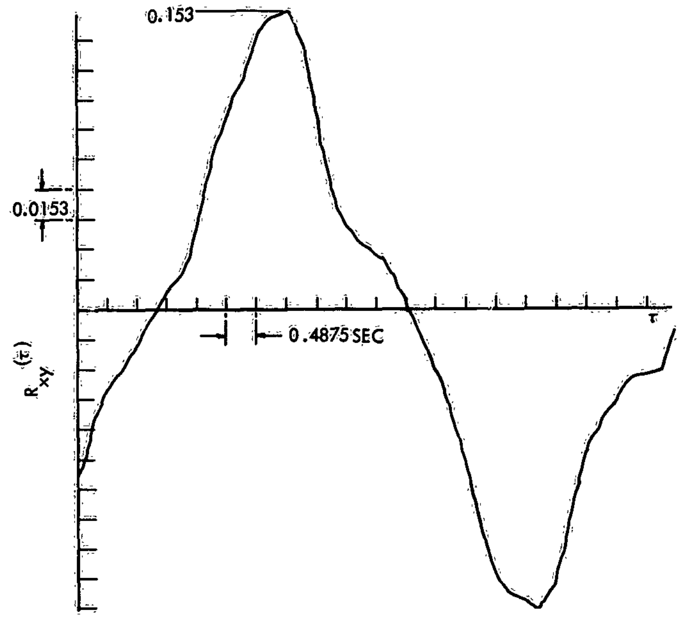

Fig. XXV-5. Crosscorrelation between pupil noise and respiration.

pupil noise can be compared with other biological signals to determine whether or not correlation exists.

As a first attempt, the pupil noise was crosscorrelated with a respiration signal. This respiration signal was obtained from a device that consisted of a thermistor (Fenwal Type BC32L1) placed inside a hollow plastic tube, which, in turn, was inserted into the nostril of the subject. As the subject inhaled and exhaled, the temperature in the environment of the thermistor changed and thus the resistance of the thermistor changed. The thermistor was used as one arm of a resistance bridge, and the signal obtained indicated, in some sense, the respiration of the subject.

The respiration was crosscorrelated with the pupil area under constant illumination conditions. Three cases were tried: (a) slow breathing, (b) regular breathing, and (c) fast breathing.

Figure XXV-4 shows a typical area and respiration signal for the slow-breathing case after digitalization, and Fig. XXV-5 shows its crosscorrelation function. The crosscorrelation function is

$$R_{xy}(\tau) = \frac{\overline{(x(t)-\bar{x})(y(t+\tau)-\bar{y})}}{\sigma_x \sigma_y}$$

Here, the bar denotes time average, x is the pupil area, y is the respiration signal, $\bar{x}$ and $\bar{y}$ are the respective time-average values, and σ_x and σ_y are the respective rms values of the signal. We see from Fig. XXV-5 that the correlation peak goes as high as 15 per cent. For regular breathing the correlation peak was approximately 11 per cent, and for fast breathing a peak of approximately 2 per cent was obtained.

No definite conclusions will be drawn now, due to the fact that the experiment was performed only once, and there is the possibility of head movement during breathing, which could add correlation.

S. F. Stanten, L. Stark

D. EYE-MOVEMENT EXPERIMENTATION

Equipment for our eye-movement experiment has been set up at the Massachusetts Eye and Ear Infirmary of the Massachusetts General Hospital. It is very similar to the experimental arrangement used for the study of the effect of pharmacological agents on

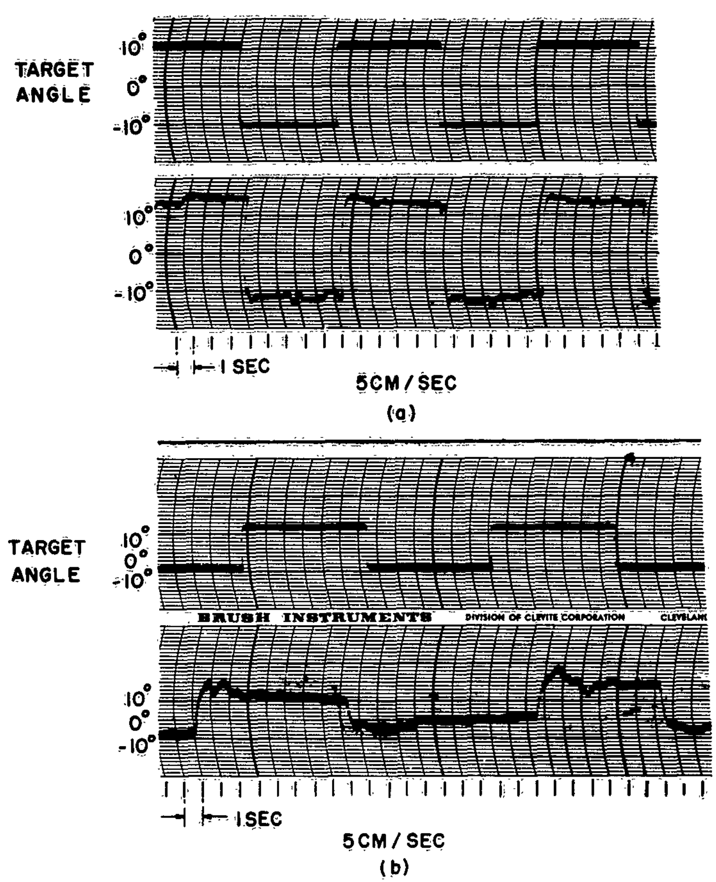

Fig. XXV-6. Response to step changes in target angle recorded from (a) normal subject, and (b) young child with possible brain tumor.

control of eye movements.[1] We are studying patients with various eye-movement disorders who sit with head fixed in a "catcher's" mask. They wear a pair of photocell goggles that measure eye movement as a moving spot of light on an oscilloscope screen is tracked.

The patient performs a varied set of tasks: (a) directed gaze in darkness — lateral and forward; (b) compensatory movements to passive head rotation; (c) directed gaze at fixation point; and (d) conjugate eye movements following moving targets of steps, constant velocity, constant acceleration, and sinusoids. These are designed to measure certain types of eye movements — saccades, pursuit, fixation, stability, and nystagmus.

Figure XXV-6a shows the response of a normal subject to step changes in target angle. Note the rapid response without much overshoot. Figure XXV-6b shows the response of a young child with a possible brain tumor. His record shows considerable oscillatory overshoot that was not seen in ordinary clinical examination.

Gabriella W. Smith, D. G. Cogan, L. Stark

(Dr. D. G. Cogan is Chief of Ophthalmology, Massachusetts Eye and Ear Infirmary.)

References

1. H. T. Hermann, G. P. Nelson, L. Stark, and L. R. Young, Effect of pharmacological agents on control of eye movements, Quarterly Progress Report No. 67, Research Laboratory of Electronics, M.I.T., October 15, 1962, pp. 231-232.

E. MODEL OF PUPIL REFLEX TO LIGHT

Work continues in an attempt to refine our model of the human pupillary response to light. Extensive use has been made of the GE 225 computer as an integral part of a hybrid analog-digital pupil model, and to obtain reliable results by the use of on-line averaging of experimental data.

From Fig. XXV-7, and from previous work[1,2] it is apparent that some form of scale compression is present early in the signal processing by the system. Figure XXV-8 illustrates the existence of a nonlinearity with memory.[1] Note the small effect of the pulsewidth on the height of the response.

The model presented previously is shown in Fig. XXV-9. The revised model shown in Fig. XXV-10 differs from the previous model in the following respects.

(i) A logarithmic scale-compression factor has been added, the results of which are shown in Fig. XXV-11.

(ii) An extra and faster time constant has been added to the transfer function of $\overline{T}$. This addition will aid in reducing the effect on response height of pulsewidths from 10 msec to 2 seconds. However, this addition decreases the dependence of time to peak on the pulsewidth in contradiction with experimental results.

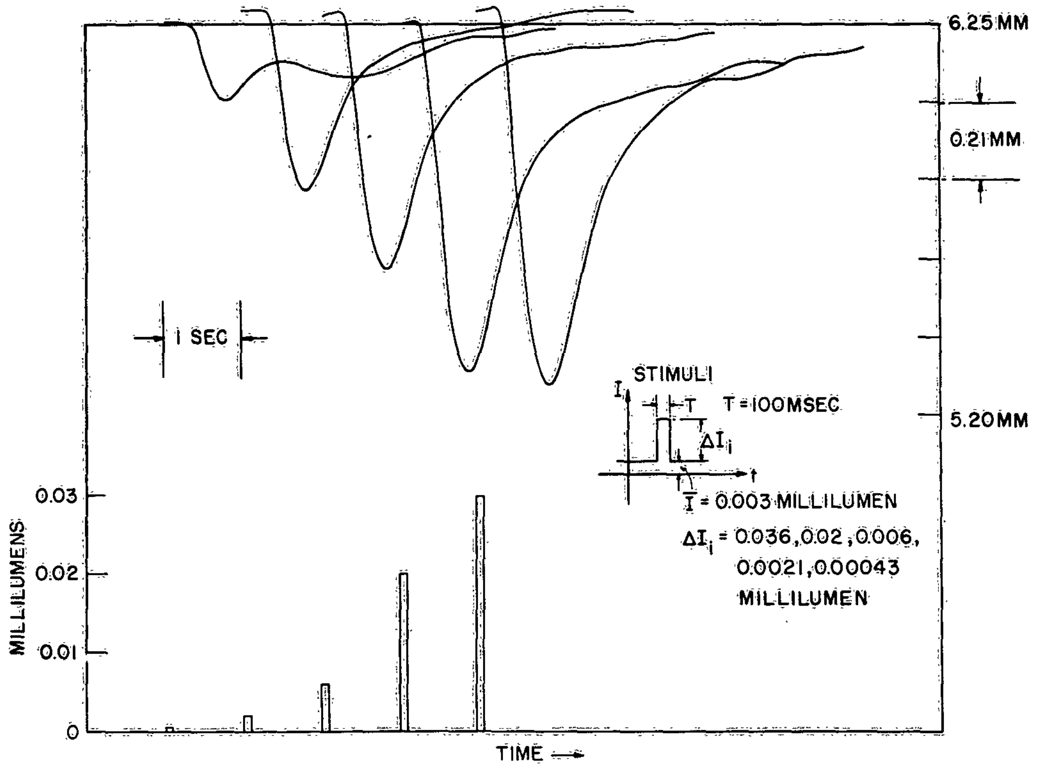

Fig. XXV-7. Pupil response to light pulses of different heights.

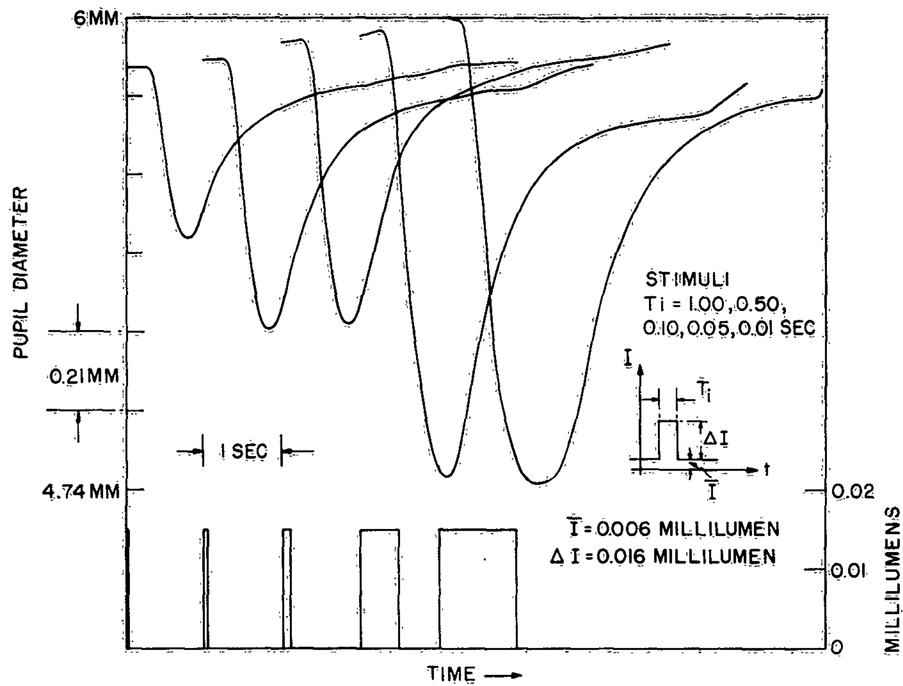

Fig. XXV-8. Average response of pupil to light pulses of decreasing width.

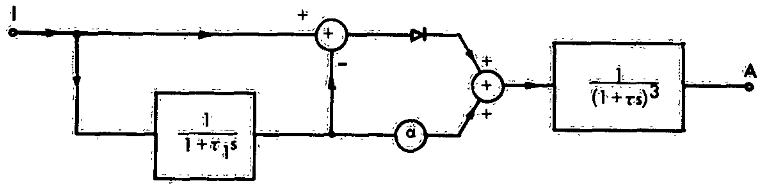

Fig. XXV-9. Old pupil model. $\tau_1 \approx 1.5$ sec; $\tau \approx 0.15$ sec; $a = 0.1$.

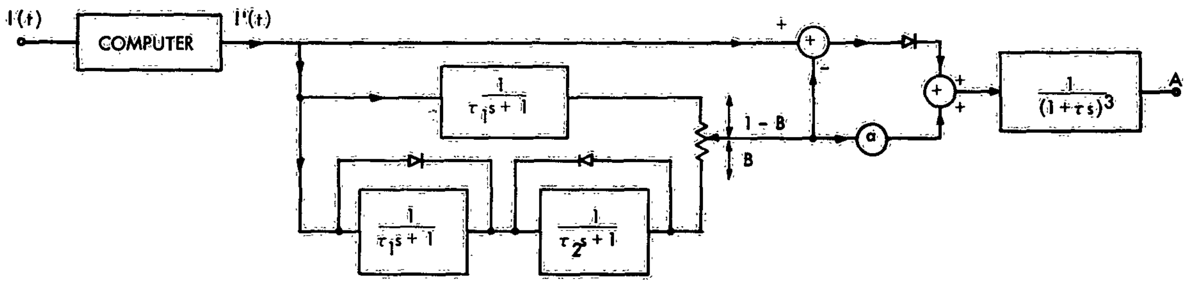

$I'(t) = LOG_2 [K I(t-T) + 1]$

$K = 6$, $\tau_1 = 1.5$ SEC, $\tau_2 = 0.2$, $\tau = 0.2$ SEC

$a = 0.05$, $\beta = 0.8$, $T = 0.2$ SEC

Fig. XXV-10. New pupil model.

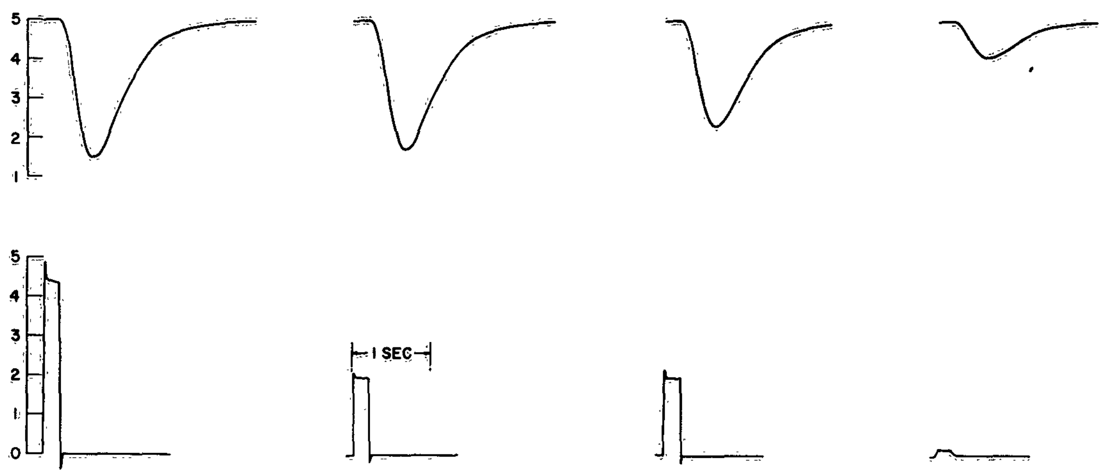

Fig. XXV-11. Response (top) of pupil model to positive pulses (bottom) of greatly varying amplitude. Note scale compression of log function. (Overshoot of the simulated stimuli is due to X-Y recorder inertia.)

(iii) The lower diodes have been introduced to make the recently introduced rapid light adaptation ineffective during dark adaptation.

A. A. Sandberg, L. Stark

References

1. L. Stark, Julia H. Redhead, and H. Van der Tweel, Pulse response of the pupil, Acta Physiol. Pharmacol. Neerl. (in press).

2. F. H. Baker, Pupil response to short-duration pulses, Quarterly Progress Report No. 65, Research Laboratory of Electronics, M.I.T., April 15, 1962, pp. 251-257.

F. HUMAN PREDICTION OF FILTERED RANDOM SEQUENCES

An experiment has been designed to investigate a human subject's strategy in predicting successive numbers in a nonindependent sequence of random numbers. The experiment is implemented in the form of a digital-computer program that interacts with the subject and the experimenter by means of typewriters. This program has been written and checked out, and the first carefully controlled experiments are now in progress.

The subject is presented with a sequence of positive and negative decimal integers, which are formed by taking a weighted sum of (a) a number obtained by an independent sampling of a uniform distribution of zero mean and (b) a linear combination of previous numbers in the output sequence.

After each number is presented, the subject is asked to predict what the next number in the sequence will be. It is apparent, and, indeed, can be proved, that he may minimize his mean-square error by setting his prediction just equal to the quantity (b) above. This is then his "optimum policy."

Figure XXV-12 gives a block diagram of the experimental configuration. The quantities shown have the following meanings:

R	Random-number generator
Fi	Filter
D_1	Delay of one discrete time unit
S	Subject
E	Experimenter
i	Discrete time variable
X(i)	Independent sample from a uniform distribution
Y(i)	Constrained random number
Q(i)	Subject's optimum prediction for Y(i)
Y(i-1)	The number presented to the subject just before he gives P(i)

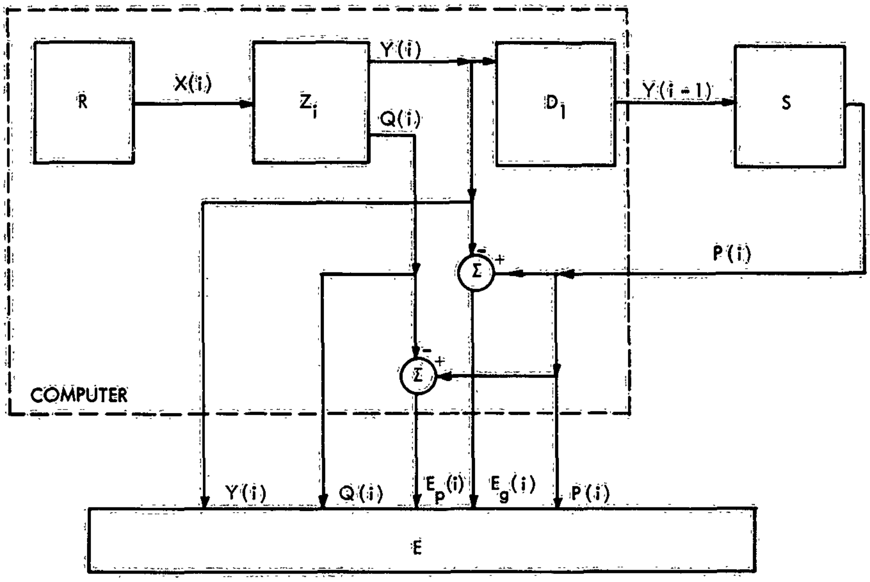

Fig. XXV-12. Experimental configuration.

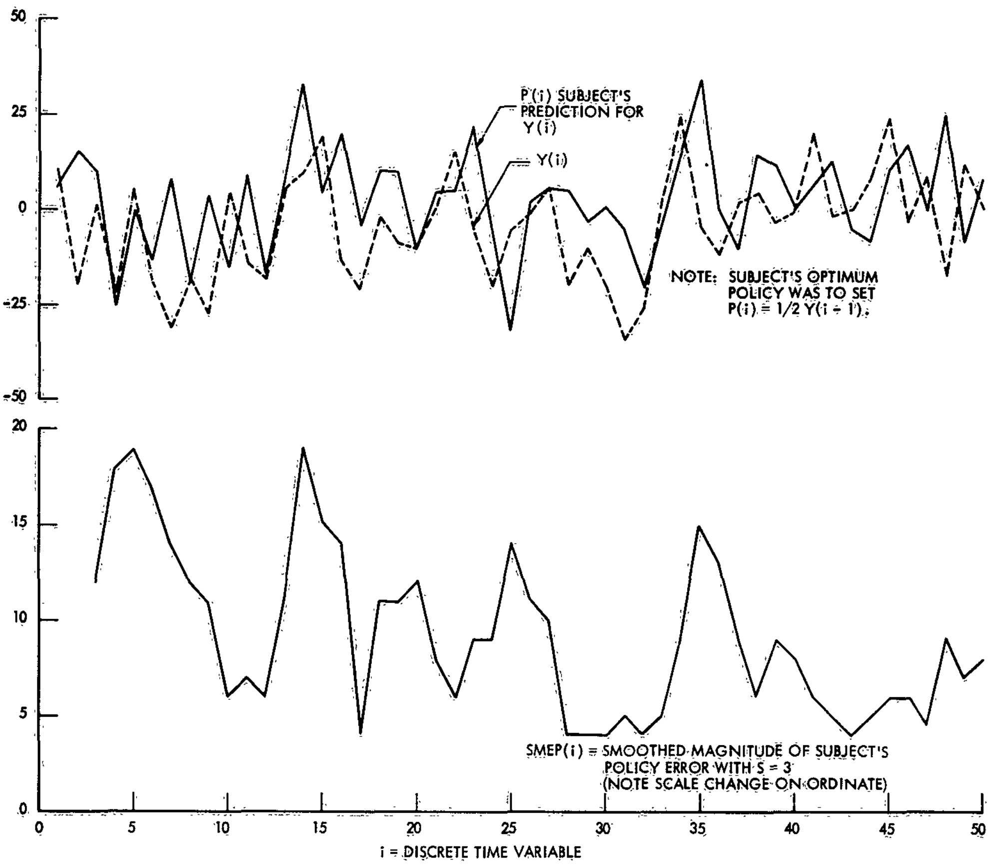

Fig. XXV-13. Results of one human prediction experiment.

$P(i)$ Subject's prediction for $Y(i)$

$Eg(i)$ Subject's guess error ($=P(i)-Y(i)$)

$Ep(i)$ Subject's policy error ($=P(i)-Q(i)$).

Another quantity that is not shown in Fig. XXV-11 and is also calculated by the computer is

$$SMEP(i) = \frac{1}{S} \sum_{j=1}^{S} \left| Ep(i-j) \right|.$$

Here, SMEP stands for "smoothed magnitude of policy error." We have found it convenient to set $S = 3$ for most of our experiments.

Figure XXV-13 is a graph of $P(i)$, $Y(i)$, and $SMEP(i)$ (with $S=3$) plotted against i for a representative sum of 50 predictions.

The hypothesis has been set forth that the subject will gradually learn to behave well with respect to the optimum policy, but that the random character of the Y's will cause him to eventually become dissatisfied with his performance. He will then make a drastic change in his policy, which, of course, will cause his policy error to increase in magnitude. He will then gradually return to the optimum policy, only to become dissatisfied again later on. Our experimentation has not progressed far enough to enable us to confirm or deny this hypothesis.

E. C. Van Horn, Jr., L. Stark

XXVI. CUTANEOUS SENSORY MECHANISMS*

Prof. R. Melzack
P. D. Donahue
J. G. Hallett
G. R. S. Bingham

RESEARCH OBJECTIVES

There is considerable evidence that severe restriction of the early perceptual experience of animals produces profound disturbances of their perceptual, emotional, and intellectual development. The purpose of our investigation is to carry out a series of studies on the physiological mechanisms that underlie the highly abnormal behavior observed in animals reared in isolation. The focus of individual studies will be on three salient characteristics of the behavior of animals reared in isolation: (a) a frequent failure to perceive and respond to the appropriate environmental cues, including stimuli that are painful to animals that are reared under normal conditions; (b) an extremely high level of excited activity that pervades virtually all of the animals' behavior; and (c) a low capacity for learning new responses in problem-solving situations. The method of procedure for the first problem is to observe the behavior of restricted and normally reared animals from the same litter in response to brief burns and pinpricks and simultaneously to record responses evoked at the midbrain, thalamus, and cortex.

R. Melzack

*This research was supported in part by the National Institutes of Health (Grant MH-04235-03).

XXVII. SENSORY AIDS RESEARCH*

Prof. S. J. Mason
Prof. D. E. Troxel
G. Cheadle
J. Dupress
W. G. Kellner
D. G. Kocher
R. C. Levine
M. A. Pilla

RESEARCH OBJECTIVES

The basic objective of our research in sensory communication is to provide a better understanding of the fundamental problems underlying the development of sensory aids for people who are blind or blind and deaf. Current and projected work includes studies of (a) tactile transmission of Braille-like codes; (b) tactile-kinesthetic transmission of stenotypelike codes; (c) tactile-kinesthetic perception of planar shapes, including modified and enlarged letter and word shapes; (d) communication by means of the thermal sense; (e) communication by simultaneous stimulation of two or more sensory modalities; (f) picture processing for drastic reduction of information content; (g) detection of skin potentials; and (h) eye-movement measurements.

S. J. Mason

*This work was supported in part by the National Institutes of Health (Grant MH-04737-02); in part by the National Science Foundation (Grant G-16526); and in part by the U. S. Air Force (Electronic Systems Division) under Contract AF19(628)-258.

XXVIII. CIRCUIT THEORY AND DESIGN*

Prof. P. Penfield, Jr.
Prof. R. P. Rafuse
Prof. C. L. Searle
Prof. R. D. Thornton

RESEARCH OBJECTIVES

Investigations of nonlinear, time-variant linear, and linear active circuits are aimed at a better understanding of the relations between theoretical models and physical devices. Current research includes:

(a) theoretical investigations, design, and experimental behavior of parametric amplifiers and frequency multipliers

(b) determination of the invariant properties of active network components under various kinds of embedding

(c) studies of transistor and tunnel-diode circuits

(d) interpretation of a general v · i conservation theorem.

P. Penfield, Jr., R. P. Rafuse, C. L. Searle, R. D. Thornton

*This work is supported in part by Purchase Order DDL B-00368 with Lincoln Laboratory, a center for research operated by Massachusetts Institute of Technology with the joint support of the U. S. Army, Navy, and Air Force under Air Force Contract AF19(604)-7400.

XXIX. NETWORK SYNTHESIS

Prof. E. A. Guillemin
S. G. Chamberlain
V. K. Prabhu
W. C. Schwab

RESEARCH OBJECTIVES

As expressed in last year's research objectives (Quarterly Progress Report No. 64, page 337), the further development of an approach to synthesis, which was started during the past two years, will continue during this and for several more years, inasmuch as many collateral problems are generated in the process of working out essential steps in this new method of network synthesis.

E. A. Guillemin

XXX. COMPUTER RESEARCH

Prof. J. B. Dennis
N. Kerllenevich
G. Y-C. Wang

RESEARCH OBJECTIVES

The purpose of this group, which is operated jointly by the Research Laboratory of Electronics, the Electronic Systems Laboratory, and the Department of Electrical Engineering, M.I.T., is threefold:

1. To provide a flexible and readily accessible computation facility oriented toward the Laboratory's research goals.
2. To develop computation techniques, especially in the sense of increasing the convenience with which operating programs for particular tasks may be produced, and of allowing the scientist easy communication with the machine about tasks that are being performed for him.
3. To provide an education facility where students may learn the principles of automatic computation, and undergraduate and graduate theses and projects may be carried out.

Computation Facility

The computation facility consists of two general-purpose digital computers. The TX-0 computer, an experimental transistorized machine,[1] was built by Lincoln Laboratory, M.I.T. Since 1958, the TX-0 computer has been made available for academic research. Its effectiveness has been increased through the expansion of its instruction code,[2] the addition of a flexible in-out facility for communicating with the users' equipment, and the installation of a magnetic tape unit for auxiliary storage. In September 1961, the Digital Equipment Corporation generously donated one of its PDP-1 machines to the Department of Electrical Engineering, M.I.T. This machine is a commercial unit that is similar in many respects to the TX-0 in its design and intended application.

Time Sharing

Our experience with TX-0 has shown that on-line communication between the user and machine allows the user to progress faster in his research with less effort on his part than is possible with a closed-shop operation: If the user can interrogate the machine at any time to observe the course of the computation and to change parameters of the problem when it is necessary, he can make quicker progress with less computation. A closed-shop operation, of course, will allow much more efficient use of the computer, since it need never stand idle while the user ponders his next step in running a computation experiment, or in testing a program.

The time sharing of one computer by a number of users operating from different consoles would combine the advantages of both modes of computer operation, and is viewed by many as the desirable goal for the future computation facility[3] at the Massachusetts Institute of Technology. The hardware and programming for time-shared operation of the PDP-1 computer from up to seven typewriter consoles has been designed and installation is nearing completion. The system is built around a magnetic drum that stores users' programs while they are waiting their turn to run. The drum permits a shift between programs in 33 msec, allowing a fast response to users' demands.

This facility will make the advantages of time-shared operation available to students and laboratory research projects, and help establish requirements for a future large-scale facility.

J. B. Dennis

References

1. J. T. Gilmore, Jr. and H. P. Peterson, A Functional Description of the TX-0 Computer, Memo 6M-4789-1, 1958.

2. Quarterly Progress Report No. 67, Research Laboratory of Electronics, M. I. T., October 15, 1962, pp. 275-282.

3. H. Teager, Report of the Long-Range Computation Study Group, M. I. T., 1961.

4. J. E. Yates, A Time Sharing System for the PDP-1 Computer, Report ESL R-140, Electronic Systems Laboratory, M. I. T., June 1962.

XXXI. ADVANCED COMPUTATION RESEARCH*

Prof. H. M. Teager
N. E. Bolen
E. L. Ivie
U. Shimony
R. L. Ward
D. U. Wilde

RESEARCH OBJECTIVES

Our objective is to develop devices, systems, and languages for fruitful interaction between scientists and computers, through the use of the computer as a powerful, on-line aid to understanding. Taking cost and computer capacity into consideration, we can provide this facility by time-sharing a slightly modified computer with a normal-sized memory. The computer is equipped with random access files and many low-cost remote consoles, each of which has low-data-rate graphical and character-producing input-output devices. The consoles can be operated simultaneously.

Work in this field has been concerned with the following problems. We have tested on-line programming and computation, utilizing a system of multiple independent typewriters. An existing digital plotter has been connected to an IBM 709 computer, and we are constructing a special-purpose computer to control multiple independent plotters. A prototype of a high-resolution graphical input device for figures and symbols that are drawn by hand is being built. Design modifications for an IBM 7090 computer have been proposed and incorporated into the Computation Center machine. Scheduling systems for time-sharing and memory allocation have been simulated and found satisfactory. An information-retrieval system for programs and data is being designed. Programming systems for recognition of handwritten input are being checked out, and new graphical languages for several major problem classes for input and output have been partially specified.[1-3]

In a wider sense, we are investigating theoretical problems, such as associate memories, information-retrieval systems, pattern recognition, and machine organization, with a view toward the development of a comprehensive theory of computation and information processing.

H. M. Teager

References

1. H. M. Teager, Marriage of on-line human decision with computer programs, Naval Research Logistics Quarterly, December 1960, pp. 379-383.

2. H. M. Teager, Systems considerations in real-time computer usage, ONR Symposium on Automated Teaching, October 12, 1961.

3. Real-time, Time-shared Computer Project, First, Second, Third, and Fourth Quarterly Progress Reports on Contract ONR 1841(69), January, March, July, October 1961.

*This work is supported in part by the Computation Center, M.I.T.

XXXII. STROBOSCOPIC RESEARCH

Prof. H. E. Edgerton
J. A. McMorris II

RESEARCH OBJECTIVES

The goal of our work with electronic flash is twofold. First, there is an intense desire to know more about the fundamental processes that occur in flash lamps so that faster, brighter, special lamps can be designed for all sorts of performance. Second, there is an unending demand for electronic flash sources to help obtain data and radiation for all sorts of research and production problems. To properly design the flash equipment, the designer must go into the problem at hand so that he can obtain useful important data in an efficient or accurate manner.

For several years there has been intense interest in the laser device. We are furnishing flash lamps that are specially designed for good optical coupling to the ruby crystal.

There is also interest in photographing small, high-velocity particles such as those that will be encountered by space ships. The duration required for this photography is approximately 10^{-8} second. Some work has been accomplished with such a short flash, and further work is under way.

For more than ten years we have worked on many applications of electronic flash-lighting equipment to underwater research with partial financial help from the National Geographic Society and interested individuals. This work has been greatly stimulated by the addition of a pressure-testing facility in Room 20D-009, M. I. T. We have assisted with the photographic devices for both existing bathyscaphes, and we have helped with the design of new photographic gear for the French bathyscaphe that is being built for ultimate depths.

H. E. Edgerton

Author Index